TECHNICAL REPORT ON THE RAVEN MINERAL DEPOSIT, MAYO MINING DISTRICT YUKON TERRITORY, CANADA

PREPARED FOR

VICTORIA GOLD CORP.
Suite 1000, 1050 West Pender Street
Vancouver, B.C V6E 3S7

PREPARED BY

GINTO CONSULTING INC.
333 West 17th Street
North Vancouver, B.C, V7M 1V9

QUALIFIED PERSON	COMPANY
Marc Jutras, P.Eng., M.A.Sc.	Ginto Consulting Inc.

VICTORIA GOLD CORP
TSX I VGCX

Report Date: October 26, 2022
Effective Date: September 15, 2022

DATE AND SIGNATURE PAGE

This report entitled Technical Report, Raven Property, Mayo Mining District effective as of October 26, 2022 was prepared and signed by the following author:

Original document signed and sealed by:

Name	*Date Signed*
Marc Jutras, P.Eng., M.A.Sc.	October 26, 2022

NOTICE

Ginto Consulting Inc. prepared this National Instrument 43-101 Technical Report, in accordance with Form 43-101F1, for Victoria Gold Corp. The quality of information, conclusions and estimates contained herein is based on: (i) information available at the time of preparation; (ii) data supplied by outside sources, and (iii) the assumptions, conditions, and qualifications set forth in this report.

Victoria Gold Corp. filed this Technical Report with the Canadian Securities Regulatory Authorities pursuant to provincial securities legislation. Except for the purposes legislated under provincial securities law, any other use of this report by any third party is at that party's sole risk.

VICTORIA GOLD CORP

Table of Contents

TABLE OF FIGURES

TABLE OF TABLES

TABLE OF APPENDICES

1 EXECUTIVE SUMMARY

1.1 Introduction

This Technical Report is produced for Victoria Gold Corp. (“Victoria” or the “Company”), a Canadian public company engaged in the business of production, development and exploration of precious metals. Victoria’s common shares are listed on the on the Toronto Stock Exchange (“TSX) and trades under the symbol VGCX.

This report summarizes exploration work performed on the Raven Deposit (the “Deposit” or the “Project”), located in central Yukon, on the Dublin Gulch Claim Block (The “Property”) and within the Traditional Territory of the First Nation of Na-Cho Nyak Dun (“FNNND”). The Raven Deposit is owned and advanced by Victoria. The report is inclusive of an initial mineral resource estimate for the Raven Deposit, a summary of all exploration conducted on the Raven Deposit to date, including but not limited to, geochemical, geological, geophysical and diamond drilling; combined with a detailed review of the Deposit’s exploration history, a discussion of the Deposit Model and its significance towards exploration potential of the Deposit, and recommendations for future work.

1.2 Project Description and Ownership

The Property, which contains the Raven Deposit, is 100% owned by Victoria. The centre of the Deposit is at approximately; UTM Coordinates 7,101,613N / 473,605E, Zone 8, North American Datum (NAD) 83.

Raven represents a potentially high-grade, on-surface gold deposit that lies in the extreme southeast contact of the Nugget Intrusive Stock within the surrounding Earn Group metasedimentary package. This large, approximately three (3) kilometres by two (2) kilometres, medium to coarse grained granodiorite stock of Cretaceous age represents the second largest intrusive body on the Dublin Gulch property (second only to the Dublin Gulch Stock that hosts the Eagle Gold Mine). The Nugget Stock is highly prospective to host Eagle-style sheeted vein mineralization, and the vast majority of the greater than five (5) square kilometre stock remains untested.

The Raven occurrence is hosted in a shear zone corridor on the Southeast portion of the Nugget Stock, in close association with the intrusion-metasediment contact on the eastern side of the Lynx Creek valley.

Exploration drilling, trenching, and soil geochemical sampling at the Raven Deposit in 2018 through 2021 field seasons have repeatedly returned high-grade gold intersections accompanied by prolific visible gold occurrences along a major and consistently mineralized corridor, which has grown sequentially since its discovery in 2018. The Raven discovery was based largely from initial-surface trenches constructed and sampled in the 2018 field season that exposed scorodite, bismuth, and siderite related sulphide veins under less than one (1) metre of overburden/cover.

1.3 History, Exploration and Drilling

The Nugget Granodiorite Stock (“Nugget Stock”) has historically been the focus of much of the exploration efforts expended to date on the eastern portion of the Dublin Gulch Property. The earliest exploration work on the Nugget Stock occurred in the 1960’s and 1970’s when it was staked for Keno-style silver-lead-zinc mineral and intrusion related tungsten potential. Samples from this period were not assayed for gold. Later, in 1993 – 2011, the area immediate to the Nugget Stock was explored for gold potential. Airborne geophysics defined a large exposed and buried intrusion flanked by several thrust faults in an area with similarities to the Eagle Deposit (JDS, 2019). Eagle-style sheeted quartz veins were identified at this time

through ground truthing efforts. A program of surface trenches on the south-east section of the Nugget Stock was completed in 1995 and returned results from trace up to 1.12 ppm Au-in-soils (TR-95-2), and from trace up to 1.35 ppm Au in grab samples; however, the trench efforts failed to reach bedrock. The gold-in-soils anomaly identified in this program was interpreted to have a NE-SW trend. Re-sampling of the trenches in 2003 resulted in six (6) panel samples over five (5) metres grading from 0.18 ppm to 2.38 ppm Au (Ross, 2003). With limited helicopter support; prospecting, mapping and sampling campaigns were conducted in 2011 and 2014 by Victoria.

The 2018 Raven discovery was aided by a geological map of the area produced by United Keno Hill Mines Aro Aho in the 1960's. The map indicated that there were large quartz boulders with minor sulphides scattered around the eastern portion of the Nugget Stock (Van Tassel, 1969). Initial prospecting in 2018 found arsenopyrite and pyrite occurring along fractures within the quartz veins as well as thin sulphide veins within the granodiorite boulders at surface. The eastern portion of the granodiorite in the Raven zone also exhibits a well-developed oxidation profile on- and near-surface, which is not evident in other parts of the Nugget Stock. A 152-metre trench was placed along a prominent north-south oriented ridge which extended through the southern contact of the Nugget Stock. The north-south orientation was used to increase the possibility of uncovering veins of an east-west orientation which is the prominent mineralization orientation in the district – as per the Potato Hills Mineralization Model developed internally by Victoria. Trench TR18-33 (124 metres) uncovered a wide mineralized shear zone under less than a metre of overburden and assayed at 3.51g/t Au. The mineralization intersected in these surface trenches consists primarily of arsenopyrite and pyrite veins with evident scorodite. The early 1990's trenching campaign occurred nearby, 200 metres south of the Raven discovery trench. The older trenches did not reach bedrock, due to depth of overburden and limited size of heavy equipment. However, trench samples did return anomalous gold values (Doherty, 1996). After the Raven discovery, soil sample assays from the 2018 soil program were received and indicated a large (1.5 x 0.5 kilometre) Au-As anomaly over the Raven Zone extending several hundred metres from the initial discovery trench.

Three holes were drilled in 2018 proximal to the discovery trench. This was followed up with a small 1,616 metre ("m") drill campaign in 2019, a large 5,438m trench program and 3,018 geochemical soil sampling survey over the area. In 2020, a larger 7,452m drilling program was completed further extending the prospect 600 metres along strike to the east – coincident with 1,958m of surface trenches and a 3,808 geochemical soil sample program. In 2021, 8,063m were drilled, along with an additional 600m of targeted surface trenches.

1.4 Geology and Mineralization

The Raven Deposit is located at the contact zone at the extreme south-eastern portion of the Nugget Stock. The area is underlain by the Devonian to Mississippian age Earn Group and the Early Carboniferous age Keno Hill Quartzite that have been subjected to greenschist facies metamorphism, folding, and thrusting (Gordey and Makepeace, 2003). The Raven target is interpreted to be hosted in a dilatational fracture zone within the Nugget Stock, in close association with the intrusion-metasediment contact.

The Raven target was discovered in 2018 during an evaluation of the Nugget Stock. Soil samples over the Raven target area returned coincident arsenic - bismuth - gold anomalies. Follow up trenches uncovered mineralization at surface with initial trench results consisting of 3.51 g/t gold over 124 metres. Subsequent drilling (2018, 2019, 2020, and 2021) outlined the mineralization for 770 metres along strike and is open at depth and to the East and West.

Mineralization consists of arsenopyrite-dominant polymetallic veins. The veins and vein sets are remarkably consistent across Raven and preliminary mapping suggests these mineralized veins occur with steep to moderate dips (~60o) to the north along a west to southwest strike. Intense shearing deforms the vein sets along a roughly east-west orientation, representing a structurally related mineralized corridor within which mineralization remains open along strike in both directions and in particular down dip. Sulphides are dominantly found in the vein material and occur in the centre, on the margin, and disseminated throughout

the veins. The most common sulphide minerals present in the Raven massive sulphide veins are: arsenopyrite, pyrite, galena, sphalerite, molybdenite, pyrrhotite, chalcopyrite, and bismuthinite. Sericite is the dominant mineral in alteration envelopes which can be found pervasively throughout the core within the Raven Mineralized Corridor or can be restricted to narrow vein selvedges. Iron oxidation alteration is generally restricted to major structures and mineralized vein selvedges, although alteration zones of this type can also occur in drill core with no direct relation to veins – where it is assumed that additional veins are nearby but were not intersected in the drill core. Gold mineralization also occurs within the metasedimentary rock package immediately adjacent to the granodiorite. Multiple phases of mineralization at Raven have been identified through overprinting of mineralization and mineralized structures, an indication of repeated re-activation of the veins over a period of protracted intrusive events.

A major focus of Victoria's future exploration plans will be to evaluate the entirety of the Nugget Stock for Eagle-style deposits while continuing to expand the high-grade footprint of Raven.

1.5 Mineral Resource Estimate

This Report presents the first mineral resource estimate ("MRE") of the Raven Deposit. The drill hole database utilized for this MRE utilizes 78 diamond drill holes collared between August 2018 and September 2021 and is comprised of 11,956 assays from 18,217 m of drilling. Additionally, 55 surface trenches with 3,464 assays and 7,443m of sampling were included in establishing the MRE.

A geologic model comprised of four mineralized domains was interpreted by Victoria's exploration team. These wireframed entities represent the Massive Sulphide Veins ("MSV") and the Lower Grade ("LG") domains above 0.2 g/t Au, 0.6 g/t Au and 4.0 g/t Au, respectively. The MSV domain was modeled based on the interpretation and measurements of veins identified in drill holes and surface exposures, structural measurements from oriented core and surface trenches, as well as high-grade gold analytical values.

Original Au assays were composited to 1.3m as it is the most common sampling length within the MSV and LG domains. Overall, 19,757 composites were generated with 1,591 composites within the MSV unit, 3,273 composites within the Lower Grade ("LG") unit above 0.2 g/t Au, 3,709 composites within the LG unit above 0.6 g/t, and 491 composites within the LG unit above 4.0 g/t Au.

The high-grade gold outliers of the 1.3m composites were capped to 25.0 g/t Au for the MSV, 5.0 g/t Au for the LG > 0.2 g/t Au domain, 6.0 g/t Au for the LG > 0.6 g/t Au domain, and 21.0 g/t Au for the LG > 4.0 g/t Au domain. Statistics conducted on the capped composites showed lognormal distributions with reasonably well-behaved gold grade distributions.

The spatial continuity of the gold grades was examined with a variographic study. Results showed main orientations of gold grade continuity along the strike of the deposit oriented approximately east-west and along the dip of the deposit at a 65° towards north. Ranges of gold grade continuity for the MSV were approximately 60m along strike and 44m down dip, while for the LG zone they were approximately 50m along strike and 40m down dip.

Gold grade estimates were estimated with an ordinary kriging technique, within each of the four mineralized domains which were each treated as hard boundary domains, into an orthogonal block model. The block model was discretized on 5.0m x 5.0m x 5.0m parent blocks and sub-blocked to 0.5m x 0.5m x 0.5m blocks. A minimum of 2 and maximum of 12 samples were used to calculate a grade estimate for each block. A two-pass estimation approach was used with the first pass having a search ellipsoid oriented and dimensioned to the second range of the variograms and the second pass having a search ellipsoid dimensioned to twice the second range of the variograms.

The mineral resource was classified as Inferred. The tonnage was calculated with a specific gravity value of 4.50 for the MSV and of 2.65 for the other LG domains. The mineral resource was constrained within a pit shell optimized from a Lerchs-Grossman algorithm with the following parameters: US$ 1,700/oz Au, US$

1.50/t mining, US$ 2.00/t processing, US$ 2.50/t G&A, 90% recovery and a 45° pit slope. The pit-constrained inferred mineral resource estimate of the Raven Gold Deposit is presented in Table 1-1.

Table 1-1: Pit-Constrained Inferred Mineral Resources at a 0.50 g/t Au Cut-Off - Effective September 15, 2022 – Raven Gold Deposit

Au Cut-Off g/t	Tonnage tonnes	Avg Au Grade g/t	Au Content oz
0.30	27,254,472	1.32	1,160,157
0.35	24,604,552	1.43	1,132,790
0.40	22,874,757	1.51	1,111,986
0.45	21,308,166	1.59	1,090,637
0.50	**19,956,934**	**1.67**	**1,070,239**
0.55	18,894,809	1.73	1,052,159
0.60	17,635,639	1.82	1,029,103
0.65	15,479,632	1.98	985,410
0.70	14,437,186	2.07	962,681

Notes:

1. The effective date for the Mineral Resource is September 15, 2022.
2. Mineral Resources which are not Mineral Reserves do not have demonstrated economic viability. The estimate of Mineral Resources may be materially affected by environmental, permitting, legal, title, taxation, sociopolitical, marketing, or other relevant issues.
3. The CIM definitions were followed for classification of Mineral Resources. The quantity and grade of reported inferred Mineral Resources in this estimation are uncertain in nature and there has been insufficient exploration to define these inferred Mineral Resources as an indicated Mineral Resource and it is uncertain if further exploration will result in upgrading them to an indicated or measured Mineral Resource category.
4. Mineral Resources are reported at a cut-off grade of 0.50 g/t Au, within a Lerchs-Grossman pit shell using a gold price of US$1,700/ounce and a US$/CAN$ exchange rate of 0.75.

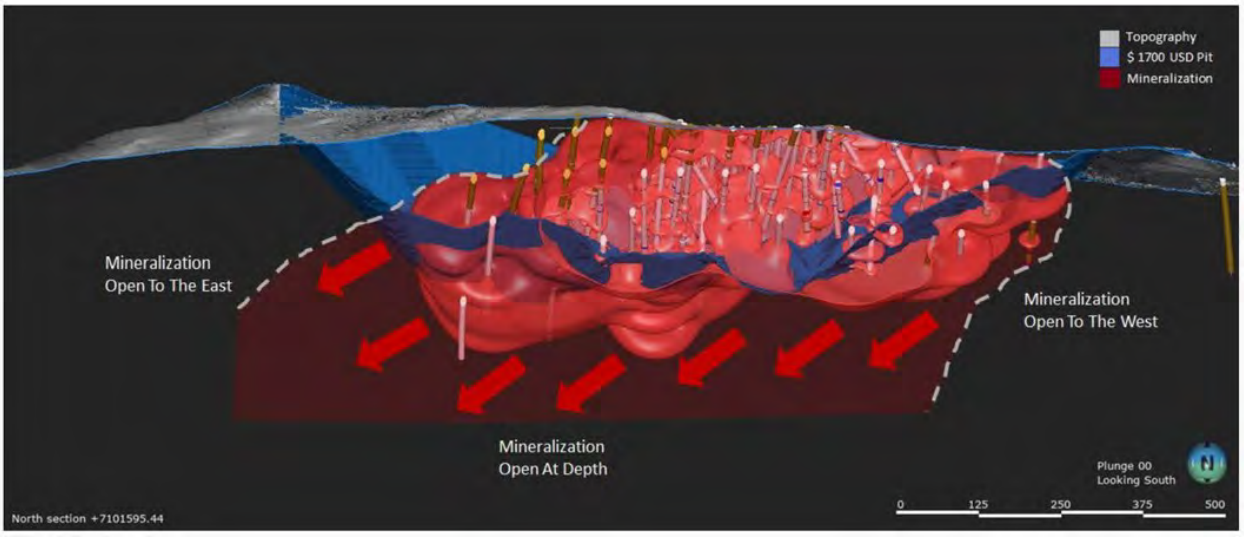

Figure 1-1: Schematic Display of the Raven Deposit Mineralization within the Resource Pit

Source: Victoria Gold Corp. (2022)

1.6 Conclusions and Recommendations

The Raven Deposit is 100% owned by Victoria. Raven represents a potentially high-grade, on-surface gold deposit that lies in the extreme southeast contact of the Nugget Intrusive Stock within the surrounding Earn Group metasedimentary package. This large, approximately 3 kilometres by 2 kilometres, medium to coarse grained granodiorite stock of Cretaceous age represents the second largest intrusive body on the Dublin Gulch property (second only to the Dublin Gulch Stock that hosts the Eagle Gold Mine). The Nugget Stock is highly prospective to host Eagle-style sheeted vein mineralization, and the vast majority of the greater than five (5) square kilometre stock remains untested.

Diamond drilling, soil sampling, and extensive surface trench construction/mapping/sampling have been conducted on the Nugget Stock with a primary focus on the Raven Deposit throughout each of 2018, 2019, 2020, and 2021 field seasons. The totals for these respective exploration activities are summarized below in Table 1-2.

The results of diamond drilling to date show that the Raven Deposit mineralization defined by the resource model Figure 1-1 is open for expansion in all directions, as well as depth. There is a strong indication that Raven mineralization can be expanded with further definition drilling and exploration.

A two (2) phase $35,000,000 exploration program is recommended for the Raven Project. Phase I will expand the Raven resource and consist of: 25,000 m of step-out drilling down-dip and along strike at the Raven Zone and the collection and testing of Raven mineralization for metallurgical testing; Phase II will upgrade the Raven resource from inferred to indicated and consist of: 25,000 m of in-fill drilling and additional metallurgical testing at the Raven Zone (Details in Section 26).

Table 1-2: Victoria Gold's Raven Deposit Exploration Work Summary

	Drilling		Trenches		Soil Samples
Year	**Meterage**	**Count**	**Meterage**	**Count**	**Count**
2018	1,754.90	9	1,447.00	13	2,448
2019	1,616.80	9	5,438.00	37	3,018
2020	7,452.60	31	558.00	5	3,808
2021	7,393.10	29	-	-	-
Total	**18,217.40**	**78**	**7,443.00**	**55**	**9,274**

Source: Victoria Gold Corp. (2022)

2 INTRODUCTION

2.1 Issuer

This report is produced for Victoria Gold Corp., a Canadian public company engaged in the business of production, development and exploration of precious metals, listed on the TSX with trading symbol - VGCX.

Marc Jutras (QP) is responsible for and has reviewed all Sections of this Technical Report. Marc Jutras has prepared the mineral resource estimates of Section 14 and has supervised the preparation of all other Sections of the Technical Report.

The Company has a 100% ownership of the Raven Deposit (“the Project”) in central Yukon.

2.2 Terms of Reference

The author was contracted by Victoria Gold to prepare this National Instrument 43-101 ("NI 43-101") Technical Report to be filed with the Toronto Stock Exchange (TSX) and the Canadian System for Electronic Document Analysis and Retrieval (SEDAR).

This report was produced for the purpose of supplying exploration information, a mineral resource estimate, and recommendations for further work. The report was written following disclosure and reporting guidance set forth in the Canadian Securities Administrations’ current “Standards of Disclosure for Mineral Projects” under provisions of National Instrument 43-101, Companion Policy 43-101 CP and Form 43-101 F1. It is a compilation of publicly available assessment reports filed with the Yukon Mining Recorder for mineral claim tenure credit, unpublished internal company reports, and property data provided by Victoria Gold Corp; supplemented by publicly-available government maps and scientific publications. The supporting documents are referenced in appropriate sections of this report.

2.3 Source of Information

The data used in the resource estimation and the development of this report was provided to the author by Victoria Gold Corp. and Ginto Consulting. Some information including the property history and regional and property geology has been sourced from previous publicly available technical assessment reports and revised or updated as required. References for information used are contained in Section 27.

2.4 Summary of Qualified Persons

The author wishes to make clear that they are a qualified person only in areas of this Report where they are identified by a “Certificate of Qualified Person”. Table 2-1 outlines the Qualified Person(s) responsible for the corresponding sections of this Report.

2.5 Site Visits

Marc Jutras, P. Eng., M.A.Sc., Principal, Ginto Consulting Inc., is an independent Qualified Person in accordance with the requirements of NI 43-101. He is independent of Victoria Gold, and the Raven Project. He has no interest in the companies, in the Property, or in any claims in the vicinity of the Property. Ginto visited the Property in 2018, 2019, and 2021. Ginto examined several core holes, drill logs and assay

certificates. Assays were examined against drill core mineralized zones. Ginto inspected the offices, core logging facilities/sampling procedures and core security. Ginto participated in a field tour of the Project geology conducted by Victoria Gold employees Paul D. Gray, P.Geo. (Vice President Technical Services) and Helena Kuikka, P.Geo. (Vice President Exploration).

Table 2-1: Qualified Persons and Areas of Responsibilities

Section	Description	Qualified Person(s)	Comments and Exceptions
1	Summary	Ginto	
2	Introduction	Ginto	
3	Reliance on Other Experts	Ginto	
4	Property Description and Location	Ginto	
5	Accessibility, Climate, Local Resources, Infrastructure, and Physiography	Ginto	
6	History	Ginto	
7	Geological Settings and Mineralization	Ginto	
8	Deposit Types	Ginto	
9	Exploration	Ginto	
10	Drilling	Ginto	
11	Sample Preparation, Analysis and Security	Ginto	
12	Data Verification	Ginto	
13	Mineral Processing and Metallurgical Testing	N/A	
14	Mineral Resource Estimate	Ginto	
15	Mineral Reserve Estimate	N/A	
16	Mining Methods	N/A	
17	Recovery Methods	N/A	
18	Property Infrastructure	N/A	
19	Market Studies and Contracts	N/A	
20	Environmental Studies, Permitting, and Social or Community Impact	Ginto	
21	Capital and Operating Costs	N/A	
22	Economic Analysis	N/A	
23	Adjacent Properties	Ginto	
24	Other Relevant Data and Information	Ginto	
25	Interpretations and Conclusions	Ginto	
26	Recommendations	Ginto	
27	References	Ginto	

2.6 Units of Measure and Abbreviations

Units of measure are metric. Assays and analytical results for precious metals are quoted in parts per million (ppm) and parts per billion (ppb). Parts per million are also commonly referred to as grams per tonne (g/t) in respect to gold and silver analytical results. Gold endowment may be referred to as ounces (oz.) as per

industry common practice. Assays and analytical results for base metals are also reported in percent (%). Temperature readings are reported in degrees Celsius (°C). Lengths are quoted in kilometres (km), metres (m) or millimetres (mm). Density measurements are reported in tonnes per cubic metre (t/m^3). All costs are in Canadian dollars (C$ or $) unless otherwise noted. A listing of abbreviations and acronyms can be found in Section 28.

3 RELIANCE ON OTHER EXPERTS

The Author relied on information from reports prepared by or for Victoria which detail surface and drill results and resource calculations, as well as other historical reports regarding the Property and Project. Victoria Gold also maintains a library of historical internal company reports that are not in the public domain. The Author has reviewed this material and believes that the relevant data has been collected in a careful and conscientious manner and in accordance with the standards set out in NI 43-101; and when data collection precedes the implementation of NI 43-101, that it was collected in accordance with contemporary industry standards.

Mineral claim information was provided by the office of the Yukon Mining Recorder via its interactive web site. Approximate claim locations shown on government claim maps and referred to on maps that accompany this Technical Report have not been verified by accurate surveys.

Information concerning claim status and ownership which are presented in Section 4 below, have been provided to the Author by Victoria and have not been independently verified by the Author. However, the Author has no reason to doubt that the title situation is other than what is presented here.

4 PROPERTY DESCRIPTION AND LOCATION

The Raven Project is located on the eastern portion of the Dublin Gulch claim block on the South East corner of the Nugget Stock (Figure 4-1) and within the Traditional Territory of the First Nation of Na-Cho Nyak Dun (FNNND). The Project area is accessible via an exploration access road 26km from the Eagle Gold Mine (Figure 4-2). Access to the area was first constructed in 2018, prior to that the Project was accessible via walking or helicopter only. A seasonal 14 sleeper tent camp, including office tent, first aid tent, kitchen, two weather haven tents and a dining room was constructed and commissioned in 2019 by Victoria, and opened again in early July 2020. A second core shack and new double cut shack was built in 2020 to increase drill core processing capacity. Groceries and supplies are brought in via Victoria and or bonded expeditors through the Eagle Mine. Road access and camp upgrades have improved steadily throughout 2021 commiserate with drilling production increase.

The centre of the Project is at approximately; UTM Coordinates 7,101,613N / 473,605E, Zone 8, North American Datum (NAD) 83.

4.1 Property Holdings

The Raven Project is located on the eastern portion of the Dublin Gulch claim block, which is a block of 1,914 quartz claims, 10 quartz leases, and one federal crown grant (Figure 4-3). All of the Dublin Gulch mineral titles are held by Victoria Gold (Yukon) Corp., a wholly owned-directly held subsidiary of Victoria Gold. The Dublin Gulch property is rectangular in shape and is approximately 35,000 ha.

A list of the claims, leases and grant that comprise the Dublin Gulch property are provided in Appendix 5 and are shown in Figure 4-3.

The primary legislation governing mining in Yukon is the Quartz Mining Act (QMA) and the Quartz Mining Land Use Regulations. The regulatory body charged with overseeing the QMA is the Department of Energy, Mines and Resources (EMR).

Ownership of quartz claims pursuant to the QMA carries the right to surface access and use for the exploitation of minerals contained within the claims. A claim holder must however make an application to the Minister of EMR to engage in development or production activities and may only conduct these activities in accordance with the terms and conditions of a license issued by the Minister. The license issued by the Minister is a Quartz Mining License (QML) which specifies the duration, activities, and claims, among other matters, that a licensee and claim holder must adhere to and operate within.

The permitting required for Property is discussed further in (Section 20).

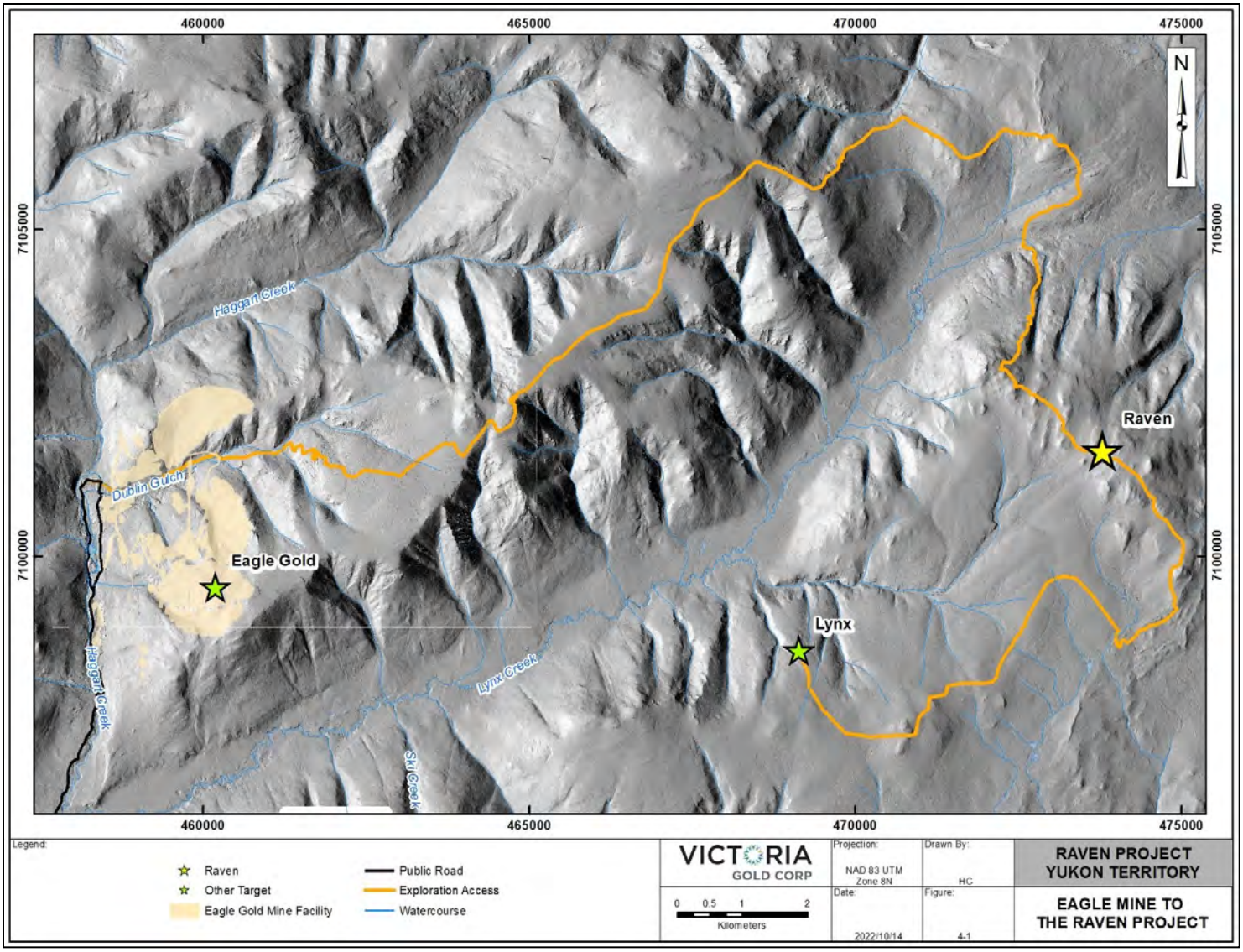

Figure 4-1: Eagle Mine to the Raven Project

Source: Victoria Gold Corp. (2022)

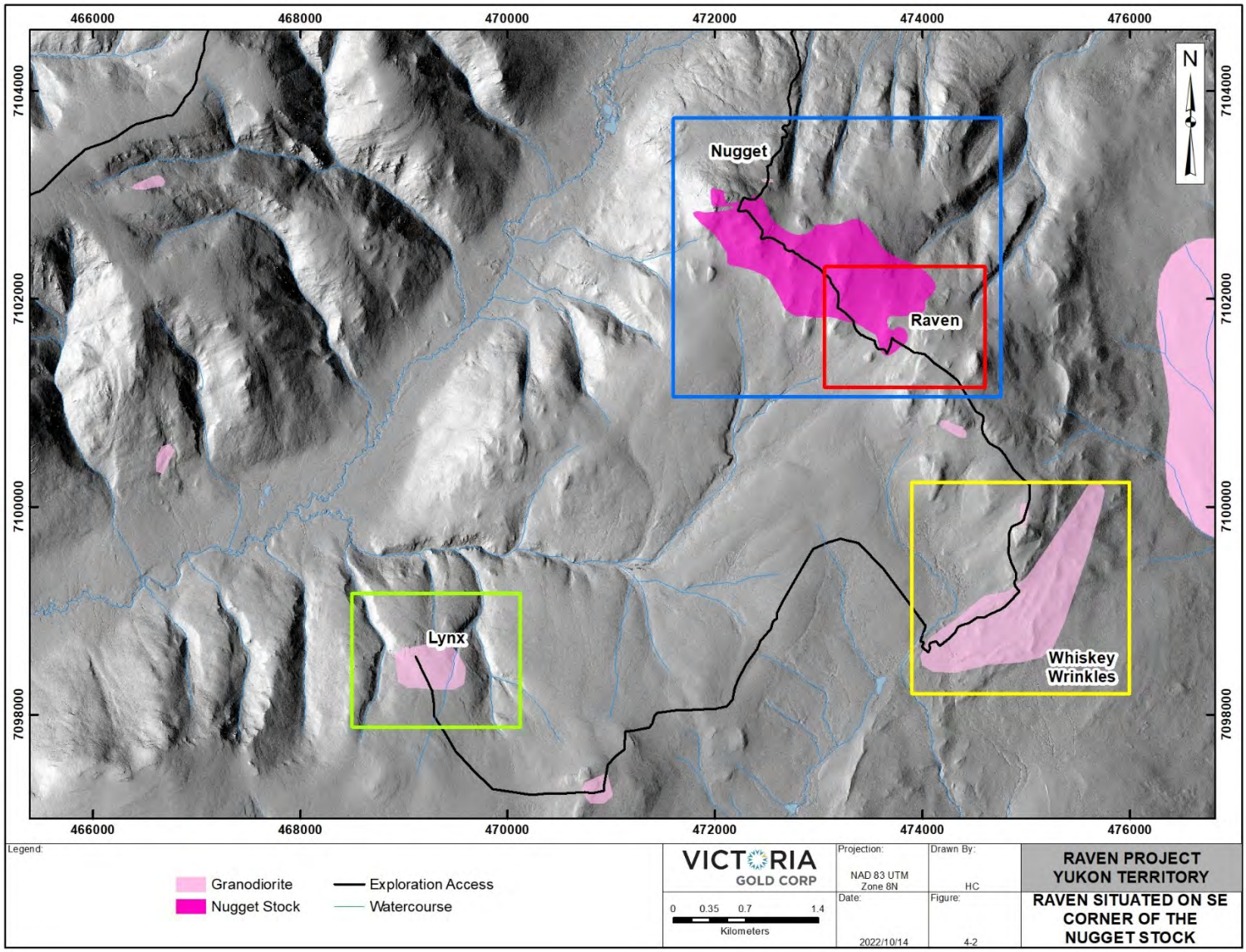

Figure 4-2: Raven Project Location within the Eastern Portion of the Dublin Gulch Claim Block

Source: Victoria Gold Corp. (2022)

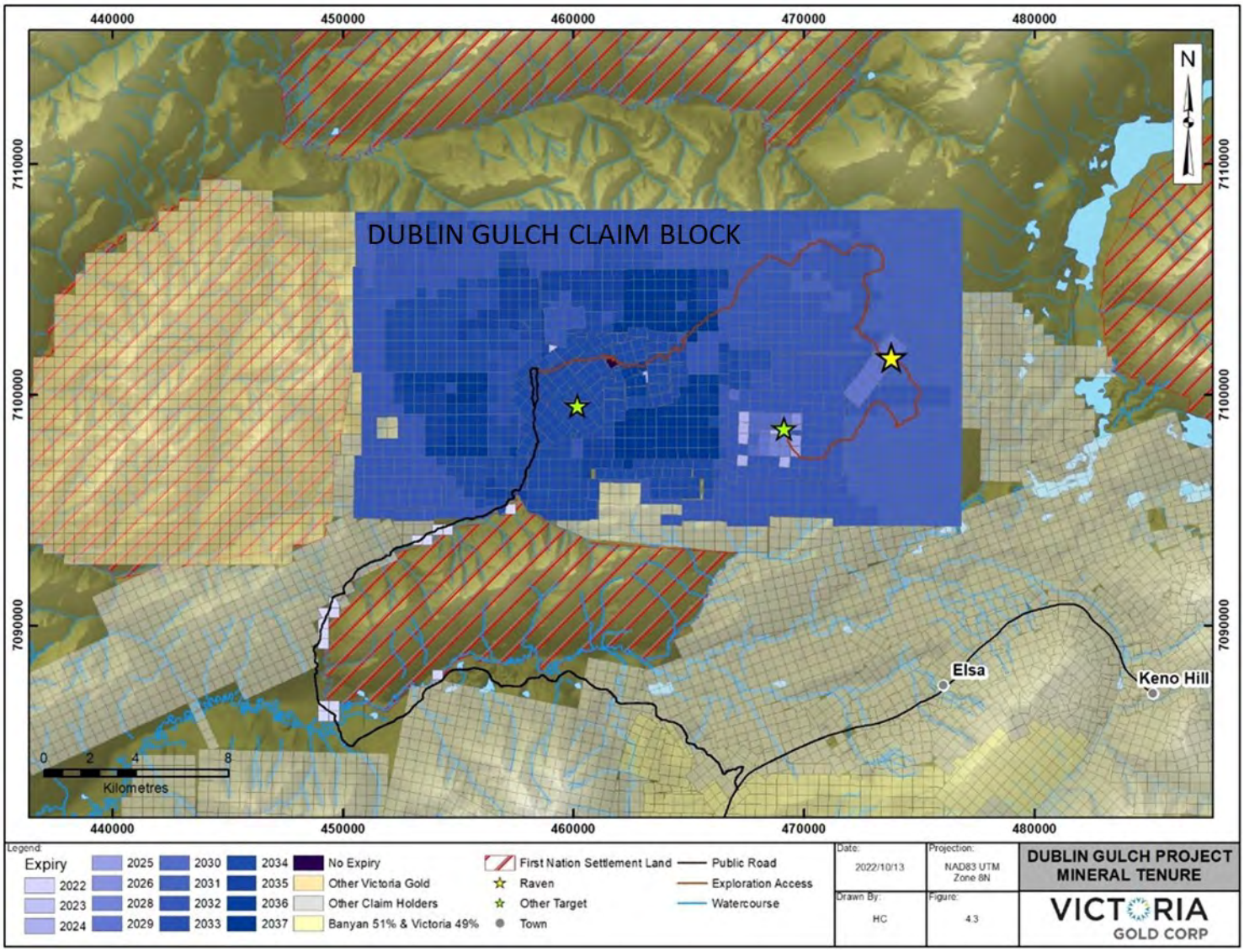

Figure 4-3: Mineral Tenure Map

Source: Victoria Gold Corp. (2022)

4.2 Property Agreements

The mineral claims which comprise the Raven Deposit are 100% owned by Victoria Gold Corp. and are not subject to underlying property agreements.

4.2.1 Raven Property

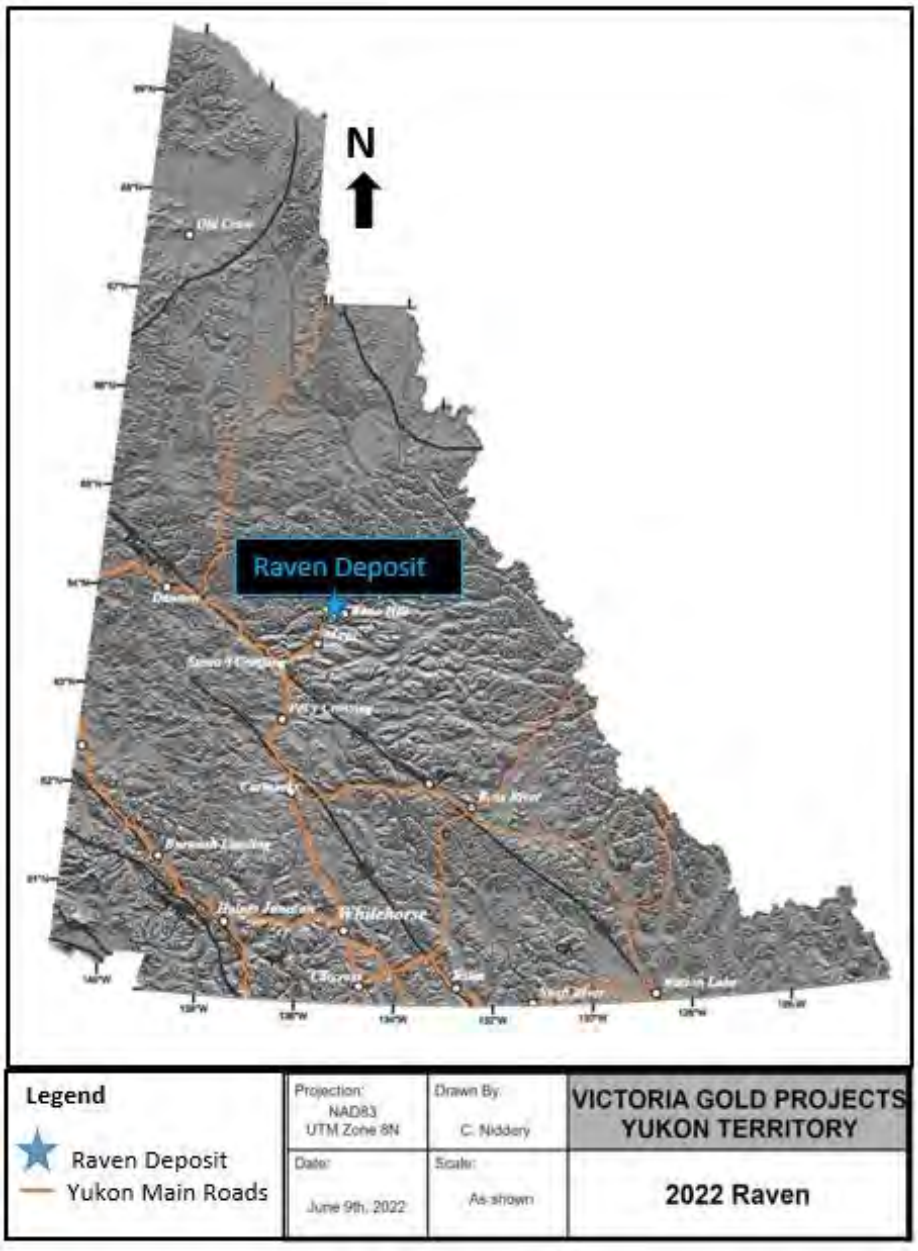

Figure 4-4: Yukon-Scale Project Location Map

Source: Victoria Gold Corp. (2022)

4.3 Land Use and Environmental

Ownership of Quartz claims in Yukon confers rights to mineral tenure, whereas surface rights are held by the Crown in favour of Yukon Territory. A Quartz Mining Land Use Approval (MLUA) is required to conduct exploration in Yukon. Activities on the property have been conducted under a current Class IV MLUA, approval number LQ00562. The permit is in good standing. The expiry date of this permit is January 18th, 2032. All contemplated exploration activities will have to be in compliance with terms and conditions set out in LQ00562. LQ00562 required Victoria to post financial security in the amount of $326,821 to cover any outstanding, or contemplated, exploration work on the Property. As of the date of this Report, the security has been posted by Victoria. There are no known environmental liabilities related to the Raven Deposit. Reclamation of drill sites and exploration work is done progressively, generally in or within the year the work is done, and the company files pre-season plans describing the general scope of work intended to be completed at each season. At the close of each year the company files post season reports detailing the actual activity undertaken and providing digital location files. At present, liability would be limited to minor reclamation (trails, trenches, and drill pads), monitoring revegetation and removal of equipment and camps.

Temporary exploration camps relevant to the Raven Deposit work have been established for by Victoria Gold and are named the Nugget and Lynx camps. The Nugget camp is comprised of canvas wall-tents, wooden outhouses, first-aid/office weather havens, core logging and sampling facilities, and is located approximately 15kms east from the Eagle Gold Mine. The Lynx camp (5km by exploration road and south west of Nugget) also has a smaller, similar set-up.

Raven's drill core has and will be stored at a large laydown at the Nugget Camp Figure 11-1.

Trenches, drill sites, and temporary access trails are reclaimed on an ongoing process. Trenches and roads, whether historical or constructed under the current MLUA, that cannot be reclaimed immediately are left in a condition that is stable and unlikely to lead to ongoing erosional issues.

Petroleum products are stored on the Project in compliance with terms of the MLUA. All petroleum products and storage containers for petroleum products are required to be removed from the site prior to the expiry of the current MLUA or any extension to the MLUA.

5 ACCESSIBILITY, CLIMATE, LOCAL RESOURCES INFRASTRUCTURE AND PHYSIOGRAPHY

5.1 Accessibility

The Raven Deposit lies approximately 15 km from Victoria's producing Eagle Gold Mine (straight-line). The Eagle Gold Mine, is approximately 90 km from the community of Mayo which in turn is 450km north of the Yukon's capital, Whitehorse, with year-round access via the Yukon Robert Campbell Highway. From Mayo, well developed year-round access via the Silver Trail (Yukon Highway 11) onto the Eagle Gold Mine access road which consists of; the South McQuesten Road (SMR) and the Haggart Creek Road (HCR) which terminates at the Project site. Together the SMR and the HCR comprise a 45 km road divided by the South McQuesten River. The first 23 km of the Eagle Mine Access Road is regulated and maintained under the Yukon Highways Act; however, the SMR is only maintained during the summer by the Yukon Government Department of Highways and Public Works (HPW), whereas the HCR is considered a "public unmaintained" road which is maintained by Victoria whom conduct snow clearing activities on both the SMR and HCR on an as needed basis and general maintenance on the HCR under the authority of permits granted by HPW.

The Raven Project has road access from the Eagle Gold Mine available for year-round service; however, is normally operated in the seasonal months of April-October in support of exploration activities.

5.2 Local Resources and Infrastructure

Mayo has a population of approximately 450 persons and offers accommodation, fuel, a nursing station, and earthmoving contractors. The Yukon Government maintains a 1,400 m gravel airstrip about 3 km north of Mayo, that has been certified by Transport Canada, and supports service by air carriers. The Project is about 60 km straight-line distance north-northeast of Mayo. Most major services and supplies are available in Whitehorse.

The Eagle Gold Mine is currently connected to the Yukon Energy Corporation electrical grid. All major facilities required by the Mine are operating on grid power. The YEC operates Three-Phase 69Kv power lines from Mayo to Elsa and Keno City – these power lines are within 6km of the Raven Deposit.

A broader range of services are available in Whitehorse, Yukon, located about six and a half hours by road to the south of the Project. Whitehorse has a population of 31,913 (Yukon Bureau of Statistics) and has regularly scheduled air service to Vancouver, Edmonton, Calgary, and Fairbanks.

An important part of Victoria's exploration program related to the Project was the establishment of infrastructure, which includes; a vehicular accessible trail, two (2) permitted - 25-person camps (Lynx – 10 sleeper tents and Nugget -15 sleeper tents), three (3) core processing shacks (one core shack at Lynx), three (3) core cutting shacks (one cut shack at Lynx), and one (1); kitchen, common room, and medical tent at each camp (weather havens). Both camps are powered by portable generators (Figure 5-1 and Figure 5-2).

There is cellular phone service at the Raven Deposit and at the Nugget and Lynx Camps.

Figure 5-1: Nugget Camp 2021

Source: Victoria Gold Corp. (2021)

Figure 5-2: Lynx Camp 2021

Source: Victoria Gold Corp. (2021)

Figure 5-3: Landscape and General Area of the Raven Deposit in 2021

Source: Victoria Gold Corp. (2021)

5.3 Climate

Climate studies have been conducted to support the Eagle Gold Mine. The findings of these studies are considered directly relevant to the Project given its proximity to the Mine. The Property area is characterized by a “continental” type climate with moderate annual precipitation and a large temperature range. Summers are short and can be hot, while winters are long and cold with moderate snowfall. Rainstorm events can occur frequently during the summer and may contribute between 30 to 40% of the annual precipitation. Higher elevations are snow-free by mid-June. Frost action may occur at any time during the summer or fall.

Monitoring data for the Property is based on two on-site climate stations located in the vicinity of the Eagle Mine. Local snow course surveys and regional data which have been extensively analyzed and the information below is briefly summarized from the climate report prepared for Victoria in Lorax (2021).

Air temperatures at the Eagle Gold Mine area, and thus comparable to the Project, are consistent with those throughout the Yukon interior. Mean annual air temperature is -3.7°C at the Eagle Mine Camp climate station (782 masl) and -3.6°C at the Potato Hills climate station (1,420 masl) over their respective periods of record. At the Eagle Gold Mine Camp station, monthly average temperature ranges from -20.0°C in January to 13.3°C in July, and -15.3°C to 10.9°C at the Potato Hills station, for the same months.

Generally, precipitation falls as snow from November through March, with precipitation falling as a mix of rain and snow in April and October. Annual average rainfall is 211 mm and 255 mm for the Eagle Mine Camp and Potato Hills stations respectively for their periods of record.

Snow depth and snow water equivalent, barometric pressure, relative humidity, wind speed and direction, and solar radiation are also measured by the site climate stations.

5.4 Physiography

The topography of the Property area is characterized by rolling hills and plateaus ranging in elevation from approximately 800 masl to a local maximum of 1,650 masl at the summit of Potato Hills and is drained by deeply incised creeks and canyons. The ground surface is covered by residual soil and felsenmeer. Outcrops are rare, comprising generally less than two percent of the surface area, and are limited to ridge tops and creek walls.

Lower elevations are vegetated with black spruce, willow, alder and moss, and higher elevations by subalpine vegetation.

6 HISTORY

In 1949, a reported piece of float containing galena was discovered near what is now the Lynx property (Aho and Tempelman-Kluit,1963)., The area remained unstaked until October,1962 when it was staked by the Titan Project Joint Venture (Noranda Mines Ltd, Canex Aerial Exploration Ltd, Homestake Explorations Ltd, and Kerr Addison Gold Mines Ltd). This area was later prospected and mapped for silver related mineralization in 1963 (Doherty and Dudka,1994)

In 1964, the Geological Survey of Canada's Operation Keno conducted regional geochemical data and following its release in June, 1965, it was re-staked by United Keno Hill Mines Ltd. These claims were prospected and soil sampled, for base metals and silver mineralization later in that same year (Doherty and Dudka,1994)

No work was conducted until March of 1969, when it was re-staked again by United Keno Hill Mines Ltd, where they continued mapping and geochemical sampling with a target for discovery of base metal and silver mineralization in both 1969 and 1970 (Van Tassel, 1970).

In July of 1971, Archer, Cathro and Associates staked the Gwaihir claims over what is now the western part of the Nugget Stock. Amax of Canada Ltd later re-staked the claims in April, 1979 and performed mapping and a trenching program focusing on the tungsten mineralization in the area. (Kidlark, 1980).

Amax re-staked again in August, 1991 as the Tag claims. HRC Development Corporation performed a geological and geochemical survey on the Tag claims in 1992, and added further claims in July, 1993. The Tag claims were staked to explore for type intrusion-hosted gold mineralization after the discovery of the Fort Knox deposit in Alaska. Amax prospected and soil sampled in August, 1993. In July, 1994 HRC carried out further prospecting and rock and soil sampling on the claims. In 1995, HRC trenched and sampled over the soil sample anomalies identified in 1994. In March 1997, HRC staked the East and South of the Tag claims and conducted a drilling program consisting of 6 diamond drill holes along strike of previously identified gold mineralization on the Lynx property (Keyser, 1997).

In July 2002, Expatriate Resources Ltd., acquired the Lynx Property from Janet Dickson. Expatriate Resources Ltd., subsequent spun out StrataGold Corporation (now known as Victoria Gold (Yukon) Corp.) with several different mineral exploration properties which included the Lynx Property. In 2004, StrataGold conducted a large staking program around the Lynx Property, which included a portion of the Raven Project area. This staking program essentially encircled the Eagle Gold Zone and Wolf Tungsten Deposit that were owned by Sterlite. In October 2004, StrataGold Corporation purchased mineral claims, including the Dublin Gulch (i.e., the Eagle Gold Zone) and Clear Creek gold properties from Sterlite and conducted a drilling program which consisted of 14 diamond drillholes totaling 2,069m focusing on the Lynx property (Hladky, 2004). In June 2009, through a Plan of Arrangement, StrataGold was acquired by Victoria Gold. In March 2010, Victoria Gold acquired the Hla Hla and Neera claims (which had been staked in 2003) by way of a purchase agreement from the estate of John Peter Ross. The Hla Hla and Neera claims are within the Raven Project area.

Sporadic and limited (largely reconnaissance and surface mapping) activities were conducted by Victoria over the general Nugget Stock area in 2009/10/11. This limited mapping, combined with the geological map of the area produced by United Keno Hill Mines in the 1960's - indicated that there were large quartz boulders with minor sulphides scattered around the eastern portion of the Nugget Stock. An access trail linking the Nugget Stock and Raven with the Eagle Gold Mine was designed and constructed starting in 2017 – with final access completed in late 2018. Initial prospecting in 2018 at Raven found arsenopyrite and pyrite occurring along fractures within the quartz veins as well as thin sulphide veins within the granodiorite boulders at surface with a notable increase in oxidation profile than in other parts of the Nugget Stock.

A 152m trench was placed along a prominent north-south oriented ridge which extended through the southern contact of the Nugget Stock. The north-south orientation was used to increase the possibility of uncovering veins of an east-west orientation which is the prominent mineralization orientation in the district – as per the Potato Hills Mineralization Model developed internally by Victoria. Trench (TR18-33) uncovered a wide mineralized shear zone under less than a meter of overburden. The mineralization intersected from these surface trenches consists of primarily arsenopyrite and pyrite veins with evident scorodite. After the Raven discovery, soil sample assays from the 2018 soil program were received and indicated a large Au-As anomaly over the Raven Zone extending several hundred meters from the initial discovery trench.

7 GEOLOGICAL SETTING AND MINERALIZATION

7.1 Geological Setting

The Nugget stock is a mid-Cretaceous (98-million-year-old), medium to coarse grained granodiorite stock and occurs on the eastern side of the Lynx Creek valley (Stevens et al. 1982). The area is underlain by the Devonian to Mississippian age Earn Group and the Early Carboniferous age Keno Hill Quartzites which have undergone regional greenschist facies metamorphism, folding, and thrusting (Gordey and Makepeace, 2003). Mineralization is hosted in a shear zone corridor within the granitic intrusive bodies, in close association with the intrusion-metasediments contact.

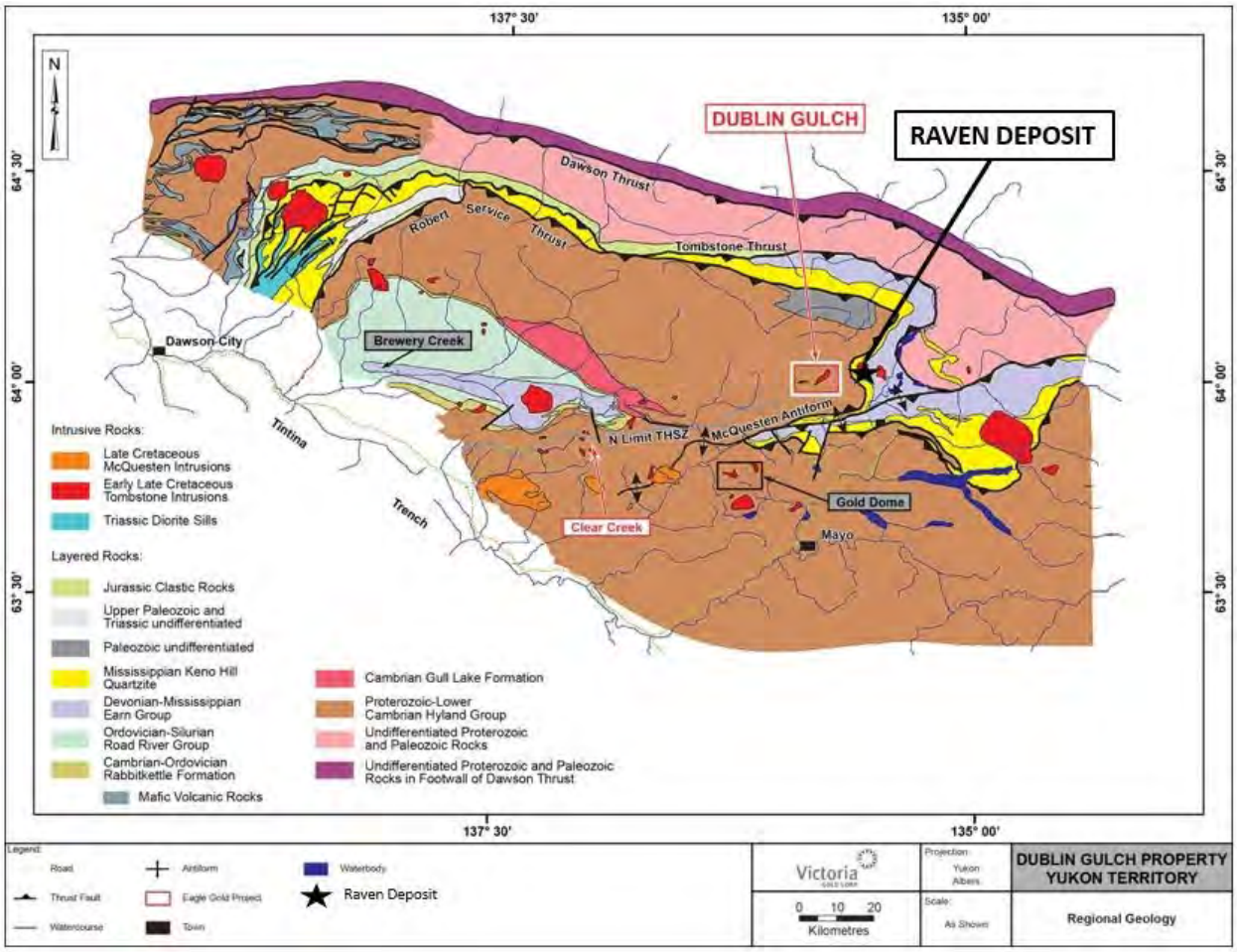

Figure 7-1: Regional Geology Map of Raven and Adjacent Deposits

Source: Modified from Scott Wilson Mining (2010)

7.2 Property Geology

7.2.1 Lithology

The dominant lithological type in Raven is granodiorite - it hosts the majority of the massive sulphide mineralized veins identified to date at Raven and accommodates major structures. These intrusive lithologies intruded a metasedimentary host rock, and these metasediments form a cap on the top of the intrusion in the Raven area, which here are interpreted to have been thrust, at low angles, on top of the intrusive. These structural contacts are interpreted to overprint the intrusive contact. Metasediments rarely host massive mineralized veins. Greenstone also appears sparsely throughout the property. Elemental concentrations and ratios are strongly characteristic of these lithologies (Zr, Y, Ti, Sr, Sc, S, P, Mg, Li, La, Cr, Co, Ni, Fe, and Ca; respectively) and have been used for preliminary geological mapping of intrusion (granodiorite), metasediments, and greenstone in unmapped areas. Lithology types can be correlated across Raven drill holes as shown in Figure 7-3.

Intrusion (Granodiorite – GND) - common to see; light orange weathering (ox) or medium grey fresh (no alt), medium to coarse grained granitoid intrusion with 30% light grey, medium to coarse grained, anhedral to subhedral quartz, 40% white medium to coarse grained, subhedral to euhedral feldspar, 30% dark brown-green, medium to coarse grained, euhedral biotite. Intrusion is weakly folded, non-foliated, non-magnetic, often with a vigorous reaction with HCl; commonly present are 1-2% white, very coarse grained, euhedral feldspar phenocrysts. Common carbonate alteration along microfractures in intrusion.

Metasediments (MSEDS) - dark brown weathering, dark grey-light green fresh, banded at mm-10's cm scale, alternating beds and laminae of very fine-grained silicate, calc silicate and carbonate metasedimentary units; brown-pink metasediments are slightly magnetic and can contain fine grained pyrrhotite; dark green bands are composed of fine-grained chlorite and actinolite; common are cm scale quartz lenses subparallel with beds and laminae; metasediments are variably foliated.

Greenstone (GNST) - dark brown-green weathering, dark green-grey fresh, foliated, fine grained dioritic to gabbroic intrusion with 85% dark green very fine-grained groundmass of chlorite after pyroxene or hornblende and 15% white to light grey, fine grained, subhedral feldspar or quartz crystals, forming whitish streaks in the groundmass that accentuate foliated structure; non-magnetic, no reaction with HCl.

Figure 7-2: Raven Lithologies of Granodiorite – Metasediments – Greenstone (left to right)

Source: Victoria Gold Corp. (2022)

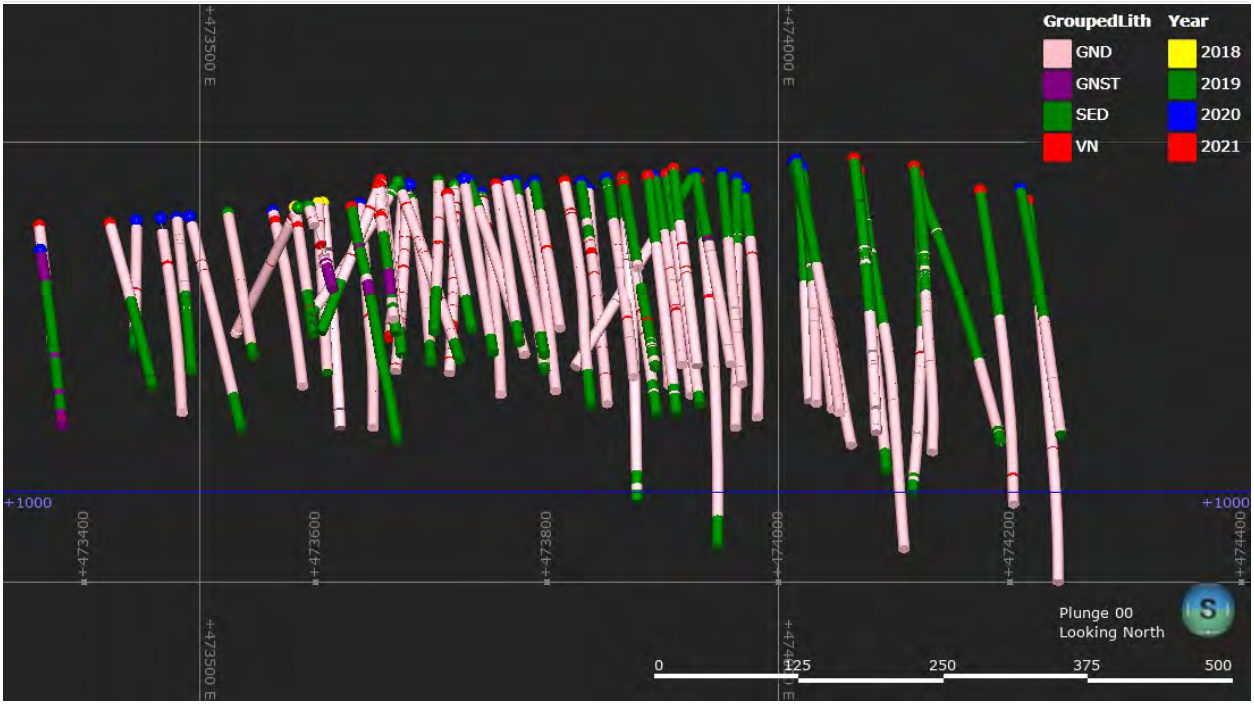

Figure 7-3: Raven Lithologies of Granodiorite – Metasediments – Greenstone (2018-2021 Diamond Drillholes)

Source: Victoria Gold Corp. (2022)

7.2.2 Structure

Structural zones at Raven include; fault, fault zone, fault gouge, shear, and breccia intervals. The dominant structural type in the intrusion and metasediments is a fault zone that includes fragmented and gouged rock; it is present in approximately one quarter of all Raven diamond drill core. This forms a major structure in the area and displays a strong E-W trend with a steep dip (Figure 7-6). Some fault zones are also present along contact zones of the intrusion with metasediments – these display shallow dipping structures (in a broad sense – no measured strike and dip), they are local, occurring among dominantly intrusive contact zones with sharp contacts between intrusion and metasediments. Vein breccia and brecciated intrusion and metasediments are minor structures.

All structures are brittle and many of them fragmented due to shearing – brittle expressions of shearing include cataclastic textures in intrusion along contacts with veins, and presence of strongly fragmented and gouged rock. All structure types are associated with moderate to strong sericite alteration, increased vein density and grey fault gouge zones. Fault and breccia zones are often associated with iron oxidation present at minimum on fractured surfaces regardless of the depth. Approximately 1/3 of all structure types (dominantly vein breccia) are associated with Au > 0.2 g/t.

The average fault and shear dip and dip azimuth was considered in the Raven structural modelling (blue rectangle in Figure 7-4), which is 263/78.

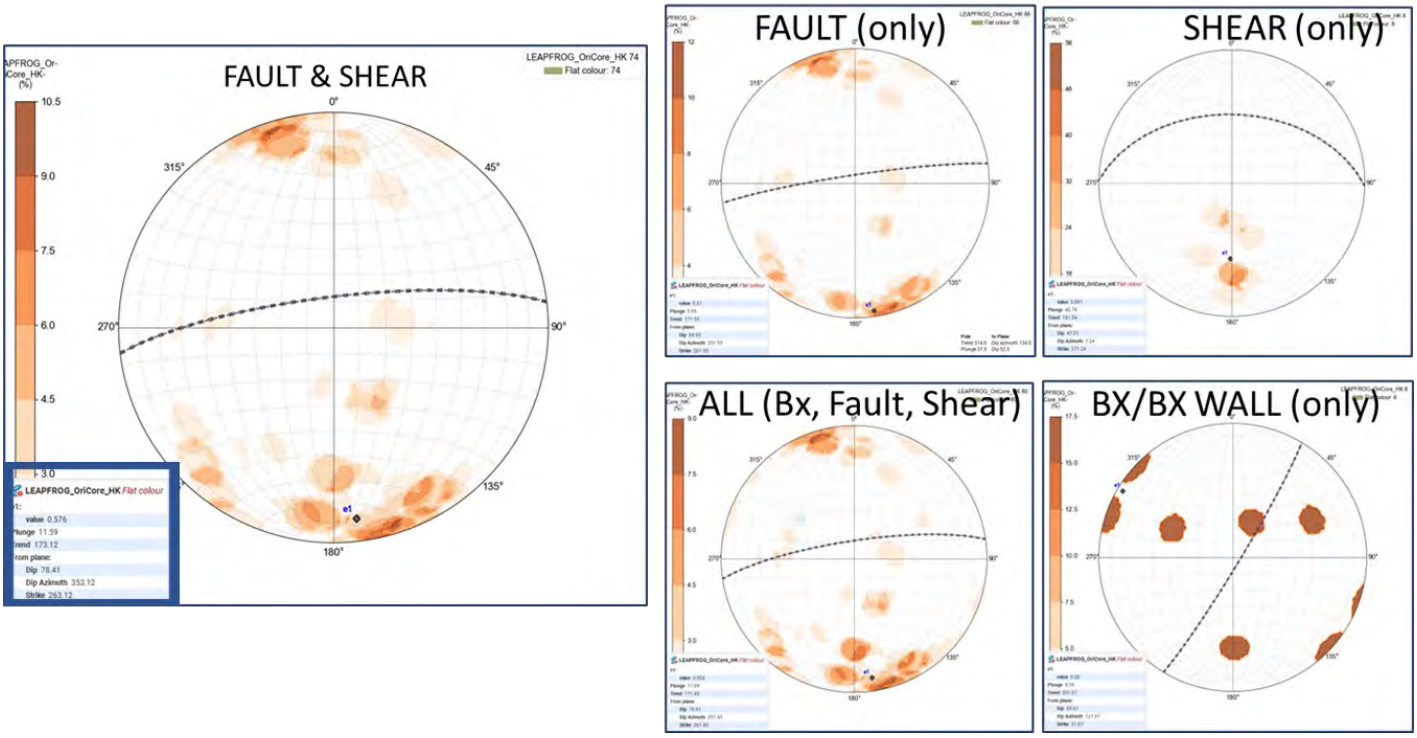

Figure 7-4: Structural Zones as Interpretated from Raven Drill Core

Source: Victoria Gold Corp. (2022)

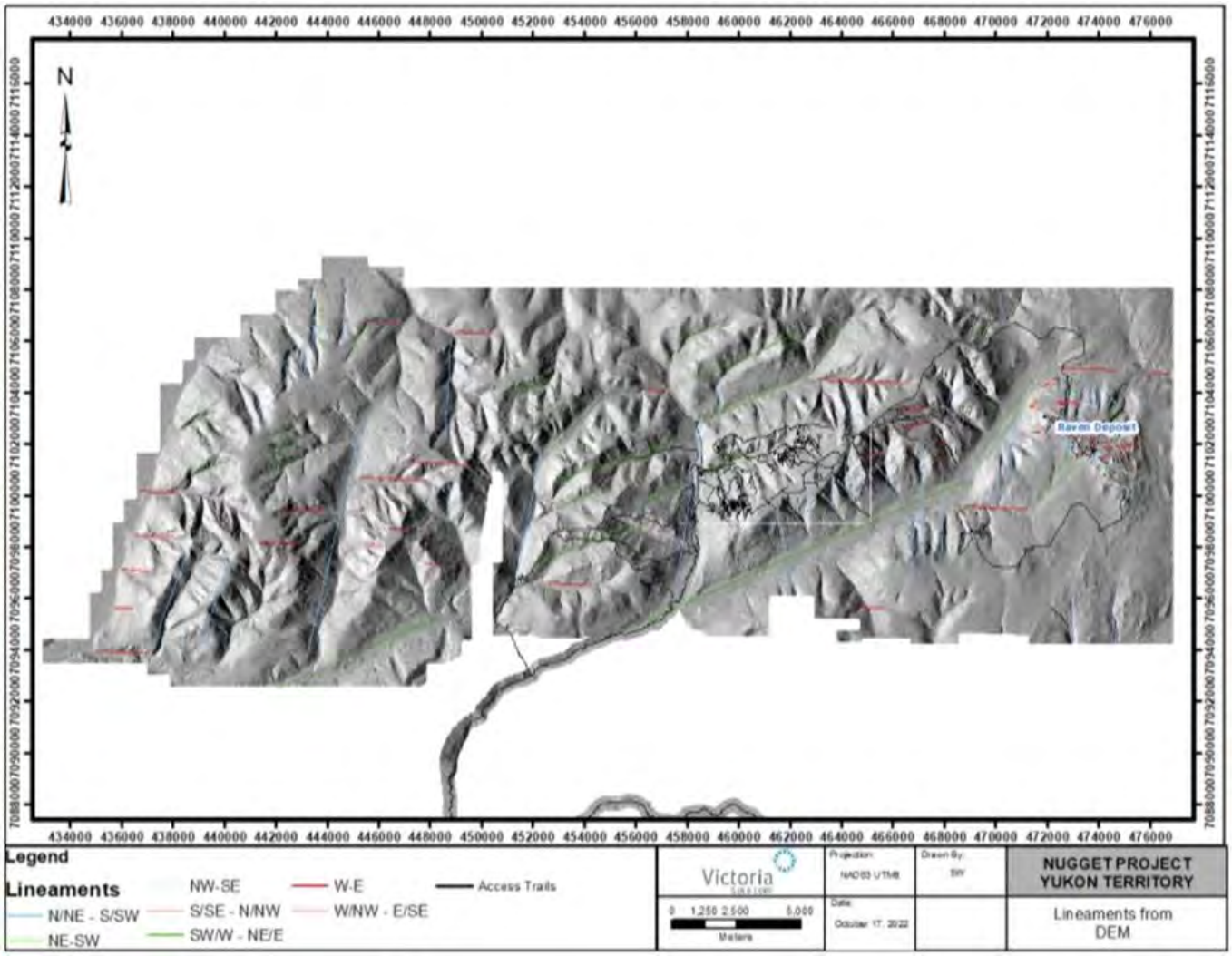

Figure 7-5: Interpreted Structural Lineaments from DEM Analysis (Dublin Gulch Claim Block)

Source: Victoria Gold Corp. (2022)

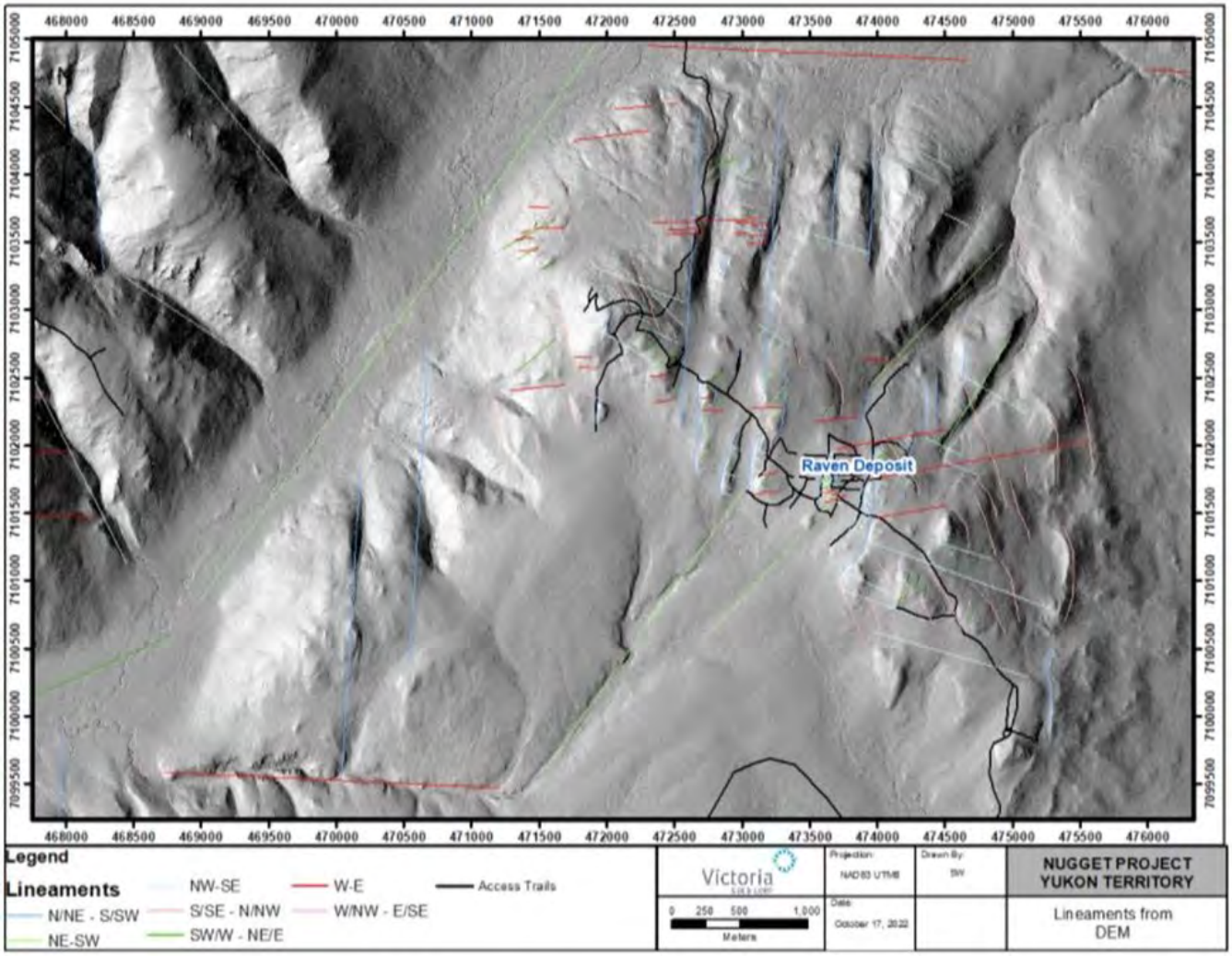

Figure 7-6: Interpreted Structural Lineaments from DEM Analysis (Raven Deposit)

Source: Victoria Gold Corp. (2022)

7.2.3 Alteration

The most abundant alteration of moderate to strong intensity at Raven is silicification, followed by sericite alteration and iron oxidation.

Sericitization at Raven is pervasive and a widespread vein envelope-style-alteration. It can be simultaneous with silica and/or carbonate and it can be overprinted with silica, carbonate, clay and iron oxides (Figure 7-7). Sericite commonly forms a peripheral halo around the core of intrusion-related porphyry deposits; and in low-sulphidation epithermal systems, sericite often occurs as wall rock alteration surrounding veins and replacement zones in permeable lithology. At Raven, sericite alteration occurs as pervasive, selectively pervasive, and veinlet-controlled styles; generally, pervasively altered exposures are white to grey (the white clay alteration at Raven could be due to sericite after feldspar in oppose to kaolinite/clays after feldspar). Textures range from selective incipient development to primary phenocrysts to total replacement of pre-existing crystals, deposition in veins and cavity infills. Sericite is interpreted to form under slightly acidic conditions (pH 4-6) and co-exists with kaolin group minerals at pH 4-5. The crystallinity of sericite increases with increasing temperature: well-formed, fine-grained sericite occurs at >200-250 degC, very coarse grained at >250-300 degC; in porphyry system it is a dominant mineral in sericitic and phyllic (ser-illite-quartz-chlorite) alteration; in epithermal precious metal deposits it is contemporaneous with or immediately follows mineralization formation. Sericite-silica combination is very common with silica dominating near the fluid source and sericite taking over the fringes; sericite alteration initiates within feldspars (especially calcic plagioclase) and the actual production of sericite generates quartz; white micas will actually alter all the minerals of the host rock and this includes quartz, the same for chlorite, carbonate (Thompson et al 1996).

Carbonate alteration is extremely common in selected zones of the intrusion in the Raven area (contact zones with metasediments) and as vein alteration envelopes - commonly overprinting sericite alteration with carbonates the resultant alteration products - which requires a fluid system containing CO^2. Alteration assemblage calcite, chlorite, hematite is common in retrograde skarn, through replacement in earlier skarn alteration, and may also affect adjacent wall rock limestones. Alteration assemblage chlorite, epidote, albite, calcite, actinolite is propylitic, commonly forms outermost alteration zone at intermediate-deep porphyry, in some is mineralogically zoned from inner actinolite-rich to outer epidote rich alteration (Thompson et al 1996).

Silica alteration is in a form of diffuse silica in vein alteration envelopes or silica flooded contact zones between intrusion and metasediments at Raven. Silica covers a wide range of temperature conditions and can be mistaken when is unusually dark (can contain very fine-grained sulphides) or pink or buff. Quartz can be in a form of pervasive replacement of the rock by silica minerals, and occurs in some epithermal systems as wall rock alteration around fractures and veins or within permeable zones at relatively shallow levels. Although adularia resembles quartz, it is characteristic of low-sulphidation epithermal deposits. Albite also resembles quartz alteration, it replaces primary plagioclase, common in alkaline porphyries, generally distributed along fracs and vein envelopes, may form a dense mass rock. Zones of silicified rock are common in many hydrothermal systems, where silica precipitation typically results from decreasing fluid temperatures. It can be pervasive over large areas (>100m^2), may be associated with sericite and adularia and mineralization, may be structurally controlled, forming envelopes around quartz veins, stockwork zones and may be stratigraphically controlled by more permeable units. Opaline silica/chalcedony may mark the paleowater table. Jasperoid can form large masses, it can be bedding or fault controlled and it is common epigenetic alteration product (mass replacement of limestone by silica). Brecciated jasperoid is characterized by multiple quartz veining events (Thompson et al 1996).

Iron-oxide alteration overprints all alteration types at Raven (Figure 7-8). It forms a subsurface oxidized zone down to ~10m and it also present at various depths to 350m in structural zones. Hematite is present in a variety of styles as bladed specular hematite in veins, vugs, matrix as a replacement of magnetite or as fine-grained hematite giving a red stain to altered rocks. It is a common alteration mineral in many intrusion related systems, commonly at higher levels with sericite-chlorite alteration. Magnetite is a widespread hydrothermal mineral that may occur in massive replacement bodies adjacent to the sediment-

intrusive contact, as thin bedded replacement horizons, dissemination or vein fills within early quartz-amphibole alteration in some porphyry deposits (Thompson et al 1996). The rare specular hematite vein exposed in a Raven trench was primarily a magnetite vein interpreted to be associated with hydrothermal activity related to intrusive emplacement.

Clay alteration is occasionally present in competent intrusion and in fault gouge at Raven. It may be mistaken for sericite alteration.

Chlorite alteration is dominantly associated with intrusive contact zones between metasediments and intrusive lithologies at Raven. Chlorite very likely replaces actinolite in these zones (Figure 7-9). Actinolite -Ca, Fe-Mg amphibole – is common in calcic skarn alteration (Thompson et al 1996).

Brown alteration in Raven holes could be due to pink-red- brown minerals such as hematite and carbonate (Figure 7-9). White sericite/clay alteration of feldspars are associated with this alteration.

Vugs can be occasionally seen in Raven quartz-carbonate-sulphide veins. Vugs are created during intense leaching (through reaction of extremely low-pH aqueous fluids/vapours of magmatic origin with rock/minerals), these fluids effectively remove all components, leaving behind quartz and rutile, leaving residual vuggy quartz. Vugs may be filled by late quartz, sulphides (Thompson et al 1996). In Raven veins, vugs appear to have formed intense leaching of interstitial carbonates, leaving behind quartz and sulphides.

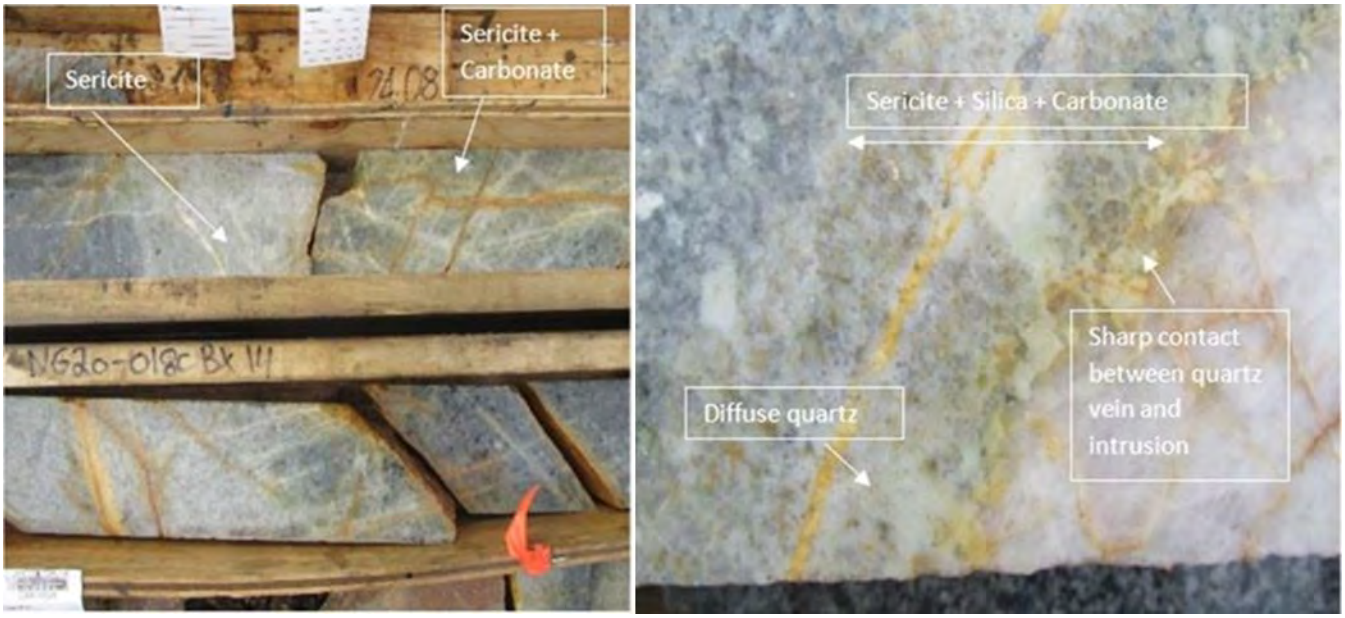

Figure 7-7: Sericite, Silica, and Carbonate Alterations in the Raven Deposit

Source: Victoria Gold Corp. (2022)

Figure 7-8: Iron Oxide and Fault Gouge Alterations in the Raven Deposit

Source: Victoria Gold Corp. (2022)

Figure 7-9: Chlorite after Actinolite and Brown Alterations in the Raven Deposit

Source: Victoria Gold Corp. (2022)

7.2.4 Veining

In 2019, logged Raven veins were classified into three (3) barren quartz vein types, and five (5) mineralized sulphide bearing veins (Table 7-1). Sulphide bearing veins are separated into arsenic-dominant and base-metal dominant. A degree of base metal veining overprinting occurs throughout the Raven area. The massive sulphide veins were the subject of the majority of the 2020 vein modelling efforts as the highest Au means are in massive sulphide veins (Figure 7-13). More specifically, highest mean and max values for gold are in massive arsenopyrite veins (M ASPY), massive pyrite veins (M PY) and massive sulphide (M SX) veins (Figure 7-14). Gold is interpreted to be closely associated with arsenopyrite; massive pyrite veins have dominant massive sulphide pyrite, but also a considerable amount of arsenopyrite, therefore they link to high Au grade; for example, massive pyrite-gasp veins (M PY-GASP) also have high Au grade, beside massive pyrite as dominant sulphide and minor galena-sphalerite overprinting massive pyrite, they have also a considerable amount of Au-bearing (semi-massive) arsenopyrite (Figure 7-16). Another example – thin quartz or massive quartz veins (QTZ and M QTZ) are not expected to show any Au grade as they have no visible sulphides (Figure 7-11)(Figure 7-12). One exception of this is if the quartz vein contains molybdenite, in that case, arsenopyrite could have been mistaken for molybdenite (Figure 7-15).

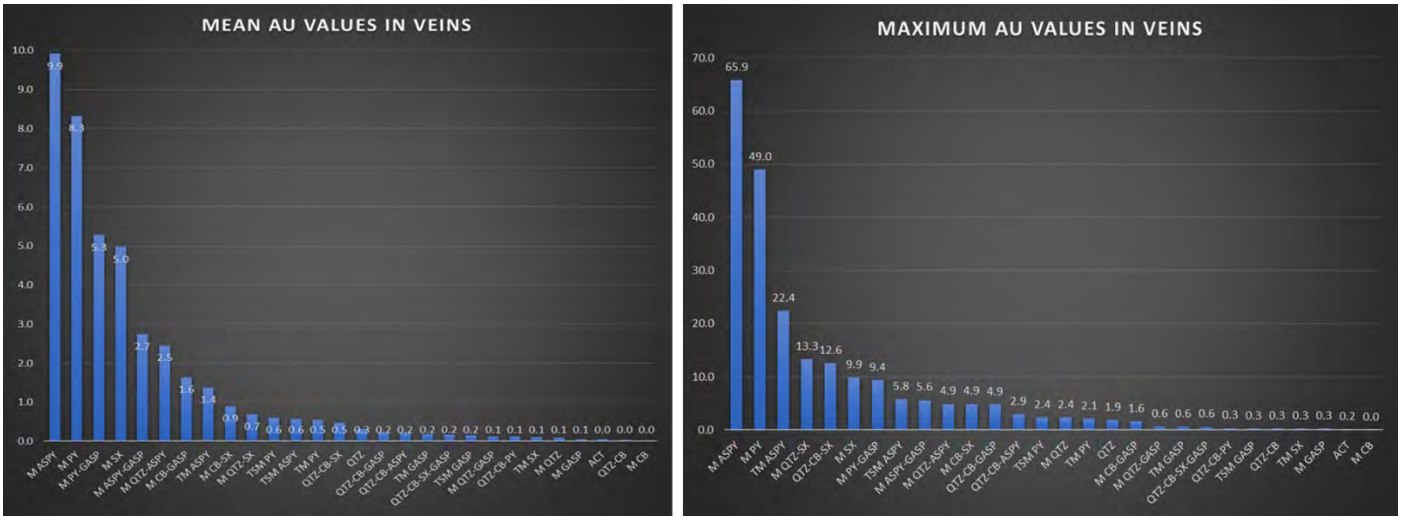

Figure 7-10: Raven Gold Values in Veins

Source: Victoria Gold Corp. (2021)

Massive brecciated sulphides do not have a higher Au mean when compared to banded sulphides, but they have higher MAX Au value. Mo and W have the highest mean values in massive quartz veins and Ag, Pb, Zn have the highest mean values in massive base metal veins. Massive base metal veins have commonly Au < 0.1 g/t, in oppose to Pb, Zn and Ag high mean values not only in base metal veins, but also in massive sulphide veins (Pb, Zn > 1000 ppm).

Massive sulphide veins have their alteration envelope at metre scale. Their alteration envelope can be unoxidized to moderately iron oxidized, moderately to strongly sericitized, with or without fault clay gouge, and non-silicified to moderately silicified. Brecciated massive sulphides are dominantly associated with breccia zones. Banded massive sulphides are dominantly not associated with any structure. Increase in the thickness of massive sulphide veins does not correspond necessarily with the higher Au grade; there are semi-massive sulphide veins that have higher Au grade than massive sulphide veins. They show a strong E-W trend with moderate to steep dips.

It is uncertain if moderate and steep dips of massive sulphide veins represent two discrete sets of major structures or if their dip variations are due to local rotations of faulted intrusion blocks, the dip difference is 32 degrees.

Massive sulphide veins are commonly associated with structure displayed within their alteration envelope, as well within themselves. Presence of breccia is dominant in brecciated massive sulphides, which is expected. Some massive sulphides are associated with fault zones. Most of the massive quartz-minor sulphide veins and banded massive sulphides have no obvious structure associated. Moderate to strong vein density is characteristic for most of the massive sulphides – it is common to find an increase in vein density towards massive veins.

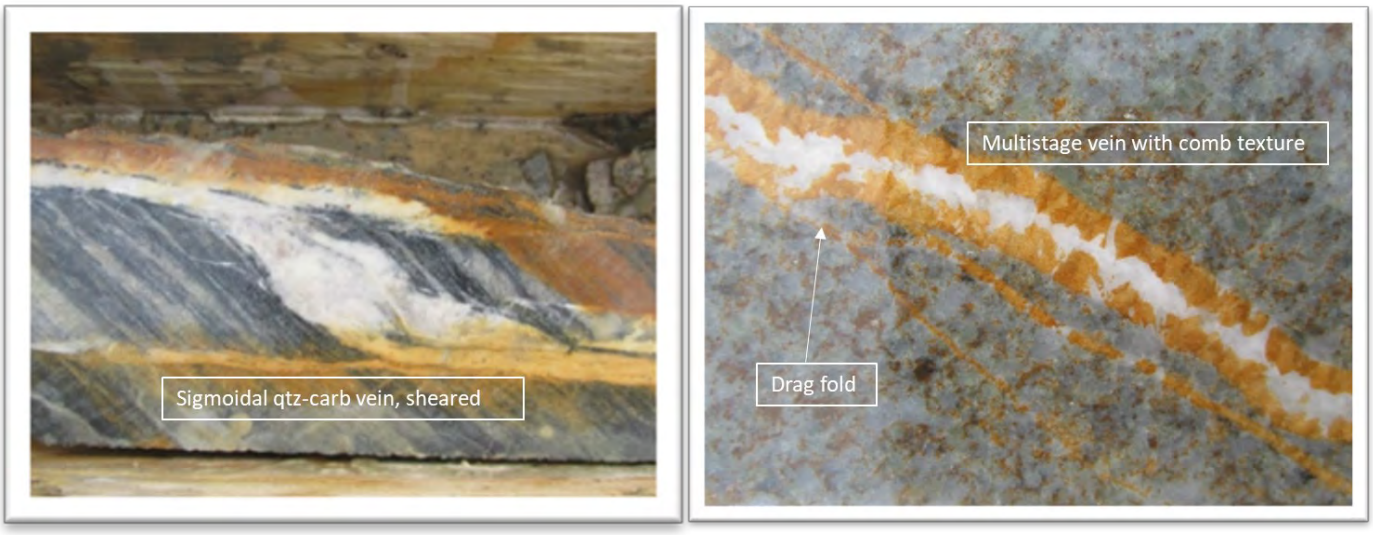

Figure 7-11: Thin Quartz-Carbonate Veins

Source: Victoria Gold Corp. (2022)

Figure 7-12: Thin Quartz-Carbonate-Sulphide Veins

Source: Victoria Gold Corp. (2022)

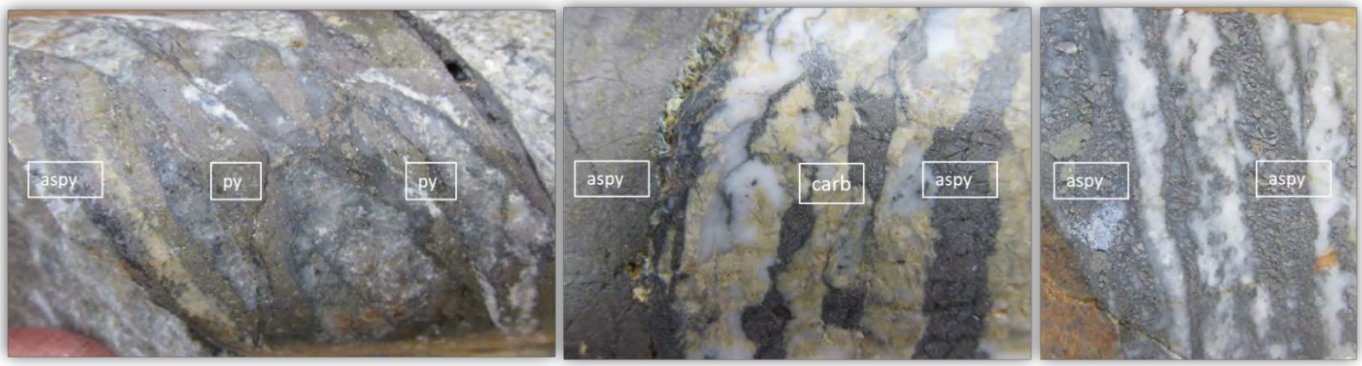

Figure 7-13: Thin Semi-Massive and Thin-Massive Sulphide Veins

Source: Victoria Gold Corp. (2022)

Figure 7-14: Massive Sulphide Veins

Source: Victoria Gold Corp. (2022)

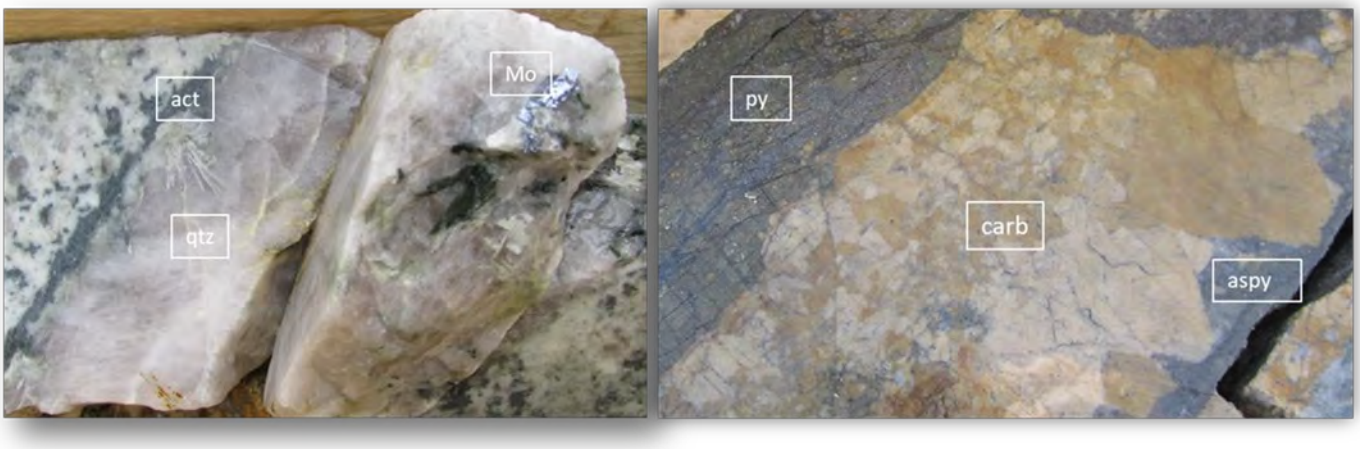

Figure 7-15: Massive Quartz and Carbonate Veins

Source: Victoria Gold Corp. (2022)

Figure 7-16: Sulphide (Arsenopyrite) Veins with Visible Gold

Source: Victoria Gold Corp. (2022)

Table 7-1: Vein Classification for Raven Deposit

#	Description	Mineralization
1a	Barren Quartz-Act	Quartz-Actinolite +/- Chlorite
1c	Barren Quartz	Quartz +/- Carb +/- Chlorite
1h	Oxidising hydrothermal fluid Quartz	Quartz-Hematite
6g	Free Gold in Calcite	Calcite-Quartz-Au +/- minor sx
6a	Arsenic dominant	Quartz-Sx [Apy +/- Py] [M ASP +/- M PY]
6i	Intermediate Phase- Overprinting 6a	Quartz-Ankerite-Sx [Apy +/- Py +/- Cpy]
6b	Base Metal	Quartz-Ankerite-Sx [Galena +/- Sphalerite +/- Pyrite +/- Sulphosalts +/- Apy] [M PY-GASP]
6m	Base Metal- Massive Sx or Ank Dominant	Sx-Ankerite [Pyrite +/- Galena +/- Sphalerite +/- Apy +/- Sulphosalts, minor Qtz] [M SX]

Raven Oriented Diamond Drill Core Analysis;

In Figure 7-17, the stereonet (R) shows general ~264 deg strike for all sulphide veins, having both, moderate and steep dips. More detailed sets of mineralized veins are presented in stereonets A, B, C, D below: these individual sets consist of smaller sample sizes (10+ sulphide veins) - and confirm that sulphide veins can have NW (13 veins) and SW (14 veins) strikes. Strike sets A and B are +/- 20 deg from 270 deg (W) azimuth and could represent a local variation of a general vein W strike. Set C includes vein strikes +/- 20 deg from 310 deg (NW) azimuth. Set D includes vein strikes +/- 20 deg from 230 deg (SW) azimuth (Figure 7-17).

In addition, massive QTZ-SX veins and thin QTZ-SX veins can have also NW strikes with moderate to shallow dips; base metal veins seem to have preferred SW strike, but their averaged azimuth comes from a variety of azimuths. Continued exploration and additional measurements on the Raven veins will help better define the Raven resource.

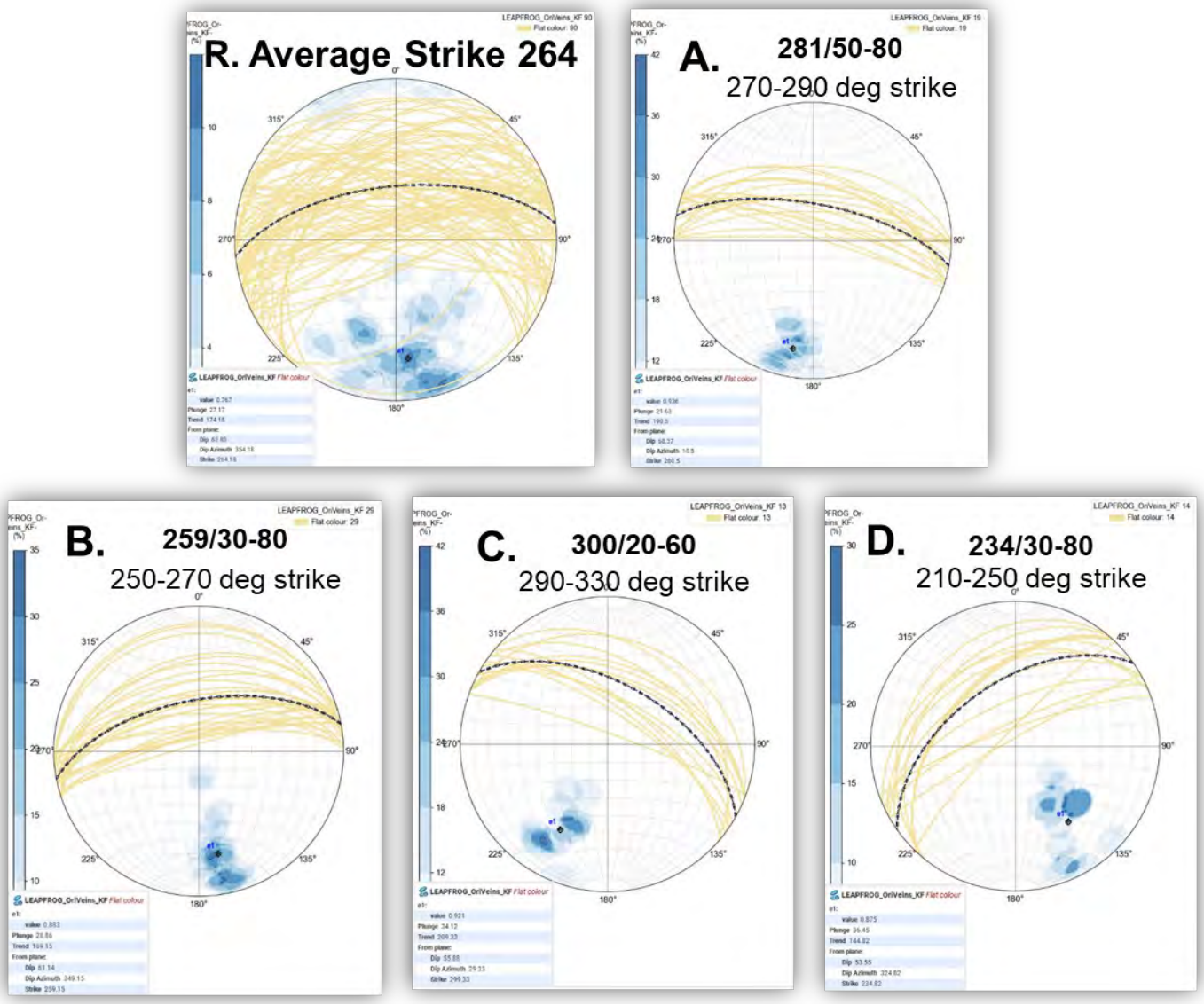

Figure 7-17: Raven Oriented Drill Core Analysis

Source: Victoria Gold Corp. (2022)

Analysis of the oriented drilling data, logging data, and field mapping confirms the persistence of these of the E-W trending structures and helped define the general trends of the mineralized veins across the Raven deposit. This data was then used to develop the Raven geologic model and aided in establishing the domains utilized in the resource estimate.

7.2.5 Raven Geophysical Surveys, LIDAR, and Orthophotography

Based on the RMI geophysical anomaly, the Nugget Stock is an elongated intrusion with E-W trend. The intrusion in the Raven project hosts sheared, mineralized, massive sulphide veins that also display a dominant E-W trend. DEM, VLF, K-radiometry support the presence of a set of N/NE-S/SW lineaments/structures which may be the traces of high angle normal faults that could be responsible for the 10-100 m scale offset of sheared mineralized zone. There is strong evidence of the presence of these

structures, but there is no clear evidence that they offset the mineralized zone. A full report on the Geophysical survey review is provided in Appendix 1.

The first geophysical survey was flown by Fugro Airborne Survey Corp. in 2004. It consisted of an Airborne DIGHEMV and Magnetic Survey which covered 3059.7-line kilometers. The survey employed the DIGHEMV-DSP electromagnetic system. Ancillary equipment consisted of a dual-sensor horizontal gradient magnetometer, radar and barometric altimeters, video camera, a digital recorder, and an electronic navigation system. The instrumentation was installed in an AS350-B2 turbine helicopter which flew at an average airspeed of 108 km/h with an EM sensor height of approximately 30 metres (Fugro Airborne Surveys, 2004). In 2011, the 2004 survey data was re-interpreted providing a full geological interpretation based on the EM and magnetic data which focused on delineating contacts and faults throughout the area and identifying unique rock units and intrusive bodies. This survey was conducted before the current extent of the Dublin Gulch claim block was staked and consequently only partially covered the Nugget stock area.

In 2017, Precision GeoSurveys Inc. conducted an airborne high-resolution magnetic and radiometric survey covering 4068-line kilometers over the current 555 square kilometer Dublin Gulch claim block. The instrumentation was installed in an AS350 helicopter which was flown at a constant height of 35 metres above the ground. The helicopter was equipped with a magnetometer, spectrometer, data acquisition system, laser altimeter, magnetic compensation system, pilot guidance unit (PGU), and GPS navigation system. In addition, two magnetic base stations were used to record diurnal magnetic variations (Precision GeoSurveys Inc., 2017) (Figure 7-18 through Figure 7-22).

In 2017, Eagle Mapping Ltd. collected LIDAR and orthophotography of the Dublin Gulch claim block. A Riegl Q1560 dual-channel LIDAR system was used for acquisition of LIDAR data. This system was installed on a Piper Navajo aircraft, which is based in Abbotsford, BC. The nominal flying height was 1300m above ground level and the flying speed was around 140 knots. Aerial photography was collected at the same time as the LIDAR data using an IQ-180 80MP digital camera co-mounted with the Q1560 LIDAR system. The photo resolution was 20 centimeters. A Digital Elevation Model (DEM) was then derived from the LIDAR data (Figure 7-23).

In 2018, Aurora Geosciences Ltd. conducted DC resistivity / Induced Polarization (IP) and total magnetic field / VLF (mag-VLF) surveys over the Nugget stock. The surveys consisted of three 2D IP lines, one downhole IP survey, 191.8-line kilometers of walk-mag where total field readings were collected once per second, and 172-line kilometers of VLF readings, where readings were collected every 10 metres (Aurora Geosciences Ltd., 2018) (Figure 7-20 and Figure 7-22).

The Nugget Stock (pink/orange polygon in Figure 7-18) shows a moderately negative magnetic anomaly from RMI (blue oval), which means the reading is lower than the average magnetic field. Raven shares magnetic response with other Mayo Suite Intrusions, considered as Reduced Intrusion Related Gold Systems (RIRGS). Elongation of the intrusion reflects W/NW – E/SE regional trend (purple dashed line in Figure 7-18). RMI (also TMI) anomalies complement some structural lineaments derived from DEM and aid in intrusion mapping and identification of contact zones.

VLF (Very Low Frequency) - Linear inversion of the electromagnetic measurements involved application of the Fraser filter; the objective of the inversion was to obtain a subsurface distribution of the electrical resistivity. VLF survey used the transmitter Jim Creek, Washington and generated 2D resistivity models, successfully identifying many N-S conductive features as strong and weak VLF linears (Figure 7-22). VLF anomalous zones are suspected fractured zones/ lithological boundaries; VLF N-S linears (yellow lines) support the presence of prominent N-S structures at Nugget.

The N/NE-S/SW oriented lineaments may be the traces of high angle normal faults that could be responsible for the 10-100 m scale offset of sheared mineralized zone. There is strong evidence of the presence of these structures, but there is no clear evidence that they offset the mineralized zone (Figure 7-24).

K-Radiometry: High K radiometry anomaly indicates locations with intrusion at or near the surface with values of greater than or equal to 0.3 %. K radiometry anomaly coincides with mapped intrusion exposures, as well it suggests the presence of structural lineaments that may or may not overlap with DEM structural linears. K radiometry is a reliable tool for locating prospective targets of intrusion-hosted mineralized veins (Figure 7-21).

Appendix 1 of this Technical Report includes the Aurora Geosciences 2018 technical memo on the Raven Geophysical compilation including detailed review and presentation of the various geophysical surveys and recommendations on future work. Appendix 2 includes Precision GeoSurvey's 2017 full report on the Dublin Gulch claim block.

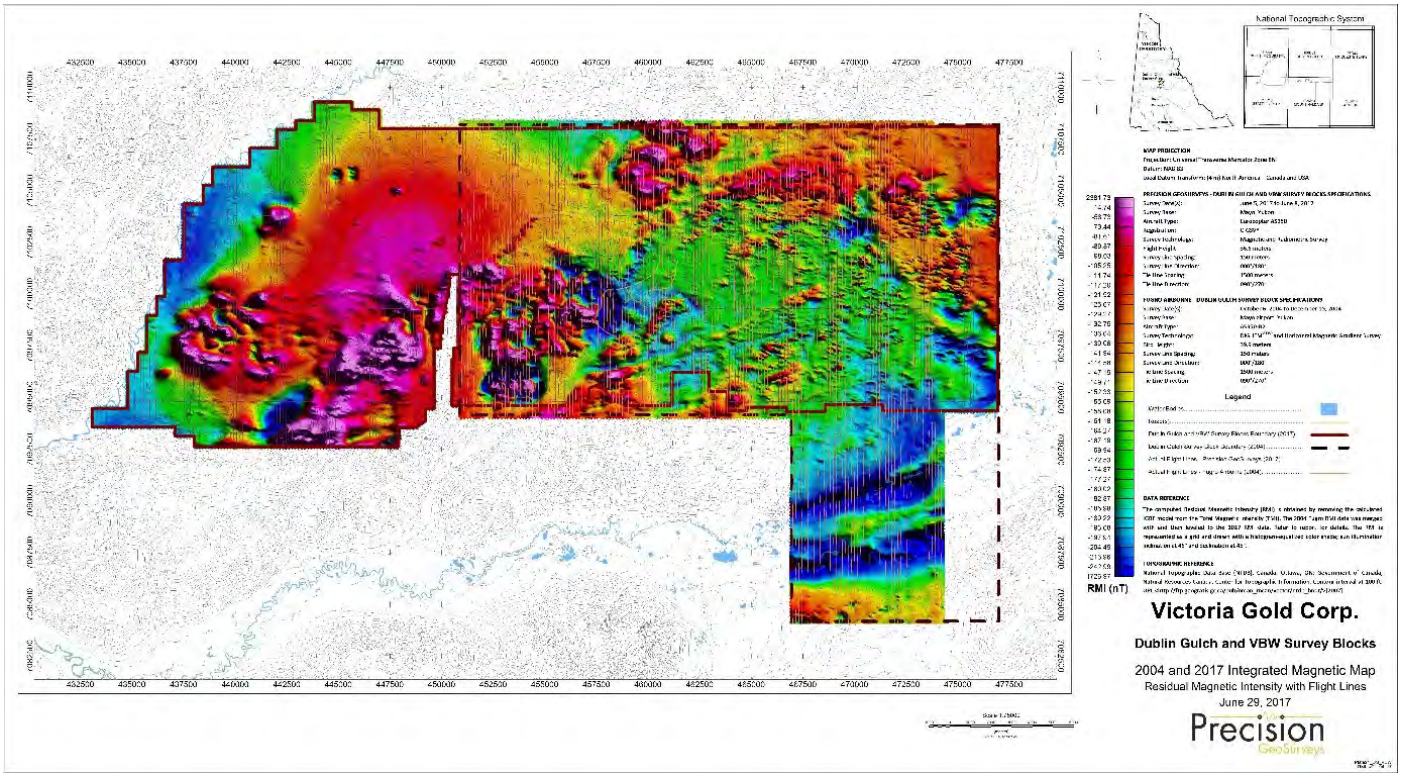

Figure 7-18: Integrated Magnetic Map (2004 and 2017) RMI with Flight lines

Source: Precision GeoSurvey Inc. (2017)

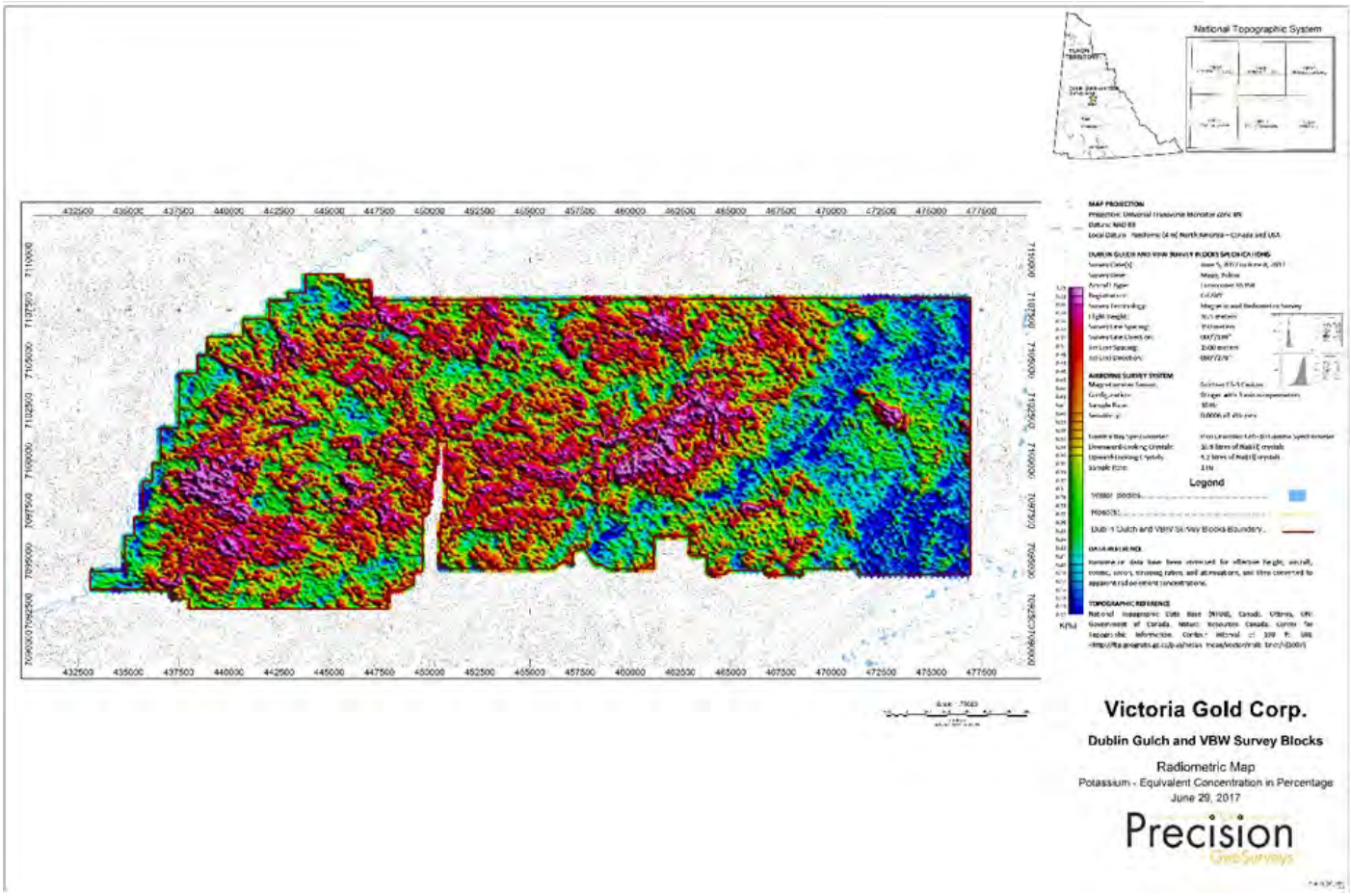

Figure 7-19: Radiometric Map of Dublin Gulch and VBW Survey Blocks

Source: Precision GeoSurvey Inc. (2017)

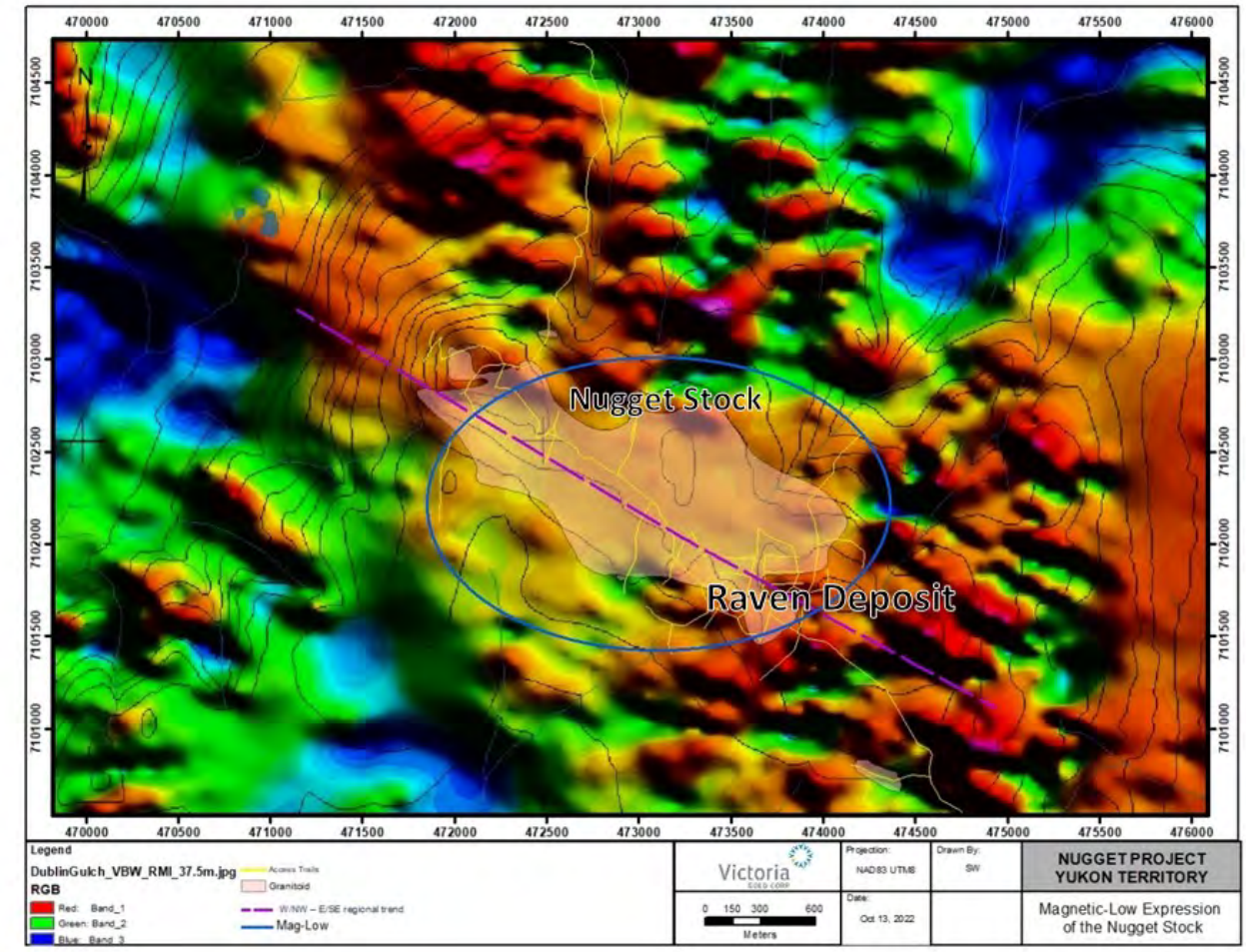

Figure 7-20: Magnetic-Low Expression of The Nugget Stock

Source: Modified from Precision GeoSurvey Inc. (2017)

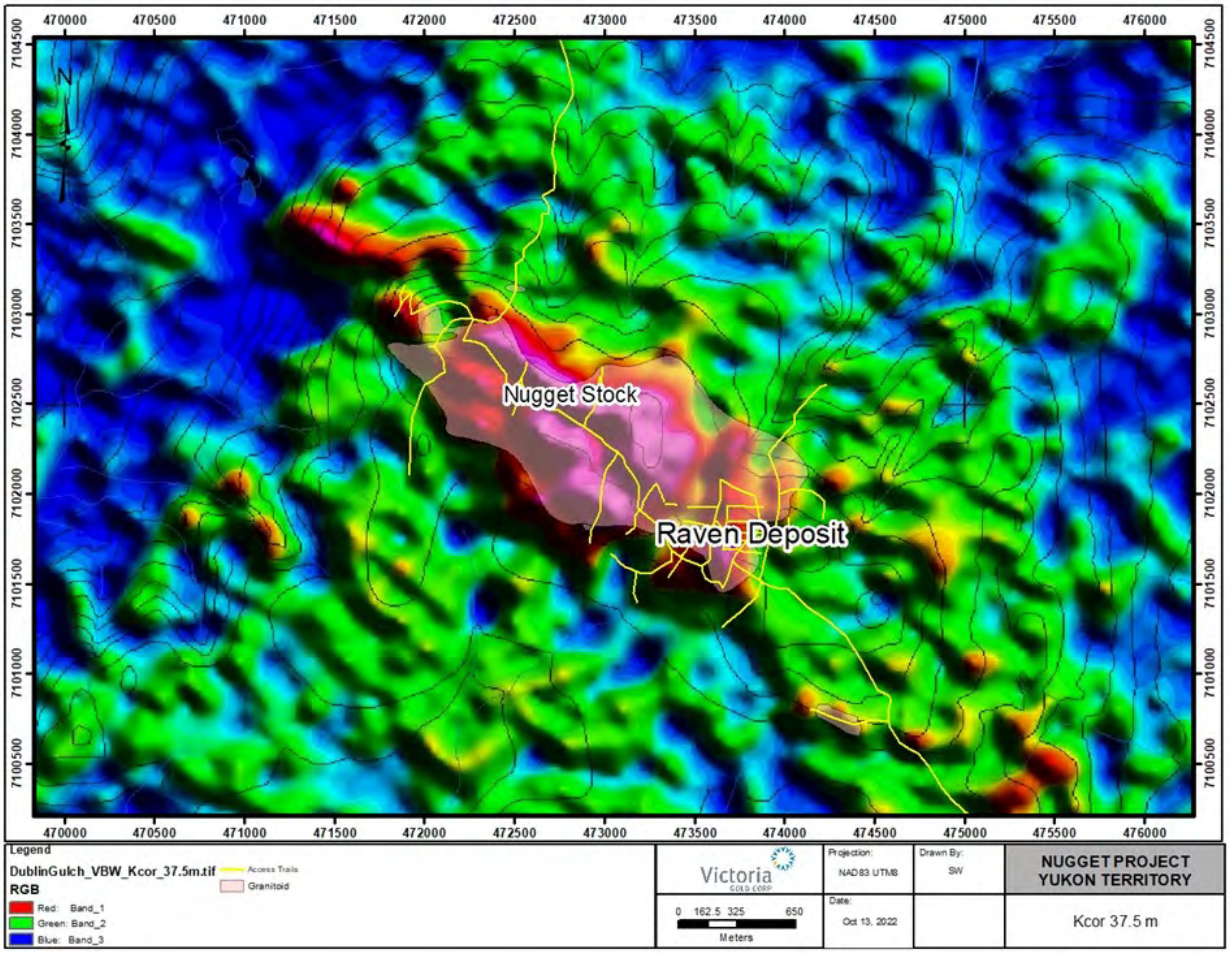

Figure 7-21: K-Radiometry of The Nugget Stock

Source: Modified from Precision GeoSurvey Inc. (2017)

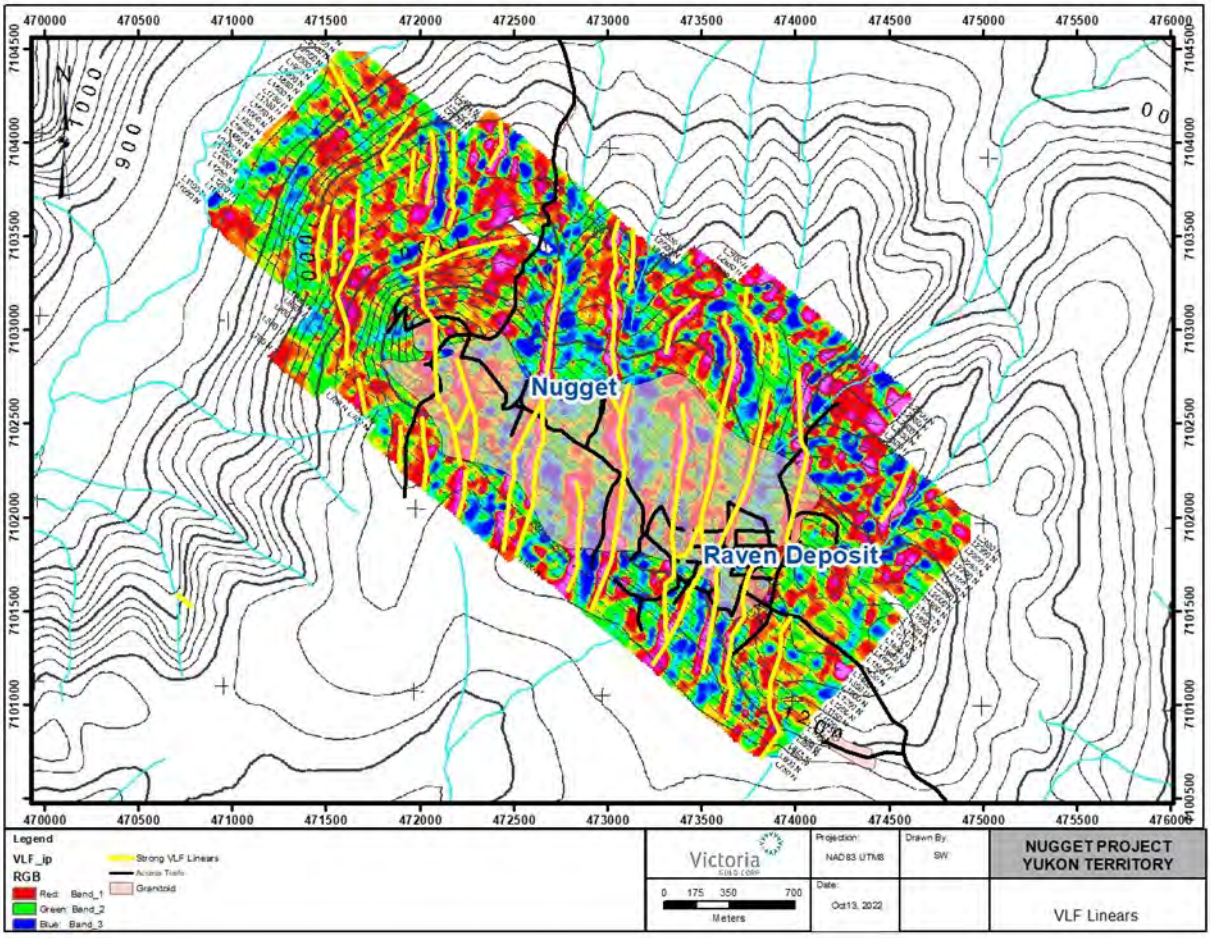

Figure 7-22: VLF Linears of The Nugget Stock

Source: Modified from Aurora Geosciences Ltd. (2018)

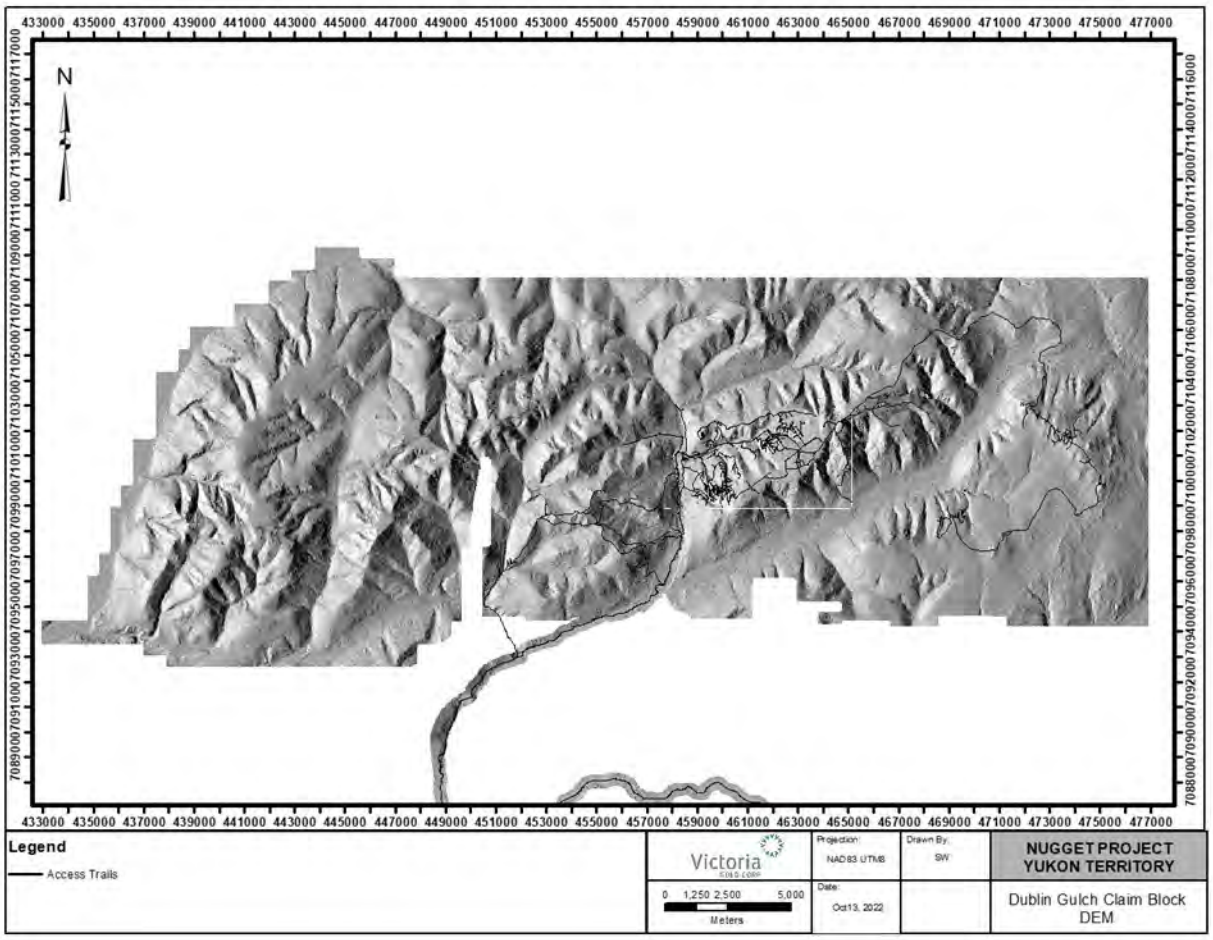

Figure 7-23: Dublin Gulch Claim Block DEM

Source: Victoria Gold Corp. (2022)

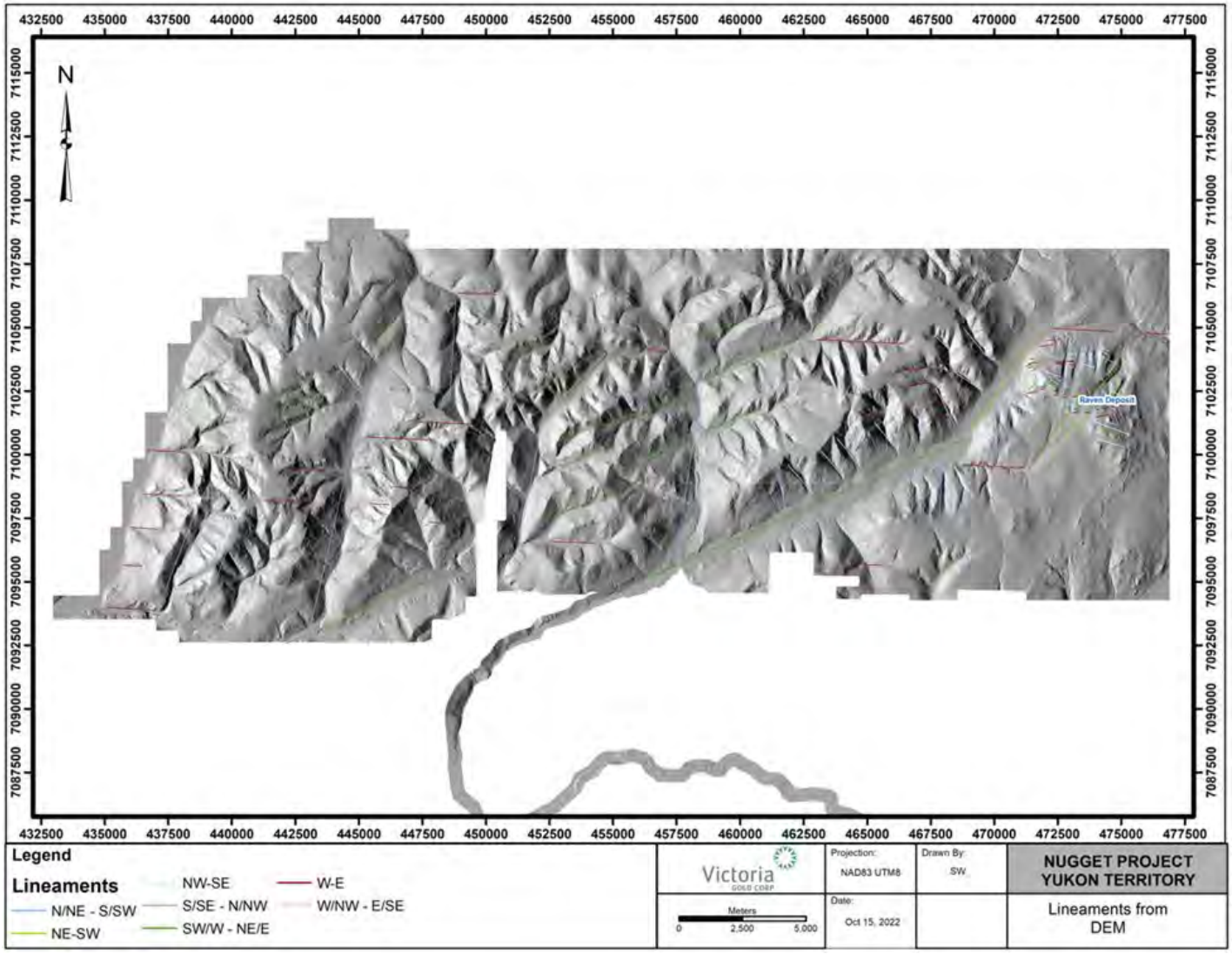

Figure 7-24: Lineaments from DEM on the Raven Deposit

Source: Victoria Gold Corp. (2022)

8 DEPOSIT TYPES

The Nugget Stock consists of Cretaceous age (98-million-year-old), medium to coarse grained granodiorite and occurs on the Eastern side of the Lynx Creek valley. The area is underlain by the Devonian to Mississippian age Earn Group and the Early Carboniferous age Keno Hill Quartzites which have been deformed by greenschist facies metamorphism, folding, and thrusting (Gordey and Makepeace, 2003). The Raven occurrence is hosted in a shear zone corridor within the Nugget Stock, in close association with the intrusion-metasediment contact.

The Raven zone and the surrounding Nugget Stock is an interpreted reduced intrusive-related gold system (RIRGS), a member of the Mayo Plutonic Suite and part of the Tombstone-Tungsten belt, which forms a narrow belt of intrusions extending 550 kilometres across the north-central Yukon within the Selwyn Basin (Hart et al., 2004) (Figure 8-1 and Figure 8-2). Like the majority of RIRGS deposits, gold mineralization at Raven occurs within the stock, although minor mineralization is noted within surrounding hornfelsed Earn Group meta-sedimentary rocks.

RIRGS' classes of mineral deposits are deposits that are:

- Metaluminous subalkalic intrusions of intermediate to felsic composition that lie near the boundary between ilmenite and magnetite series;
- Associated with carbonic hydrothermal fluids;
- A metal assemblage that variably combines gold with elevated bismuth, tungsten, arsenic, molybdenum, tellurium, and antimony as well as low concentrations of base metals;
- Associated with commonly weak hydrothermal alteration that is really restricted;
- In a tectonic setting well inboard of inferred or recognized convergent plate boundaries; and
- Located in magmatic provinces best or formerly known for tungsten and/or tin deposits.

The RIRGS class of gold deposits was developed based on studies of gold and other mineral deposits hosted in granitoids in the Yukon and Alaska (Hart, C. R., 2007)

Additionally:

- RIRGS deposits are best developed in intrusions that were emplaced into ancient continental margins behind accretionary or collisional orogens and subduction-related magmatic arcs. Preferred host strata include reducing basinal miogeoclinal sedimentary or metasedimentary rocks;
- Thermal gradients surrounding cooling plutons are steep and result in temperature-dependent concentric metal zones that develop outward from pluton margins for distances up to a few kilometres or just beyond the thermal halo;
- Skarns and replacements are generally pluton-proximal with an increase in structural control on more distal mineralization. There is also crustal-scale vertical zonation with epizonal occurrences forming at shallower levels;
- The most distinctive style of gold mineralization in RIRGS deposits is sheeted arrays of parallel, low sulphide, single-stage quartz veins that are found over widths of tens to hundreds of metres and are preferentially located in the cupola of the pluton. These veins are unlike multidirectional, interconnected stockworks characteristic of porphyry systems or antithetic tensional vein arrays typical of orogenic deposits;
- Mineralized plutons have characteristics that indicate the likelihood of generation of hydrothermal fluids, high volatile contents, fluid exsolution, rapid fractionation and zonation, including the

presence of porphyritic textures, aplite and pegmatite dikes, quartz and tourmaline veins, greisen alteration, miarolitic cavities and unidirectional solidification textures, preferably in pluton apices;

- RIRGS deposits are associated with felsic, ilmenite-series plutons that lack magnetite, have low magnetic susceptibilities and aeromagnetic response, and have ferric-ferrous ratios of less than 0.3. These types of plutons are uncommon in arc and fore-arc settings where orogenic gold deposits are most common; and Intrusion-related deposits are coeval with their associated, causative pluton.

Table 8-1 to Source: From (Corbett, 2009), (Hart, 2007), and (Victoria Gold Corp 2021)

Table 8-4 below represent the differences of the Nugget-Raven stock classification of RIRGS compared to that of a Porphyry system.

Table 8-1: Nugget-Raven RIRGS vs Prophyry

	RIRGS	Au (Au-Cu) Porphyry	Nugget
Geological Setting	• Mineralization is intrusion hosted, in tensional zones in plutons brittle carapace near country rock, in the hornfels thermal aureole • Elongate plutons, cylindrical-shaped plutons- reflect structural controls on pluton emplacement intruding metaseds • Shoulders provide region of structural, geological contrast-enhance development of fluid focusing structures • Depth 5-7 km-greater depth prevent stwk or breccia formtn, meteoric water reach and broad altrn haloes • It is thermally driven hydrothermal system	• Calc-alkaline stratovolcanoes – traditional model • Epizon-mesozone • subvolcanic • Shallower depth : allow for stwk and breccia, extensive altrn haloes by mixing meteoric waters	• Similar to Dublin Gulch (RIRGS) • Elongate pluton based on RMI • Mineralization is veins that are intrusion hosted dominantly, less metasediment hosted • Veins are in pluton's brittle carapace near and partially in country rock • Banded skarn is W poor, retrograde min assemblage?? – very fine grained to identify mineralogy
Tectonic Setting	Post-collision extension behind thickened continental margin Depth 5-7 km-greater depth prevent stwk or breccia formtn, meteoric water reach and broad altrn haloes It is thermally driven hydrothermal system	Calc-alkaline stratovolcanoes – traditional model Epizon-mesozone Subvolcanic True continental margin arcs, subdactn zone Along regional structures	• Similar to DG • Post-collision extension behind thickened continental margin
Deposit Size	• Small, < 2km sq isolated plutons • OR as a larger (2-10km sq) pluton's apophyses	• Large	• A few km long oval intrusion or pluton's apophysis based on VLF and mapping
Deposit Morphology	• Sheeted vein arrays within intrusion commonly, less common in well-developed hornfels zones • Following the same extensional fractures that controlled pluton emplacements: filled w pegmatite, aplite, lamprophyre dikes	• Ore bodies overlap, or separate, or stacked on top of each other • Ore bodies zoned: barren cores-> concentric metal zones-> barren py haloes -> skarns, peripheral vein, replacement mantos, epithermal precious dep • Complex, irregular ore and alteratn	• based on drilling: intrusion carapace with stoping metasediment blocks and mineralized veins extend down 200 m • based on trench and outcrop mapping on Raven: contact zone • Based on RMI: The shape of intrusion may likely follow regional structures: W-E, based • Based on mapping: could rhyolite dyke be actually aplite dykes typical features following the same extensional features that controlled pluton emplacement- not enough dyke attitude measurements
Magmatic Association	Reduced-Ilmenite series Felsic intrusion Granites, monzonite, granodiorites w Bio>>hbl>px qtz monzonite, sulph pyrrhotite	Oxidized – Magnetite series Intermediate- Mafic intrusion Diorite, granodiorite, alk monz Magnetite, ilmenite, py (domint sx), po, anhydrite	lack of magnetite? – reduced Demagnetized magnetite – oxidized – petrography will help, no magnetite observed in handspecimen • Felsic to intermediate (qtz monzogranite?), seems to be biotite rich – similar to RIRGS, commonly porphyritic • Recrystallization texture overprinting original textures

Source: From (Corbett, 2009), (Hart, 2007), and (Victoria Gold Corp 2021)

Table 8-2: Nugget-Raven RIRGS vs Porphyry

	RIRGS	Au (Au-Cu) Porphyry	Nugget
Ore Paragenesis	• Early ore stages: high temp anhydr diop-plag skarns w sheelite • Overprintd by low temp hydr bio-zois-act skarn where Au w sx • High temp sx: po>>cpy • Low temp sx: Bi-Te-Sb-Pb-Au minerals and alloys • Low sulphidation - Thin sheeted vns qtz-Au-Bi-Te-W	High sulphidation:enargite-py-barite-alunite-Au-Cu Low sulphidatino: cpy-ga-sph, chlorite wall rock, qtz-cpy vns High sulphidation epithermal typical	• Mineralized veins likely form in extension regime; veins occur roughly normal to the axis of extension • Shear is a post-mineralization event, subparalleling veins • Qtz-FeOx and Hematite veins are the most common veins, they are often found together and they are always present in locations of scorodite veins • Hematite veins occur as marginal, sheared and gouged veins, bounding scorodite, qtz-feox +/- sulph, lim-ser veins OR in the center of scorodite veins • Barren actinolite, carbonate veins are commonly not associated with hematite veins
Mineralogy	• Skarns lack garnet – reduced skarns • Au w Bi-Te-Sb-Pb-Au minerals and alloys: tellurobismuthite, maldonite, tetradymite, native Bi, boulangerite, Bi-Pb sulphosalts, gal, moly • OR Au w Py-as py-aspy-lim	Py-cpy-bor-/+Au Au-Cu-Mo Au-Cu (deeper-covellite)-+/-Ag, Te-Sb in the uppermost portions Cu-Au dep: cpy-bor-chalcoc-ten-native Au, electrum, tellurides, py, aspy, magnet, quartz, biot, kspar, anhydr, epid, chlor, scapol, albite, cc, fluorite, garnet	**Veins:** **Au – Bi – Sb – Cu - Ag – As – S** **Ag – Cu – Bi – Sb – S** **As – Pb – Sb – Zn – Fe – S** **Bi – Cu – Sb – S** **Cu – Sb – S** **Pb – Zn** **Sb – S** **Chalcopyrite, pyrite** **pyrrhotite** **Enargite-copper, arsenic sulfosalt – mod to low temp hydrothermal dep** **Pyrargyrite-prustite: sulfaosalt-silver sulfarsenide – hydrothermal deposits, oxidized and supergene zone** **Jamesonite: sulfosalt-lead, iron, antimony sulphide – moder temperature hydrothermal deposits** **Tetrahedrite - tennantite: sulphosalt-copper, antimony, arsenic – moderate temperature hydrothermal dep, contact zones**
Veins	Early sheeted veins: alk fspar-mica-sheel-qtz, lack Au Low temp sheeted veins: aspy-py-Au-Bi-Te alloys Outside of intrn: aspy and antim vns Late veins beyond contact metamorphic aureole: Ag-Pb-Zn-qtz vns = Ag-rich-ga-sph-qtz-cb vns	Comb-quartz vein w Au py-cpy, deeper +spec hem-po-marc-opal Qtz-sx Au+/- Cu Au-Cu-Bi or Au-Cu-Te = deeper levels Carbonate-base metal Au vns : qtz-sx-Au-sph-ga-cpy-ten-tetra-late stage cb Epthermal qtz-Au-Ag vns – high grade Au-bonanza Au Banded chalcedony-ginguro epithermal Au-Ag vns – adularia-sericite = low sulphidation vns Polymetalic Ag-Au banded fissure vns: qtz-sx (py)-cb+/-Cu-Ag (argentite-freibergite-polybasite)-sph	In trenches: • qtz-sx vns (py-aspy) • Qtz-sx vn (qtz-ga) • Sheared scor-ser-lim-hem vns • Lim-ser vns / zones • Qtz-cb vn • Qtz-act vn In drill core: • Sheared Qtz-sid-mass sx (aspy) • Planar qtz-sx (aspy? Or ga?) • Sheeted qtz-? Vns • Planar qtz-tour? Or act/ampb?

Source: From (Corbett, 2009), (Hart, 2007), and (Victoria Gold Corp 2021)

Table 8-3: Nugget-Raven RIRGS vs Porphyry

	RIRGS	Au (Au-Cu) Porphyry	Nugget
Ore Paragenesis	• Early ore stages: high temp anhydr diop-plag skarns w sheelite • Overprintd by low temp hydr bio-zois-act skarn where Au w sx • High temp sx: po>>cpy • Low temp sx: Bi-Te-Sb-Pb-Au minerals and alloys • Low sulphidation - Thin sheeted vns qtz-Au-Bi-Te-W	• High sulphidation:enargite-py-barite-alunite-Au-Cu • Low sulphidatino: cpy-ga-sph, chlorite wall rock, qtz-cpy vns • High sulphidation epithermal typical	Relative Timing on Mineralization & Structure: • Multiple stage veining and mineralization • Both, low and high angle mineralized veins appear to be sheared implying that mineralization occurred prior to shearing, eventually were contemporaneous • Low angle shear + mineralization could possibly pre-date the steep angle shear + mineralization • Low angle shear + mineralization could occur during the thrusting metasediments onto intrusion • Steep angle structure x-cuts and perhaps offsets low angle structure • Low angle, sheared scorodite veins appear to have wide U shape along the trench line and appear to be "terminated" by a steep angle structure; they tend to be persistent at m scale along the trench lines – drag fold resemblance • Steep angle structure can be persistent from the bottom to the top of the trench wall, sometimes tracible across the trench bottom
Mineralogy	• Skarns lack garnet – reduced skarns • Au w Bi-Te-Sb-Pb-Au minerals and alloys: tellurobismuthite, maldonite, tetradymite, native Bi, boulangerite, Bi-Pb sulphosalts, gal, moly • OR Au w Py-as py-aspy-lim	• Py-cpy-bor-/+Au • Au-Cu-Mo • Au-Cu (deeper-covellite)-+/-Ag, Te-Sb in the uppermost portions • Cu-Au dep: cpy-bor-chalcoc-ten-native Au, electrum, tellurides, py, aspy, magnet, quartz, biot, kspar, anhydr, epid, chlor, scapol, albite, cc, fluorite, garnet	**Veins:** **Au – Bi – Sb – Cu - Ag – As – S** **Ag – Cu – Bi – Sb – S** **As – Pb – Sb – Zn – Fe – S** **Bi – Cu – Sb – S** **Cu – Sb – S** **Pb – Zn** **Sb – S** • **Chalcopyrite, pyrite, pyrrhotite** • **Enargite-copper, arsenic sulfosalt – mod to low temp hydrothermal dep** • **Pyrargyrite-prustite: sulfaosalt-silver sulfarsenide – hydrothermal deposits, oxidized and supergene zone** • **Jamesonite: sulfosalt-lead, iron, antimony sulphide – moder temperature hydrothermal deposits** • **Tetrahedrite - tennantite: sulphosalt-copper, antimony, arsenic – moderate temperature hydrothermal dep, contact zones**
Veins	• Early sheeted veins: alk fspar-mica-sheel-qtz, lack Au • Low temp sheeted veins: aspy-py-Au-Bi-Te alloys • Outside of intrn: aspy and antim vns • Late veins beyond contact metamorphic aureole: Ag-Pb-Zn-qtz vns = Ag-rich-ga-sph-qtz-cb vns	• Comb-quartz vein w Au py-cpy, deeper +spec hem-po-marc-opal • Qtz-sx Au+/- Cu • Au-Cu-Bi or Au-Cu-Te = deeper levels • Carbonate-base metal Au vns : qtz-sx-Au-sph-ga-cpy-ten-tetra-late stage cb • Epithermal qtz-Au-Ag vns – high grade Au-bonanza Au • Banded chalcedony-ginguro epithermal Au-Ag vns – adularia-sericite = low sulphidation vns • Polymetalic Ag-Au banded fissure vns: qtz-sx (py)-cb+/-Cu-Ag (argentite-freibergite-polybasite)-sph	In trenches: • qtz-sx vns (py-aspy) w sheared hem margins • Qtz-sx vn (qtz-ga) • Sheared scor-ser-lim-hem vns • Lim-ser vns / zones • Qtz-cb vn (late stage, undeformed) • Qtz-act vn (late stage, undeformed) In drill core: • Sheared Qtz-sid (gangue min of hydrotherm metallic vns)-mass sx (aspy?) • Planar qtz-sx (aspy? Or ga?) • Sheeted qtz-? Vns • Planar qtz-tour? Or act/amph?
Alteration	• Not extensive, not intensive	Broad, extensive Potassic, propylitic, argillic – prograde atrn Phyllic, argillic – retrograde altrn	• Surface to 15 -45 m: oxide zone w hem-lim-ser altern • 45m: sericite-silica altern at m scale • Probably can be considered as not extensive when compared to porphyry alteration

Source: From (Corbett, 2009), (Hart, 2007), and (Victoria Gold Corp 2021)

Table 8-4: Nugget-Raven RIRGS vs Porphyry

	RIRGS	Au (Au-Cu) Porphyry	Nugget
Zonation	• Proximal Au-W-As metal assoctn • Distal Ag-Pb-Zn metal assoctn	Vertical zonation: • Cu>Au at depth • Zn, Pb w Au-Ag in central portion • high grade Ag>Au in the uppermost portion	• Difficult to say – not enough area covered by trench mapping • The same mineralized vn types occur on the surface and 200m downhole
Geochemical Features	• Lack of anomalous Cu • Dominance in Au, associated W Fort Knox • Au-Bi-Te correl • W, Mo, Sb, As don't corell w Au CC • Au-As+/-Bi, Te –W, and base metal vn Ag-Bi-Pb+/- As, Au correl DG • Au-Bi-Te? SheelDome • Au-Te-Bi+/-W,As and Ag-Pb-Zn-Cd-Sb+/-Cu,Au Brewery • Au-As and As-Sb-Hg	• Anomalous Cu or poor-Cu • Huge sulphur anomalies	• Lack of anomalous Cu • Low sulphur anomalies (?) Soils: • Na- K-Ca-Mg anomaly concentrated at Nugget North – metaseds • Au-As-Bi-W-Mo (weak anomaly?) in Nugget Top – intrusion • Cu-Mo-Ag (weak anomaly) in Nugget NE – intrusion • Au-As-Bi on Raven – intrusion DrillCore - intrusion: **Au – Bi** **Au – Cu – Fe – S** **Ag – Pb - S** **Ag – Cu – S** **As – S** **Bi – Fe – S** **Sb - S** **Fe – S** **Drill core – metaseds:** **Au – As** **Ag – Pb – Sb – Zn** **Cu – Fe – S** **Fe - S** **Trench – intrusion:** **Au – Bi** **Ag – Sb – Pb** **Trench – metaseds:** **Au – Bi** **Au – Cu – Bi – Fe – Te – As** **Ag – Pb - Sb – Te ?** **Trench – All:** **Au – Bi** **Ag - Pb – Sb**
Geophysics	• Low magnetic signature • Plutons have low magnetic responses, however pyrrhotite concentrations in hornfelsed aureoles may yeld doughnut-shaped signatures for exposed plutons	• IP chargeability anomaly – barren pyrite from phyllic altrn or mineralized py • Magnetic anomaly from abundant hydrotherm magnetite, po, mag-bearing skarn-caution estructed magnetite in phyll zones • Gamma ray spectrometry surveys-K altrn	• Low magnetic signature – demagnetized (retrograde) magnetite or a lack of magnetite ??

Source: From (Corbett, 2009), (Hart, 2007), and (Victoria Gold Corp 2021)

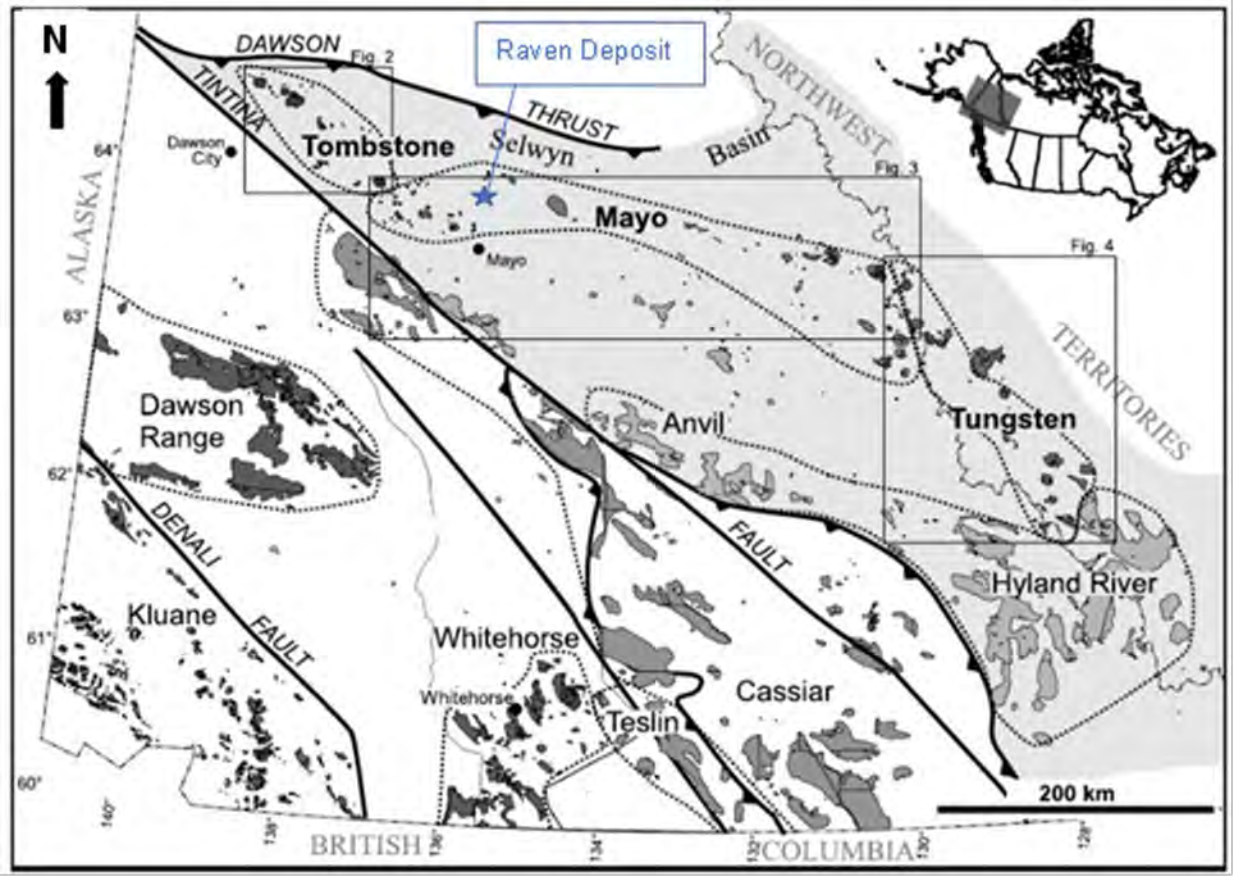

Figure 8-1: Regional Tectonic Elements of Yukon and Distribution of Mid-Cretaceous Plutonic Suites

Source: Modified from (Hart et al. 2002)

Figure 8-2: Map of the Tintina Gold Province for the Yukon Territory and Alaska

Source: Modified from (Hart et al. 2002)

9 EXPLORATION

9.1 Victoria Gold Exploration on the Raven Property

The Nugget stock is the second largest on the Dublin Gulch Property (second only the Dublin Gulch Stock that hosts the Eagle Gold Mine). The Nugget intrusion is akin to the Eagle Deposit host rock, and has been the subject of limited historic exploration work due to historic inaccessibility of the area. In 2017, an access trail was constructed that allowed vehicular access to the high-priority Nugget target. During this trail construction, a float sample of galena was discovered in what is now the Raven Zone, this eventually led to the 2018 Raven Zone trench discovery that was accomplished through surface trenches designed to test the contact of the Nugget Stock and exposed a series of parallel northernly dipping massive sulphide veins up to 2.5m in width.

Victoria Gold's Exploration team has repeatedly conducted successful exploration programs through the years of; 2018, 2019, 2020, and 2021. A total of 78 diamond drill holes have been collared in the Raven Zone (18,217.40 metres), 55 sampled trenches (7,443.00 metres), and 9,274 soil geochemical samples have been collected and assayed. Additionally, multiple airborne and ground-based geophysical surveys have been completed over the Nugget Stock/Raven Zone. The compiled extent from each season's exploration programs is presented in Table 9-1.

Structural controls related to the mineralization at Raven is evident within the surface trenches and diamond drill-core and this information has been of critical importance to the creation of the Raven Mineralization model utilized in the development of the maiden Mineral Resource Estimate presented in this report. The on-going collection of similar data will continue to inform and guide all next phase efforts at Raven, to vector in to the large high-grade dilatational fracture zone which is interpreted to host the Raven Deposit.

Table 9-1: Raven Exploration Work Summary

	Drilling		Trenches		Soil Samples
Year	**Meterage**	**Count**	**Meterage**	**Count**	**Count**
2018	1,754.90	9	1,447.00	13	2,448
2019	1,616.80	9	5,438.00	37	3,018
2020	7,452.60	31	558.00	5	3,808
2021	7,393.10	29	-	-	-
Total	**18,217.40**	**78**	**7,443.00**	**55**	**9,274**

9.1.1 (2017) Raven Exploration Program

Grab samples collected during prospecting of the general area in 2017 from galena bearing veins uncovered during Nugget access construction returned values from trace up to;

- 1,440 g/t Ag
- 63.44 % Pb
- 1.435 % Zn

Other grab samples from additional bearing veins (jamesonite) returned values from trace up to;

- 0.515 g/t Au
- 82 g/t Ag
- 20.30 % Pb
- 8.34 % Sb
- 4.20 % As

Grab samples collected from a historic trench within the Nugget Stock returned values from trace up to;

- 0.202 g/t Au
- 3.7 g/t Ag
- 1.3 % As

One drill hole was designed and conducted late in the 2017 season (DG17-970C) to test the Nugget Stock. The hole was drilled at 150.00 metres with low returns of Au and Ag. Additional work completed on the Raven Deposit in 2017 area included; orthophotographs, LIDAR, airborne magnetic and radiometric surveys (See Section 7).

9.1.2 (2018) Raven Exploration Program:

The 2018 Raven exploration program was designed to build upon the previously discovered grab sample noted above from 2017. This season's exploration program consisted of; surface trenches, preliminary structural analyses, mapping, and soil geochemical sampling. The season completed with; 13 surface trenches (highlights in Table 9-2) totalling 1,447.00 metres, 2,448 soil geochemical samples, and nine (9) diamond drillholes totalling 1,520 metres. Raven trenches with Au and Ag values are shown in Figure 9-6 and Figure 9-7. Trench TR18-33 sampled in 2018 assayed at 3.51g/tonne gold over 124.00m (Figure 9-1). Additional work conducted in the 2018 season was comprised of; a 192 line-kilometre ground-based magnetometer, 6,600 metres of 2D Induced Polarization lines, and a 172 line-kilometre VLF survey plus downhole geophysical investigations.

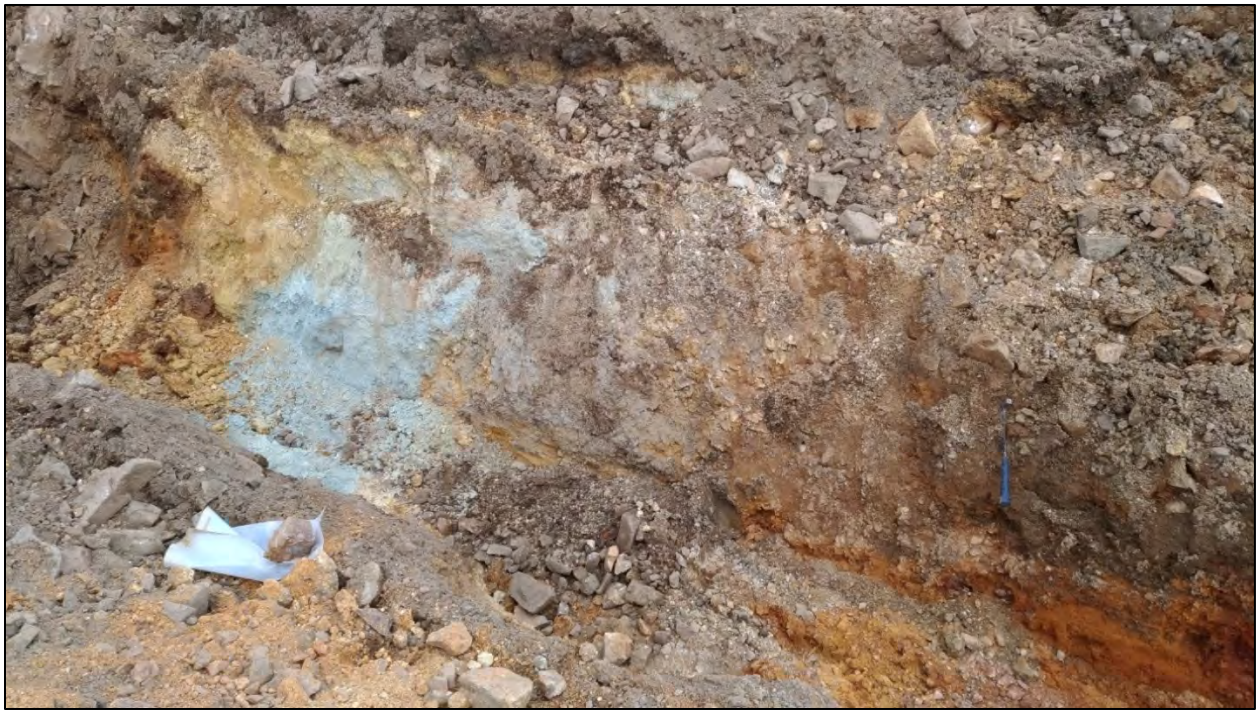

Figure 9-1: 2018 Raven Discovery Trench

Source: Victoria Gold Corp. (2018)

Table 9-2: Highlighted 2018 Raven Surface Trench Analytical Results

Trench	From (m)	To (m)	Length (m)	Gold (g/t)	Silver (g/t)
TR18-24	**10.0**	**26.0**	**16.0**	**0.22**	**-**
TR18-33	**28.0**	**152.0**	**124.0**	**3.51**	**-**
including	54.0	56.0	2.0	76.1	-
including	82.0	140.0	58.0	4.68	10.16
including	100.0	108.0	8.0	11.4	11.78
TR18-37	**0.0**	**4.0**	**4.0**	**1.07**	**1.7**
including	20.0	70.0	50.0	4.15	7.21
including	20.0	38.0	18.0	7.15	5.56
including	52.0	70.0	18.0	4.31	13.22
TR18-38	**0.0**	**4.0**	**4.0**	**7.25**	**25.55**
including	16.0	36.0	20.0	0.95	8.62

Source: Victoria Gold Corp. (2022)

9.1.3 (2019) Raven Exploration program

The 2019 Raven drill program was designed to follow up on the high-grade, on surface, gold mineralization discovered in late of 2018 from surface trenches and limited diamond drilling. The 2019 program consisted of the construction, mapping, and sampling of surface trenches built in all directions from the 2018 Discovery Trench and drill testing of the Raven Zone on nominal 50-metre step outs from the 2018 drill fence and surface trenches.

During the 2019 drilling campaign, further evaluation of the Nugget Intrusive Stock, was undertaken as well as new access construction into areas in the eastern Dublin Gulch claim block that were previously inaccessible. Nine (9) short angled diamond drill holes (average hole depth of 180 metres) totaling 1,616.80 metres were drilled over approximately 400 m^2 of the > 1 km^2 Raven Zone (as defined from 2018 soils geochemical survey coincident As-Bi-Au; which tested over 300 metres of strike length across the target.

In total, 37 surface trenches (5,438.00 metres) were constructed, mapped, and sampled at Nugget, with over 3,300 metres of those trenches focused on Raven (exploration trenches also tested Nugget NW (Figure 9-8). Soil geochemical sampling collected 3,018.00 samples this season.

At Raven, the trench program returned strongly anomalous scorodite, bismuth, and siderite bearing sulphide veins within altered granodiorite lithologies along strike of the previously discovered mineralization (Figure 9-2). The veins and vein sets exposed were remarkably consistent across Raven and preliminary mapping suggested these mineralized veins occur with steep to moderate dips (~60) with West to Southwest strike. Intense shearing deforms the exposed vein sets along an East-West direction. Notably, the assays returned from the 2019 trenches (highlights in Table 9-3) exhibited markedly reduced silver grades as compared to the high silver grades identified in 2018. Raven trenches with Au values are shown in Figure 9-9.

The 2019 Raven trenches covered an area of over 800 m^2 out of the large 1,800 metre long by 900-metre-wide soil anomaly, that remains open to the South and East.

Figure 9-2: Trench Sampling in 2019

Source: Victoria Gold Corp. (2019)

Table 9-3: Highlighted 2019 Raven Surface Trench Analytical Results

Trench	From (m)	To (m)	Length (m)	Gold (g/t)	Silver (g/t)
TR19-05	**76.0**	**102.0**	**26.0**	**1.22**	**-**
including	76.0	78.0	2.0	5.58	8.00
including	90.0	92.0	2.0	6.54	7.00
including	100.0	102.0	2.0	3.18	6.00
including	214.0	256.0	42.0	0.70	-
including	214.0	226.0	12.0	1.15	-
including	214.0	216.0	2.0	2.41	-
including	224.0	226.0	2.0	3.83	29.00
TR19-06	**0.0**	**68.0**	**68.0**	**0.58**	**-**
including	46.0	56.0	10.0	2.14	-
including	46.0	48.0	2.0	4.21	21.00
TR19-07	**0.0**	**126.0**	**126.0**	**0.74**	**-**
including	12.0	18.0	6.0	1.57	-
including	48.0	108.0	60.0	1.12	-
including	72.0	76.0	4.0	7.34	2.00
TR19-12	**0.0**	**94.0**	**94.0**	**0.54**	**-**
including	4.0	6.0	2.0	16.40	3.00
including	86.0	90.0	4.0	2.56	22.00
TR19-13	**24.0**	**34.0**	**10.0**	**6.64**	**-**
including	24.0	30.0	6.0	11.05	13.00
TR19-15	**0.0**	**66.0**	**66.0**	**1.48**	**-**
including	18.0	30.0	12.0	7.91	-
including	24.0	26.0	2.0	35.70	8.00
TR19-20	**236.0**	**248.0**	**12.0**	**0.80**	**-**
including	246.0	248.0	2.0	4.31	-
TR19-23	**6.0**	**10.0**	**4.0**	**1.65**	**-**
including	8.0	10.0	2.0	3.09	3.00
TR19-29	**4.0**	**10.0**	**6.0**	**0.45**	**-**
including	26.0	28.0	2.0	0.49	123.00
TR19-32	**70.0**	**72.0**	**2.0**	**1.12**	**-**
including	136.0	140.0	4.0	0.98	-
TR19-37	**8.0**	**10.0**	**2.0**	**2.50**	**-**

Source: Victoria Gold Corp. (2020)

9.1.4 (2020) Raven Exploration Program

The 2020 Raven exploration campaign increased the mineralized strike length of the Raven target to 750 metres, more than doubling the previously known strike length. Diamond drilling in conjunction with surface trenches, geologic mapping and soil geochemical surveys were utilized during the course of the campaign. Oriented core (over 900 measurements taken) was collected over Raven in this season using Reflex's Act 3 and, in unison with the detailed core logging and surface mapping, was utilized to help vector in on mineralization controls. The Exploration Program culminated in the collaring of 31 diamond drill holes totalling 7,452.60 metres; 558.00 metres of surface trenching (5 trenches–Figure 9-3), and the collection of 3,808 soil samples. Raven trenches from 2018 through 2021 are shown in Figure 9-10.

Figure 9-3: Scorodite in Trench - Sampled in 2020

Source: Victoria Gold Corp. (2020)

9.1.5 (2021) Raven Exploration Program

The 2021 Raven exploration program was designed to build upon the previously defined 750m mineralized strike length defined from 2018-2020 fence-based diamond drilling. Surface trenches, detailed structural analysis, geologic mapping/prospecting, and diamond drilling were used to this end. The 2021 program successfully increased the strike length of Raven to ~1.3 km (particularly to the east in an area covered by overlying metasedimentary lithologies), and completed 29 drill holes with a total of 7,393.10 metres.

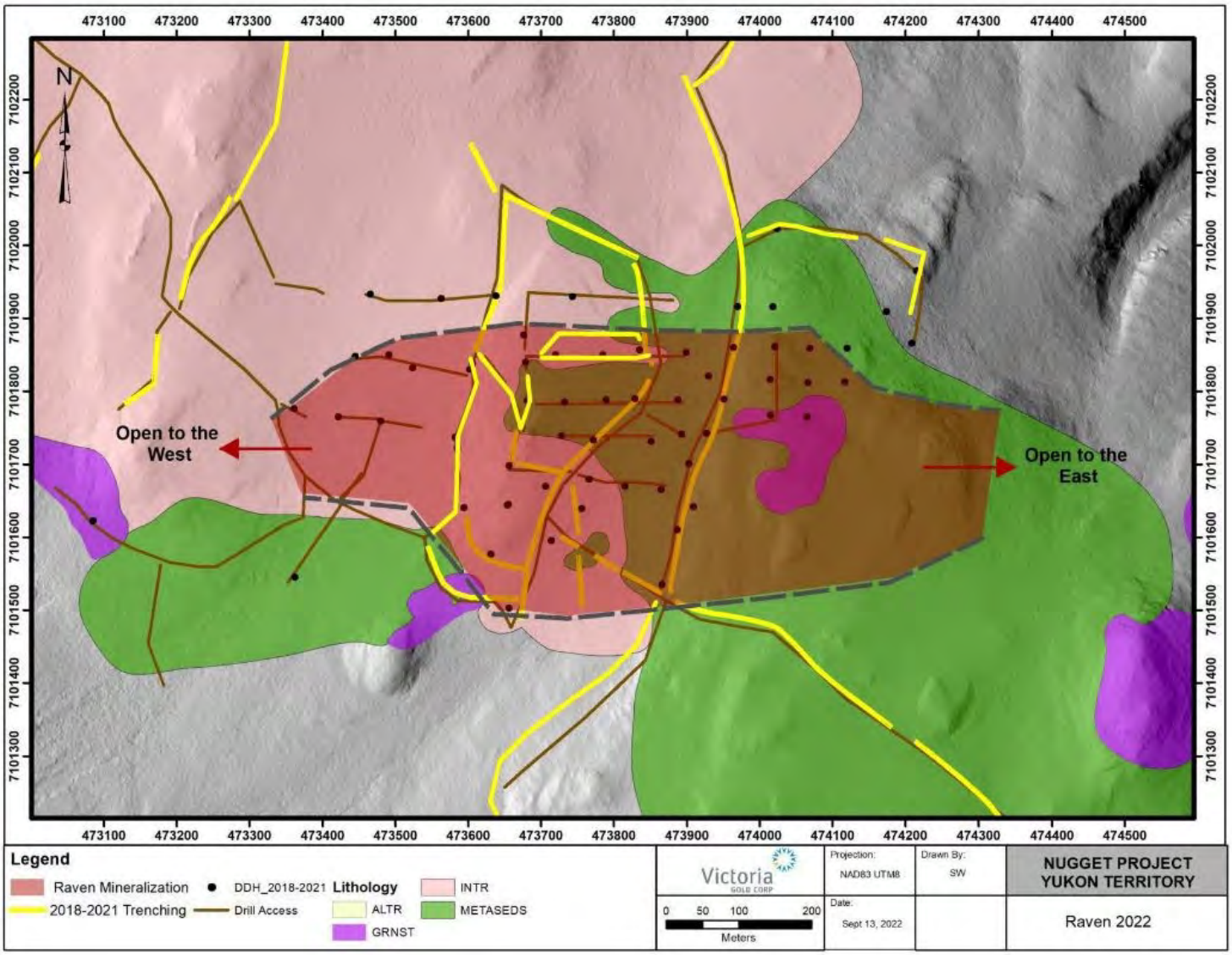

Figure 9-4: Raven Project Trenches and Geology (2018-2021)

Source: Victoria Gold Corp. (2022)

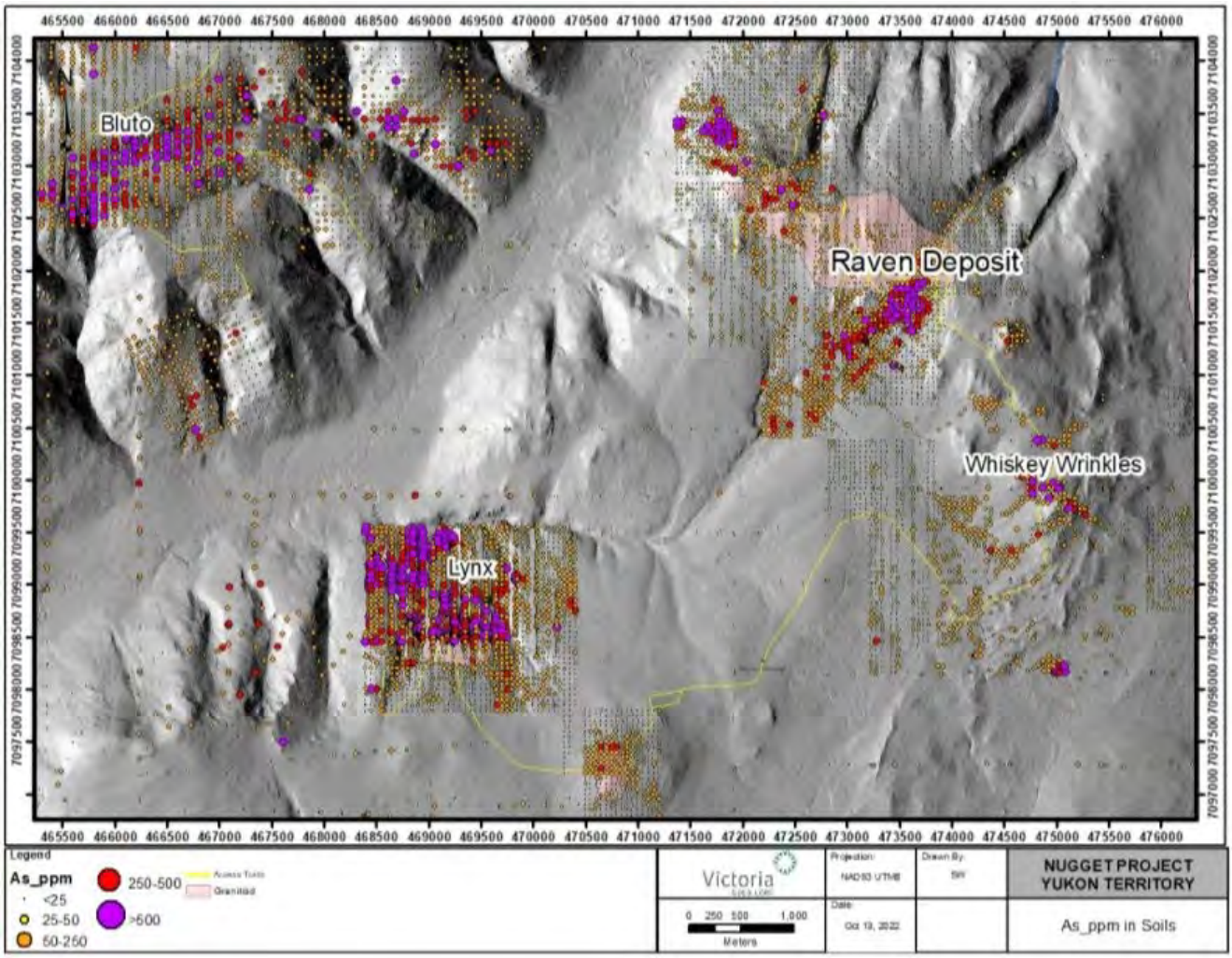

Figure 9-5: Raven Deposit As-in-Soils Map

Source: Victoria Gold Corp. (2022)

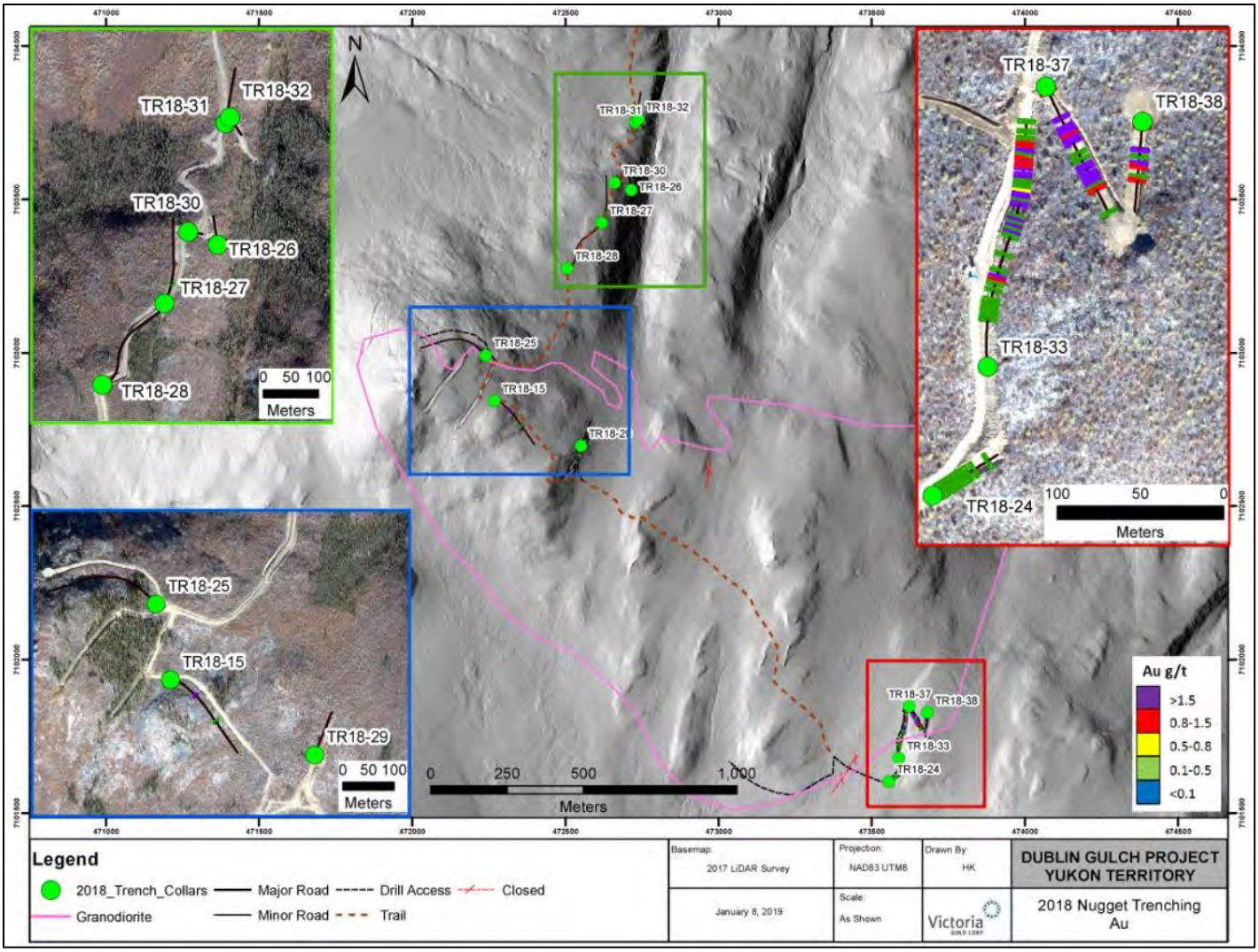

Figure 9-6: Nugget-Raven Trenching Au (2018)

Source: Victoria Gold Corp. (2018)

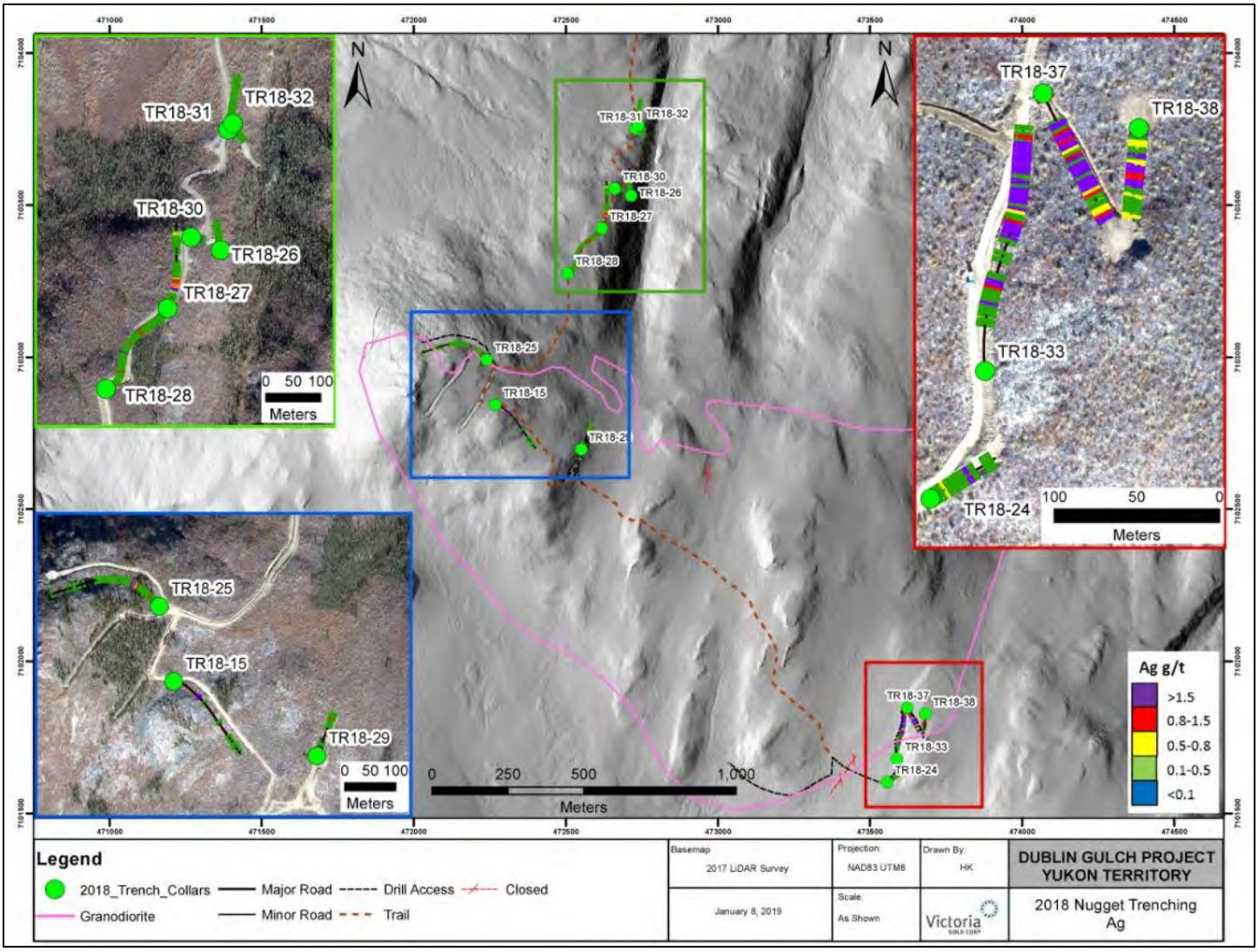

Figure 9-7: Nugget-Raven Trenching Ag (2018)

Source: Victoria Gold Corp. (2018)

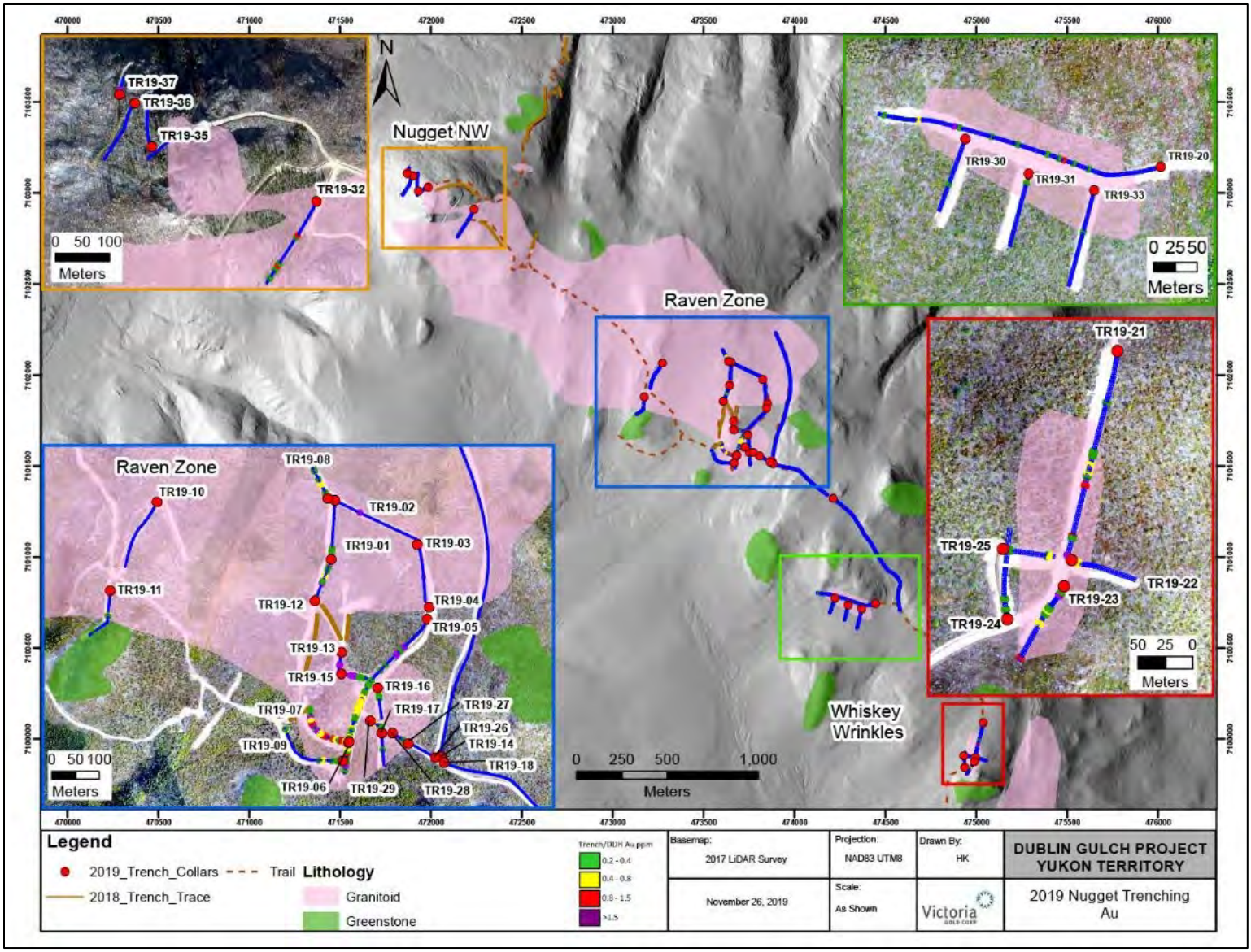

Figure 9-8: Nugget-Raven Trenching Au (2019)

Source: Victoria Gold Corp. (2019)

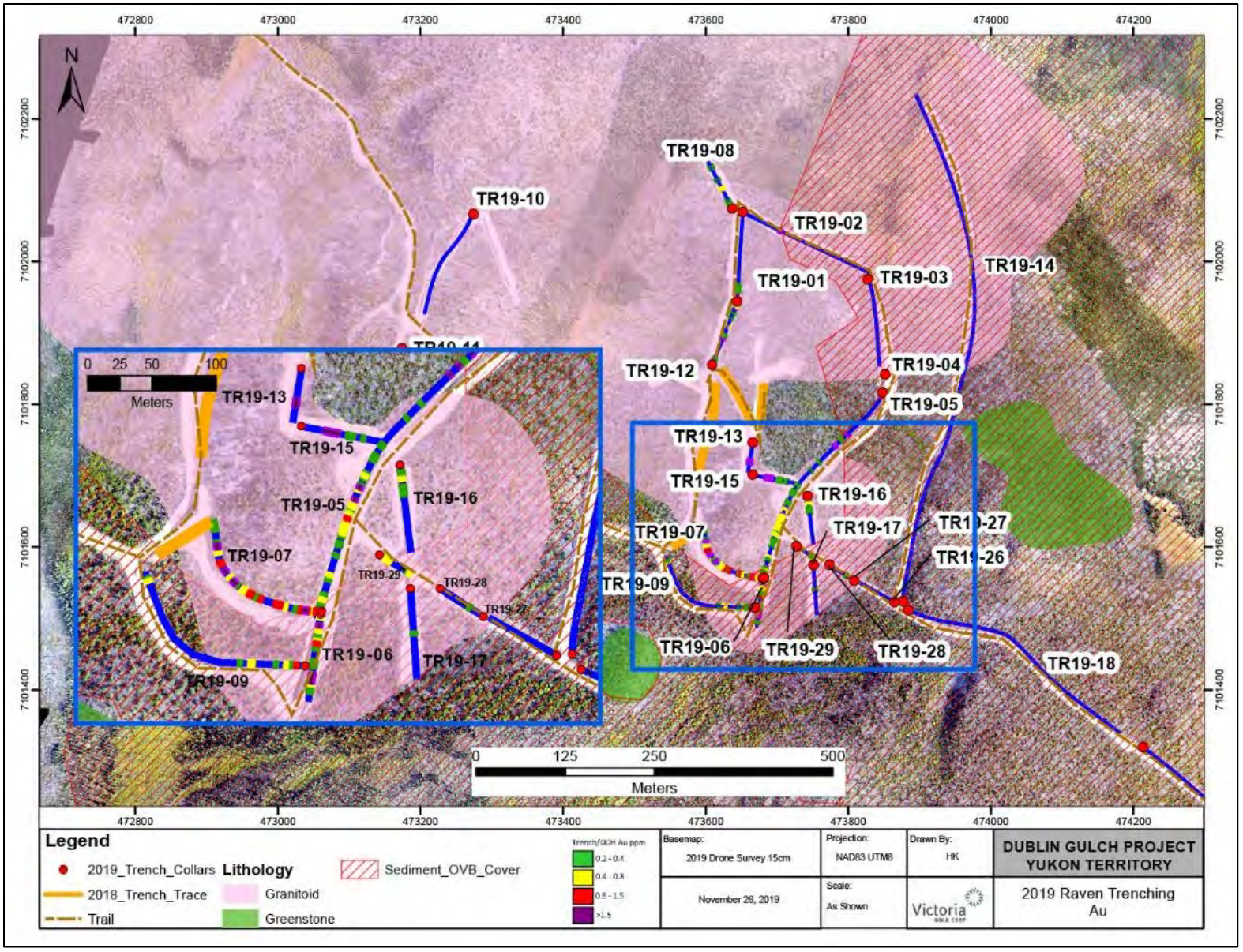

Figure 9-9: Raven Zone Trenching Au and Lithologies Detail (2019)

Source: Victoria Gold Corp. (2022)

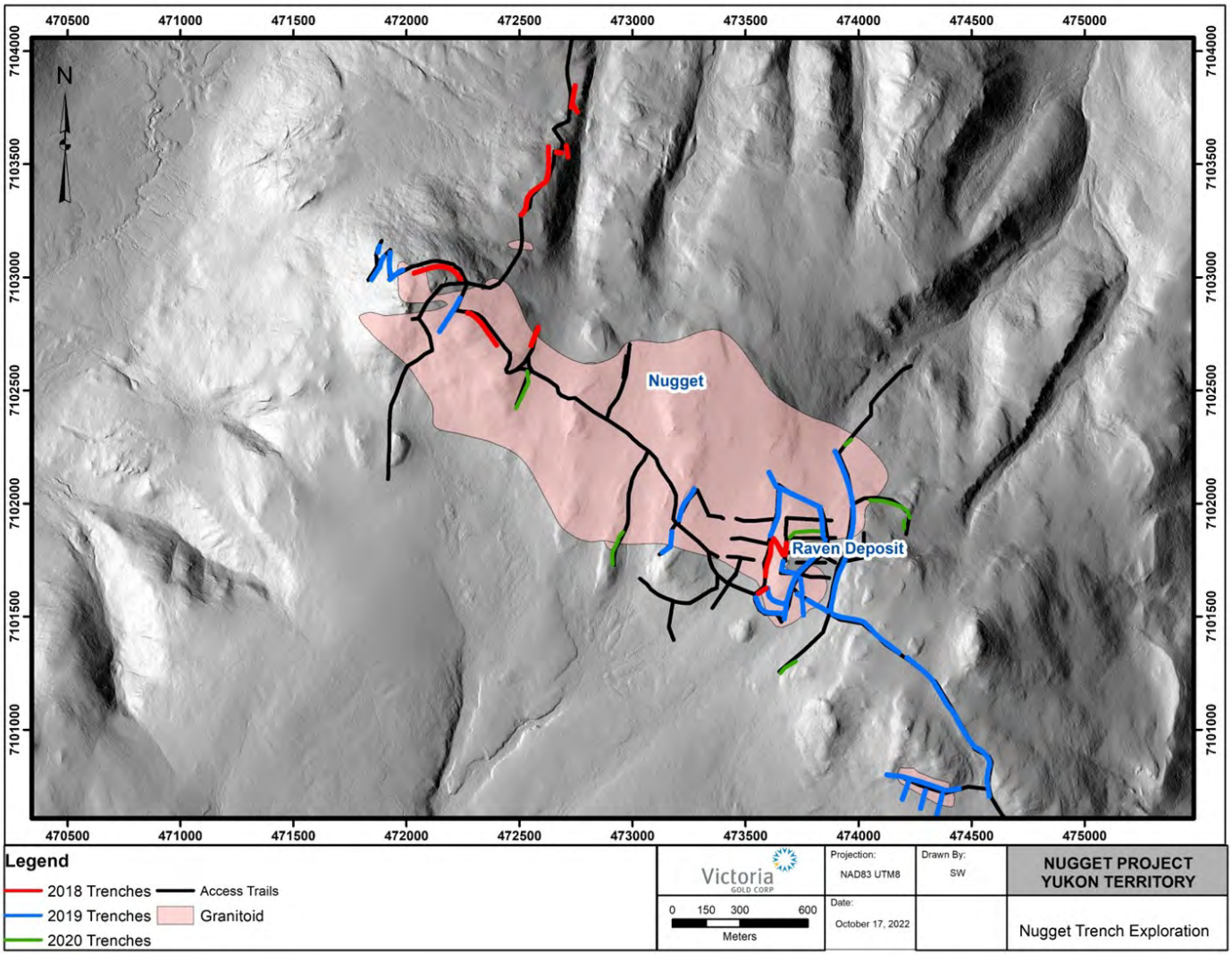

Figure 9-10: Raven Trench Compilation Map

Source: Victoria Gold Corp. (2022)

10 DRILLING

Drilling in the Eastern regions of the Dublin Gulch Claim Block has been focused primarily on the Raven Zone, with the Lynx and Whiskey Wrinkles targets at subordinate levels. Victoria Gold has conducted diamond drilling programs in each of 2018, 2019, 2020, and 2021 (Figure 10-5 and Figure 10-6). Table 10-5 presents total metres drilled at the Raven Deposit through 2021. Highlighted assay results from these drill programs are presented in the sections and associated tables below. The resultant data was sufficient for the initial Mineral Resource estimation for the Raven Deposit, as described in Section 14 of this report.

10.1 (2018) Raven Drilling Program:

The Raven diamond drill program in 2018 was to test the potential of a high-grade, on surface, gold mineralization that was discovered without the aid of analytical results as both surface trenches and soils geochemical results were not received at the time the drills were collared.

Victoria Gold completed nine (9) diamond drillholes for 1,754.90 metres (highlights in Table 10-1). An example of mineralized Raven core from 2018 is shown in Figure 10-1.

Figure 10-1: Raven Diamond Drill Hole Core (2018)

Source: Victoria Gold Corp. (2018)

Table 10-1: Highlighted 2018 Raven Diamond Drill Hole Intercepts

Hole ID	From (m)	To (m)	Length* (m)	Gold (g/t)	Silver (g/t)
NG18-006C	**3.4**	**207.6**	**204.2**	**0.32**	**1.44**
including	3.4	104.9	101.5	0.57	2.27
including	39.6	41.0	1.4	9.6.0	48.00
including	61.8	94.8	33.0	1.03	3.46
including	61.8	78.0	16.2	1.76	1.54
including	61.8	71.9	10.1	2.79	8.6.0

Hole ID	From (m)	To (m)	Length* (m)	Gold (g/t)	Silver (g/t)
including	61.8	63.0	1.1	12.1	28.80
including	93.8	104.9	11.1	0.64	2.57
including	93.8	94.8	1.0	4.95	22.00
including	180.1	191.3	11.2	0.49	4.91
including	180.1	180.9	0.8	4.43	35.10
NG18-007C	**67.7**	**88.3**	**20.6**	**1.49**	**11.56**
including	80.6	88.3	7.7	3.36	30.60
NG18-008C	**52.8**	**60.9**	**8.1**	**0.48**	**1.06**

Source: Victoria Gold Corp. (2018)

10.2 (2019) Raven Drilling Program

The Raven drill program was to follow up on the high-grade, on surface, gold mineralization discovered in late 2018 by surface trenches and limited diamond drilling. The 2019 program consisted of extensive surface trenches and drill testing of the Raven Target on nominal 50-metre step outs from the 2018 drill fence and surface trenches.

During the 2019 drilling campaign, further evaluation of the Nugget intrusive stock, which hosts the Raven Target, was undertaken as well as new access construction into areas in the eastern Dublin Gulch claim block that were previously inaccessible. An example of mineralized Raven core from 2019 is shown in Figure 10-2.

Nine short angled diamond drill holes (average hole depth of 180 metres) totaling 1,617 metres were drilled over approximately 400 m^2 of the > 1 km^2 Raven Target in 2019; which tested over 300 metres of strike length across the target (highlights in Table 10-2).

Figure 10-2: Raven Diamond Drill Hole Core (2019)

Source: Victoria Gold Corp. (2019)

Table 10-2: Highlighted 2019 Raven Diamond Drill Hole Intercepts

Hole ID	From (m)	To (m)	Length (m)	Gold (g/t)
NG19-009C	**81.1**	**98.1**	**17.1**	**0.39**
NG19-010C	**81.3**	**134.3**	**53.0**	**0.45**
including	81.3	89.4	8.1	2.04
NG19-011C	**28.8**	**117**	**88.1**	**0.60**
including	16.7	40.5	23.9	0.92
including	28.8	31.6	2.8	7.72
including	91.1	117	25.9	1.15
including	91.1	93	1.8	9.27
NG19-012C	**29.4**	**195.7**	**166.4**	**0.46**
including	29.4	71.8	42.4	1.05
including	29.4	30.5	1.1	14.90
including	65.9	71.8	5.9	4.48
NG19-013C	**14.1**	**153.4**	**139.3**	**0.41**
including	72.5	91.7	19.2	0.89
including	72.5	73.5	1.0	9.90
NG19-014C	**16.8**	**119.1**	**102.4**	**0.32**
including	16.8	17.2	0.4	18.20
including	78.2	97	18.8	0.95
NG19-015C	**4.4**	**198.3**	**193.9**	**0.35**
including	48.6	91.4	42.8	0.94
including	68.2	84.1	15.9	2.35
including	82.1	84.1	2.0	12.80
NG19-016C	**33.9**	**176.4**	**142.6**	**0.45**
including	100.1	106.1	6.0	2.64
including	161.6	176.4	14.8	2.05
NG19-017C	**15.2**	**62.3**	**47.1**	**0.43**
including	58.1	62.3	4.2	3.93

10.3 (2020) Raven Drilling Program

The Raven drilling program in 2020 was designed to test underneath the known metasedimentary cap. Drill core results and analyses appeared to represent low angle thrusting of the metasediments over top of the granodiorite (Figure 10-3). The contact zone between the metasediments and the granodiorite was defined by structures analysed in the drill core, such as; gouge, slickenlines, fault zones, and brecciation. The contact contained stronger alteration (sericite, silica, oxidation) and was consistently mineralized throughout. The program culminated in the collaring of 31 diamond drill holes totalling 7,452.60 metres (highlights in Table 10-3); 558.00 metres of surface trenches, the collection of 3,808 soil samples and the shipment of more than 6,000 core and trench samples.

Figure 10-3: Raven Diamond Drill Hole Core Contact Zones (2020)

Source: Victoria Gold Corp. (2020)

Table 10-3: Highlighted 2020 Raven Diamond Drillhole Intercepts

Hole ID	From (m)	To (m)	Length (m)	Gold (g/t)	Silver (g/t)
NG20-036C	**115.6**	**128.0**	**12.4**	**0.59**	**1.23**
NG20-037C	**35.7**	**209.9**	**174.2**	**0.76**	**2.33**
including	90.4	109.4	19.0	3.95	2.63
including	96.9	97.9	1.0	61.10	10.00
including	153.7	157.0	3.3	12.00	45.05
NG20-038C	**141**	**267.0**	**126.0**	**0.68**	**4.31**
including	166.1	253.0	86.9	0.93	5.59
including	175.1	215.4	40.3	1.39	9.58
including	183.1	193.6	10.5	2.13	24.80
including	192.1	193.6	1.5	7.56	100.00
including	210.4	215.4	5.0	3.44	13.54
including	248.5	253.0	4.5	3.75	5.43
NG20-039C	**48.0**	**105.0**	**57.0**	**0.32**	**2.31**
including	81.6	105.0	23.4	0.46	2.12
including	81.6	83.3	1.7	3.57	16.00
NG20-040C	**5.2**	**194.2**	**189.0**	**0.31**	**9.46**
including	44.2	45.7	1.5	6.26	2.00
including	146.1	171.1	25.0	0.45	58.47
NG20-041C	**111.3**	**169.3**	**58.0**	**0.37**	**2.65**

Hole ID	From (m)	To (m)	Length (m)	Gold (g/t)	Silver (g/t)
including	111.3	127.2	15.9	0.98	5.44
NG20-042C	**167.9**	**332.0**	**164.1**	**0.40**	**3.40**
including	206.7	241.4	34.7	0.81	3.31
including	219.2	221.0	1.8	6.16	1.00
including	289.8	332.0	42.2	0.59	5.67
including	299.8	306.5	6.7	1.70	26.21
NG20-043C	**45.9**	**185.9**	**140.0**	**0.40**	**4.48**
including	45.0	53.9	8.9	2.78	3.84
including	45.9	46.8	0.9	19.40	26.00
including	106.3	149.4	43.1	0.58	10.60
including	144.8	149.4	4.6	2.87	59.30
NG20-044C	**191.4**	**317.6**	**126.2**	**0.32**	**2.19**
including	191.4	192.2	0.8	13.20	11.00
including	239.4	240.3	0.9	8.29	8.00
including	295.7	317.6	21.9	0.45	4.33
NG20-045C	**113.5**	**220.8**	**107.3**	**0.92**	**3.13**
including	121.5	172.2	50.7	1.63	3.66
including	132.7	146.4	13.7	4.48	10.64
including	143.1	144.4	1.3	42.80	68.00
including	157.2	159.2	2.0	5.37	2.00
including	209.1	220.8	11.7	0.92	2.10
NG20-047C	**75.9**	**217.1**	**141.2**	**0.47**	**2.95**
including	130.1	152.7	22.6	1.23	5.83
including	130.1	130.7	0.6	14.30	36.00
including	149.6	150.2	0.6	12.40	7.00
including	216.1	217.1	1.0	25.10	66.00
NG20-048C	**35.8**	**94.5**	**58.7**	**0.70**	**3.50**
including	55.9	64.2	8.3	1.75	6.72
including	63.1	64.2	1.1	9.71	28.00
including	93.2	94.5	1.3	15.20	74.00

10.4 (2021) Drilling Program

The 2021 Raven exploration program was designed to build upon a previously defined 750m strike length from fence-based diamond drilling, surface trenches, additional detailed structural analysis, and mapping. The 2021 program successfully increased the strike length of Raven to ~1.3 km (particularly to the west in an area covered by overlying metasedimentary lithologies), and completed 29 drill holes with a meterage total of 7,393.10 (m) (highlights in Table 10-4). An example of mineralized Raven core from 2021 is shown in Figure 10-4.

Figure 10-4: Raven Diamond Drill Hole Core (2021)

Source: Victoria Gold Corp. (2021)

Table 10-4: Highlighted 2021 Raven Diamond Drill Hole Intercepts

Hole ID	From (m)	To (m)	Length (m)	Gold (g/t)
NG21-048C	**116.3**	**154.0**	**37.7**	**0.54**
including	152.8	154.0	1.2	8.71
NG21-049C	**100.3**	**184.8**	**84.5**	**0.40**
including	146.4	184.8	38.4	0.63
NG21-050C	**46.9**	**176.9**	**130.0**	**0.50**
including	46.9	111.2	64.3	0.65
including	97.7	111.2	13.5	1.67
including	109.7	111.2	1.5	10.10
including	148.6	176.9	28.3	0.78
including	155.8	176.9	21.1	1.01
NG21-051C	**39.5**	**144.5**	**105.0**	**0.50**
including	70.8	84.4	13.6	1.07
including	106.5	107.7	1.2	15.00
NG21-052C	**199.0**	**208.5**	**9.5**	**1.64**
including	199.9	200.5	0.6	18.40
including	317.8	318.7	0.9	16.60
NG21-053C	**91.0**	**103.2**	**12.2**	**1.16**
NG21-058C	**19.5**	**112.8**	**93.3**	**0.41**
including	19.5	30.6	11.1	1.23

Hole ID	From (m)	To (m)	Length (m)	Gold (g/t)
including	75.7	76.4	0.7	16.10
NG21-061C	**70.1**	**146.8**	**76.7**	**0.45**
including	92.4	107.5	15.1	1.74
including	92.4	94.8	2.4	7.12
NG21-062C	**219.5**	**307.7**	**88.2**	**0.62**
including	286.7	307.7	21.0	1.49
including	299.0	301.0	2.0	6.23
NG21-063C	**9.1**	**133.8**	**124.7**	**0.44**
including	10.9	12.2	1.3	29.60
NG21-065C	**197.7**	**213.5**	**15.8**	**1.21**
including	197.7	198.4	0.7	17.50
including	235.1	260.0	24.9	0.82
NG21-067C	**245.0**	**315.0**	**70.0**	**1.25**
including	264.5	265.0	0.5	33.80
including	313.5	315.0	1.5	8.30

10.5 Drilling Process

Since 2018, core drilling was contracted out to Kluane Drilling of Whitehorse, Yukon. Holes were surveyed by a downhole instrument from REFLEX, as soon as the hole was stable, and with no interference from casing, at 30 m intervals thereafter, and at the bottom of the hole.

Core was drilled primarily as HTW core size with reduced drilling in NTW size when drilling production declined due to ground conditions. Core was transferred from the core tube into boxes by the drill crew who marked the end of each run with a crayon marker. Hole depth was measured in imperial units (feet) and subsequently converted into metric units (metres) on the depth markers. Core was transported by the drilling company from the drill site to the core logging facility that is located in the camp.

Core was laid out for geo-teching/logging inside the core shed to be washed and prepped for sampling. Core was first geo-teched, including measurements of: block interval measurements (proper lengths, correct drilling numbers), core recovery (metre lengths and total rock competency % of drill run), RQD (Rock Quality Designation – quality of core taken from borehole), vein density (number of veins over run, veins per metre, average thickness), natural breaks, and rock hardness.

Core logging observations were then executed and transferred into an organized computer database. Significant observations include rock type, weathering, alteration, foliation angle and intensity, fracture angle and intensity as well as descriptions of any veins present. Several types of alteration (oxidation, silicification, sericitization) were quantified from zero to five with zero equating to no alteration and five representing complete alteration. There is no unique convention with respect to fracture intensity although the attempt was made among those logging to apply the same criteria. The majority of the samples were 1.5 m in length but did not exceed 2.0 m in length and were shorter if lithological contacts or significant variations in sulphide content were present. In general, the entire length of the hole was sampled.

When logging was complete, sample tags were affixed to the core box at the start of each sample interval. Each sample tag was comprised of three pieces: one for the core box, one for the sample bag into which the sample was placed, and the third which remains in the sample book.

Given the variable orientation of mineralized quartz veins, the relationship between sample length and thickness of mineralization is also variable. However, given that the sampling was continuous, and the mineralization is a bulk target, the variability of this relationship is not considered to be detrimental to the objectives of the sampling program.

Drilling was done as angle holes across the primary strike orientation of the mineralization. The drilling methods, and sample handling procedures are in line with industry norms and are acceptable methods for defining the gold mineralization at the Raven Deposit.

Table 10-5: Total Drilled Meters at the Raven Deposit

	Drilling	
Year	**Meterage**	**Count**
2018	1,754.90	9
2019	1,616.80	9
2020	7,452.60	31
2021	7,393.10	29
Total	**18,217.40**	**78**

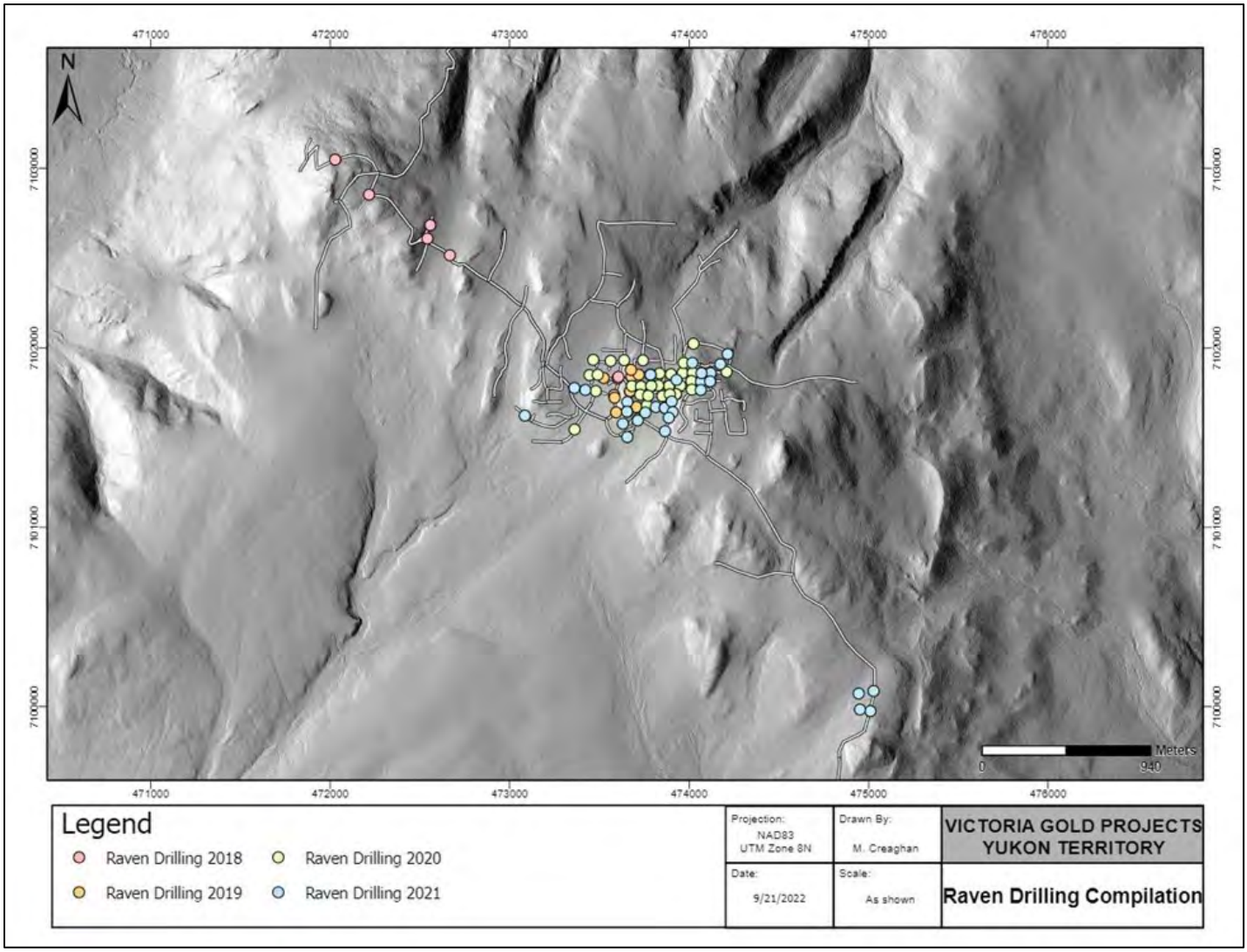

Figure 10-5: Victoria Gold Project Drilling Compilation Map

Source: Victoria Gold Corp. (2022)

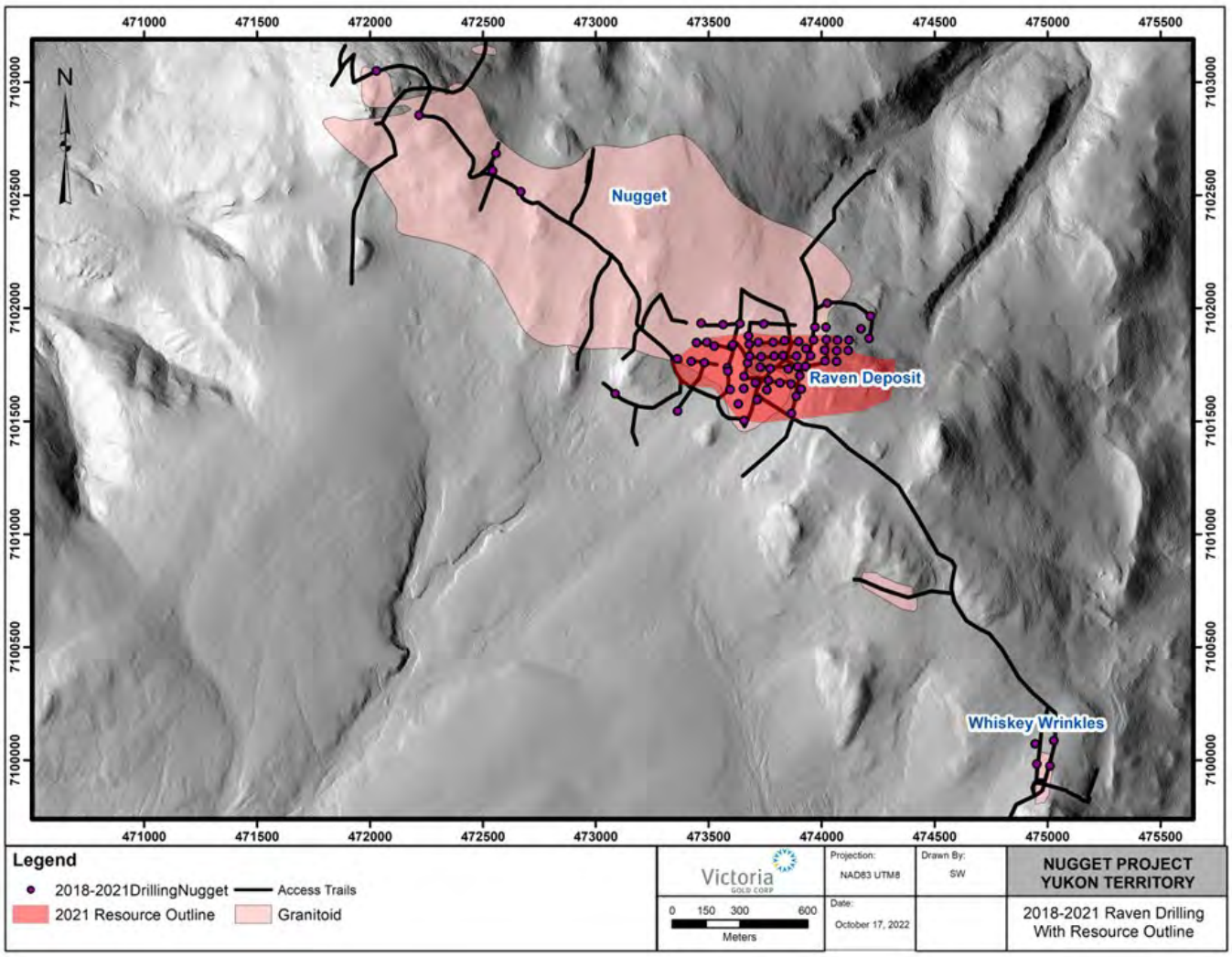

Figure 10-6: Victoria Gold Project Drilling Compilation Map with Raven Resource Outline

Source: Victoria Gold Corp. (2022)

11 SAMPLE PREPARATION, ANALYSES AND SECURITY

11.1 Sample Preparation, Analyses, and Security Overview

The methods of sample preparation, analysis and security for the 2018 through 2021 programs by Victoria Gold are well documented in the Yukon Assessment Reports. All drill core and field rock samples collected were processed in the below procedures. In the author's opinion, the sample preparation, security, and analytical procedures utilized to date are adequate for the MRE reported herein and follow industry standard practices.

Core was sawn in half by diamond saw; one half was bagged for assaying and the other half was kept for reference. The sample to be analyzed was put in a plastic bag that contained a sample tag. The sample number was also written on the outside of the bag. Each bag was then closed by zip ties and combined with others to fill woven plastic "rice bags" for shipping. Each rice bag was labelled with the numbers of the samples it contained. The rice bags were expedited by a contract shipper who picked up the samples in camp and delivered them to the assigned laboratory in Whitehorse and Burnaby. Standard chain-of-custody forms were used for the shipping process (Figure 11-2).

The boxes with the half-core are stored outside and cross-piled on pallets at Raven's core storage facility located at the Nugget Camp (Figure 11-1).

Holes were sampled in their entirety, unless recovery was particularly poor in any single drilled interval. Below presents a summary of each year's sample preparation, analysis and security.

11.1.1 (2018) Raven Core Processing

All exploration drill core from the 2018 program was logged, photographed, and split for shipment at Victoria Gold's Bluto Exploration Camp (Figure 9-5). Once split, half samples were placed back in the core boxes with the other half of split samples sealed in poly bags with one part of a three-part sample tag inserted within. Victoria's Bluto Exploration Camp where they were subsequently delivered to the Whitehorse, Yukon, sample preparation facility of Bureau Veritas Minerals. There, samples were crushed with prepared samples sent to Bureau Veritas Minerals', Vancouver, B.C. laboratory facilities. Bureau Veritas Minerals of Vancouver, B.C. subsequently pulverized all samples and utilized the aqua regia digestion ICP-MS 36-element AQ200 analytical package with FA450 50-gram Fire Assay with AAS finish for gold on all samples. A comprehensive system of standards, blanks and field duplicates was implemented for the 2018 drilling programs and were monitored as chemical assay data became available.

All 2018 soils samples were sent to the Bureau Veritas preparation facility in Whitehorse where samples were sorted and shipped to Bureau Veritas' Vancouver analysis facility where soils were dried, prepped and assayed utilizing a the AQ201 - 35 element ICP/MS Finish analytical package.

All exploration trench samples from the 2018 program were collected *in situ* by Victoria Geologists from constructed trenches and prepared for shipment at Victoria Gold's Bluto Exploration Camp where samples were subsequently delivered to the Whitehorse, Yukon, sample preparation facility of Bureau Veritas Minerals. There, samples were crushed with prepared samples sent to Bureau Veritas Minerals', Vancouver, B.C. laboratory facilities. Bureau Veritas Minerals of Vancouver, B.C. subsequently pulverized all samples and utilized the aqua regia digestion ICP-MS 36-element AQ200 analytical package with FA450 50-gram Fire Assay with AAS finish for gold on all samples. A comprehensive system of standards, blanks and field duplicates was implemented for the 2018 programs and were monitored as chemical assay data became available.

11.1.2 (2019) Raven Core Processing

All exploration drill core from the 2019 program was logged, photographed, split, and shipped from Victoria Gold's Nugget Exploration Camp with half samples placed back in the core boxes and alternate halves of split samples sealed in poly bags with one part of a three-part sample tag inserted within. Half core samples were sent directly to SGS Canada Inc.'s on-site assay laboratory at the Eagle Gold Mine where samples were crushed, pulverized and analyzed by 30-gram Fire Assay with AAS finish for gold via SGS protocol 'GC_FAA35V10'. A comprehensive system of standards, blanks and field duplicates was implemented for the 2019 Raven drilling programs and were monitored as chemical assay data became available. Samples above 0.2 ppm Au were sent for a repeat Fire Assay analysis as well as multi-element ICP.

All exploration trench samples from the 2019 program were collected by Victoria's geological team and shipped from Victoria Gold's Nugget exploration camp. Trench samples were sealed in poly bags with one part of a three-part sample tag inserted within. The trench samples were then delivered to the SGS sample preparation facility in Whitehorse, Yukon. There, samples were crushed and subsequently pulverized and sent to the SGS lab in Burnaby, British Columbia. All samples underwent the 4-acid digestion ICP-MS 33-element analytical package with FAA50V5 50-gram fire assay with AAS finish for gold on all samples. A comprehensive system of standards, blanks, field and prep duplicates was implemented for the 2019 programs and were monitored as chemical assay data became available.

11.1.3 (2020) Raven Core Processing

All exploration drill core from the Raven 2020 program was analyzed at SGS Canada Inc. of Burnaby, B.C. utilizing the GE_ICP40Q12, 34-element analytical package with GE_FAA50V5 50-gram fire assay with gravimetric finish for gold on all samples. All core samples were split on-site at Victoria's Nugget exploration camp and shipped to SGS Canada Inc.'s Whitehorse preparation facility. There, samples were sorted and crushed to appropriate particle size (coarse crush) and representatively split to a smaller size (250 grams) for shipment to SGS Canada Inc.'s Burnaby analytical laboratory facilities. A comprehensive system of standards, blanks and field duplicates has been implemented for the 2020 exploration campaign and is monitored as chemical assay data become available.

All exploration trench samples from the 2020 program were collected by Victoria's geological team and shipped from Victoria Gold's Nugget exploration camp. Trench samples were sealed in poly bags with one part of a three-part sample tag inserted within. The trench samples were then delivered to the SGS sample preparation facility in Whitehorse, Yukon. There, samples were crushed and subsequently pulverized and sent to the SGS lab in Burnaby, British Columbia. All samples underwent the 4-acid digestion ICP-MS 33-element analytical package with FAA50V5 50-gram fire assay with AAS finish for gold on all samples. A comprehensive system of standards, blanks, field and prep duplicates was implemented for the 2020 programs and were monitored as chemical assay data became available.

11.1.4 (2021) Raven Core Processing

All exploration drill core from the 2021 programs were analyzed at SGS Canada Inc. of Burnaby, B.C. utilizing the GE_ICP40Q12, 34-element analytical package with GE_FAA50V5 50-gram fire assay with gravimetric finish for gold on all samples. All core samples were split at Victoria's exploration facilities and shipped to SGS Canada Inc.'s Whitehorse preparation facility. There, samples were sorted and crushed to appropriate particle size (coarse crush) and representatively split to a smaller size (250 grams) for shipment to SGS Canada Inc.'s Burnaby analytical laboratory facilities. A comprehensive system of standards, blanks and field duplicates was implemented for the 2021 exploration campaign and is monitored as chemical assay data become available.

All exploration trench samples from the 2021 program were collected by Victoria's geological team and shipped from Victoria Gold's Nugget exploration camp. Trench samples were sealed in poly bags with one part of a three-part sample tag inserted within. The trench samples were then delivered to the SGS sample preparation facility in Whitehorse, Yukon. There, samples were crushed and subsequently pulverized and sent to the SGS lab in Burnaby, British Columbia. All samples underwent the 4-acid digestion ICP-MS 33-element analytical package with FAA50V5 50-gram fire assay with AAS finish for gold on all samples. A comprehensive system of standards, blanks, field and prep duplicates was implemented for the 2021 programs and were monitored as chemical assay data became available.

Figure 11-1: Raven Drill Core at Nugget Camp

Source: Victoria Gold Corp. (2021)

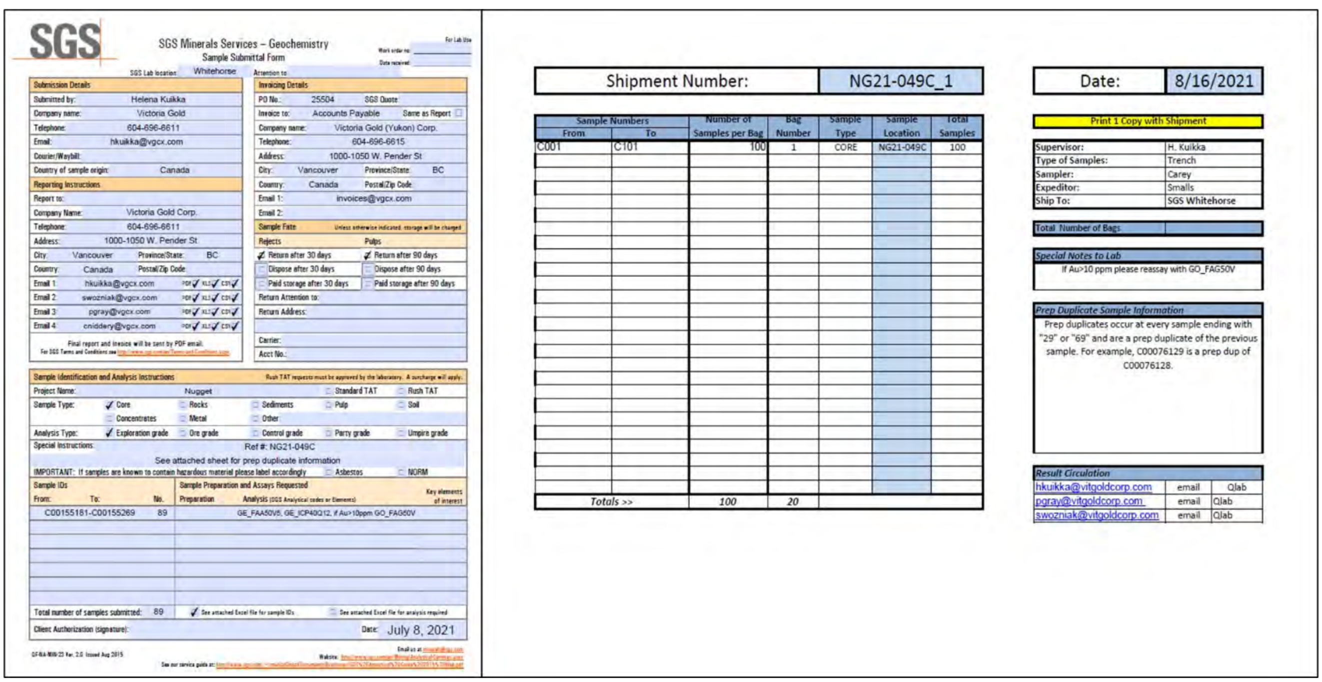

SGS

SGS Minerals Services – Geochemistry
Sample Submittal Form

For Lab Use
Work order no:
Date received:

SGS Lab location: Whitehorse
Attention to:

Submission Details	
Submitted by:	Helena Kuikka
Company name:	Victoria Gold
Telephone:	604-696-6611
Email:	hkuikka@vgcx.com
Courier/Waybill:	
Country of sample origin:	Canada
Reporting Instructions	
Report to:	
Company Name:	Victoria Gold Corp.
Telephone:	604-696-6611
Address:	1000-1050 W. Pender St
City:	Vancouver Province/State: BC
Country:	Canada Postal/Zip Code:
Email 1:	hkuikka@vgcx.com PDF ✓ XLS ✓ CSV ✓
Email 2:	swozniak@vgcx.com PDF ✓ XLS ✓ CSV ✓
Email 3:	pgray@vgcx.com PDF ✓ XLS ✓ CSV ✓
Email 4:	cniddery@vgcx.com PDF ✓ XLS ✓ CSV ✓

Final report and invoice will be sent by PDF email.
For SGS Terms and Conditions see http://www.sgs.com/en/Terms-and-Conditions.aspx

Invoicing Details	
PO No.:	25504 SGS Quote:
Invoice to:	Accounts Payable Same as Report ☐
Company name:	Victoria Gold (Yukon) Corp.
Telephone:	604-696-6615
Address:	1000-1050 W. Pender St
City:	Vancouver Province/State: BC
Country:	Canada Postal/Zip Code:
Email 1:	invoices@vgcx.com
Email 2:	
Sample Fate	Unless otherwise indicated, storage will be charged
Rejects	**Pulps**
✓ Return after 30 days	✓ Return after 90 days
☐ Dispose after 30 days	☐ Dispose after 90 days
☐ Paid storage after 30 days	☐ Paid storage after 90 days
Return Attention to:	
Return Address:	
Carrier:	
Acct No.:	

Sample Identification and Analysis Instructions — Rush TAT requests must be approved by the laboratory. A surcharge will apply.

Project Name: Nugget ☐ Standard TAT ☐ Rush TAT
Sample Type: ✓ Core ☐ Rocks ☐ Sediments ☐ Pulp ☐ Soil ☐ Concentrates ☐ Metal ☐ Other
Analysis Type: ✓ Exploration grade ☐ Ore grade ☐ Control grade ☐ Party grade ☐ Umpire grade
Special Instructions: Ref #: NG21-049C
See attached sheet for prep duplicate information
IMPORTANT: If samples are known to contain hazardous material please label accordingly ☐ Asbestos ☐ NORM

Sample IDs From: To:	No.	Preparation	Analysis (SGS Analytical codes or Elements)	Key elements of interest
C00155181-C00155269	89		GE_FAA50V5, GE_ICP40Q12, if Au>10ppm GO_FAG50V	

Total number of samples submitted: 89 ✓ See attached Excel file for sample IDs ☐ See attached Excel file for analysis required

Client Authorization (signature): Date: July 8, 2021

GF-NA-MIN-23 Rev. 2.0 Issued Aug 2015

Shipment Number:	NG21-049C_1

Date:	8/16/2021

Sample Numbers From	Sample Numbers To	Number of Samples per Bag	Bag Number	Sample Type	Sample Location	Total Samples
C001	C101	100	1	CORE	NG21-049C	100
Totals >>		100	20			

Print 1 Copy with Shipment

Supervisor:	H. Kuikka
Type of Samples:	Trench
Sampler:	Carey
Expeditor:	Smalls
Ship To:	SGS Whitehorse
Total Number of Bags	

Special Notes to Lab
If Au>10 ppm please reassay with GO_FAG50V

Prep Duplicate Sample Information
Prep duplicates occur at every sample ending with "29" or "69" and are a prep duplicate of the previous sample. For example, C00076129 is a prep dup of C00076128.

Result Circulation		
hkuikka@vitgoldcorp.com	email	Qlab
pgray@vitgoldcorp.com	email	Qlab
swozniak@vitgoldcorp.com	email	Qlab

Figure 11-2: Example of Sample Shipment Form and Chain of Custody Form - Raven Samples

Source: Victoria Gold Corp. (2022)

12 DATA VERIFICATION

12.1 Quality Assurance and Quality Control Procedures 2018 to 2021

Two analytical laboratories were used to prep and assay core and trench samples over the 2018-2021 period. Samples from the 2018 program were processed at Bureau Veritas Commodities Canada Ltd. In Vancouver for Fire Assay Au and multi-element ICP. For the 2019 program, all core samples were processed through the Eagle Gold Mine on-site analytical facility for Fire Assay gold. Samples above 0.2 ppm Au were then sent to SGS Laboratories in Burnaby for a repeat Fire Assay analysis as well as multi-element ICP. All trench samples from the 2019 program were processed at the SGS Burnaby Lab for Fire Assay and multi-element ICP. For the 2020-2021 programs, all core and trench samples were processed at SGS Laboratories in Burnaby for Fire Assay and multi-element ICP.

The exploration programs employed blanks, duplicates and standards as part of the quality assurance/quality control (QA/QC) program, the amount and type of QAQC over all drilling and trenching is presented in Table 12-1 below.

Table 12-1: QAQC Insertion Rate

	QAQC Type	#	Percent of total samples
VGCX	Standards	382	3.2%
	Blanks	389	3.3%
	Field Duplicates	243	2.1%
	Pulp Duplicates	215	1.8%
		Total	**10.4%**
Assay Lab	Reject Duplicate	166	1.4%
	Pulp Duplicates	713	6.0%
	Total		**7.4%**
	Grand Total		**17.8%**

The QAQC samples used for the Raven programs are described below:

- Crushed dolomite, purchased from a garden-supply centre, was used as blank material. Blanks were made by scooping roughly 500 g of crushed dolomite into a bag which was then added to the sample stream. Three blank controls were added for every 100 samples, usually where the sample numbers ended in 16, 56 and 96, although some were added in other locations according to local mineralizing conditions and at the discretion of the logging geologists.
- Drill core duplicates were obtained by submitting both halves of the core for analysis; with one half representing the original (normal) sample and the other half the duplicate. The gap left in the core box was marked by a piece of wood or polyvinyl chloride plastic pipe;
- Pulp duplicates were collected at the sample preparation stage by splitting a pulverized portion of the sample. Additional pulp duplicates were collected on every batch by the analytical lab- replicate samples.
- Reject duplicates were collected at the sample preparation stage by splitting a sample of crushed mineralized material which was then pulverized. These were inserted at the prep lab.
- Standard Reference Material (standards) were obtained from CDN Resource Laboratories Ltd, Langley, who supplied seven certified standards. One OREAS standard was also used. These are all listed in Table 12-2, together with their mean values and lower and upper limits of two standard deviations.

Table 12-2: Standard Reference Material Statistics

Standard	Mean Value (Au ppm)	Low Threshold (Au ppm)	High Threshold (Au ppm)
CDN-GS-1K	0.867	0.769	0.965
CDN-GS-1U	0.968	0.881	1.055
CDN-GS-P4C	0.362	0.326	0.398
CDN-GS-P4G	0.468	0.416	0.520
CDN-GS-P6	0.626	0.552	0.700
CDN-GS-P6C	0.767	0.689	0.845
CDN-GS-P8G	0.818	0.758	0.878
Oreas 67a	2.238	2.046	2.430

12.1.1 Assessment of Precision Error of 2018-2021 Exploration Programs

Precision error at Raven is quantified by comparing field, pulp, and coarse reject duplicates assayed at the same laboratory. Field duplicates used half-core samples for drill core, and a duplicate rock sample for trenches. The field duplicate represents the heterogeneity produced by sampling and is expected to produce the highest precision error due to local variation in gold location and content at Raven. Coarse reject duplicates are used to assess the precision error due to sample preparation at the laboratory and pulp duplicates are used to assess the analytical and instrument errors. Relative precision error was measured for field, reject and pulp duplicates using the coefficient of variation (CV). For the 2018-2021 Raven samples, the CV for field duplicates is 0.183, CV for reject duplicates is 0.125, and the CV for pulp duplicates is 0.099. This aligns with the expected increase in precision for duplicates from field to pulp samples and is considered within acceptable targets.

The gold CV for field duplicates (half-core and trench duplicates), reject and pulp duplicates for sample analyses performed from 2018-2021 are shown in Figure 12-1. This scatter plot shows that gold duplicates are most varied with field duplicates and least varied with pulp duplicates.

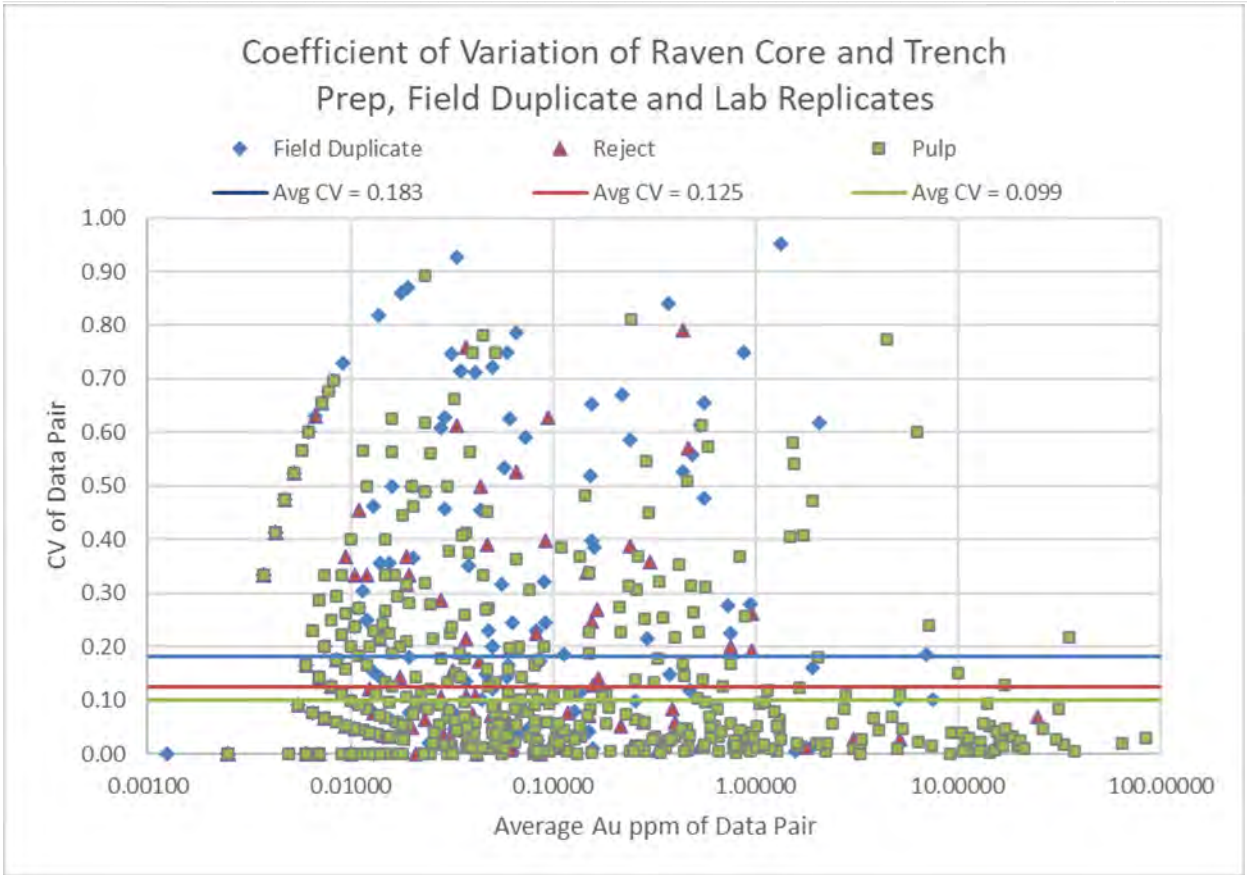

Figure 12-1: Coefficient of Variation (CV) for Raven Drill Core and Trench Field, Reject and Pulp Duplicates

Source: Victoria Gold Corp. (2022)

12.1.2 Assessment of Accuracy of 2017, 2018 and 2019 Drill Programs

Assay accuracy is measured for the Raven exploration program with inserted standard reference materials (SRM) using the expected tolerance of the expected recommended values (RV). Victoria Gold used 8 different standard reference materials summarized in Table 12-3.

Table 12-3: Standard Reference Values used at Raven during 2018-2021

Standard Type	Recommended Value (RV) Au ppm	Between Laboratory 2 SD
CDN-GS-1K	0.867	0.098
CDN-GS-1U	0.968	0.087
CDN-GS-P4C	0.362	0.036
CDN-GS-P4G	0.468	0.052
CDN-GS-P6	0.626	0.074
CDN-GS-P6C	0.767	0.078
CDN-GS-P8G	0.818	0.060
Oreas 67a	2.238	0.192

Percent relative difference (%RD) is calculated from the replicate analyses of the reference materials using:

$\%RD = 100 \times (\mu_i - RV) / RV$

Where μ_i = mean value of element i in the standard over a number of analytical runs; and RV = 'known' or 'certified' value of i in the standard or reference material. Values for %RD can be negative or positive depending on whether values are less than the known value (i.e., %RD < 0). In general, %RD values of ±0–3% are considered to have excellent accuracy, and values from 3–7% are considered to have very good accuracy; 7–10% have good accuracy; and values above 10% are not accurate (Jenner, 1996). The %RD for each standard reference material is shown in Table 12-4.

Table 12-4: Sample Stream Standard Reference Material Control

Reference Material	# Samples	RV Au ppm	Standard Deviation	% RD	Accuracy
CDN-GS-1K	7	0.865	0.047	-0.2	Excellent
CDN-GS-1U	132	0.981	0.054	1.3	Excellent
CDN-GS-P4C	1	0.380	0.000	5.0	N/A
CDN-GS-P4G	20	0.451	0.034	-3.5	Very Good
CDN-GS-P6	48	0.649	0.040	3.7	Very Good
CDN-GS-P6C	22	0.795	0.121	3.7	Very Good
CDN-GS-P8G	149	0.819	0.036	0.1	Excellent
Oreas 67a	3	2.277	0.027	1.7	Excellent
Blanks	771	0.004	0.005	N/A	N/A

Blanks were used to test for contamination introduced during sample preparation and analysis. Material used for the blanks in Raven consists of dolomite crush rock and is known to contain little to no gold mineralization. Monitoring blanks inserted into the sample stream is shown in Figure 12-2. The gold detection limit for samples assayed at the Eagle Gold Mine onsite laboratory is higher than the detection limit at Bureau Veritas or the SGS Burnaby lab (0.02 vs. 0.005). Samples below detection limit are assigned a value of ½ of the detection limit. Figure 12-3 to Figure 12-6 show this clustering around the different detection limits.

Analytical batches with analyses falling outside of the between laboratory 2-standard deviation were checked for other batch errors. Batches generally contained multiple standards and blanks to check against. Multiple standard or blank failures within a batch was not seen, however some batches were re-run anyway if located within a mineralized zone.

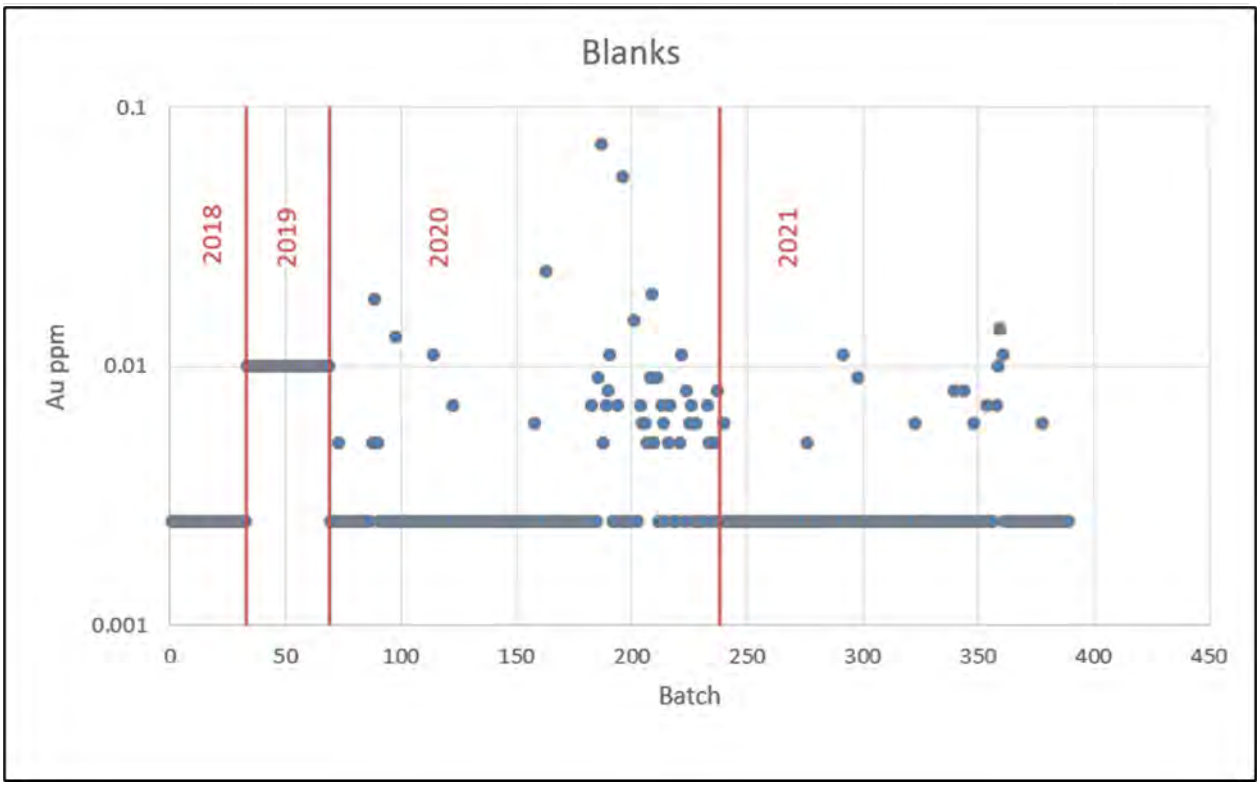

Figure 12-2: Blank Assays in Raven 2018 – 2021

Source: Victoria Gold Corp. (2022)

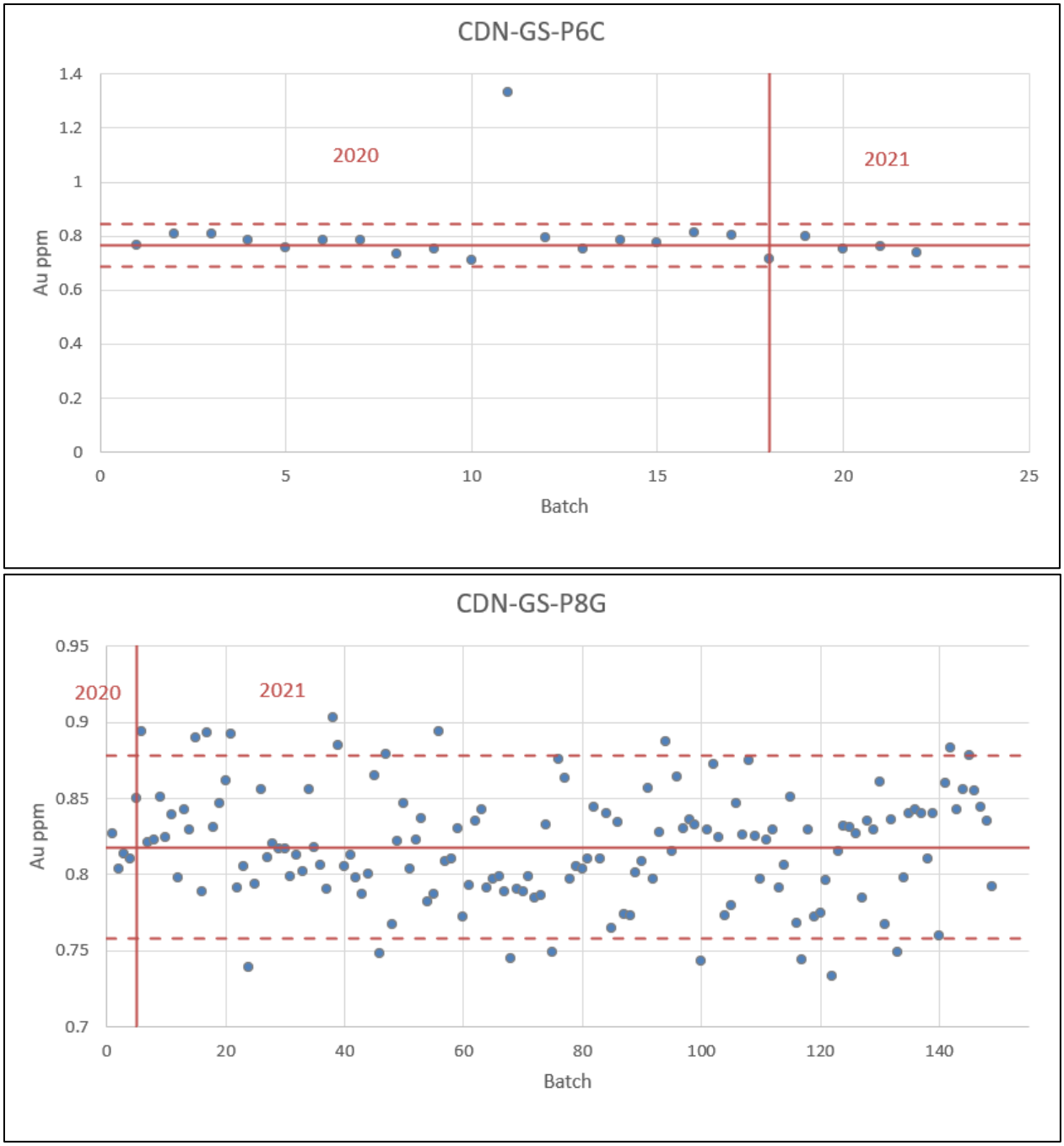

Figure 12-3: Performance Summary for CDN-GS-1Q and CDN-ME-1605 Standard Reference Materials

Source: Victoria Gold Corp. (2022)

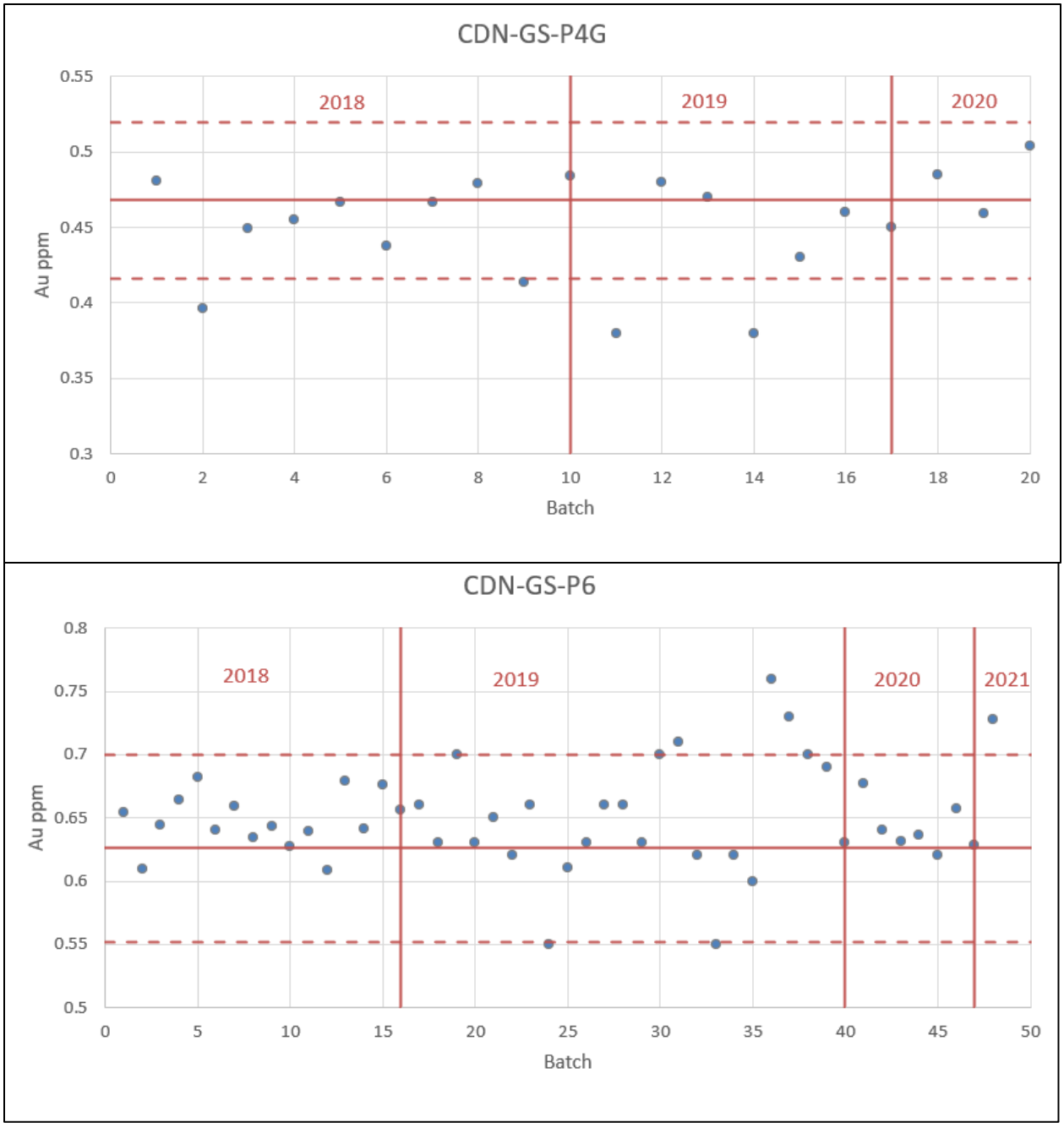

Figure 12-4: Performance Summary for CDN-GS-1Q and CDN-ME-1605 Standard Reference Materials

Source: Victoria Gold Corp. (2022)

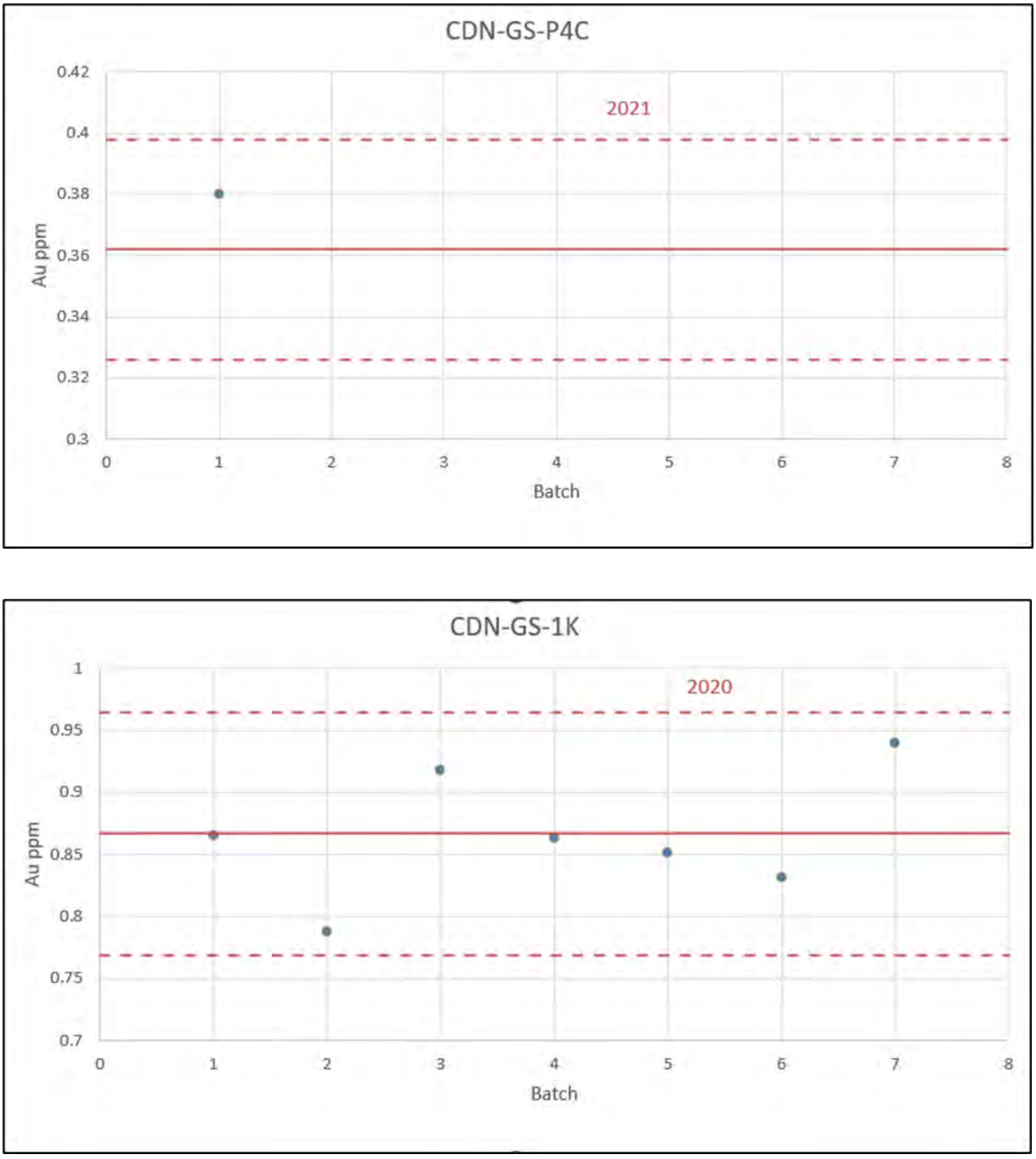

Figure 12-5: Performance Summary for CDN-GS-1Q and CDN-ME-1605 Standard Reference Materials

Source: Victoria Gold Corp. (2022)

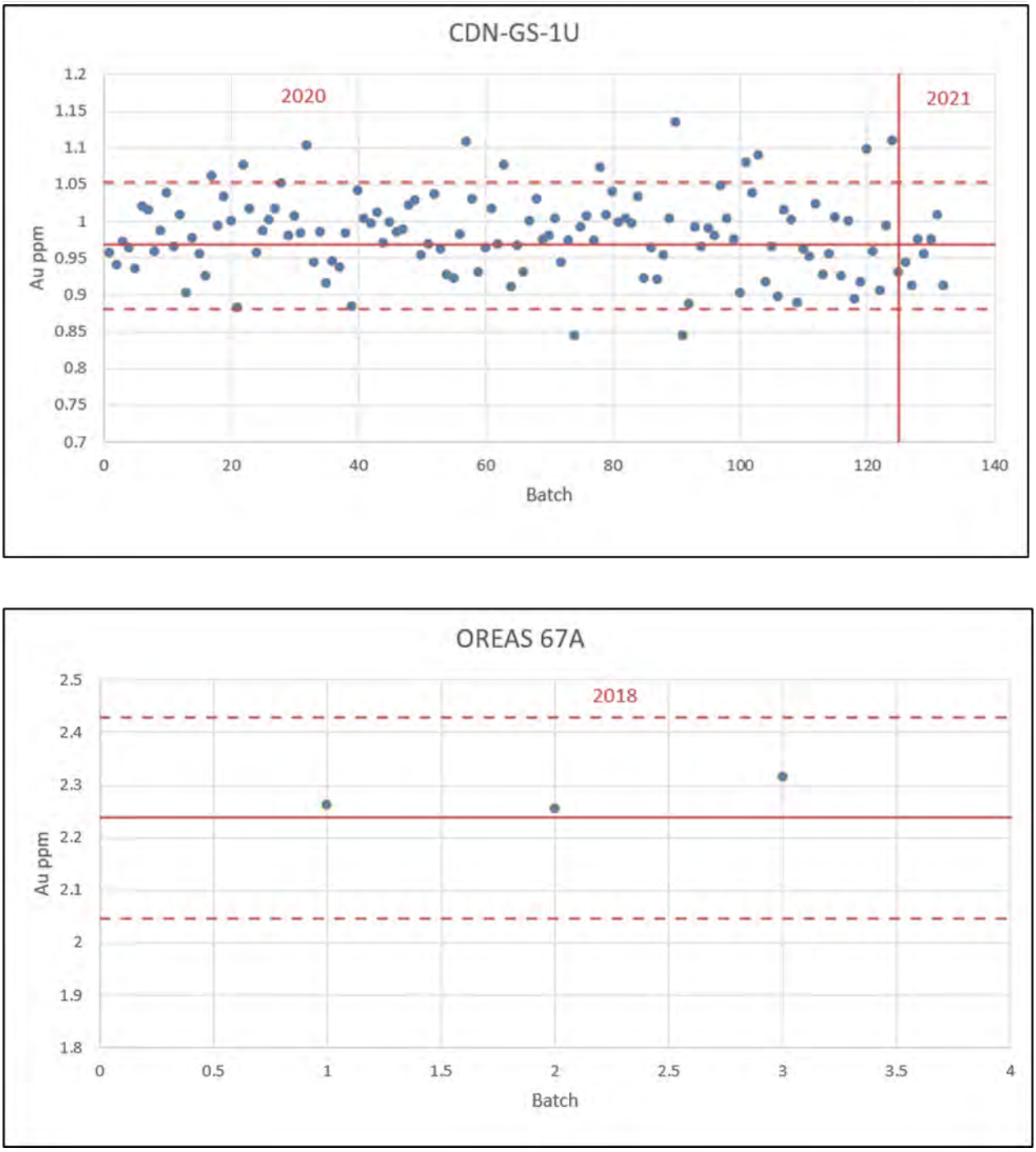

Figure 12-6: Performance Summary for CDN-GS-1Q and CDN-ME-1605 Standard Reference Materials

Source: Victoria Gold Corp. (2022)

The author is confident that the data from drilling on the Raven Project has been obtained in accordance with contemporary industry standards, and that the data is adequate for the calculation of an inferred mineral resource, in compliance with National Instrument 43-101.

13 MINERAL PROCESSING AND METALLURGICAL TESTING

13.1 Petrographic Analyses:

Helena Kuikka of Victoria Gold Corp. submitted nine (9) polished thin sections to Fabrizio Colombo (Ultra Petrography & Geoscience Inc.) for petrographic analysis. The samples were selected from mineralized veins and altered rock from the 2018 exploration drilling program. The aim of this study was to define alteration and mineralogical associations which would aid determining the mineralization type and help with exploration techniques.

The Petrographic Descriptions section provided the following for each sample:

1. The petrographic rock classification according to the British Geological Survey Classification Scheme (Gillespie and Styles, 1999; Gillespie et al., 2011; Hallsworth and Knox, 1999; Robertson, 1999).
2. A brief microstructural description linking the feature visible mesoscopically and on the stained offcut of the thin section (a 20x40 image of the offcut is included in the report) and the features detected under the microscope.
3. A table with the modal percentage and average grain size for each mineral;
4. A detailed description of the minerals in decreasing order of abundance.
5. Photomicrographs describing the most relevant microstructures and mineral intergrowths observed and described in points 1 and 4. The photomicrographs are in .tiff format, and the native copy of the high-resolution images included in the report are also provided separately.

Examples of microphotographs are shown in Figure 13-1 through Figure 13-3.

The Ultra Petrography & Geoscience Inc. report can be found in Appendix 3.

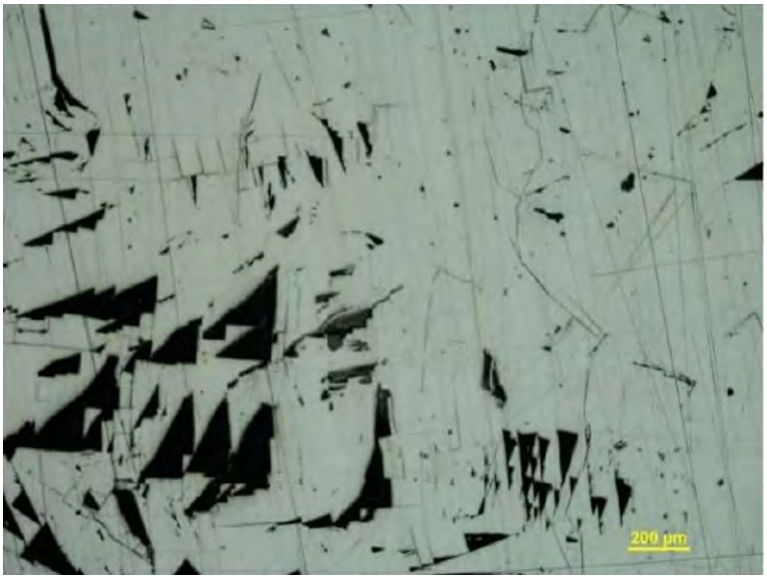

Figure 13-1: Triangular poke marks in the massive aggregate of galena indicate the cubic symmetry of the mineral.

Source: Ultra Petrography & Geoscience Inc. (2021)

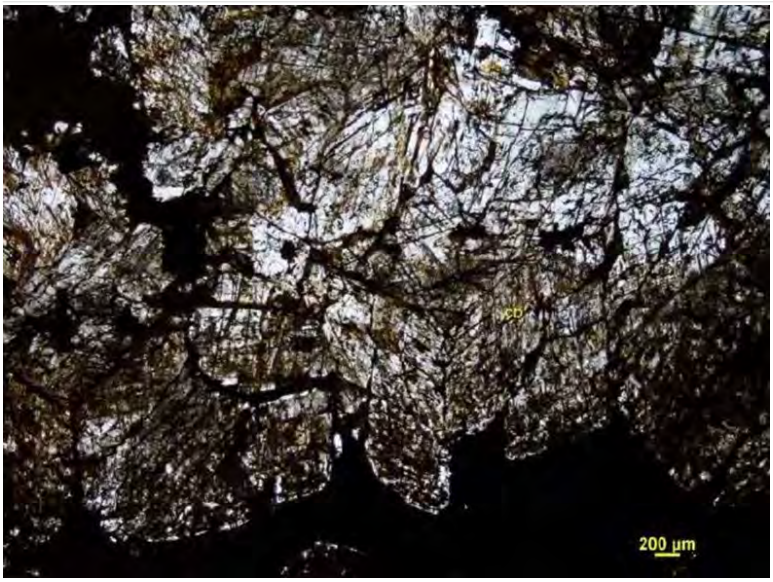

Figure 13-2: Medium-grained crystals of carbonate are intergrown with subordinate dispersions of partially oxidized pyrite and limonitic material. The carbonate domain shows an irregular boundary at the contact with the massive galena.

Source: Ultra Petrography & Geoscience Inc. (2021)

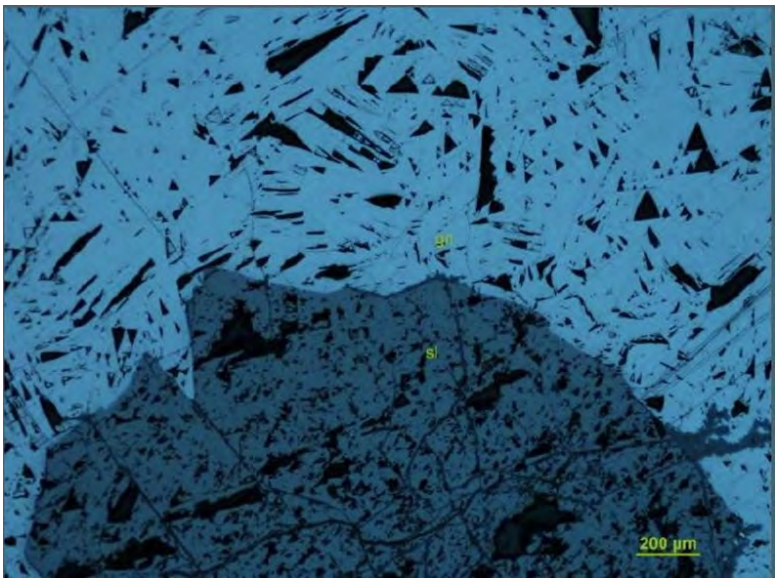

Figure 13-3: A subhedral sphalerite crystal is immersed within the massive galena.

Source: Ultra Petrography & Geoscience Inc. (2021)

14 MINERAL RESOURCE ESTIMATES

This study represents the first mineral resource estimate of the Raven Gold Deposit. The Raven deposit is located approximately 15 km northeast of Victoria's Eagle Gold Mine, and is approximately 375 km north of the city of Whitehorse, Yukon.

The geologic interpretation of the Raven deposit was performed by Victoria's exploration team, while the estimation of the mineral resources was carried out by Mr. Marc Jutras, P.Eng., M.A.Sc., Principal, Mineral Resources at Ginto Consulting Inc. Mr. Jutras is an independent Qualified Person as defined under National Instrument 43-101.

The mineral resource estimation was primarily undertaken with the Maptek™ Vulcan™ software and utilities internally developed in GSLIB-type format. The following sections outline the procedures undertaken to calculate the mineral resources of the Raven Gold Deposit.

14.1 Drill Hole Database

The drill hole database was provided by Victoria's exploration team on July 7, 2022. The drill data is comprised of 78 diamond drill holes collared between August 2018 and September 2021 and is comprised of 11,956 assays from 18,217 m of drilling. Additionally, 55 surface trenches with 3,464 assays and 7,443m of sampling were included in the mineral resource database. Statistics on the number of drill holes and trenches, and number of meters by year are presented in Table 14-1. Statistics from the mineral resource database are shown in Table 14-2. Gold is the element of interest in g/t.

The drill hole location is shown in Figure 14-1.

Table 14-1: Drill Hole Database Statistics by Year – Raven Gold Deposit

Year	Diamond Drill Holes		Surface Trenches		Drill Hole and Trenches	
	Number of Holes	Metres	Number of Trenches	Metres	Number of Holes and Trenches	Metres
2018	9	1,754.9	13	1,447.0	21	3,201.9
2019	9	1,616.8	37	5,438.0	46	7,054.8
2020	31	7,452.6	5	558.0	36	8,010.6
2021	29	7,393.1	-	-	29	7,393.1
Total	**78**	**18,217.4**	**55**	**7,443.0**	**133**	**25,660.4**

Source: Ginto Consulting (2022)

Table 14-2: Drill Hole Database Statistics – Raven Gold Deposit

Raven Gold Deposit - Yukon - All Drill Hole Data

Collar Data	Number of Data	Mean	Standard Deviation	Coefficient of Variation	Minimum	Lower Quartile	Median	Upper Quartile	Maximum	Number of 0.0 values	Number of < 0.0 values
Easting (X)	133	473593.0	628.828	0.001	471873.0	473516.0	473706.0	473894.0	475037.0	—	—
Northing (Y)	133	101874.0	710.084	0.007	99843.0	101645.0	101789.0	101916.0	104718.0	—	—
Elevation (Z)	133	1244.06	49.355	0.04	930.83	1237.35	1261.63	1268.45	1295.79	—	—
Hole Depth	133	192.935	115.259	0.597	6.0	111.0	188.98	250.02	758.0	—	—
Azimuth	133	163.18	73.195	0.449	0.0	160.3	170.0	183.25	351.0	—	—
Dip	133	-28.161	23.907	-0.849	-70.0	-46.0	-44.6	0.0	12.0	—	—
Overburden	133	0.0	0.0	0.0	0.0	0.0	0.0	0.0	0.0	—	—
Survey Data											
Azimuth	406	171.947	64.886	0.377	0.1	168.61	173.41	180.5	362.4	—	—
Dip	406	-34.622	21.128	-0.61	0.0	0.0	0.0	0.0	0.0	—	—
Assay Data											
Interval Length (from-to)	15345	1.639	0.584	0.357	0.06	1.34	1.68	2.0	10.73	0	0
AU_GPT	15345	0.241	1.829	7.579	0.0	0.003	0.006	0.023	76.113	3	75

Source: Ginto Consulting (2022)

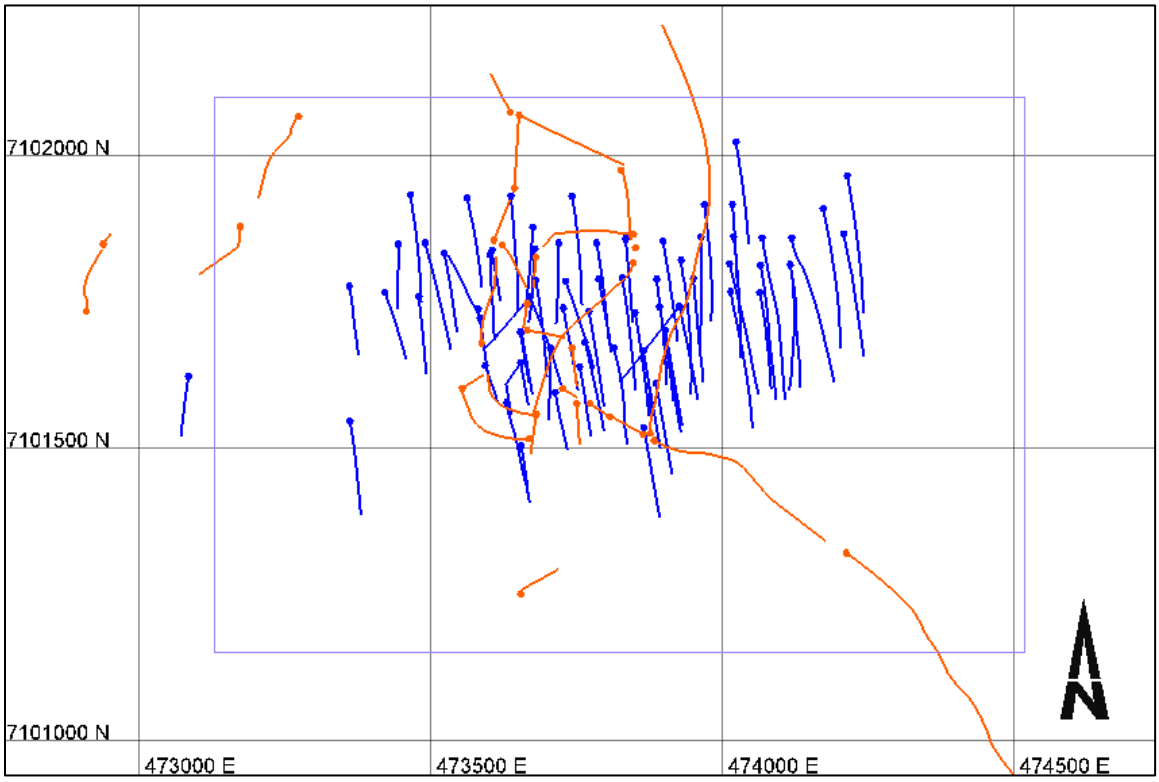

Figure 14-1: Drill Hole (Blue) and Trench (Orange) Locations Within the Block Model Limits (Purple) – Raven Gold Deposit

Source: Ginto Consulting (2022)

14.2 Geology Model

The geology model was developed by Victoria's exploration team with the Leapfrog© software and consists of four mineralized units as follows: the massive sulphide veins' domain ("MSV"), the lower grade greater than 0.2 g/t Au domain ("LG>0,2"), the lower grade greater than 0.6 g/t Au domain ("LG>0.6") and the lower grade greater than 4.0 g/t Au domain ("LG>4.0"). Table 14-3 presents additional details of the different domains.

The MSV unit's interpretation is based on the geologic controls on gold mineralization, including veins identified in drill holes and surface exposures, structural measurements from oriented core and surface trenches as well as high-grade gold analytical values. The MSV domain is made of individual veins oriented at an azimuth of approximately 85° and dipping 65° to the north.

The lower grade ("LG") domains were modeled at three different gold grade cut-offs based on the gold grade distribution outside the MSV domain. From the probability plot of gold grades outside the MSV domain, three different grade populations were observed with breaks at 0.2 g/t, 0.6 g/t and 4.0 g/t Au. The geologic controls on gold grade mineralization within the LG domains are not entirely understood and for such gold grade envelopes at increasing grade thresholds were selected to model gold mineralization within these areas. Similarly, to the MSV domain, the LG domains are oriented at an azimuth of approximately 85° and dipping 65° to the north.

Table 14-3: Geology Model – Raven Gold Deposit

Rock Type	Rock Code	Description	Volume (m^3)
1	MSV	Massive Sulphide Veins	6,615,702
2	LG>0.2	Lower Grade ≥ 0.2 g/t and < 0.6 g/t Au	70,347,259
3	LG>0.6	Lower Grade ≥ 0.6 g/t and < 4.0 g/t Au	8,038,514
4	LG>4.0	Lower Grade ≥ 4.0 g/t Au	558,448
		TOTAL	**85,559,923**

Source: Ginto Consulting (2022)

The wireframes of the different gold mineralization domains are presented in Figure 14-2 to Figure 14-4. The gold mineralization was modeled over an area of approximately 1,100m east-west by 700m north-south and down to a depth of approximately 400m below surface.

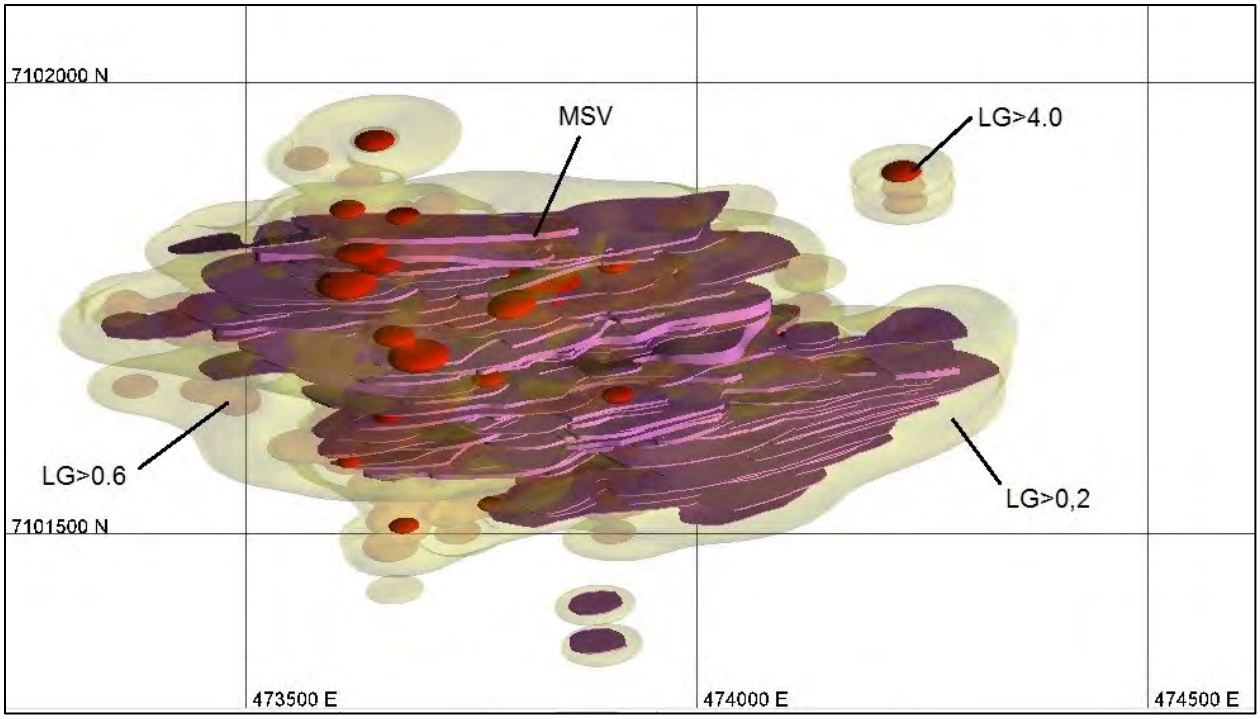

Figure 14-2: Geology Model – Plan View – Raven Gold Deposit

Source: Ginto Consulting (2022)

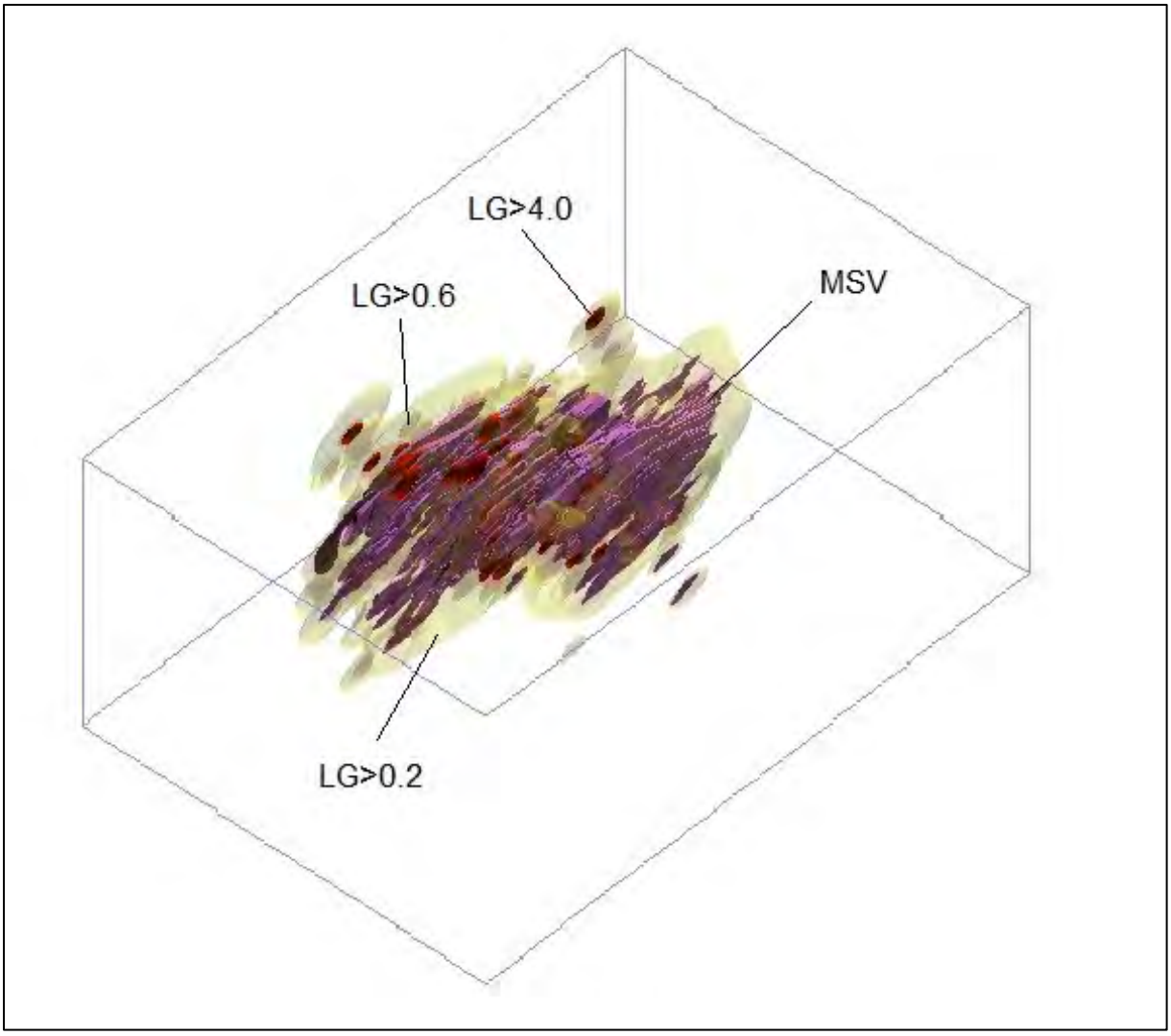

Figure 14-3: Geology Model – Perspective View Looking to the Northeast – Raven Gold Deposit

Source: Ginto Consulting (2022)

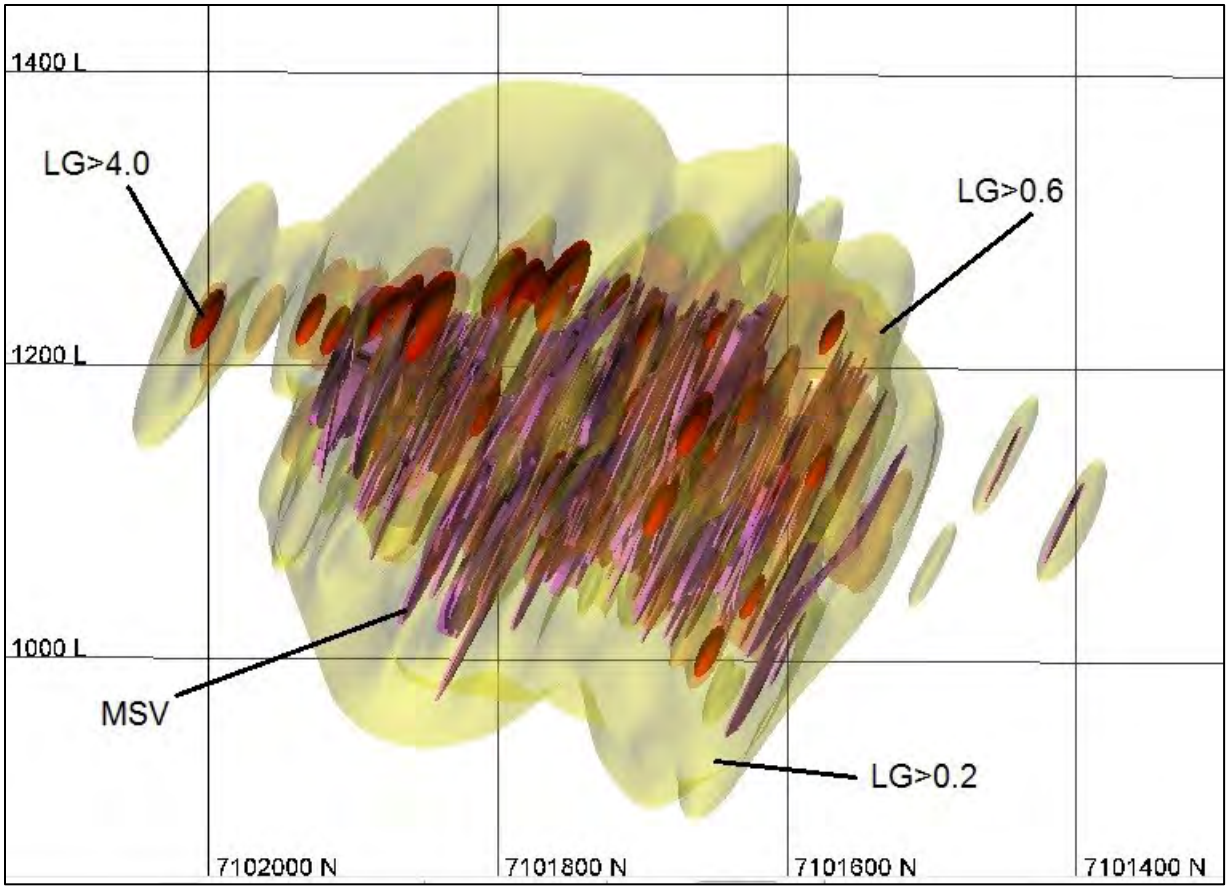

Figure 14-4: Geology Model – Profile View Looking to the East – Raven Gold Deposit

Source: Ginto Consulting (2022)

A model of the overburden and topography surface were also provided for this study. The thickness of the overburden varies from non-existent to a maximum of approximately 40m in the northwest portion of the area of interest, with most of the modeled overburden varying from 1m to 5m when present. Figure 14-5 displays the overburden model and the topography surface. The topography shows changes in elevation up to a maximum of approximately 50m with low ridges oriented to the north-northeast.

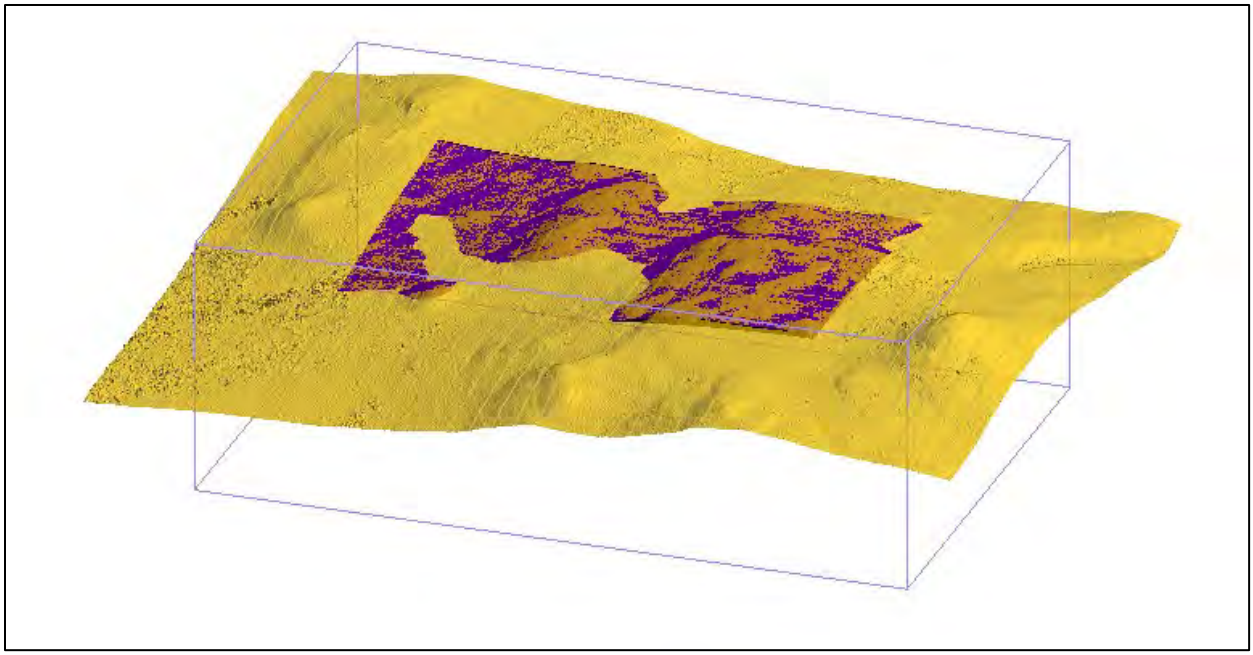

Figure 14-5: Overburden (Purple) and Topography Surface (Yellow) – Perspective View Looking to the Northeast – Raven Gold Deposit

Source: Ginto Consulting (2022)

14.3 Compositing

The original samples were composited to regular 1.3m lengths as it is the most common sampling interval within the MSV and the LG domains with 14% and 12% of the data, respectively. A dynamic compositing process was selected for this task. In this setting, the residual composites are re-distributed to the full-length composites to allow for all composites within a domain to have the same composite length. This will avoid artifacts possibly created by the shorter residual composites.

The selection of 1.3m as the composite length is base on the most common sampling length as well as on the envisioned block height of 5m. This provides a ratio of block height to composite length of 3.85 (5.0m/1.3m), which is within guideline limits of ratios between 2 and 5.

The geology model (section 14.2) was utilized for the compositing process with each mineralized unit serving as a domain boundary for this procedure.

A total of 9,064 composites were generated from 72 holes and 19 trenches located only within the mineralized domains as defined by the geology model (less than the overall number of holes (78) and trenches (55)).

14.4 Exploratory Data Analysis (EDA)

The exploratory data analysis (EDA) is an exercise that allows for a better understanding of the different geometric and statistical properties of the Raven deposit's gold grades.

14.4.1 Drill hole Spacing and Orientation

The drill hole spacing within the Raven area is at 55.6m on average with a median of 36.7m. The average and median drill hole spacing for the different domains are presented in Table 14-4. The drill hole spacing statistics were calculated by pairing the closest sample from another drill hole to each sample and storing this 3-D distance for the computation of the average and median spacing.

Table 14-4: Drill Hole Spacing – Raven Gold Deposit

Domain	Average Spacing m	Median Spacing m	Number of Composites
MSV	29.8	29.2	1,591
LG>0.2	38.7	36.9	3,273
LG>0.6	29.8	27.4	3,709
LG>4.0	49.7	45.3	491
ALL LG	31.7	29.9	7,473
ALL MIN	31.0	29.3	9,064
OUT MIN	78.7	50.0	10,693
ALL	55.6	36.7	19,757

Source: Ginto Consulting (2022)

The orientation of drill holes is mainly to the south throughout the deposit at azimuths ranging from 160° to 185° and at dips ranging from -40° to -70°. Surface trenches can be found at various orientations in the project area with the north-northeast and south-southwest directions as major orientations. Figure 14-6 displays the orientations and dips of the drill holes of the Raven deposit. The azimuths and dips of Figure 14-6 are displayed on a stereonet-type of plot with the azimuth angles represented on the outer circle and the dips on the inner circles.

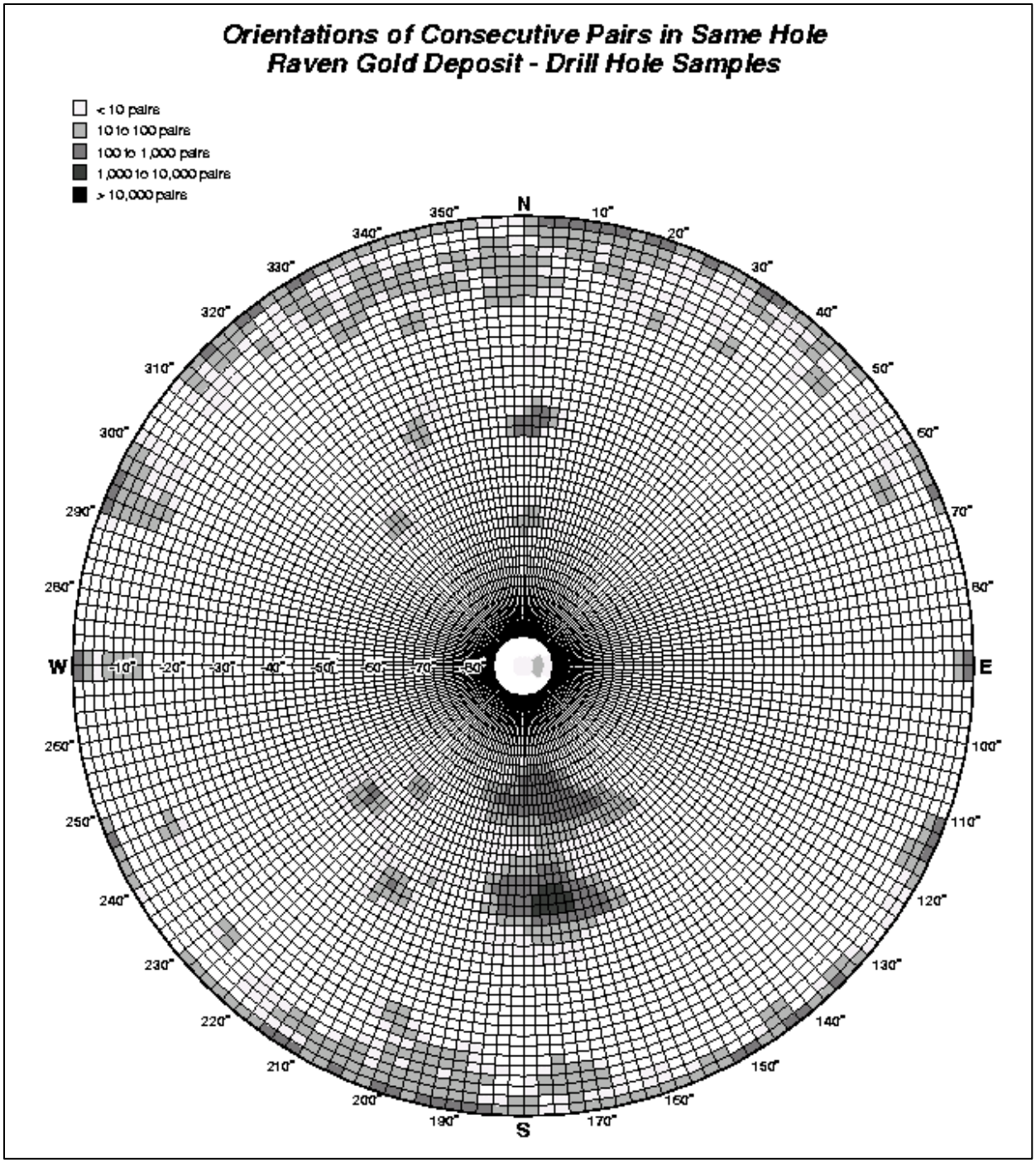

Figure 14-6: Orientations and Dips of Drill Holes and Trenches – Raven Gold Deposit

Source: Ginto Consulting. (2022)

14.4.2 Basic Statistics

Basic statistics were conducted on composited gold grades with histograms, probability plots, and boxplots for each domain of the geology model. These various analyses have shown positively skewed lognormal distributions of gold grades. Results are presented in the boxplots of Figure 14-7 for each domain.

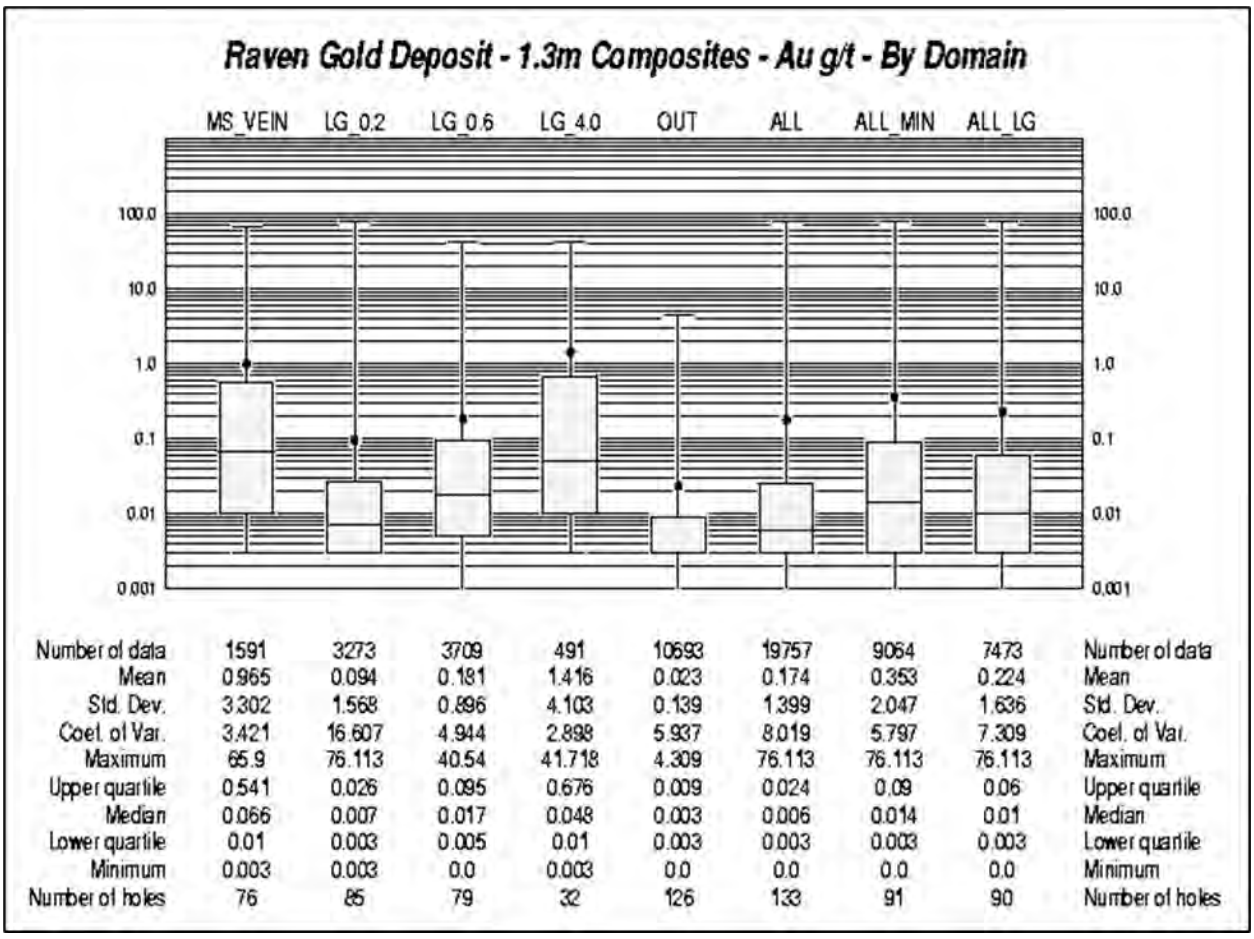

Figure 14-7: Boxplots of Composited Gold Grades by Domain – Raven Gold Deposit

Source: Ginto Consulting (2022)

As seen in Figure 14-7, greater variability of gold grades, with coefficients of variation (CV) above 3.0, are noted for three of the four mineralized domains. The LG>4.0 domain displays a more homogeneous (less variable) distribution of gold grades with a CV less than 3.0.

It can be observed that the statistical characteristics of the gold mineralization from the different domains vary in accordance to the interpreted units of the geology model.

14.4.3 Capping Of High-Grade Outliers

It is common practice to statistically examine the higher grades within a population and to trim them to a lower grade value based on the results from specific statistical utilities. This procedure is performed on high-grade values that are considered outliers and that cannot be related to any geologic feature. In the case of the Raven deposit, the higher gold grades were examined with three different tools: the probability plot, the decile analysis, and the cutting statistics. The usage of various investigating methods allows for a

selection of the capping threshold in a more objective and justified manner. For the probability plot method, the capping value is chosen at the location where higher grades depart from the main distribution. For the decile analysis, the capping value is chosen as the maximum grade of the decile containing less than an average of 10% of metal. For the cutting statistics, the selection of the capping value is identified at the cut-off grade where there is no correlation between the grades above this cut-off or where a jump in the coefficient of variation is observed. The resulting compilation of the capping thresholds is listed in Table 14-5. One of the objectives of the capping strategy is to have less than 10% of the metal affected by the capping process. This was achieved for three of the four domains of the Raven deposit. The stronger reduction of the LG>0.2 domain's metal content is mainly attributable to a single high-grade value that represents a large portion of the metal content for this lower grade domain.

Table 14-5: List of Capping Thresholds of High-Grade Outliers – Raven Gold Deposit

Rock Code	Probability Plot Au g/t	Cutting Statistics Au g/t	Decile Analysis Au g/t	Final Au g/t	% Metal Capped	Number Capped
MSV	25.0	20.0, 25.0	25.1	25.0	4	7
LG>0.2	2.5, 5.0	4.0, 5.0	4.7	5.0	40	4
LG>0.6	6.0, 9.0	6.0, 9.0	5.9	6.0	6	6
LG>4.0	15.0, 21.0	21.0	21.4	21.0	8	4

Source: Ginto Consulting (2022)

Basic statistics were re-computed with the gold grades capped to the thresholds listed in Table 14-5. Boxplots of Figure 14-7 display the basic statistics resulting from the capping of the higher gold grade outliers.

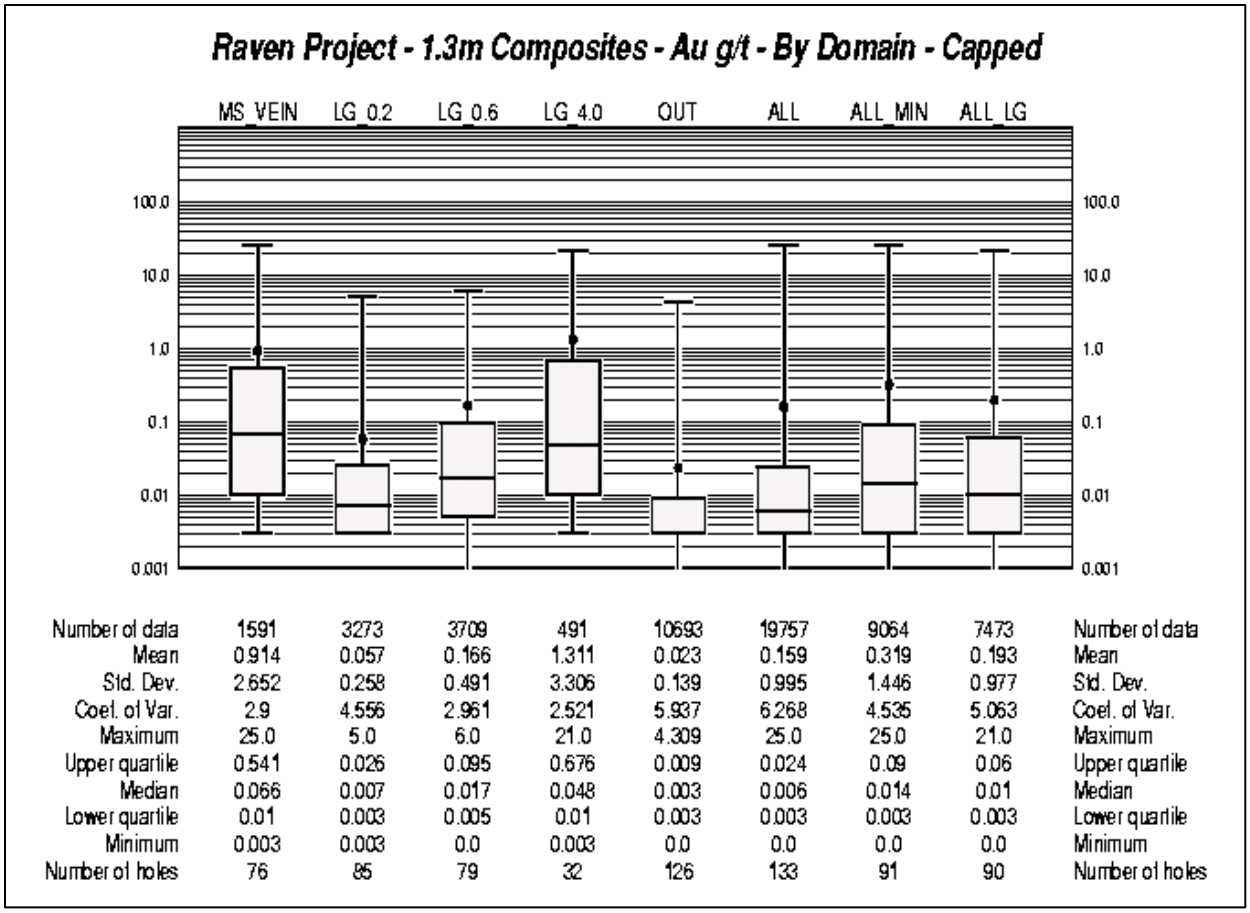

	MS_VEIN	LG_0.2	LG_0.6	LG_4.0	OUT	ALL	ALL_MIN	ALL_LG	
Number of data	1591	3273	3709	491	10693	19757	9064	7473	Number of data
Mean	0.914	0.057	0.166	1.311	0.023	0.159	0.319	0.193	Mean
Std. Dev.	2.652	0.258	0.491	3.306	0.139	0.995	1.446	0.977	Std. Dev.
Coef. of Var.	2.9	4.556	2.961	2.521	5.937	6.268	4.535	5.063	Coef. of Var.
Maximum	25.0	5.0	6.0	21.0	4.309	25.0	25.0	21.0	Maximum
Upper quartile	0.541	0.026	0.095	0.676	0.009	0.024	0.09	0.06	Upper quartile
Median	0.066	0.007	0.017	0.048	0.003	0.006	0.014	0.01	Median
Lower quartile	0.01	0.003	0.005	0.01	0.003	0.003	0.003	0.003	Lower quartile
Minimum	0.003	0.003	0.0	0.003	0.0	0.0	0.0	0.0	Minimum
Number of holes	76	85	79	32	126	133	91	90	Number of holes

Figure 14-8: Boxplots of Composited and Capped Gold Grades by Domains – Raven Gold Deposit

Source: Ginto Consulting (2022)

It can be observed from Figure 14-8 that the coefficients of variation from the capped composites are below 3.0 for three of the mineralized domains, with the exception of the LG>0.2 domain where greater variability is observed.

The effect of the capping of the high-grade outliers has reduced the overall average gold grade of the mineralized domains by 9.6%.

Because of the lower coefficients of variation observed for the gold grade populations in general, it was concluded that there is no need to treat the higher-grade composites differently than the lower grade composites during the estimation process. Ordinary kriging is thus a well-suited estimation technique in this case.

14.5 Variography

A variographic analysis was carried out on the capped gold grade composites within the mineralized domains of the geology model. The objective of this analysis was to spatially establish the preferred directions of gold grade continuity. In turn, the variograms modeled along these directions would be later utilized to select and weigh the composites during the block grade interpolation process. For this exercise, all experimental variograms were of the type relative lag pairwise, which is considered robust for the assessment of gold grade continuity.

Variogram maps were first calculated to examine general gold grade continuities in the XY, XZ, and YZ planes. The next step undertaken was to compute omni-directional variograms and down-hole variograms. The omni-directional variograms are calculated without any directional restrictions and provide a good assessment of the sill of the variogram. As for the down-hole variogram, it is calculated with the composites of each hole along the trace of the hole. The objective of these calculations is to provide information about the short scale structure of the variogram, as the composites are more closely spaced down the hole. Thus, the modeling of the nugget effect is usually better derived from the down-hole variograms.

Directional variograms were then computed to identify more specifically the three main directions of continuity. A first set of variograms were produced in the horizontal plane at increments of 10 degrees. In the same way a second set of variograms were computed at 10° increments in the vertical plane of the horizontal direction of continuity (plunge direction). A final set of variograms at 10° increments were calculated in the vertical plane perpendicular to the horizontal direction of continuity (dip direction). The final variograms were then modeled with a 2-structure spherical variogram, and resulting parameters presented in Table 14-6 for gold populations of the different mineralized domains.

The directions of gold grade continuity are in general agreement with the orientation of the mineralized domains, with best directions of continuity trending approximately east-west and down-dip to the north at approximately -65°. The ranges of gold grade continuity along the principal direction (strike) vary from 24m to 60m, along the minor direction (dip) from 21m to 47m, and along the vertical direction (across strike and dip) from 10m to 32m. The modeled variograms have relatively low nugget effects with values varying from 9% to 21% of the sill. The experimental variograms are considered of acceptable quality overall, however infill drilling would benefit the modeling of the variograms' continuity structures at shorter lag distances.

Plots of variogram models can be found in Appendix 4.

Table 14-6: Modeled Variogram Parameters for Gold – Raven Gold Deposit

Parameters	1 – MSV			2 – LG>0.2		
	Principal	Minor	Vertical	Principal	Minor	Vertical
Azimuth*	85°	175°	175°	80°	170°	170°
Dip**	0°	65°	-25°	0°	60°	-30°
Nugget Effect C0	0.486			0.142		
1st Structure C1	0.852			0.904		
2nd Structure C2	0.926			0.498		
1st Range A1	39.3m	40.4m	27.5m	29.7m	29.7m	8.2m
2nd Range A2	59.7m	43.6m	31.8m	51.2m	46.9m	31.8m
Parameters	**3 – LG>0.6**			**4 – LG>4.0**		
	Principal	Minor	Vertical	Principal	Minor	Vertical
Azimuth*	85°	175°	175°	90°	180°	180°
Dip**	5°	65°	-25°	-10°	65°	-25°
Nugget Effect C_0	0.216			0.452		
1st Structure C_1	1.196			1.798		
2nd Structure C_2	0.505			0.358		
1st Range A_1	3.8m	9.2m	3.8m	11.3m	11.3m	4.9m
2nd Range A_2	54.4m	41.3m	18.9m	24.1m	20.9m	10.2m

Source: Ginto Consulting (2022)

* Positive clockwise from north

** Negative below horizontal

14.6 Gold Grade Estimation

The estimation of gold grades into a block model was carried out with the ordinary kriging technique. The estimation strategy and parameters were tailored to account for the various geometrical, geological, and geostatistical characteristics previously identified. The block model's structure is presented in Table 14-7. It should be noted that the origin of the block model corresponds to the lower left corner, the point of origin being the exterior edges of the first block. A parent block size of 5m (easting) x 5m (northing) x 5m (elevation) with sub-blocks of 0.5m (easting) x 0.5m (northing) x 0.5m (elevation) was selected to better reflect the mineral deposit's geometrical configuration and anticipated production rate. The block model is orthogonal with no rotation applied to it.

Table 14-7: Block Grid Definition – Raven Gold Deposit

Coordinates	Origin m	Rotation (azimuth)	Distance m	Parent Block Size m	Number of Parent Blocks	Sub-Block Size m
Easting (X)	473,130.0	0°	1,390.0	5.0	278	0.5
Northing (Y)	7,101,150.0		950.0	5.0	190	0.5
Elevation(Z)	900.0		500.0	5.0	100	0.5
Number of Parent Blocks		5,282,000				

Source: Ginto Consulting (2022)

The database of 1.3m capped gold grade composites was utilized as input for the grade interpolation process along with the modeled mineralized domains. The size and orientation of the search ellipsoid for the estimation process was based on the variogram parameters modeled for gold. A minimum of 2 samples and maximum of 12 samples were selected for the block grade calculations along with hard boundaries between the mineralized domains. No other restrictions, such as a minimum number of informed octants, a minimum number of holes, a maximum number of samples per hole, etc., were applied to the estimation process. A 2-pass estimation strategy was utilized for the grade interpolation process. The first grade estimation run utilized a search ellipsoid oriented along the directions of best gold grade continuity defined by the variogram models, and dimensioned to the second range of gold grade continuity from the variograms. Similar estimation parameters were utilized for the second grade estimation run with a search ellipsoid dimensioned to twice the second range of gold grade continuity from the variograms. The gold grade estimation parameters for the first run are summarized in Table 14-8.

Table 14-8: Estimation Parameters for Gold – Raven Gold Deposit

Rock Code	minimum # of samples	maximum # of samples	search ellipsoid – long axis - azimuth/dip	search ellipsoid – long axis - size	search ellipsoid – short axis - azimuth/dip	search ellipsoid – short axis - size	search ellipsoid – vertical axis - azimuth/dip	search ellipsoid – vertical axis - size
1	2	12	85°/0°	60.0m	175°/65°	44.0m	175°/-25°	32.0m
2	2	12	80°/0°	51.0m	170°/60°	47.0m	170°/-30°	32.0m
3	2	12	85°/0°	54.0m	175°/65°	42.0m	175°/-25°	19.0m
4	2	12	90°/-10°	24.0m	180°/65°	21.0m	180°/-25°	10.0m

Source: Ginto Consulting (2022)

14.7 Validation of Grade Estimates

A set of validation tests were carried out on the estimates to examine the possible presence of a bias and to quantify the level of smoothing/variability.

The visual and statistical validation tests were conducted on gold grade estimates regularized to a 2.5m x 2.5m x 2.5m block size and, declustered and capped 1.3m composites.

14.7.1 Visual Inspection

A visual inspection of the block gold grade estimates with the drill hole gold grades on plans, east-west and north-south cross-sections was performed as a first check of the estimates. Observations from stepping through the estimates along the different planes indicated that there was overall a good agreement between the drill hole grades and the estimates. The orientations of the estimated grades were also according to the projection angles defined by the search ellipsoid. Examples of cross-sections and level plans for gold grade estimates are presented in Figure 14-9 to Figure 14-11.

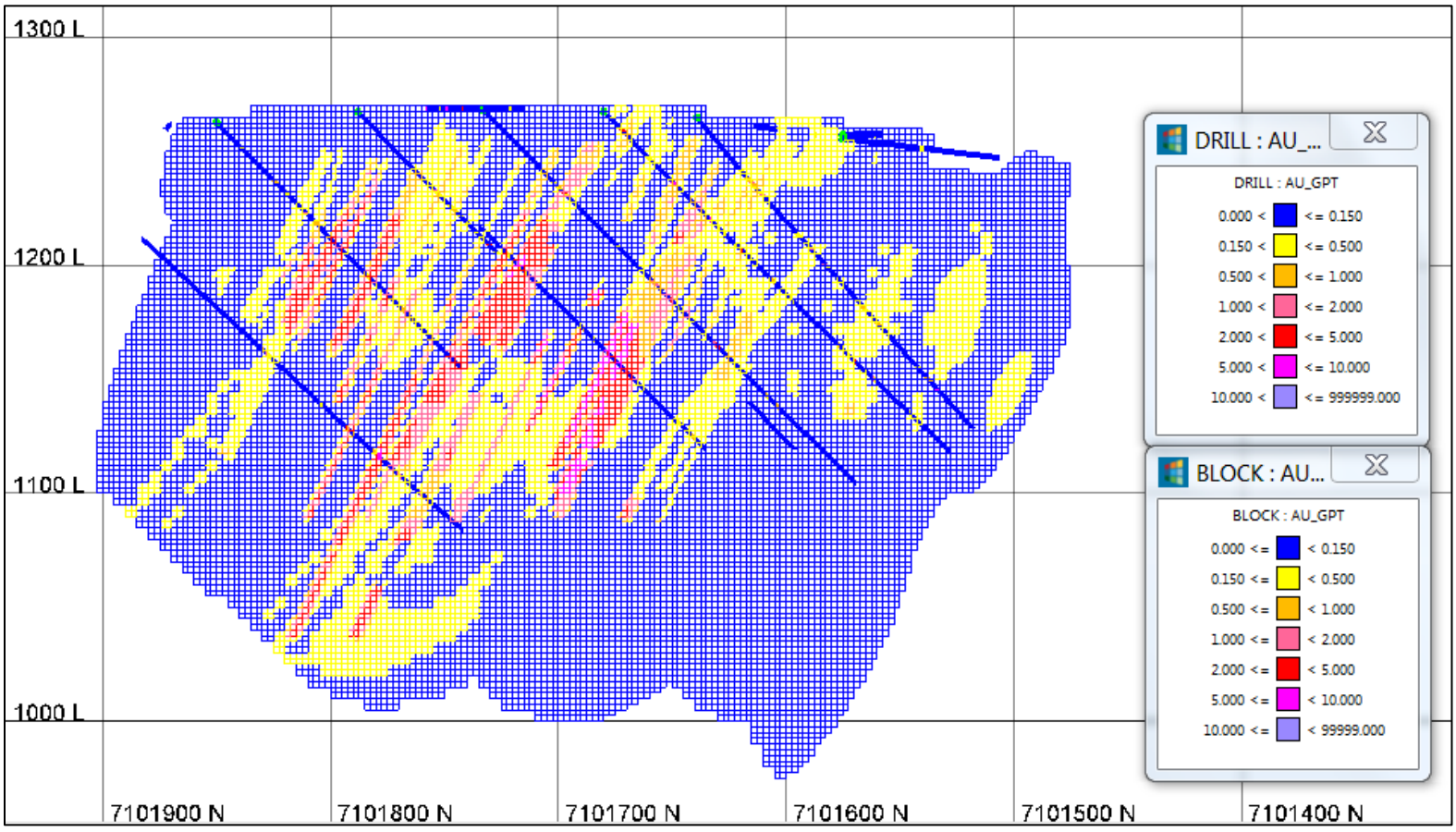

Figure 14-9: Gold Block Grade Estimates and Drill Hole Grades – Section 473,775E Looking East – Raven Gold Deposit

Source: Ginto Consulting (2022)

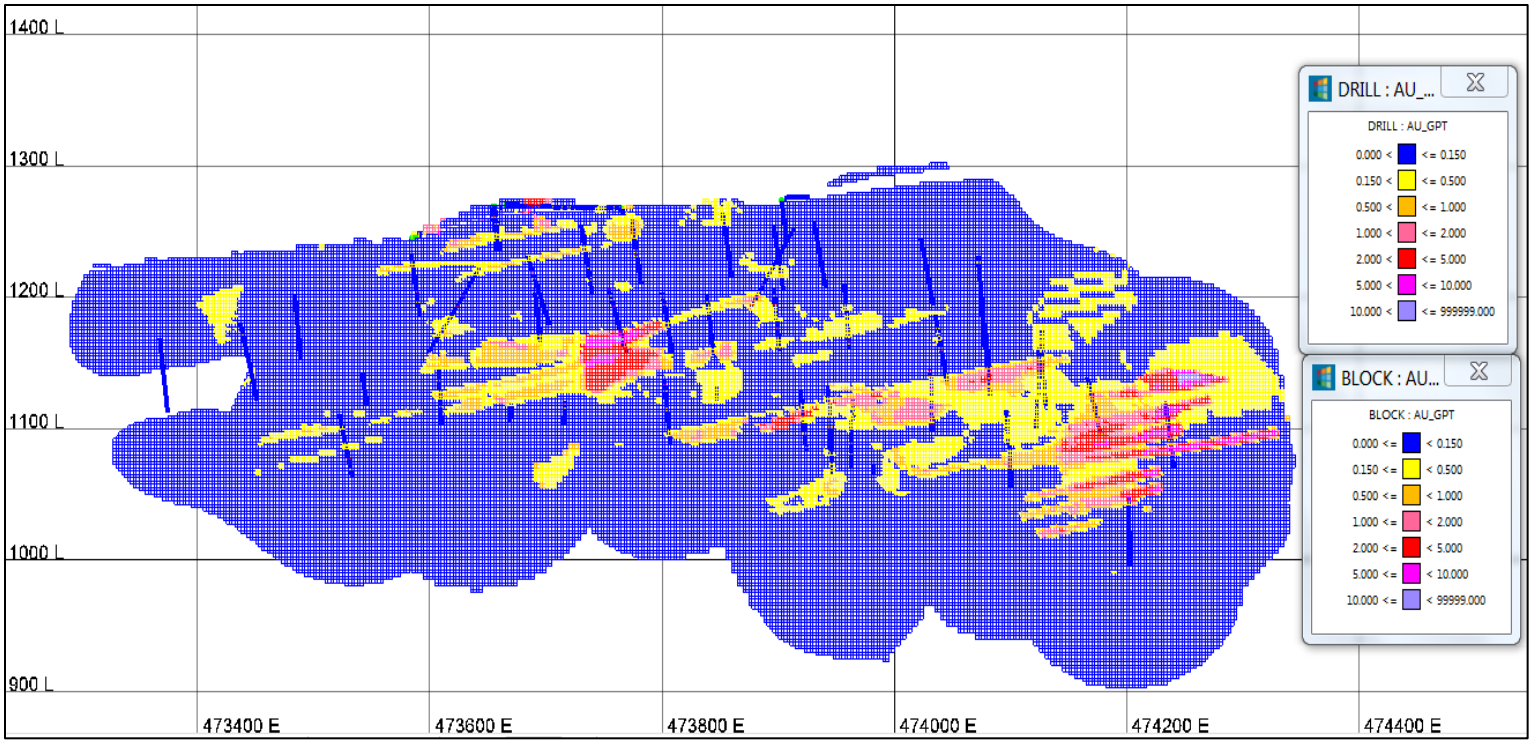

Figure 14-10: Gold Block Grade Estimates and Drill Hole Grades – Section 7101700N Looking North – Raven Gold Deposit

Source: Ginto Consulting (2022)

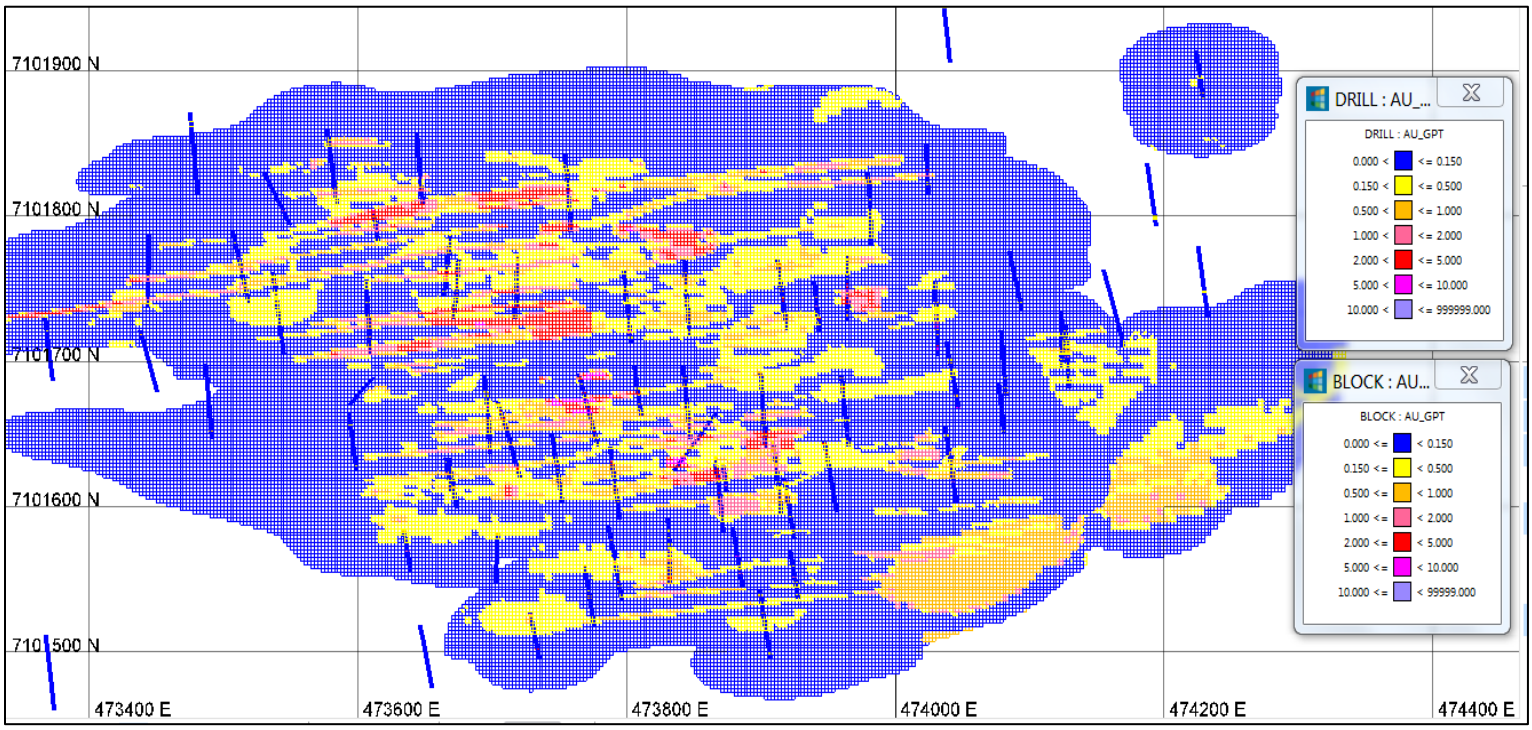

Figure 14-11: Gold Block Grade Estimates and Drill Hole Grades – Plan 1150 Elevation – Raven Gold Deposit

Source: Ginto Consulting (2022)

14.7.2 Global Bias

The comparison of the average gold grades from the declustered composites and the estimated block grades examines the possibility of a global bias of the estimates. As a guideline, a difference between the average gold grades of more than ± 10% would indicate a significant over- or under-estimation of the block grades and the possible presence of a bias. It would be a sign of difficulties encountered in the estimation process and would require further investigation.

Results of this average gold grade comparison are presented in Table 14-9.

Table 14-9: Average Gold Grade Comparison – Polygonal-Declustered Composites with Block Estimates – Raven Gold Deposit.

Statistics	Declustered Composites	Block Estimates
Average Gold Grade g/t	0.210	0.190
Difference	-9.5%	

Source: Ginto Consulting. (2022)

As seen in Table 14-9, the average gold grades between the declustered composites and the block estimates are within the limits of acceptability. It can be concluded that no significant global bias is present in the gold grade estimates.

14.7.3 Local Bias

A comparison of the gold grade from composites within a block with the estimated grade of that block provides an assessment of the estimation process close to measured data. Pairing of these grades on a scatterplot gives a statistical valuation of the estimates. It is anticipated that the estimated block grades should be similar to the composited grades within the block, however without being of exactly the same value. Thus, a high correlation coefficient will indicate satisfactory results in the interpolation process, while a medium to low correlation coefficient will be indicative of larger differences in the estimates and would suggest a further review of the interpolation process. Results from the pairing of composited and estimated grades within blocks pierced by a drill hole are presented in Table 14-10.

As seen in Table 14-10 for gold, the block grade estimates are similar to the composite grades within blocks pierced by a drill hole, with a high correlation coefficient, indicating satisfactory results from the estimation process.

Table 14-10: Gold Grade Comparison for Blocks Pierced by a Drill Hole – Paired Composite Grades with Block Grade Estimates – Raven Gold Deposit

Block Composites Avg. Au (g/t)	Block Estimates Avg. Au (g/t)	Difference	Correlation Coefficient
0.288	0.310	7.7%	0.724

Source: Ginto Consulting (2022)

14.7.4 Grade Profile Reproducibility

The comparison of the grade profiles of the declustered composites with that of the estimates allows for a visual verification of an over- or under-estimation of the block estimates at the global and local scales. A qualitative assessment of the smoothing/variability of the estimates can also be observed from the plots. The output consists of three graphs displaying the average grade according to each of the coordinate axes (east, north, elevation). The ideal result is a grade profile from the estimates that follows that of the

declustered composites along the three coordinate axes, in a way that the estimates have lower high-grade peaks than the composites, and higher low-grade peaks than the composites. A smoother grade profile for the estimates, from low to high grade areas, is also anticipated in order to reflect that these grades represent larger volumes than the composites.

Gold grade profiles are presented in Figure 14-12.

From the plots of Figure 14-12, it can be seen that the grade profiles of the declustered composites are well reproduced overall by those of the block estimates and consequently that no global or local bias is observed. As anticipated, some smoothing of the block estimates can be seen in the profiles, where estimated grades are higher in lower grade areas and lower in higher grade areas. To quantify the level of smoothing of the estimates, further investigation is required (see Section 14.7.5, Level of Smoothing/Variability).

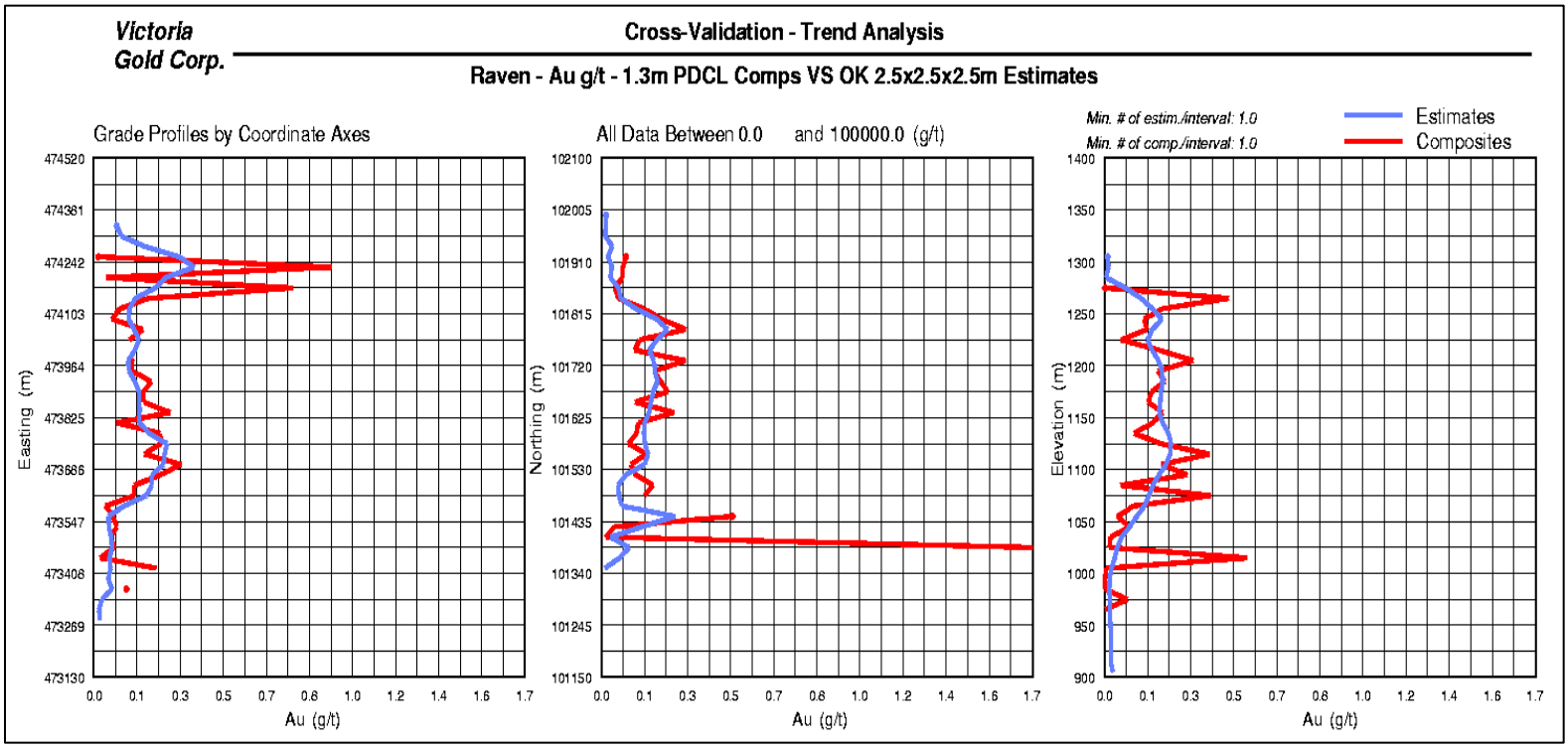

Figure 14-12: Gold Grade Profiles of Declustered Composites and Block Estimates – Raven Gold Deposit

Source: Ginto Consulting (2022)

14.7.5 Level of Smoothing/Variability

The level of smoothing/variability of the estimates can be measured by comparing a theoretical distribution of block grades with that of the actual estimates. The theoretical distribution of block grades is derived from that of the declustered composites, where a change of support algorithm is utilized for the transformation (Indirect Lognormal Correction). In this case, the variance of the composites' grade population is corrected (reduced) with the help of the variogram model, to reflect a distribution of block grades (2.5m x 2.5m x 2.5m). The comparison of the coefficient of variation (CV) of this population with that of the actual block estimates provides a measure of smoothing. Ideally a lower CV from the estimates by 5 to 30% is targeted as a proper amount of smoothing. This smoothing of the estimates is desired as it allows for the following factors: the imperfect selection of mineralized blocks at the mining stage (misclassification), the block grades relate to much larger volumes than the volume of core (support effect), and the block grades are not perfectly known (information effect). A CV lower than the 5 to 30% range for the estimates would indicate

a larger amount of smoothing, while a higher CV would represent a larger amount of variability. Too much smoothing would be characterized by grade estimates around the average grade, where too much variability would be represented by estimates with abrupt changes between lower and higher-grade areas.

Results of the level of smoothing/variability analysis are presented in Table 14-11. As observed in this Table, the CV of the gold grade estimates is within the targeted range, indicating an appropriate amount of smoothing/variability of the gold grade estimates.

Table 14-11: Level of Smoothing/Variability of Gold Grade Estimates – Raven Gold Deposit

CV – Theoretical Block Grade Distribution	CV – Actual Block Grade Distribution	Difference
4.373	2.793	-14.6%

Source: Ginto Consulting (2022)

14.8 Mineral Resource Classification

The mineral resource was classified as inferred at this stage of the project. This decision mainly stems from the wider spacing of the drill holes with regards to the configuration of the gold mineralization within the Massive Sulphide Veins and Low-Grade domains.

14.9 Mineral Resource Calculation

14.9.1 Specific Gravity

Average specific gravity values were assigned to blocks within each of the MSV, LG, and overburden domains as presented in Table 14-12.

Table 14-12: Specific Gravity by Domain – Raven Gold Deposit

Domain	MSV	LG>0.2	LG>0.6	LG>4.0	OVB	OUT
SG	4.50	2.65	2.65	2.65	2.00	2.65

Source: Ginto Consulting (2022)

14.9.2 Mineral Resource Constraint

With the objective to satisfy the NI 43-101 requirement of reporting a mineral resource that provides “reasonable prospects for economic extraction”, an open pit shell was optimized to constrain the mineral resources. A summary of the mineral resource pit constraining parameters is shown in Table 14-13. The constraining pit shell optimized with the Lerchs-Grossman algorithm is shown in Figure 14-13.

Table 14-13: Mineral Resource Constraining Parameters* – Raven Gold Deposit

Gold Price	$1,700/oz
Mining Cost	$1.50/t
Processing Cost	$2.00/t
G&A Cost	$2.50/t
Heap Leach Recoveries	90%
Pit Slopes	45°

Source: Ginto Consulting (2022)

*All dollar amounts in US$

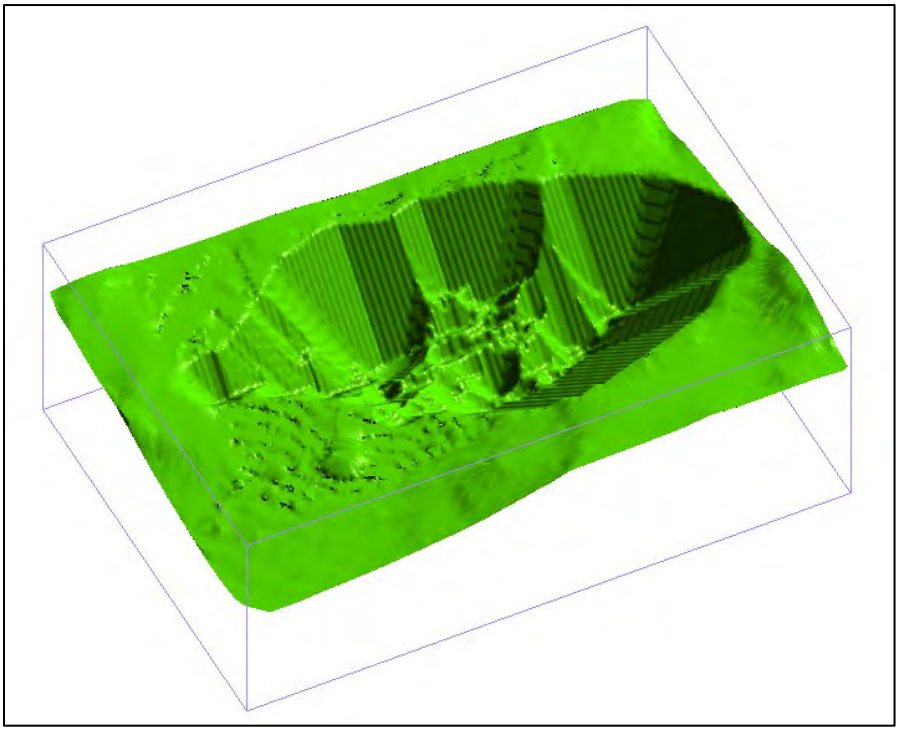

Figure 14-13: Mineral Resource Open Pit Shell – Perspective View Looking to the Northeast – Raven Gold Deposit

Source: Ginto Consulting (2022)

The pit-constrained inferred mineral resources are presented at various gold grade cut-offs in Table 14-14. The pit-constrained inferred mineral resources within the Massive Sulphide Veins domain are presented in Table 14-15 and within the Low-Grade domain in Table 14-16.

At a 0.50 g/t Au cut-off, the pit-constrained, inferred mineral resources, are of 20.0 million tonnes at an average gold grade of 1.67 g/t for a total of 1.1 million ounces of gold.

It should be noted that mineral resources are not mineral reserves and do not have demonstrated economic viability. There is no certainty that all or any part of the mineral resources estimated will be converted into mineral reserves. The estimate of mineral resources may be materially affected by future changes in environmental, permitting, legal, title, taxation, socio-political, marketing, mining, metallurgy, infrastructure, or other relevant issues. However, there are no currently known issues that negatively impact the stated mineral resources.

The CIM definitions were followed for the classification of inferred mineral resources. The inferred mineral resources have a lower level of confidence and must not be converted to mineral reserves. It is reasonably expected that the majority of inferred mineral resources could be upgraded to indicated mineral resources with continued exploration.

Table 14-14: Pit-Constrained Inferred Mineral Resources (Massive Sulphide Veins + Low-Grade Domains) – Raven Gold Deposit

Au Cut-Off g/t	Tonnage tonnes	Avg Au Grade g/t	Au Content oz
0.30	27,254,472	1.32	1,160,157
0.35	24,604,552	1.43	1,132,790

Au Cut-Off g/t	Tonnage tonnes	Avg Au Grade g/t	Au Content oz
0.40	22,874,757	1.51	1,111,986
0.45	21,308,166	1.59	1,090,637
0.50	**19,956,934**	**1.67**	**1,070,239**
0.55	18,894,809	1.73	1,052,159
0.60	17,635,639	1.82	1,029,103
0.65	15,479,632	1.98	985,410
0.70	14,437,186	2.07	962,681

Source: Ginto Consulting (2022)

Notes:

1. The effective date for the Mineral Resource is September 15, 2022.
2. Mineral Resources which are not Mineral Reserves do not have demonstrated economic viability. The estimate of Mineral Resources may be materially affected by environmental, permitting, legal, title, taxation, sociopolitical, marketing, or other relevant issues.
3. The CIM definitions were followed for classification of Mineral Resources. The quantity and grade of reported inferred Mineral Resources in this estimation are uncertain in nature and there has been insufficient exploration to define these inferred Mineral Resources as an indicated Mineral Resource and it is uncertain if further exploration will result in upgrading them to an indicated or measured Mineral Resource category.
4. Mineral Resources are reported at a cut-off grade of 0.50 g/t Au, within a Lerchs-Grossman pit shell using a gold price of US$1,700/ounce and a US$/CAN$ exchange rate of 0.75.

Table 14-15: Pit-Constrained Inferred Mineral Resources - Massive Sulphide Veins Domain – Raven Gold Deposit

Au Cut-Off g/t	Tonnage tonnes	Avg Au Grade g/t	Au Content oz
0.30	18,601,644	1.63	976,626
0.35	17,581,942	1.71	965,485
0.40	16,782,742	1.77	956,131
0.45	16,037,440	1.84	946,155
0.50	**15,390,060**	**1.89**	**936,165**
0.55	14,775,490	1.95	925,859
0.60	14,042,379	2.02	911,975
0.65	13,326,222	2.10	897,598
0.70	12,671,963	2.17	883,679

Source: Ginto Consulting (2022)

Table 14-16: Pit-Constrained Inferred Mineral Resources - Low-Grade Domain – Raven Gold Deposit

Au Cut-Off g/t	Tonnage tonnes	Avg Au Grade g/t	Au Content oz
0.30	8,652,829	0.66	184,165
0.35	7,022,610	0.74	167,305
0.40	6,092,015	0.80	156,103
0.45	5,270,727	0.86	144,886
0.50	**4,566,873**	**0.92**	**134,348**
0.55	4,119,320	0.96	126,744
0.60	3,593,261	1.01	117,028
0.65	2,153,409	1.26	87,511

Au Cut-Off g/t	Tonnage tonnes	Avg Au Grade g/t	Au Content oz
0.70	1,765,223	1.39	79,114

Source: Ginto Consulting (2022)

14.10 Discussion and Recommendations

This study provides an initial estimation of the mineral resource of the Raven Gold Deposit. This mineral resource is classified as inferred due to the wider spacing of the drill hole data with regards to the configuration of the gold mineralization within the Massive Sulphide Veins and Lower Grade domains. For such, additional infill drilling is needed to increase the confidence level of the mineral resource estimate. This will allow to better understand and model the different, more intricate, geologic controls on gold mineralization. Within the Massive Sulphide Veins domain, infill drilling will benefit the modelling of the individual veins with a better delineation of their shape and extent. Within the Low-Grade domain, additional drilling will help better understand and define the geologic controls on gold mineralization.

The variographic analysis produced variograms of acceptable quality, however additional infill drilling would provide a better definition of the gold grade continuity at a more local scale.

The specific gravity values used for tonnage calculation are preliminary in nature and require additional statistical evaluation.

Based on the visual and statistical validation tests, the pit-constrained inferred mineral resources of the Raven Gold Deposit are considered to be representative of the gold mineralization, as currently understood from the available drill hole information.

Potential for additional mineral resources is good and for such, additional exploration drilling along trends outlined from the current gold grade model is recommended.

15 MINERAL RESERVE ESTIMATES

There are no mineral reserve estimates stated on this project. This section does not apply to the Technical Report.

16 MINING METHODS

This section does not apply to the Technical Report.

17 RECOVERY METHODS

This section does not apply to the Technical Report.

18 PROJECT INFRASTRUCTURE

This section does not apply to the Technical Report.

19 MARKET STUDIES AND CONTRACTS

This section does not apply to the Technical Report.

20 ENVIRONMENTAL STUDIES, PERMITTING AND SOCIAL OR COMMUNITY IMPACT

20.1 Regulatory Requirements

The regulatory approval process for major hard rock mines in Yukon, which the Raven Project would be subject to, currently occurs in two stages:

The first stage involves assessment of a proposed project pursuant to the *Yukon Environmental and Socio-economic Assessment Act (*YESAA).

In the first stage, YESAA provides a broadly scoped planning process whereby affected governments (territorial, federal or First Nations) use an assessment report prepared by an arms-length assessment body (the Yukon Environmental and Socio-economic Assessment Board or YESAB) to evaluate whether a project can proceed to the regulatory approvals process (permits, authorizations and licences). Government agencies make the final YESAA assessment decisions by issuing a “decision document” and continue to manage their respective permitting and licensing processes.

The second stage involves acquiring certain major regulatory approvals. For the Raven Project, the following major regulatory approvals will be required:

- Quartz Mining License – required under the Yukon *Quartz Mining Act* and administered by the Government of Yukon Department of Energy, Mines and Resources.
- Type A Water Use License – required under the Yukon *Waters Act* and administered by the Yukon Water Board.

Based on certain triggering activities and/or project design considerations, additional approvals will also likely be necessary including, but not limited to;

- authorization required the *Fisheries Act* and administered by the DFO.
- authorization required under the *Navigable Waters Protection Act* and administered by Transport Canada.
- Explosives Factory and Storage License – required under the *Explosives Act* and administered by NRCan.

The regulatory approval processes can occur concurrently, however, permits and licences cannot be issued until after the YESAA assessment is complete, and a positive assessment decision issued.

To support the regulatory requirements to advance a project to the construction and mining phase, environmental, and socio-economic data collection programs are necessary. As the Eagle Gold Mine has successfully completed these regulatory phases and the environmental and socio-economic data collections scopes are generally within the same area as Raven, there is some applicability of the already collected date; however, additional programs specific to the Raven Deposit will be necessary.

21 CAPITAL AND OPERATING COSTS

This section does not apply to the Technical Report.

22 ECONOMIC ANALYSIS

This section does not apply to the Technical Report.

23 ADJACENT PROPERTIES

23.1 Eagle Gold Mine

Victoria Gold's Dublin Gulch Property, including the producing Eagle Gold mine open pit and associated infrastructure lies approximately 15km west southwest of the Raven Project (Figure 23-1). The Dublin Gulch Property, which Raven lies within, is accessible by road year-round, and is connected to Yukon Energy's electrical grid.

The Eagle deposit represents a large-tonnage reduced intrusion-related gold systems associated with Cretaceous Tombstone and Mayo suite granodiorite intrusions and structurally controlled high-grade gold-sulphide veins.

The Dublin Gulch property covers an area of approximately 555 km^2 and is the site of the Company's Eagle and Olive Gold Deposits. The Eagle Gold Mine is Yukon's newest operating gold mine reaching commercial production July 1, 2020. The Eagle and Olive deposits include Proven and Probable Reserves of 3.3 million ounces of gold from 155 Mt of mineralization with a grade of 0.65 g/t Au, as outlined in a National Instrument 43-101 Technical Report for the Eagle Gold Mine dated December 3, 2019. The Mineral Resource under National Instrument 43-101 – *Standards of Disclosure for Mineral Projects* (“NI 43-101”) for the Eagle and Olive deposits has been estimated to host 227 Mt averaging 0.67 g/t Au, containing 4.7 million ounces of gold in the "Measured and Indicated" category, inclusive of Proven and Probable Reserves, and a further 28 Mt averaging 0.65 g/t Au, containing 0.6 million ounces of gold in the "Inferred" category (JDS Energy and Mining, 2019).

23.2 Lynx

Lynx is located centrally in the Dublin Gulch claim block, approximately five kilometres southwest of Raven, and is centered on a 400 by 700-metre elliptical exposure of Cretaceous granodiorite stock that intrudes overlying metasedimentary Proterozoic Hyland Group and Devonian-Mississippian Keno Hill Quartzite Formations (Figure 23-1). The Lynx target exhibits similar characteristics to the Nugget and Raven targets and has seen limited exploration by previous operators including a preliminary drilling/trenching campaign in 1997 that received follow-up drill testing in 2004.

During the 2021 season, there were 11 drill holes for 2,706 m drilled at Lynx, combined with 22 surface trenches totalling 2,362 metres. Additionally, mapping and soils geochemical surveys were conducted.

Highlighted assay results received from the first 2021 Lynx holes follow:

- 2.00 g/t Au over 32.3m in LX21-025C
- 1.14 g/t Au over 31.4m in LX21-026C
- 2.52 g/t Au over 10.2m in LX21-027C
- 3.42 g/t Au over 18.3m in LX21-026C

23.3 Keno Hill - Hecla Mining Corp.

Previous to the recent purchase of Alexco Resource Corp., Alexco was a Canadian primary silver company that owned the majority of the historic high-grade Keno Hill silver district in Canada's Yukon territory. Alexco had a long history of expanding Keno Hill's mineral resources through successful exploration and advanced

Keno Hill to production. In 2019, the company published a prefeasibility study that estimated production of 1.18 Mt of mineralization at an average rate of 430 t/d - at an average grade of 805 g/t Ag over an eight-year mine life from the Flame & Moth, Bermingham, Bellekeno, and Lucky Queen deposits.

According to the Yukon government's Minfile database, between 1913 and 1989 the Keno Hill Silver District produced in excess of 200 million ounces of silver from over 5.3 Mt of mineralization with average grades of 44 oz/t Ag, making it the second-largest historical silver producer in Canada. In 1989, with falling metal prices and increased environmental standards, the former owners of the Keno Hill Silver District, United Keno Hill Mines Limited, terminated its mining activities in the District.

Today, the Keno Hill Silver District is owned by Hecla Mining.

Historically, Alexco's Bellekeno silver mine, one of the world's highest-grade silver mines with a production grade of up to 1,000 g/t Ag, commenced commercial production at the beginning of 2011 and was Canada's only operating primary silver mine from 2011 to 2013 (Figure 23-1). The opening of Bellekeno marked the rebirth and rejuvenation of one of Canada's most famous and prolific historic mining districts.

Following suspension of operations at Bellekeno in 2013 and subsequent discovery of two new high-grade silver deposits, Alexco published a Pre-feasibility Study ("PFS"), the results of which were announced in March 2019.

The PFS anticipates sequential production from four high-grade silver deposits (Bermingham, Flame & Moth, Bellekeno and Lucky Queen) over an eight-year mine life producing 1.18 Mt of mineralization with an average silver grade of 805 g/t, 2.98% lead and 4.13% zinc. Silver production is anticipated to be approximately 4 million ounces per year.

Alexco had resumed mining operations at KHSD in 2021 after receiving a Water License for production from the Bermingham deposit. The Company had the requisite permits and authorizations for future production of mineralized material from the Bellekeno, Flame & Moth, Lucky Queen, and Onek. Hecla Mining is now in the process of taking over the properties completely (JDS Energy and Mining, 2019).

23.4 AurMac Property - Banyan Gold Corp.

Located South of the Raven Property (Figure 23-1). The AurMac Project is an advanced gold prospect located in the Mayo Mining District of central Yukon, approximately 40 km north of the community of Mayo, Yukon (65km from the Raven Property). The Property consists of 907 claims totaling approximately 173 km^2 and contains three areas of known gold mineralization, the Airstrip, Powerline and the Aurex Hill Zones.

Gold mineralization has been discovered in several areas across the AurMac Project. The Airstrip, Powerline and Aurex Hill Zones have received the most exploration and have the best-known examples of:

- Gold mineralization associated with pyrrhotitic retrograde skarn-like assemblages: Shear and contact metamorphic-induced calc-silicate altered sediments (calcareous siltstones) contain abundant pyrrhotite (locally in massive bands) along low angle shear planes and later veins and fractures. The pyrrhotite occurs as stretched grains and blebs orientated along the foliation bands within the calc-silicate altered rocks, in areas of intense shear strain. Pyrrhotite can form aggregates up to several millimetres in size where entire limestone beds have been skarnified. Pyrrhotite forms >99% of the sulphide mineralization associated with the calc-silicate alteration, with minor/trace amounts of chalcopyrite, pyrite and sphalerite. Scheelite is also common mineral in the pyrrhotitic rich horizons. This style of mineralization occurs in the Airstrip Zone, Powerline Zone and Aurex Hill Zone;
- Gold mineralization associated with quartz-arsenopyrite veins: Tend to occur in clusters of dilatant zones which suggest easterly to north-easterly strike; the dip of the veins are somewhat irregular

but commonly steep south to vertical to steep north. The veins range from 2 -60 mm in thickness. The veins have been identified in the Airstrip Zone, Powerline Zone and Aurex Hill Zone and are seen crosscutting schistose quartzites, phyllites, graphitic schist, calc-silicate sediments, greenstones, and granitic intrusions; and

- Gold mineralization associated with siderite-galena-sphalerite veins/breccias: Are siderite healed brittle fault zones with coarsely crystalline galena and marmatite sphalerite. This style of mineralization has only been observed in the Airstrip Zone.

The Airstrip and Powerline Zones occur in the south-dipping limb of the McQuesten antiform, a broad, west-southwest-plunging arch of older planar features (including bedding); all of which are well faulted as the result of the Robert Service and Tombstone thrusts and associated Strain Zone. The rocks in the Airstrip Zone and Powerline Zone consist of repeated cycles of non-calcareous foliated rocks (thinly bedded quartzites, graphitic schist, quartz-muscovite schists) separating assemblages of mixed calcareous foliated rock types (limestone, calcareous siltstones, retrograde skarn horizons [sulphide >5%], retrograde calc-silicate horizons). In the Airstrip Zone, these repeated cycles of non-calcareous and calcareous lithologies overlie a thick package of thinly-bedded graphitic quartzite; there are at least two felsic-aplitic dykes cutting through the Airstrip Zone. The Powerline Zone lies stratigraphically above the Airstrip Zone, and physically approximately one km to the south. In the Powerline Zone there are multiple gabbroic foliaform sills. Mineralized structures are interpreted as coeval with the emplacement of Tombstone intrusions.

As announced on May 17, 2022, the Updated AurMac Mineral Resource comprises a total inferred mineral resource of 3,990,000 ounces of gold on the road accessible AurMac Property (JDS Energy and Mining, 2022).

23.5 McConnell's Jest - (Zonte Metals Inc.)

The McConnell's Jest project, owned by Zonte Metals Inc., is located in the Yukon Territory about 65 km northeast of the town of Mayo. Zonte Metals Inc. properties – Victoria/Zonte are approximately 5km East of the Raven Project (Figure 23-1). The project is composed of 172 contiguous quartz claims covering approximately 3,371 hectares and is accessible by a helicopter, trails, and a road on the eastern edge of the property. Zonte completed a short exploration program during the summer of 2017 which included prospecting and drilling of five drill holes in three targets. Drilling made a discovery on the Two-Four target where the company intersected 20.28 m of 0.69 g/t Au and 20.45m of 0.72 g/t in drill hole MJ-04. MJ-03 also intersected long intervals of anomalous gold including 81.81m of 0.20 g/t Au. These results have not yet been followed up with additional exploration (Randell et al., 2017).

The project is considered an Intrusion Related Gold System and is located within the Tintina Gold Belt which stretches across Alaska and the Yukon and is host to a significant number of large deposits including Donlin Creek (32 Moz Au), Dublin Gulch (6.3 Moz) and Fort Knox (4.7 Moz) with the latter two classified as Intrusion Related Gold Deposits as well (Randell et al., 2017).

23.6 Shanghai

The Shanghai Property, owned by Yankee Hat Minerals Ltd. is located Southwest of the Raven Property (Figure 23-1). The Shanghai vein is a strong, anastomosing, transverse type structure, cutting Late Proterozoic-Early Cambrian Hyland Group schist and Mississippian Keno Hill quartzite on the north limb of the McQuesten Anticline. Mineralization is comprised of sphalerite as well as sporadic lenses of galena and tetrahedrite. The best assays reported from more than 305 m of drifted vein are 51.8 m grading 37.0 g/t Ag, 0.4% Pb, 13.6% Zn and 0.5% Cu over an average width of 2.5 m, and 9.1 m grading 1182.8 g/t Ag, 8.2% Pb and 7.2% Zn across an average width of 1.5 m. The Shanghai vein has right-lateral movement and dips to the northwest. This orientation is completely opposite of the neighbouring vein system in the Keno Hill District (YGS, 2022).

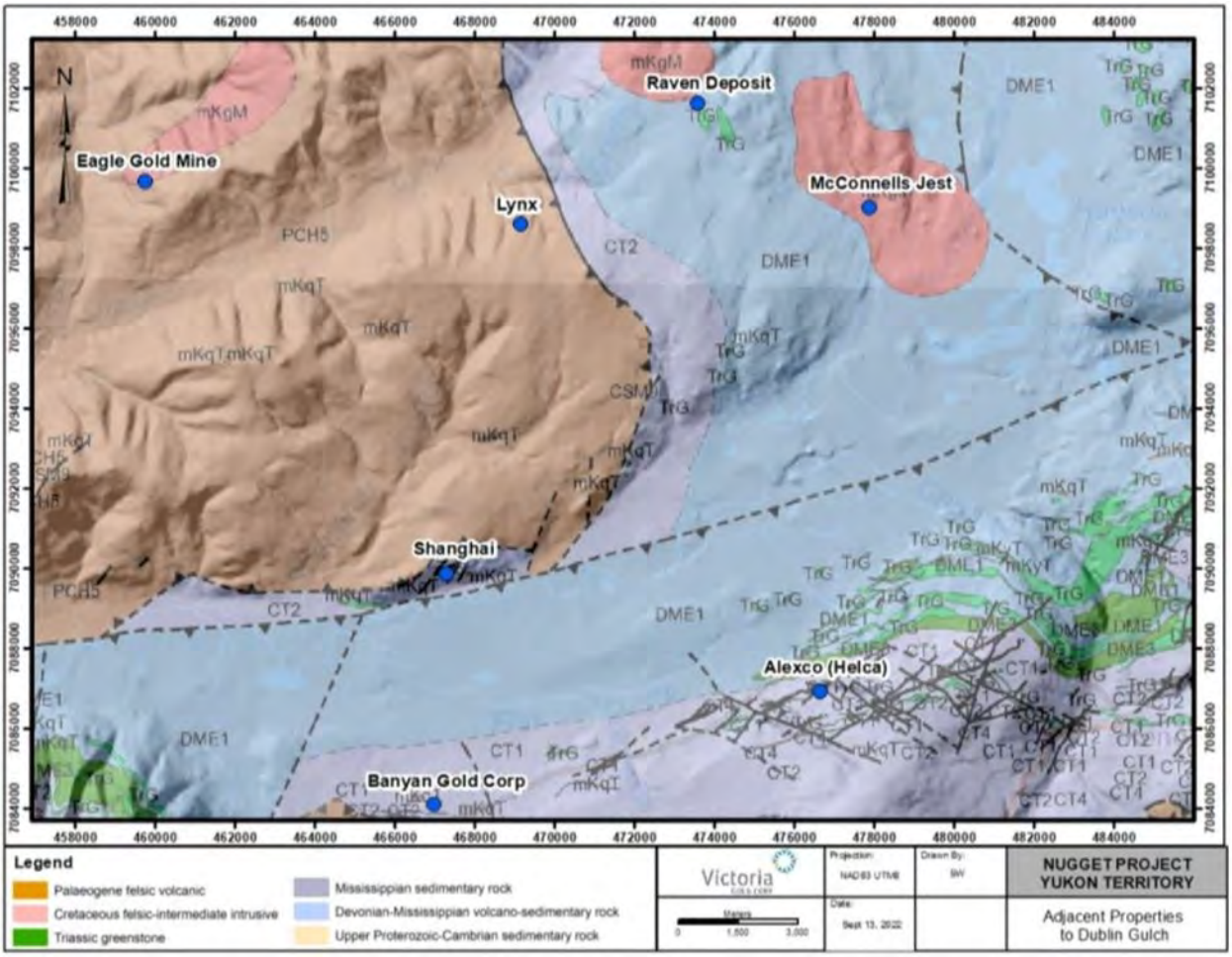

Figure 23-1: Adjacent Properties to the Raven Deposit

Source: Victoria Gold Corp. (2022)

24 OTHER RELEVANT DATA AND INFORMATION

Subsequent to the Raven resource drilling described in this report, Victoria's exploration team continued to explore the Raven Deposit in 2022. From June 2022 through October 2022, Victoria drilled ninety-one (91) holes (25,117 metres) within and proximate to the Raven Deposit. There were 1,344 Bulk Density measurements collected.

Additionally, Victoria drilled six (6) holes (1,971 metres) at Lynx with commensurate trench construction/samples - 12 trenches (932 metres); and collected over 1800 soil geochemical samples in the eastern portion of the Dublin Gulch claim block. This exploration work from the 2022 season was not included in the MRE on the Raven Deposit.

25 INTERPRETATION AND CONCLUSIONS

The Raven Project represents a potentially high-grade, on/near-surface gold deposit that lies in the extreme Southeast contact of the Nugget Intrusive Stock and the surrounding Earn Group metasedimentary package. This large, approximately three (3) kilometres by two (2) kilometres, medium to coarse grained granodiorite stock of Cretaceous age represents the second largest intrusive body on the Dublin Gulch property (second only to the Dublin Gulch stock that hosts the Eagle Gold Mine).

The Project area has been explored for gold and silver intermittently since the late 1940's and continues to produce meaningful results from on-going mineral exploration. Mineral exploration work has included; large scale remote sensing to focused prospecting, hand and mechanized trenching, extensive soil sampling, multiple geophysical surveys (airborne and ground based), and numerous diamond drilling campaigns. This work has resulted in the discovery of the Raven gold deposit as well as a series of additional mineralized targets across the Dublin Gulch Claim Block.

Exploration programs conducted by Victoria from 2018 to 2021 took Raven from a conceptual target based on the internally developed Potato Hills Trend Mineralization model, to an initial mineral resource estimate released on September 15th, 2022 (Table 25-1). Exploration conducted through 2022 is expected to further refine the geological understanding of the deposit and expand the mineralized footprint to increase the size and confidence of this inferred resource.

Table 25-1: Pit-Constrained Inferred Mineral Resources at various Au Cut-Offs Effective September 15, 2022 – Raven Deposit

Au Cut-Off g/t	Tonnage tonnes	Avg Au Grade g/t	Au Content oz
0.30	27,254,472	1.32	1,160,157
0.35	24,604,552	1.43	1,132,790
0.40	22,874,757	1.51	1,111,986
0.45	21,308,166	1.59	1,090,637
0.50	19,956,934	1.67	1,070,239
0.55	18,894,809	1.73	1,052,159
0.60	17,635,639	1.82	1,029,103
0.65	15,479,632	1.98	985,410
0.70	14,437,186	2.07	962,681

Notes:

1. The effective date for the Mineral Resource is September 15, 2022.
2. Mineral Resources which are not Mineral Reserves do not have demonstrated economic viability. The estimate of Mineral Resources may be materially affected by environmental, permitting, legal, title, taxation, sociopolitical, marketing, or other relevant issues.
3. The CIM definitions were followed for classification of Mineral Resources. The quantity and grade of reported inferred Mineral Resources in this estimation are uncertain in nature and there has been insufficient exploration to define these inferred Mineral Resources as an indicated Mineral Resource and it is uncertain if further exploration will result in upgrading them to an indicated or measured Mineral Resource category.
4. Mineral Resources are reported at a cut-off grade of 0.50 g/t Au, within a Lerchs-Grossman pit shell using a gold price of US$1,700/ounce and a US$/CAN$ exchange rate of 0.75.

This is the first mineral resource estimate ("MRE") of the Raven Deposit. The drill hole database utilized for this MRE utilizes 78 diamond drill holes collared between August 2018 and September 2021 and is comprised of 11,956 assays from 18,217 m of drilling. Additionally, 55 surface trenches with 3,464 assays and 7,443m of sampling were included in establishing the MRE.

The confidence classification of the resource (Inferred) is due to the wider spacing of the drill hole data, hindering the modelling of tighter geologic controls on gold mineralization. Based on the visual and statistical validation tests, the pit-constrained inferred mineral resource of the Raven deposit (Table 25-1) is considered to be representative of the gold mineralization, as currently understood from the available drill-hole information.

All geological data used for the resource estimate was reviewed and verified by the author as being accurate to the extent possible and to the extent possible all geologic information was reviewed and confirmed. The sample preparation, security, assay sampling, and extensive QA/QC sampling of core by Victoria Gold Corp. provides adequate and good verification of the data and it is believed that the work has been done within the guidelines of NI 43-101. The confirmation of the historic data by the Victoria Gold Corp. drill holes has provided sufficient comfort to be used for the estimation of an inferred mineral resource.

There are no significant risks or uncertainties specifically relevant to this Project, only the normal uncertainties associated with future changes in political, regulatory, financial, and metal market environments.

26 RECOMMENDATIONS

The results of diamond drilling, trenching, and soil geochemical sampling from 2018 to 2021 by Victoria's exploration team has been the development and validation of the geological model for the Raven Zone. The significant results to date show that the Raven Zone is open to expansion along strike and down dip.

The confidence classification of the resource (Inferred) is due to the wider spacing of the drill hole data, hindering the modelling of tighter geologic controls on gold mineralization. Based on the visual and statistical validation tests, the pit-constrained inferred mineral resource of the Raven deposit is considered to be representative of the gold mineralization, as currently understood from the available drill-hole information.

A two (2) phase $35,000,000 exploration program is recommended for the Raven Project. Phase I will expand the Raven resource and consist of: 25,000 m of step-out drilling down-dip and along strike at the Raven Zone and the collection and testing of Raven mineralization for metallurgical testing; Phase II will upgrade the Raven resource from inferred to indicated and consist of: 25,000 m of in-fill drilling and additional metallurgical testing at the Raven Zone. The Raven Project's recommended budget is shown in Table 26-1.

Table 26-1: Recommended Raven Project Exploration Budget

Phase I 150 Day Field Program		
Work/Employee Description	**Time and Per Day Unit Cost**	**Cost**
GIS data compilation/3D modelling (Annual license + Training)		$50,000
Mobilization/Demobilization/Travel Related (RE construction + monthly rental)		$325,000
Project Geologist (4)	150 days @ $500 per day	$300,000
Core-Processing (Logger, Tech, Cutter – 16)	150 days @ $425 per day	$1,020,000
Soil Sampling/Trenching (5)	150 days @ $600 per day	$ 450,000
Equipment Operator (5)	150 days @ $1200 per day	$900,000
Vehicle Rental (5)	150 days @ $150 per day	$112,500
Excavator (3) & Dozer (2)	9000 hours @ $150 per hour	$1,350,000
Geochemical Analysis	20000 @ $30 per sample	$600,000
Diesel Fuel + Tank Rental	150,000 litres @ $1 per litre	$162,500
Freight/Expediting		$150,000
Camp Required Materials (Gen, pumps)	150 days @ $180 per day	$27,000
Access Upgrades		$250,000
Environmental Baseline Studies		$2,800,000
Environmental Characterization Studies		$1,000,000
Metallurgical Sampling (drilling)		$500,000
Flotation Studies		$150,000
Permitting		$1,000,000
Community Outreach Projects		$250,000
Communications (monthly rental)	150 days	$95,000
Diamond Drilling	25,000 m @ $150 per m	$3,750,000
Contingency @ 15%		$2,286,300
Phase I Total		**$17,528,300**

Phase II 150 Day In-fill Program		
Work/Employee Description	**Time and Per Day Unit Cost**	**Cost**
GIS data compilation/3D modelling (Annual license + Training)		$50,000
Mobilization/Demobilization/Travel Related (RE construction + monthly rental)		$325,000
Project Geologist (4)	150 days @ $500 per day	$300,000
Core-Processing (Logger, Tech, Cutter – 16)	150 days @ $425 per day	$1,020,000
Soil Sampling/Trenching (5)	150 days @ $600 per day	$ 450,000
Equipment Operator (5)	150 days @ $1200 per day	$900,000
Vehicle Rental (5)	150 days @ $150 per day	$112,500
Excavator (3) & Dozer (2)	9000 hours @ $150 per hour	$1,350,000
Geochemical Analysis	20000 @ $30 per sample	$600,000
Diesel Fuel + Tank Rental	150,000 litres @ $1 per litre	$162,500
Freight/Expediting		$150,000
Camp Required Materials (Gen, pumps)	150 days @ $180 per day	$27,000
Access Upgrades		$250,000
Environmental Characterization Studies		$1,500,000
Environmental Assessment		$1,000,000
Metallurgical Testing		$580,000
Flotation Studies		$150,000
Permitting		$1,000,000
Community Outreach Projects		$250,000
Communications (monthly rental)	150 days	$95,000
Diamond Drilling	25,000 m @ $150 per m	$3,750,000
Contingency @ 15%		$2,103,300
Phase II Total		**$16,125,300**

27 REFERENCES

Aho, A., Tempelman-Kluit, D., (1963). The Report on the Bob Group Mineral Claims, Mayo M. D. Y. T

Aurora Geosciences Ltd. (2018). Interpretation Report Nugget 2018 Geophysics – Mag-VLF & IP Surveys.

Doherty, R. A., Dudka, S., (1994). Report on the 1994 Geological and Geochemical Assessment Work on the TAG Property

Doherty, R. A., (1996). Report on the 1995 Trenching Program on the TAG Property. Assessment Report #093383.

Columbo, F., (2021). Petrographic Report on 9 polished thin sections from the exploration target "Raven" for Victoria Gold Corp.

Corbett, G., (2009). Anatomy of porphyry-related Au-Cu-Ag-Mo mineralised systems: Some exploration implications. FOR: Australian Institute of Geoscientists North Queensland Exploration Conference June 2009, AIG Bulletin 49, p. 33-46.

Fugro Airborne Surveys (2011). INTERPRETATION REPORT - Airborne DIGHEMV and Magnetic Survey Dublin Gulch Area, Yukon for Victoria Gold Corp.

Gordey, S.P. and Makepeace, A.J. (comps.), (2003). Yukon digital geology, version 2.0; Geological Survey of Canada Open File 1749; Yukon Geological Survey Open File 2003-9(D).

Hart, C. J. R., Mair, J. L, Goldfarb, R. J., and Groves, D. I., (2004). Source and redox controls on metallogenic variations in intrusion-related ore systems, Tombstone-Tungsten Belt, Yukon Territory, Canada.

Hart, C. (2007). Reduced Intrusion-related Gold Systems.

Hart, C.J.R, (2007). Reduced intrusion-related Au systems, in Goodfellow, W.D., ed., Mineral Deposits of Canada: A Synthesis of Major Deposit Types, District Metallogeny, the Evolution of Geological Provinces, and Exploration Methods: Geological Association of Canada, Mineral Deposits Division, Special Publication No. 5, p. 96-112.

Hart, C. J. R., McCoy, D. T., Goldfarb, R. J., Smith, M., Roberts, P., Hulstein, R., Bakke, A. A., & Bundtzen, T. K., (2002). Geology, exploration and discovery in the Tintina Gold Province. In Goldfarb R. J. & Neilson, R. (eds) Geology, Exploration and Discovery in the Tintina Gold Province, Alaska and Yukon. Society of Economic Geologists Special Volume 9, 241–74.

Hladky, D., (2004). 2004 [Dublin Gulch] Geophysical Survey. Assessment Report # 094788

JDS ENERGY & MINING INC. (2019). TECHNICAL REPORT FOR THE EAGLE GOLD MINE YUKON TERRITORY, CANADA FOR VICTORIA GOLD CORP.

JDS ENERGY & MINING INC. (2022). TECHNICAL REPORT FOR AURMAC PROPERTY. YUKON TERRITORY, CANADA FOR BANYAN GOLD CORP.

Jenner, G.A., (1996). Trace element geo-chemistry of igneous rocks: Geo-chemical nomenclature and analytical geochemistry, in Wyman, D.A., ed., Trace Element Geochemistry of Volcanic Rocks: Applications for Massive Sulfide Exploration, 12, Geological Association of Canada, Short Course Notes, p. 51–77.

Keyser, H.J., (1997). Report on the 1997 Diamond Drilling Program on the Len Property. Assessment report for Panamex Resources Inc., November 28, 1997.

Kidlark, R. G., (1980). 1979 Geological and Geochemical Assessment Report. For AMAX of Canada Ltd. Assessment Report #090560.

Precision GeoSurveys Inc. (2017). Airborne Geophysical Survey Report – Dublin Gulch, VBW, and Clear Creek Survey Blocks. Mayo, YT.

Randell, A., Kirk, F., and Wilkie, D., (2017). NI 43-101 Technical Report describing GEOLOGY, MINERALISATION, GEOCHEMICAL SURVEYS, AND ENVIRONMENTAL SURVEYS on the McConnell's Jest Intrusion-Related Gold Property Yukon, Canada for Zonte Metal Inc.

Ross, J. P., (2003). Geochemical and Prospecting Report on the HLA HLA 1-14, NEERA 1-2 Claims. Mayo Mining District. Assessment Report #060724.

Scott Wilson Mining (2010). Technical Report on the Dublin Gulch Property, Yukon Territory, Canada NI 43-101 Report April 23, 2010.

Van Tassel, R. E., (1969). Geological and Geochemical Report on the Erin 1 to 28 and 31 to 189 Mineral Claims Inclusive. Assessment Report #094768.

Yukon Geological Survey (2022). Shanghai, Occurrence # 105M 028. https://data.geology.gov.yk.ca/Occurrence/13656#InfoTab, accessed: Oct 11, 2022

28 UNITS OF MEASURE, ABBREVIATIONS AND ACRONYMS

Symbol/Abbreviation	Description
'	Minute (Plane Angle)
"	Second (Plane Angle) or Inches
°	Degree
°C	Degrees Celsius
Au	Gold
AXU	Alexco Resource Corp
BD	Bulk Density
C$	Dollar (Canadian)
CEE	Canadian Exploration Expense
CIM	Canadian Institute of Mining and Metallurgy
CIM	Canadian Institute of Mining
cm	Centimetre
cm^2	Square Centimetre
cm^3	Cubic Centimetre
CV	Coefficient of Variation
EMR	Energy, Mines and Resources
ft	Foot
ft^2	Square Foot
ft^3	Cubic Foot
g	Gram
g/t	Grams Per Tonne
GSC	Geological Survey of Canada
ICP	Inductively Coupled Plasma
ICP-MS	Inductively Coupled Plasma Mass Spectrometry
in	Inch
in2	Square Inch
in3	Cubic Inch
kg	Kilogram
kg/h	Kilograms Per Hour
kg/m^2	Kilograms Per Square Metre
kg/m^3	Kilograms Per Cubic Metre
km	Kilometre
km^2	Square Kilometre
L	Litre

Symbol/Abbreviation	Description
m	Metre
Mt	Million Tonnes
m^2	Square Metre
m^3	Cubic Metre
mg	Milligram
mg/L	Milligrams Per Litre
min	Minute (Time)
mL	Millilitre
NI 43-101	National Instrument 43-101
NND	Na-Cho Nyak Dunn First Nation
NQ	Drill Core Diameter of 47.6 Mm
oz	Troy Ounce
P.Eng.	Professional Engineer
P.Geo.	Professional Geoscientist
ppb	Parts Per Billion
ppm	Parts Per Million
PSD	Particle Size Distribution
psi	Pounds Per Square Inch
QA/QC	Quality Assurance/Quality Control
QKNA	Qualitative Kriging Neighbourhood Analysis
QP	Qualified Person
QQ	Quartile-Quartile
RC	Reverse Circulation
SGC	StrataGold Corporation
t	Tonne (1,000 Kg) (Metric Ton)
VGCX	Victoria Gold Corp.
YEC	Yukon Energy Corporation
YESAA	Yukon Environmental and Socio-Economic Assessment Act
YESAB	Yukon Environmental and Socio-Economic Assessment Board
YG	Yukon Government
YRM	Yukon Revenue Mines Ltd
µm	Microns
µm	Micrometre

29 CERTIFICATES OF QUALIFIED PERSONS

Marc Jutras, M.A.Sc., BSc., P. Eng QP Certificate.

I, Marc Jutras, P. Eng., M.A.Sc., do hereby certify that:

1. This certificate applies to the technical report entitled “Technical Report on the Raven Mineral Deposit, Mayo Mining District, Yukon Territory, Canada” (this “Technical Report”) dated October 26, 2022 prepared for Victoria Gold Corp. with an effective date of September 15, 2022;

2. I am currently employed as Principal, Mineral Resources with Ginto Consulting Inc. with an office at 333 West 17th Street, North Vancouver, British Columbia, V7M 1V9;

3. I am a graduate of the University of Quebec in Chicoutimi in 1983, and hold a Bachelor’s degree in Geological Engineering. I am also a graduate of the Ecole Polytechnique of Montreal in 1989, and hold a Master’s degree of Applied Sciences in Geostatistics;

4. Since 1984, I have worked continuously in the field of mineral resource estimation of numerous international exploration projects and mining operations. I have been involved in the evaluation of mineral resources at various levels: early to advanced exploration projects, preliminary studies, preliminary economic assessments, prefeasibility studies, feasibility studies and technical due diligence reviews;

5. I am a Registered Professional Engineer with the Engineers and Geoscientists British Columbia (license # 24598) and Engineers and Geoscientists Newfoundland and Labrador (license # 09029). I am also a Registered Engineer with the Quebec Order of Engineers (license # 38380);

6. I have read the definition of "qualified person" set out in National Instrument 43-101 (NI 43-101) and certify that by reason of my education, affiliation with a professional association (as defined in NI 43-101) and past relevant work experience, I fulfill the requirements to be a "qualified person" for the purposes of NI 43-101;

7. I have visited the project site on August 30, 2021, on November 27, 2019 and on September 15, 2018. During these site visits, the core logging and sample preparation facilities were visited. Core logging procedures and drill core were reviewed. A geologic tour of the trenches and drill hole locations of the Raven deposit was also carried out, along with discussions with the exploration staff. Overall, the site visits were beneficial in better understanding the geological setting of the gold mineralization at the Raven property;

8. I am responsible for and have reviewed all Sections of this Technical Report. I have prepared the mineral resource estimates of Section 14 and have supervised the preparation of all other Sections of the Technical Report;

9. I am independent of the Issuer, Victoria Gold Corp., and related companies applying all of the tests in Section 1.5 of the NI 43-101;

10. I have had no prior involvement with the property that is the subject of this Technical Report;

11. As of the effective date of this Technical Report, to the best of my knowledge, information and belief, this Technical Report contains all scientific and technical information that is required to be disclosed to make the Technical Report not misleading;

12. I have read NI 43-101, and the Technical Report has been prepared in accordance with NI 43-101 and Form 43-101F1.

Effective Date: 15 September 2022

Signing Date: 26 October 2022

<Original signed by>

Marc Jutras, P. Eng., M.A.Sc.

Principal, Mineral Resources, Ginto Consulting Inc.

APPENDIX 1

RAVEN GEOPHYSICAL REVIEW AURORA GEOSCIENCES LTD.

WORK PERFORMED:
August 27 – September 14, 2018

Prepared for:

Victoria GOLD CORP

Prepared by:

AURORA GEOSCIENCES

Field Report
Nugget 2018 Geophysics – Mag-VLF & IP Surveys

Prepared for:
Victoria Gold Corp.
303 – 80 Richmond Street West
Toronto, ON
M5H 2A4
Attn: Paul Gray

Prepared by:
Dave Hildes Aurora
Geosciences Ltd.
34A Laberge Road, Whitehorse, Yukon, Y1A5Y9
Phone: (867) 668.7672 Fax: (867) 393.3577
www.aurorageosciences.com

CONTENTS

1 SUMMARY

This report describes the DC resistivity-induced polarization (IP), total magnetic field (mag) and very-low frequency electromagnetic (VLF) surveys conducted for Victoria Gold Corporation on the Nugget prospect of the Dublin Gulch Property northwest of Mayo, Yukon.

The surveys consisted of three 2D IP lines, one downhole IP survey, 191.8 line-km of walk-mag where total field readings were collected once per second, and 172 line-km of VLF readings, where readings were collected every 10 m (nominal). The survey plan was fluid and more mag-VLF was surveyed than originally anticipated to ensure complete coverage of the (known) intrusion. Full use was made of the existing road and trail network, but with exception of a northern extension, future mag-VLF survey production will be reduced unless the trail network is expanded or the survey is helicopter assisted.

Aurora Geosciences completed the work in a single deployment from August 27th to September 14th, 2018. The crew stayed in Victoria Gold's Bluto exploration camp and accessed the work area daily by truck. A rock was struck on the access road disabling the truck and for one day the crew relied on Victoria Gold personnel for access while a replacement truck was driven to site from Whitehorse. A full survey log is attached to the digital version of this report.

2 CREW AND EQUIPMENT

The personnel who conducted the survey are detailed in Table 1.

Table 1: Crew detail.

Crew Member	Job Role	Dates on Site
Dave Hildes	Onsite Project Manager	Aug 27 – Sep 14, 2018
Nicholas McKay	Mag-VLF Crew Chief	Aug 27 – Sep 14, 2018
Vince VanDelft	Technician	Aug 27 – Sep 14, 2018
Dimitry Spasoff	Technician	Aug 27 – Sep 14, 2018
Mathew Ford	Technician	Aug 27 – Sep 14, 2018
Madeline Vainionpaa	Technician	Aug 27 – Sep 06, 2018

The crew was equipped with instruments and equipment as detailed in Table 2.

Table 2: Instrument and equipment detail.

Equipment	Model	Serial Numbers
IP receivers	1 X Iris Elrec Pro 1 X GDD GRx24	2315-2758300063-165 1312
IP transmitters	2 X GDD 3.6kW TxII	267 & 438
VLF-Magnetometers	8 X Gem GSM-19V	1024107, 1024108,8017965, 8017966, 8017978,8017979, 8017980, 8017981,
Magnetometers (base)	2 X Gem GSM-19	708719 & 703649
Non-differential handheld GPS	8 X Garmin 64 CSX	
Handheld radios	7 X iCom handheld 1 X Base	
Communication	1 X Iridium Sat phone 1 X InReach	
IP equipment	50 X 50 m cables 50 X 25 m cables 2 X Honda 5 kW generators Misc. IP equipment	
Office equipment	2 X Laptops with Geosoft 1 X Laptop (dumping) Office box including repair kit & bear deterrents	
Vehicles	2 X Trucks (4X4)	

3 SURVEY LOCATION

Victoria Gold's Dublin Gulch property is located approximately 85 km northwest by road of Mayo, YT. The main camp at the Eagle Deposit was at capacity with mine construction activity and the surveys at Nugget were staged from the Bluto exploration camp at 465950E, 7102850N (NAD83, UTM Zone 8 coordinates) approximately 5 km from Eagle over the Potato Hills. Work at Nugget was accessed daily via a 40-minute drive on the 5 km access road. The work described in this report is located within NTS map sheet 106

D/04.

The mag-VLF survey covered the full extent of the known Nugget intrusion. Lines were extended to the northwest to cover another potential intrusion and favorable preliminary soil results. Lines were surveyed at an azimuth of 130°. The base magnetometers and the levelling grid were located adjacent to Bluto camp in a magnetically quiet area.

The IP survey comprised of two lines, each 3.3 km long at an azimuth of 130° completely traversing the extent of the know Nugget intrusion surveyed with 50 metre dipoles and a third line with 25 metre dipoles at an azimuth of 010° starting over the intrusion and extending significantly to the north. A radial array with downhole current sources in NG18-03 was surveyed over the northern margin of the intrusion close to Line 3 with 25 metre dipoles. A similar survey was planned for a hole on the southeast margin (NG1806) but insufficient casing was left in the hole and it was collapsed at less than 2 metres depth.

An overview of the survey grids is shown in Figure 1.

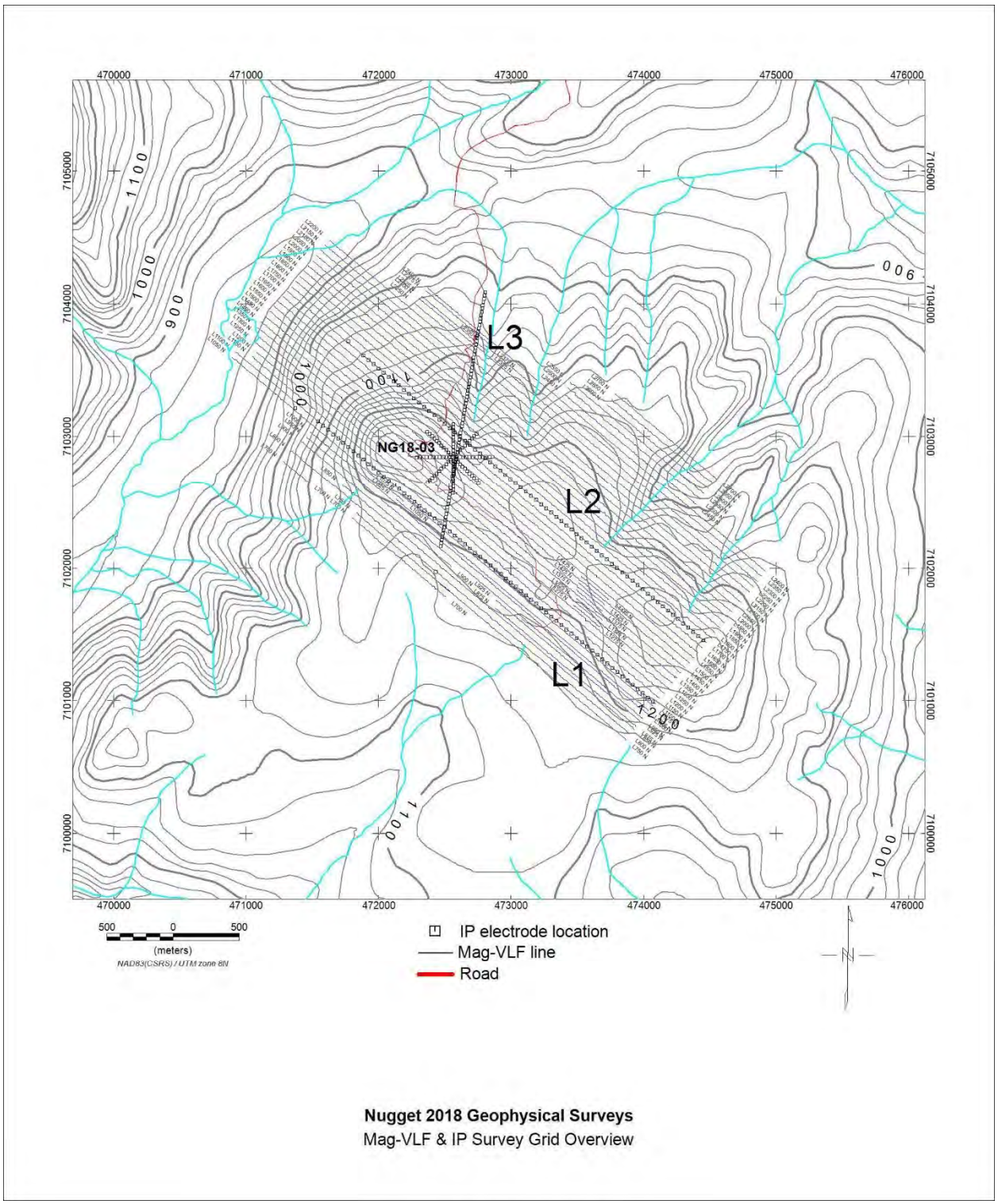

Figure 1: Survey Location and Road Access.

4 SURVEY SPECIFICATIONS

The total magnetic field and VLF-EM surveys were conducted according to specifications detailed in Table 3.

Table 3: Mag-VLF survey specifications.

Mag station spacing	1 s with a minor amount of data collected at a 2 s interval.
VLF station spacing	Nominal 10 m with a minor amount of data collected at a 20 m spacing.
Line spacing	50 m with a minor amount of data collected at a 25 m line spacing.
Line azimuth	130°.
Registration	Navigation by GPS only. NAD83, UTM Zone 8N coordinates were used. No line cutting was required and no stations are marked.
Temporal geomagnetic variation	The primary base station magnetometer was installed in a magnetically quiet area at 466062 E, 7102908 N (NAD83 UTM Zone 8N coordinates) for the duration of the survey. The secondary base station magnetometer was installed at at 466057 E, 7102914 N. Both were cycled at 3 s during the survey. Base stations and field magnetometers were synchronized daily to GPS time prior to surveying. Temporal geomagnetic variation was removed by linear interpolation and subtraction of the base station drift using a reference value of 56858 nT for the primary base and 56865 nT for the secondary base.
Temporal Geomagnetic noise threshold	The survey would have been suspended if geomagnetic variation exceeded 10 nT over 10 s on a sustained basis. No data were collected when geomagnetic noise exceeded this specification and therefore no data were removed from the final data set due to this stipulation.
Magnetic levelling	All operators surveyed a 20 point box with four perpendicular lines each of five stations daily. The levelling grid was adjacent to the base magnetometers.
VLF-EM stations	NLK (Jim Creek, Washington) - 24.8 kHz NAA (Cutler, Maine) - 24.0 kHz NPM (Lualualei, Hawaii) - 21.4 kHz
VLF components	In-phase, quadrature and total field strength.

The IP-resistivity survey was conducted according to specifications detailed in Table 4.

Table 4: IP-resistivity survey specifications.

Array	Expanding dipole-dipole and static radial array with downhole current sources (borehole).
Dipole spacing	50 m for Lines 1 & 2, 25 m for Line 3 and borehole array.
Line spacing	Variable – lines not on a grid.
Registration	Navigation by GPS only. NAD83, UTM Zone 8N coordinates were used. No line cutting was required and no station markings were used.
Current locations	Roving current 50 m behind potential spread on Lines 1 & 2 and 25 m from potential spread on Line 3. Current electrodes for the downhole survey at surface and depths of 29, 79, 104, 129 and 154 – they were 46 m more shallow than planned due to a (soft) blockage at 154 m. Stationary current electrodes as follows:

Line	UTM Zone 8 Easting	UTM Zone 8 Northing
1	471361	7103201
2	471760	7103706
3	472419	7101962
NG18-03	472731	7103743

Tx	Time domain, 50% duty cycle, reversing polarity, 0.125 Hz.
Rx windows	20 channels, semi-log scheme. Time delay of 40 ms. 7 channels of 40 ms, 7 channels of 80 ms and 6 channels of 160 ms.
Stacks	Minimum 15, more as required dependent on noise.
Rx error	Standard deviation of 5 mV/V or less, otherwise repeated several times until repeatability assured.

5 DATA PROCESSING

The mag and VLF data were downloaded at the end of each survey day and the raw, unedited data archived. A suite of internal processing scripts was run on the data to diurnally correct with a base station and to append positioning data collected during the survey with non-differential handheld GPS units.

5.1 Magnetic Data

Base serial number 703649 located at 466062 E, 7102908 N (NAD83 UTM Zone 8N coordinates) was generally used for diurnal corrections using a reference field of 56858 nT. A backup base station was always set up and on September 3rd the backup base, serial number 708719 located a few metres away at 466057 E, 7102914 N was used due to a instrument error of the primary base timing after the morning time synch. A reference field of 56865 nT was used for the secondary base location.

A levelling box of 4 lines each with 5 stations read by all operators on a daily basis was used to determine and apply a first correction of the daily data for each operator. A second estimate of levelling was done by hand. The data were then despiked with a filter width of 4 fiducials followed by a 10 fiducial low-pass filter and then gridded with a minimum curvature algorithm with a cell size of 12.5 metres. Microlevelling was used to eliminate residual down line artifacts with a 1000 metre filter on the decorrugation noise determination and a 200 nT, 125 m Naudy filter as the final microlevelling step.

To make the dataset consistent with the airborne total magnetic field data flown in 2017, further processing levelled the 2018 ground data to the 2017 airborne data. First the ground data were upward continued by 35 metres to bring the measurement height to the mean bird height of the airborne survey over the 2018 survey area. The difference between the upward continued ground data and the airborne residual magnetic field data was calculated on a 12.5 metre grid and then a first-order best-fit surface was derived from the difference grid. This is used as the final levelling step to produce a residual magnetic field from the 2018 ground data consistent with the 2017 airborne products.

The total magnetic field database with channels as described in Table 5 is provided in Geosoft database and ASCII comma delimited formats. The RMI channel is gridded with a 12.5 cell size and the first vertical derivative and tilt derivative are then calculated.

Table 5: List and description of channels in total magnetic field database.

Channel Name	Description
Grid	Name of grid / prospect
Line	Local coordinate – line
LineCoord	Line coordinate direction (n/s/e/w)
Station	Local coordinate – station
StationCoord	Station coordinate direction (n/s/e/w)
Time	Time of data acquisition
Date	Date of data acquisition
SerialNum	Identifier of data acquisition instrument
Base649	Raw magnetic readings from primary base, interpolated (nT)
Base719	Raw magnetic readings from secondary base, interpolated (nT)
RoverMag	Raw magnetics readings from the rover magnetometers (nT)
SQ	Signal Quality of RoverMag
CorrectedMag	Diurnally corrected magnetics readings (nT)
Lev1	Correction based on daily levelling grid (nT)
Lev1Mag	CorrectedMag + Lev1 (nT)
Lev1Mag_edit	Lev1Mag with hand edited points removed (nT)
Lev2	Further hand levelling (nT)
Lev2Mag	Lev1Mag + Lev2 (nT)
Lev2Mag_ds	Lev2Mag after despiking filter

Lev2Mag_lp	Lev2Mag_ds after low-pass filter

Lev3 Microlevelling correction (nT)

Lev3Mag Lev2Mag + Lev3 (nT)

Lev4 Correction to make consistent with 2017 airborne survey (nT)

Lev4Mag Lev3Mag + Lev4 (nT)

RMI Residual Magnetic Intensity, equal to Lev4Mag (nT)

UTME_Z8_NAD83 UTM Zone 8N NAD83 easting

UTMN_Z8_NAD83 UTM Zone 8N NAD83 northing

5.2 VLF Data

VLF profiles were reviewed on a line-by-line basis, and bad data manually removed. Data quality varied dramatically with VLF station; data collected using the Washington station are generally high quality with good signal strength, data from Maine was consistently poor and signal strength from Hawaii was sometimes high and other times very low, consistent with observation of Hawaii operation throughout the summer of 2018. Therefore, the data processing flow has two branches, one for Washington and the other for Maine and Hawaii.

Washington data had polarity problems identified and corrected; then the in-phase data were despiked with a filter width of one fiducial, low-pass filtered with a filter width of four fiducials and Fraser-filtered with a 5-point positive Fraser filter. A minimum curvature gridding algorithm with a cell size of 12.5 m was used to project these data on a plan view map. The result is of high quality.

Hawaii and Maine data were filtered based on signal strength with any readings less than 0.4 pT rejected. The polarity problems were identified and corrected although the poor data quality frustrated this process, particularly for the Maine data. In-phase data were despiked with a with a filter width of two fiducials, low-pass filtered with a filter width of four fiducials and Fraser-filtered with a 5 point positive Fraser filter. A minimum curvature gridding algorithm with a cell size of 12.5 m was used to project these data on a plan view map. The result is of marginal quality for Hawaii and of poor quality for Maine, which is exasperated by the sub-parallel orientation of the survey lines with conductors well-coupled to Maine.

Because of the poor quality, the Fraser filtered grids were enhanced in the direction of transmitter (maximum coupling) by applying a directional cosine filter with a degree of 1 passing features in the 080° (Maine) and 210° (Hawaii) directions. These products should be used with caution because of the underlying poor data quality. For completeness an analogous product is made for Washington with enhancement in the 142° direction.

The VLF database with channels as described in Table 6 is provided in Geosoft database and ASCII comma delimited formats.

Table 6: List and description of channels in VLF-EM database.

Channel Name	Description
Grid	Name of grid / prospect
Line	Local coordinate – line
LineCoord	Line coordinate direction (n/s/e/w)

Station Local coordinate – station

StationCoord Station coordinate direction (n/s/e/w)

Time Time of data acquisition

Date Date of data acquisition

SerialNum Identifier of data acquisition instrument

IP_214_raw Raw vertical component of in-phase for 21.4 kHz (%)

IP_214_edit Hand-edited vertical component of in-phase for 21.4 kHz (%)

IP_214 Sign-flipped (if required) vertical component of in-phase for 21.4 kHz (%)

IP_214_ds IP_214 after despiking filter (%)

IP_214_lp IP_214_ds after low-pass filter (%)

IP_214_ff IP_214_ds after Fraser filter (%)

OP_214_raw Raw vertical component of quadrature (out-phase) for 21.4 kHz (%)

OP_214_edit Hand-edited vertical component of quadrature (out-phase for 21.4 kHz (%))

OP_214 Sign-flipped (if required) vertical component of quadrature (out-phase) for 21.4 kHz (%) pT_214 Signal strength for 21.4 kHz (pT)

IP_240_raw through
Analogous to the previous 10 channels but for 24.0 kHz pT_240
IP_248_raw through
Analogous to the previous 10 channels but for 24.8 kHz
pT_248 kHz_1 Frequency of station 1, Lualualei, Hawaii (kHz) kHz_2

Frequency of station 2, Cutler, Maine (kHz) kHz_3 Frequency of station 3,

Jim Creek, Washington (kHz) h1_214 Horizontal component for 21.4 kHz

h2_214 Vertical component for 21.4 kHz h1_240 Horizontal component for

24.0 kHz h2_240 Vertical component for 24.0 kHz h1_248 Horizontal

component for 24.8 kHz h2_248 Vertical component for 24.8 kHz

UTME_Z8_NAD83 UTM Zone 8N NAD83 easting

UTMN_Z8_NAD83 UTM Zone 8N NAD83 northing

5.3 IP Data

IP data were downloaded nightly from the receiver and imported into the Geosoft Oasis Montaj IP package. Every reading was inspected and poor-quality readings or those which did not repeat were rejected from the database. The apparent resistivity is recalculated using a four-electrode equation assuming a homogeneous earth using georeferenced coordinates and images for the downhole sources. The apparent resistivity and total chargeability are averaged.

The data quality was very high for most areas. In a few areas, particularly over talus slopes on the west ends of L1 & L2 and L270 and L235 for the downhole survey in NG18-03, electrodes had to be doubled up and salted kitty litter was used in some cases to provide better contact.

Station coordinates were derived prior to surveying the line and crew navigated to those stations using handheld non-differential GPS units. Crew members recorded the locations of the current and receiver electrodes that differed significantly from the planned locations. Those coordinates replaced the provided ones in the final databases. Elevations were determined from a digital elevation model for NTS map sheet 106 D/04 equivalent to NTS 1:50 000 map.

Data are presented as pseudosections.

In order to be able to group the downhole survey by current sources while still maintaining unique station numbers, the station value (25, 50, …, 275) was added to 10 times the line number which is equal to the azimuth. Two special lines of dipoles near the centre are labelled as L2222 and L3333.

Both QA/QC databases, where all data appear and final databases where only the accepted, averaged data appear are appended to this report and have channels as described in Table 7. Databases are provided in Geosoft database and ASCII comma delimited formats.

Table 7: List and description of channels in IP-resistivity databases.

Channel Name	Description
X	Local Coordinate Plot point - Station
Y	Local Coordinate Plot point - Line
Z	Local Coordinate Plot point - Depth
Stn	Stn, defined by Geosoft as the midpoint between RX1 and TX1
X_UTM	Easting of Stn
Y_UTM	Northing of Stn
Topo	Elevation of Stn
T1X	Local Coordinate of T1 (roving current electrode)
T2X	Local Coordinate (or designated coordinate) of T2 (stationary current electrode)
R1X	Local Coordinate of R1 - potential electrode closest to T1
R2X	Local Coordinate of R2 - potential electrode further from T1
T1_UTMN	UTM Easting NAD83 Zone 8 coordinate of T1X
Vp_raw	Primary voltage as measured 1260 into the on-time window (mV)
Vp	Primary voltage, with sign correction if required (mV)
I	Transmitter current (A)
Sp	Spontaneous potential (mV)
RsCheck	Contact resistance of potential electrodes (kOhm)
Stack	Number of transmitter cycles measured during the course of the reading

Date	Date of data acquisition
DayTime	Time of data acquisition
QC_IP	Quality control for chargeability
QC_RES	Quality control for resistivity
IP_Avg	Calculated average chargeability (mV/V)
Q	Standard deviation of the average chargeability during the reading (mV/V)
IP[0]	Normalized Voltage measurement in the 40-80 ms offtime window (mV/V)
IP[1]	Normalized Voltage measurement in the 80-120 ms offtime window (mV/V)

IP[2] Normalized	Voltage measurement in the 120-160 ms offtime window (mV/V)
IP[3] Normalized	Voltage measurement in the 160-200 ms offtime window (mV/V)
IP[4] Normalized	Voltage measurement in the 200-240 ms offtime window (mV/V)
IP[5] Normalized	Voltage measurement in the 240-280 ms offtime window (mV/V)
IP[6] Normalized	Voltage measurement in the 280-360 ms offtime window (mV/V)
IP[7] Normalized	Voltage measurement in the 360-440 ms offtime window (mV/V)
IP[8] Normalized	Voltage measurement in the 440-520 ms offtime window (mV/V)
IP[9] Normalized	Voltage measurement in the 520-600 ms offtime window (mV/V)
IP[10] Normalized	Voltage measurement in the 600-680 ms offtime window (mV/V)
IP[11] Normalized	Voltage measurement in the 680-760 ms offtime window (mV/V)
IP[12] Normalized	Voltage measurement in the 760-840 ms offtime window (mV/V)
IP[13] Normalized	Voltage measurement in the 840-1000 ms offtime window (mV/V)
IP[14] Normalized	Voltage measurement in the 1000-1160 ms offtime window (mV/V)
IP[15] Normalized	Voltage measurement in the 1160-1320 ms offtime window (mV/V)
IP[16] Normalized	Voltage measurement in the 1320-1480 ms offtime window (mV/V)
IP[17] Normalized	Voltage measurement in the 1480-1640 ms offtime window (mV/V)
IP[18] Normalized	Voltage measurement in the 1640-1800 ms offtime window (mV/V)
IP[19] Normalized	Voltage measurement in the 1800-1960 ms offtime window (mV/V)
IP_Mask[0] Geosoft	mask value in the 40-80 ms offtime window (mV/V)
IP_Mask[1] Geosoft	mask value in the 80-120 ms offtime window (mV/V)
IP_Mask[2] Geosoft	mask value in the 120-160 ms offtime window (mV/V)
IP_Mask[3] Geosoft	mask value in the 160-200 ms offtime window (mV/V)
IP_Mask[4] Geosoft	mask value in the 200-240 ms offtime window (mV/V)
IP_Mask[5] Geosoft	mask value in the 240-280 ms offtime window (mV/V)
IP_Mask[6] Geosoft	mask value in the 280-360 ms offtime window (mV/V)
IP_Mask[7] Geosoft	mask value in the 360-440 ms offtime window (mV/V)
IP_Mask[8] Geosoft	mask value in the 440-520 ms offtime window (mV/V)
IP_Mask[9] Geosoft	mask value in the 520-600 ms offtime window (mV/V)
IP_Mask[10] Geosoft	mask value in the 600-680 ms offtime window (mV/V)
IP_Mask[11] Geosoft	mask value in the 680-760 ms offtime window (mV/V)
IP_Mask[12] Geosoft	mask value in the 760-840 ms offtime window (mV/V)
IP_Mask[13] Geosoft	mask value in the 840-1000 ms offtime window (mV/V)
IP_Mask[14] Geosoft	mask value in the 1000-1160 ms offtime window (mV/V)
IP_Mask[15] Geosoft	mask value in the 1160-1320 ms offtime window (mV/V)
IP_Mask[16] Geosoft	mask value in the 1320-1480 ms offtime window (mV/V)
IP_Mask[17] Geosoft	mask value in the 1480-1640 ms offtime window (mV/V)
IP_Mask[18] Geosoft	mask value in the 1640-1800 ms offtime window (mV/V) IP_Mask[19]
Geosoft mask value in	the 1800-1960 ms offtime window (mV/V) calcAppRes Resistivity calculated
using four electrode	equation.
T1_UTME UTM Zone	8N NAD83 Easting of T1
T1_UTMN UTM Zone	8N NAD83 Northing of T1
T1_Z Elevation of T1	

T1_Z_Img Image of T1	(above surface if borehole electrode)
T2_UTME UTM Zone	8N NAD83 Easting of T2
T2_UTMN UTM Zone	8N NAD83 Northing of T2
T2_Z Elevation of T2	
T2_Z_Img Image of T2	(above surface if borehole electrode)
R1_UTME UTM Zone	8N NAD83 Easting of R1
R1_UTMN UTM Zone	8N NAD83 Northing of R1
R1_Z Elevation of R1	
R1_Z_Img Image of R1	(above surface if borehole electrode)
R2_UTME UTM Zone	8N NAD83 Easting of R2
R2_UTMN UTM Zone	8N NAD83 Northing of R2
R2_Z Elevation of R2	
R2_Z_Img Image of R2	(above surface if borehole electrode)
Line Local Coordinate -	Line
Stn Local Coordinate -	Station
Stn_UTME UTM Zone	8N NAD83 Easting of Stn
Stn_UTMN UTM Zone	8N NAD83 Northing of Stn
Topo Surface elevation	of Stn
Depth Depth of	borehole electrode (T1)
Type Geosoft indicator	of averaged or unaveraged reading
Time Length of the	reading window
IP_Index Necessary	channel for Geosoft Database
ResCalc (Ohm*m)	Apparent resistivity calculated by Geosoft (without correction for proximal infinite)
Chg Average	chargeability calculated by the receiver
MF Calculated Metal	Factor
N The dipole number	in the array (calculated in geosoft)
Gfact Calculated	geometric factor based on 4 electrode equation
Final_IP Final averaged	chargeability
Final_Res Final	averaged resistivity
Final_Err Final	averaged chargeability error

6 PRODUCTS

The following are attached to the digital version of this report.

Folder / File	**Description of Contents**
Victoria Gold – Nugget 2018 Geophysics Crew Log.pdf	Production summary, daily log and personnel tracking sheet in PDF format.

Victoria Gold – Nugget 2018 Geophysics Field Report.pdf	A copy of this report in PDF format.
Data\GeosoftDB*.gdb	Processed final databases in Geosoft format.
Data\ASCIIDB*.csv	Processed final databases in ASCII format.
Figures\Geosoft Packed Maps*.map	Figures in Geosoft packed map format.
Figures\PDFs*.pdf	Figures in 11” X 17” PDF format
Raster Images\GeosoftGrid*.grd	Gridded data in Geosoft .GRD format
ShapeFiles*.shp	Selected ESRI shape files.
Raw\	Daily archive of instrument and gps dump files.

Respectfully submitted,

Dave Hildes, P.Geo., Ph. D. Project Manager, Geophysics

Aurora Geosciences Ltd.

1.2 Appendix II

Victoria Gold – Nugget 2018 Petrophysics Field Report

Nugget 2018 Geophysics – Mag-VLF & IP Surveys Interpretation Report

Summary Report
2018 Drill Core Petrophysics

Prepared for:

Victoria Gold Corp.
250-2237 2nd Ave
Whitehorse, YT Y1A0K7

Prepared by:

Aurora Geosciences Ltd.
34A Laberge Road, Whitehorse, Yukon, Y1A5Y9
Phone: (867) 668.7672 Fax: (867) 393.3577
www.aurorageosciences.com

1.3 Contents

1.3.1

1 SUMMARY

This report describes the petrophysics program conducted by Aurora Geosciences Ltd (AGL) on behalf of Victoria Gold Corp. (VIT) of drill core samples from their Dublin Gulch project. Victoria Gold arranged to have 5 samples delivered to Aurora Geosciences for testing. These samples were selected by Victoria Gold personnel to represent a variety of units of host rock and mineralized zones. The goal of the testing is is to establish a data set that can serve as an aid to interpreting upcoming geophysical surveys, reinterpret past surveys and provide insight into the utility of different geophysical methods when planning for future programs in the area.

At the request of Victoria Gold, the report describes a variety of physical properties detailed in the table below.

Table 1: Properties Measured

IP Average	mv/V
Resistivity	ohm/m
Mag Sus Average	SI 0.001
Remnant Magnetism	mA/m
Rem. Mag. Declination	°
Rem. Mag. Inclination	°
Koenigsberger Ratio	(Q)
Specific Gravity (adjusted to 4°C)	g/cm³
Porosity	%

2 METHODOLOGY

Upon arrival all samples were photographed and initial measurements of length and diameter were taken. Notes written on the samples by geologists on site were also transcribed to the database; these notes typically detailed the drill hole of origin, the start and end depths of the sample and any geochemical sample reference previously used. Samples were cut into two manageable sizes to accommodate the restriction of the IP setup (<10 cm) and the densimeter setup (<300 g.) These new sizes were also recorded.

Prior to recording measurements for IP chargeability, resistivity or specific gravity were saturated with distilled water in an attempt to emulate conditions in the water table. All samples were independently soaked inside of a vacuum desiccator for at least 24 hours, ensuring that air bubbles were no longer forming on the sample.

<u>Specific Gravity</u>

Specific gravity was measured using an Electronic Densimeter MD-300S. Small, saturated samples were measured in air and then in distilled water with the densimeter calculating volume and specific gravity. Air and water temperature were monitored and remained stable near 14˚ Celsius. Results were compensated to represent specific gravity at 4˚ Celsius, where that of water is 1 g per 1 cm^3.

Figure 1: Electronic Densimeter MD-300S used for specific gravity readings

Inductive Conductivity

Inductive conductivity was measured using a GDD-MPP-EM25 multi parameter probe. Prior to measuring the instrument was left powered on for one hour to reduce the potential drift of the response. After the one hour settling period the instrument was re-initialized every 60 seconds. Each sample was measured 10 times and the average taken. It is important to note that there is a lower threshold that must be met to allow for detection by the multi parameter probe, below this the response reads as zero.

Figure 2: GDD-MPP-EM25 used for inductive conductivity and magnetic susceptibility

Magnetic Susceptibility

As with inductive conductivity, magnetic susceptibility was also measured using a GDD-MPP-EM25 multi parameter probe. Prior to measuring the instrument was left powered on for one hour to reduce the potential drift of the response. After the one hour settling period the instrument was re-initialized every 60 seconds. Each sample was measured 10 times and the average taken.

IP Chargeability

IP chargeability is measured using a GDD TXII transmitter and Iris ProSys receiver. Signal is a 0.125Hz square wave with a 50 % duty cycle, typically using 3 different voltage outputs (150 V, 180 V, 350 V). Data is recorded across 20 time channels and results are stacked a minimum of 15 times or until the standard deviation is below 5 mv/V.

Figure 3: Iris Elrec Pro was used to measure IP chargeability and resistivity

Calculated Resistivity

Like the IP chargeability, resistivity was measured using the Elrec Pro. Resistance was measured end to end on the samples with contact across the full area of the sample end being ensured by soaking sponges in a saturated cupric sulphate solution. The resulting value was used to calculate the resistivity of the sample where resistivity =((resistance)*(sample area))/(sample length.)

Remnant Magnetism

Remnant magnetism is measured using a molspinner instrument from Molspin Inc. Samples are measured in six orientations and Molspin Spbig6 software is used to calculate final intensity and orientation values. The instrument is calibrated every thirty minutes using a 170 mA/m sample.

Figure 4: Moslpin instrument used to measure remnant magnetism

Porosity

Porosity was calculated by comparing the measured mass of saturated and fully dried samples where posority % = ((mass$_{saturated}$-mass$_{dry}$)/sample volume)*100. Samples were saturated with distilled water inside of a vacuum chamber for 24 hours before being measured with the MD-300S Electronic Densimeter. Samples were then dried in an oven at 200°C for 24 hours before being measured again.

3 RESULTS

Table 2: Results - Induced Polarity and Resistivity

Sample	DDH	Depth (m)	IP Average (mv/V)	Resistivity (ohm/m)
1	NG18-003C	59.80	8.104	3036.915
2	NG18-003C	208.82	2.888	522.668
3	NG18-18007C	87.50	11.117	1977.216
4	NG18-005	132.90	7.302	4510.725
5	NG18-007C	86.97	150.105	9.190

Table 3: Results - Specefic Gravity and Porosity

Sample	Mass Saturated (g)		Mass Dry (g)		Volume (cm^3)	Specific Gravity (g/cm^3)	Porosity (%)
1	98.07	97.78	35.930	2.730	0.81		
2	82.07	80.75	31.274	2.624	4.22		
3	61.98	61.70	22.832	2.715	1.23		
4	47.14	46.96	17.678	2.666	1.02		
5	55.26	55.23	15.797	3.498	0.19		

Table 4: Results - Remnant Magnestism and Magnetic Susceptibility

Sample	Declination (°)		Inclination (°)		Remnant Mag (mA/m)	Mag Sus Average (SI 0.001)	K ratio
1	282.0	0.7	144.253		0.17	18.71	
2	242.4	6.3	0.425	0.38	0.02		
3	226.2	3.7	1.917	0.25	0.17		
4	239.3	9.1	1.389	0.03	1.02		
5	186.8	53.3	1.487	1.04	0.03		

Respectfully submitted,

Shawn Scott

Aurora Geosciences, Ltd.

APPENDIX 2

RAVEN GEOPHYSICAL REVIEW PRECISION GEOSURVEYS INC.

Precision GeoSurveys

AIRBORNE GEOPHYSICAL SURVEY REPORT

Dublin Gulch, VBW, and Clear Creek Survey Blocks

Mayo, YT

Victoria Gold Corp.

Precision GeoSurveys Inc.
www.precisiongeosurveys.com
Hangar 42 Langley Airport
21330 - 56th Ave., Langley, BC
Canada V2Y 0E5
604-484-9402

June 2017

Table of Contents

List of Figures

List of Tables

List of Appendices

List of Plates (in pocket)

Dublin Gulch/VBW (scale 1:75000)

Plate 13_DG_VBW: Dublin Gulch and VBW - Total Count – Equivalent Dose Rate (TCcor)
Plate 14_DG_VBW: Dublin Gulch and VBW - Total Count – Exposure Rate (TCexp)
Plate 15_DG_VBW: Dublin Gulch and VBW - Potassium over Thorium Ratio (%K/eTh)
Plate 16_DG_VBW: Dublin Gulch and VBW - Potassium over Uranium Ratio (%K/eU)
Plate 17_DG_VBW: Dublin Gulch and VBW - Uranium over Thorium Ratio (eU/eTh)
Plate 18_DG_VBW: Dublin Gulch and VBW - Uranium over Potassium Ratio (eU/%K)
Plate 19_DG_VBW: Dublin Gulch and VBW - Thorium over Potassium Ratio (eTh/%K)
Plate 20_DG_VBW: Dublin Gulch and VBW - Ternary Map (TM)
Plate 21_DG_VBW: Dublin Gulch and VBW – 2004 and 2017 Residual Magnetic Intensity with Flight Lines (RMI_wFL_04_17)
Plate 22_DG_VBW: Dublin Gulch and VBW – 2004 and 2017 Calculated Vertical Gradient (CVG_04_17)

Clear Creek -

(scale 1:25000)

Plate 1_CC: Clear Creek - Actual Flight Lines (FL)
Plate 2_CC: Clear Creek - Digital Terrain Model (DTM)
Plate 3_CC: Clear Creek - Total Magnetic Intensity with Plotted Flight Lines (TMI_wFL)
Plate 4_CC: Clear Creek - Total Magnetic Intensity (TMI)
Plate 5_CC: Clear Creek - Residual Magnetic Intensity (RMI)
Plate 6_CC: Clear Creek - Calculated Vertical Gradient (CVG) of RMI
Plate 7_CC: Clear Creek - Calculated Horizontal Gradient (CHG) of RMI
Plate 8_CC: Clear Creek - Reduced to Pole (RTP) of RMI
Plate 9_CC: Clear Creek - First Vertical Derivative (1VD) of RTP
Plate 10_CC: Clear Creek - Potassium – Equivalent Concentration (%K)
Plate 11_CC: Clear Creek - Thorium – Equivalent Concentration (eTh)
Plate 12_CC: Clear Creek - Uranium – Equivalent Concentration (eU)
Plate 13_CC: Clear Creek - Total Count – Equivalent Dose Rate (TCcor)
Plate 14_CC: Clear Creek - Total Count – Exposure Rate (TCexp)
Plate 15_CC: Clear Creek - Potassium over Thorium Ratio (%K/eTh)
Plate 16_CC: Clear Creek - Potassium over Uranium Ratio (%K/eU)
Plate 17_CC: Clear Creek - Uranium over Thorium Ratio (eU/eTh)
Plate 18_CC: Clear Creek - Uranium over Potassium Ratio (eU/%K)
Plate 19_CC: Clear Creek - Thorium over Potassium Ratio (eTh/%K)
Plate 20_CC: Clear Creek - Ternary Map (TM)

1998 and 2017 Integrated Data (scale 1:40000)

Plate 21_CC: Clear Creek – 1998 and 2017 Residual Magnetic Intensity with Flight Lines (RMI_wFL_98_17)
Plate 22_CC: Clear Creek – 1998 and 2017 Residual Magnetic Intensity (%K_98_17)
Plate 23_CC: Clear Creek - 1998 and 2017 Residual Magnetic Intensity (eTh_98_17)
Plate 24_CC: Clear Creek - 1998 and 2017 Residual Magnetic Intensity (eU_98_17)
Plate 25_CC: Clear Creek - 1998 and 2017 Residual Magnetic Intensity (TCexp_98_17)

1.0 Introduction

This report outlines the geophysical survey operations and data processing procedures taken during the high resolution helicopter-borne magnetic and radiometric survey flown for Victoria Gold Corp. The airborne survey is comprised of two survey blocks: adjacent Dublin Gulch and VBW, and Clear Creek located in central Yukon (Figure 1). The geophysical survey started on June 5, 2017, and was completed on June 8, 2017.

Figure 1: Survey area location map.

1.1 Survey Area

The two survey blocks cover a total area of 599 km^2, centered 56 northwest of Mayo, YT (Figure 2). Dublin Gulch and VBW were contracted as separate blocks but were flown as one contiguous survey block.

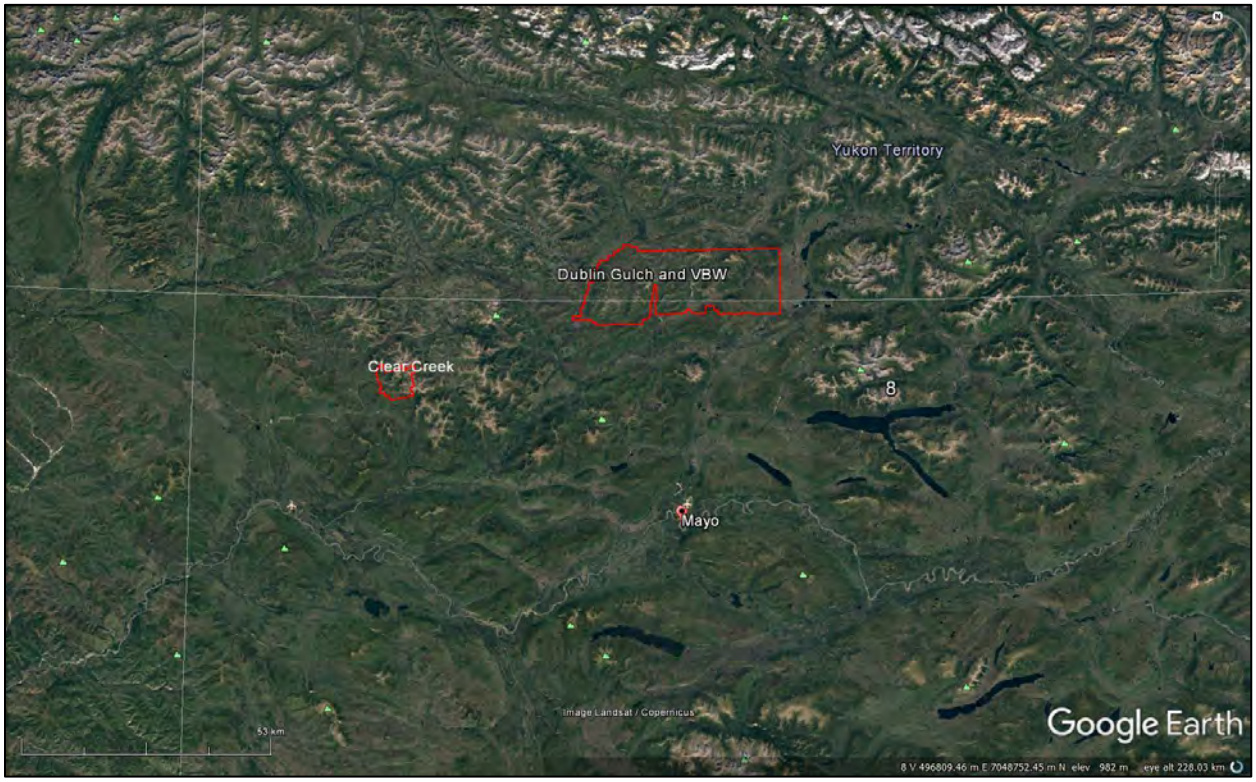

Figure 2: Survey block boundaries in red. Dublin Gulch and VBW merged into one block, north of Mayo, YT and Clear Creek, northwest of Mayo, YT.

A total of 4550 line km of data was collected on 387 survey lines and 20 tie lines over two survey blocks. Dublin Gulch/VBW was flown at 150 meter spacing at a 000°/180° heading; tie lines were flown at 1500 meter spacing at a heading of 090°/270° (Figures 3 and 4).

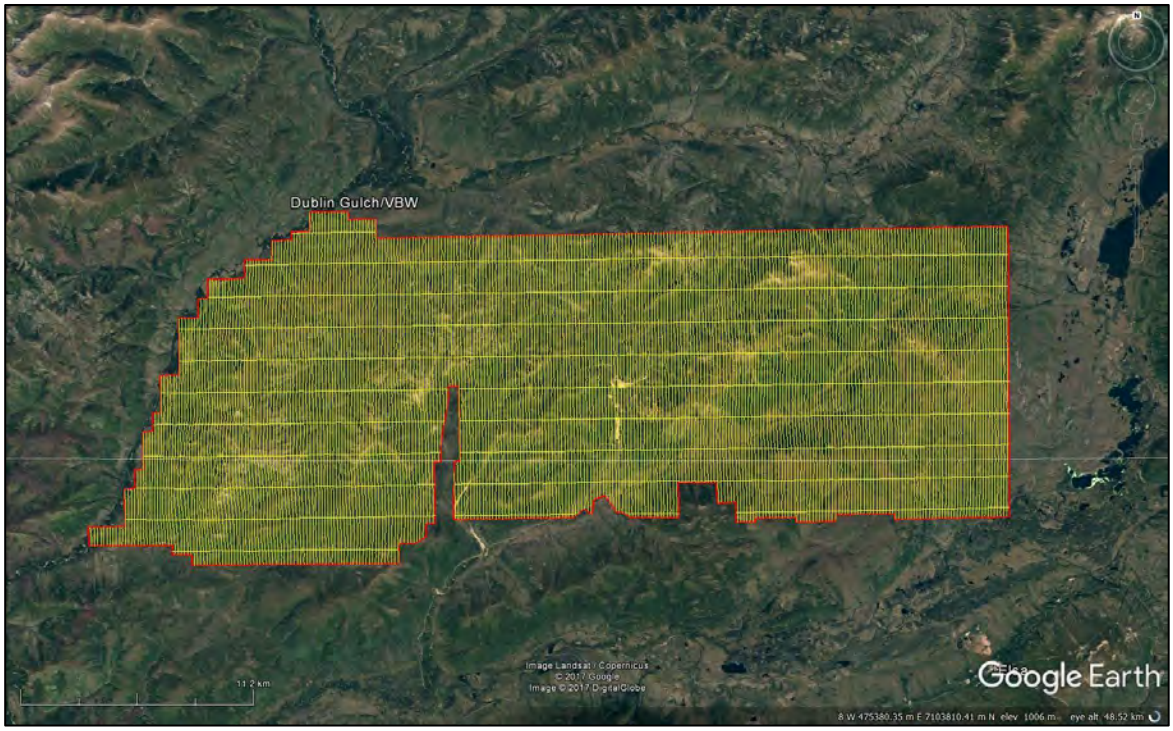

Figure 3: Plan View – Dublin Gulch/VBW with actual flight lines displayed in yellow and the block boundary in red.

Figure 4: Terrain View – Dublin Gulch/VBW with actual flight lines displayed in yellow.

Precision GeoSurveys

Clear Creek survey block was flown at 100 meter spacing at a 045°/225° heading; tie lines were flown at 1000 meter spacing at a heading of 135°/315° (Figures 5 and 6).

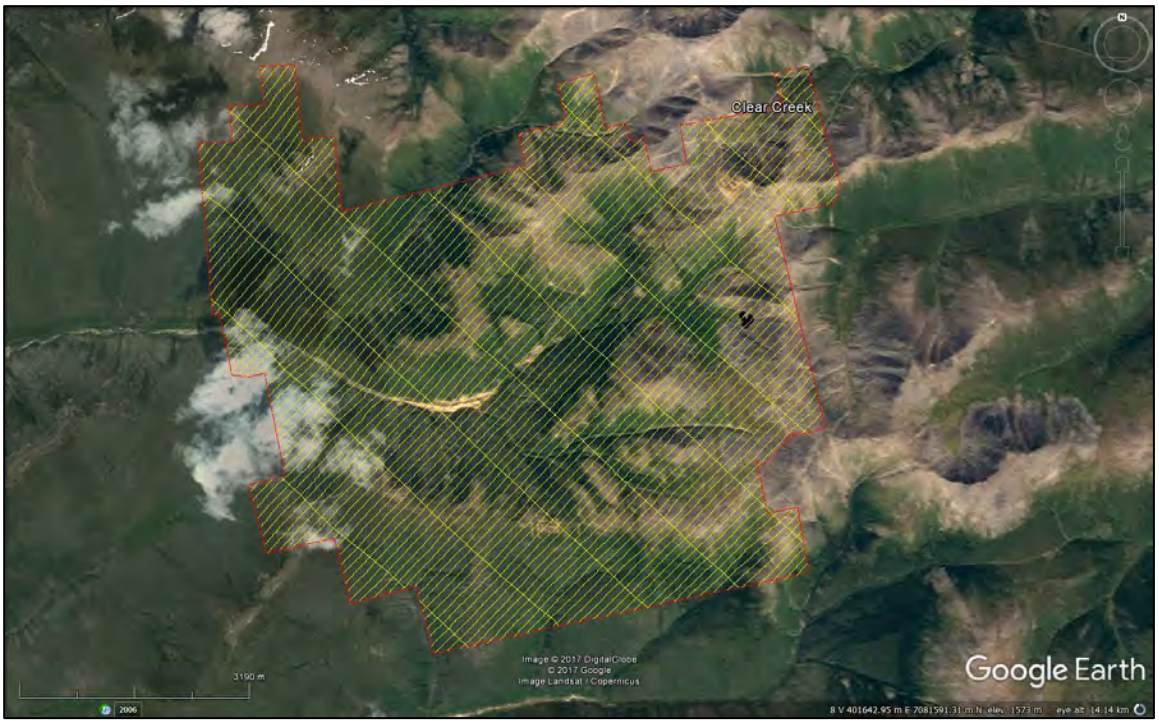

Figure 5: Plan View – Clear Creek survey block with actual flight lines displayed in yellow and the block boundary in red.

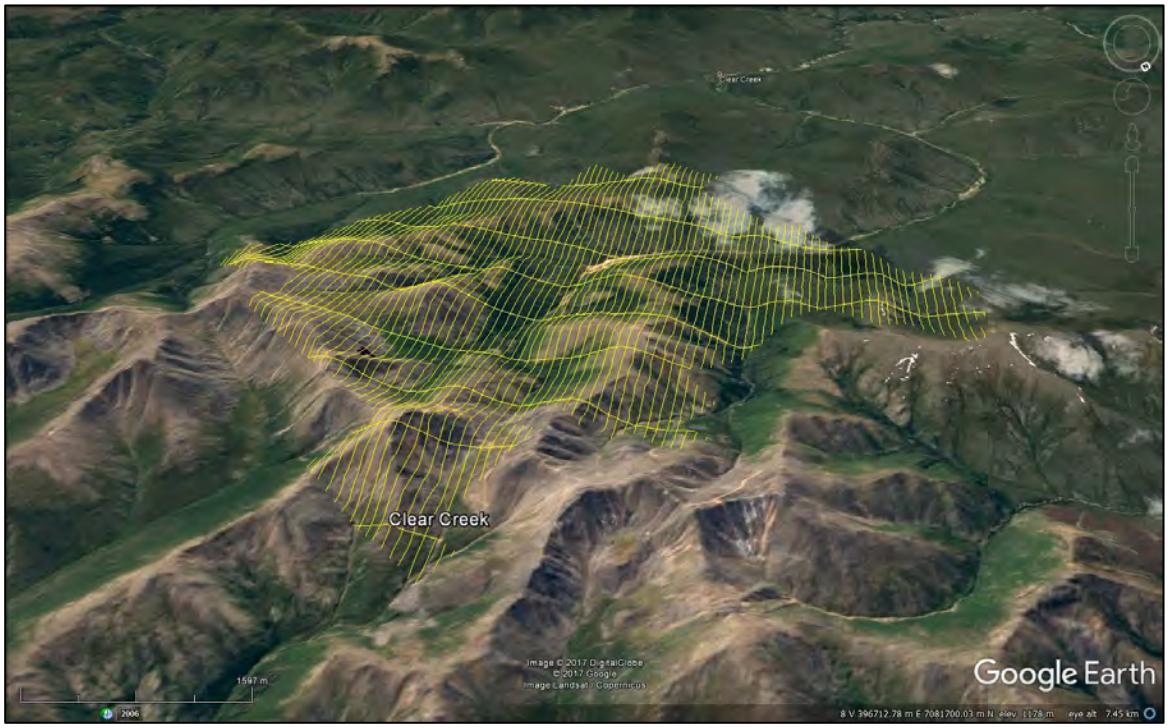

Figure 6: Terrain View – Clear Creek survey block with actual flight lines displayed in yellow.

1.2 Survey Specifications

The geodetic system used for the geophysical survey was WGS 84 and the area is contained in zone 8N. A total of 4550 line km was flown over the three survey blocks (Table 1). Polygon coordinates for the surveys are specified in Tables 1 to 3.

Block Name	Area (km^2)	Line Type	Planned No. of Lines	Line Spacing (m)	Line Orientation	Nominal Survey Height (m)	Total Planned Line km	Total Actual km Flown
Dublin Gulch and VBW (combined)	555	Survey	292	150	000°/180°	35	3699	3703
		Tie	11	1500	090°/270°	35	365	365
		Total:	**303**				**4064**	**4068**
Clear Creek	44	Survey	95	100	045°/225°	35	437	437
		Tie	9	1000	135°/315°	35	45	45
		Total:	**104**				**482**	**482**
						Total:	**4546**	**4550**

Table 1: Flight line specifications. All directions refer to WGS 84 8N.

Longitude	Latitude	Easting	Northing	N/S	E/W
135.47319403	64.09883173	476937	7108113	N	W
135.47110701	63.97535401	476937	7094353	N	W
135.58487873	63.97494010	471367	7094353	N	W
135.58493176	63.97747962	471367	7094636	N	W
135.64178042	63.97723937	468584	7094636	N	W
135.64208227	63.97436623	468566	7094316	N	W
135.68023165	63.97403089	466698	7094298	N	W
135.67991432	63.97610547	466716	7094529	N	W
135.71951990	63.97591452	464777	7094529	N	W
135.72021415	63.97431361	464741	7094351	N	W
135.73873905	63.97422049	463834	7094351	N	W
135.73896655	63.98284384	463834	7095312	N	W
135.75677322	63.98242901	462962	7095276	N	W
135.75736985	63.99088887	462944	7096219	N	W
135.79373045	63.99085618	461165	7096237	N	W
135.79331873	63.97632860	461165	7094618	N	W
135.84019493	63.97606479	458870	7094618	N	W
135.84627727	63.97791412	458575	7094828	N	W
135.85300030	63.97796451	458246	7094838	N	W
135.86501166	63.98518983	457669	7095651	N	W
135.87547922	63.98337701	457154	7095456	N	W
135.87716204	63.97708457	457062	7094756	N	W
135.88501709	63.97934338	456681	7095013	N	W
135.89583343	63.97576790	456146	7094622	N	W

136.01132995	63.97497307	450491	7094618	N	W
136.01043005	63.99985775	450579	7097390	N	W
136.00476774	63.99989704	450856	7097390	N	W
136.00591827	64.03189341	450856	7100956	N	W
136.01557772	64.03182623	450384	7100956	N	W
136.01568091	64.02678165	450370	7100394	N	W
136.02318941	64.00770222	449969	7098274	N	W
136.02320596	63.99976830	449954	7097390	N	W
136.02986983	63.99972119	449628	7097390	N	W
136.02890941	63.97360198	449628	7094479	N	W
136.03738462	63.97354164	449213	7094479	N	W
136.03718263	63.96808630	449213	7093871	N	W
136.04767495	63.96521072	448694	7093559	N	W
136.06400768	63.96509186	447894	7093559	N	W
136.06399572	63.95670927	447879	7092625	N	W
136.26520248	63.95509363	438020	7092625	N	W
136.26571276	63.95961279	438005	7093129	N	W
136.28447593	63.95958248	437086	7093144	N	W
136.28434657	63.96344307	437101	7093574	N	W
136.36664936	63.96269101	433069	7093574	N	W
136.36704547	63.97081023	433069	7094479	N	W
136.33164072	63.97113950	434803	7094479	N	W
136.33239994	63.98710001	434803	7096258	N	W
136.32241564	63.98731698	435292	7096272	N	W
136.32279934	63.99543631	435292	7097177	N	W
136.31401182	63.99551611	435722	7097177	N	W
136.31476813	64.01161126	435722	7098971	N	W
136.30536205	64.01169610	436182	7098971	N	W
136.30574080	64.01980649	436182	7099875	N	W
136.29725237	64.01988253	436597	7099875	N	W
136.29798733	64.03570858	436597	7101639	N	W
136.27917924	64.03587533	437516	7101639	N	W
136.28029503	64.06021561	437516	7104352	N	W
136.26147029	64.06038010	438435	7104352	N	W
136.26183710	64.06849057	438435	7105256	N	W
136.25210430	64.06857467	438910	7105256	N	W
136.25246892	64.07669413	438910	7106161	N	W
136.21569842	64.07700598	440704	7106161	N	W
136.21604630	64.08498200	440704	7107050	N	W
136.18900327	64.08520543	442023	7107050	N	W
136.18935513	64.09345067	442023	7107969	N	W
136.17081495	64.09360096	442927	7107969	N	W
136.17096616	64.09719874	442927	7108370	N	W
136.15271053	64.09734442	443817	7108370	N	W
136.15305184	64.10558976	443817	7109289	N	W
136.11533906	64.10588346	445655	7109289	N	W

136.11520037	64.10242020	445655	7108903	N	W
136.08811894	64.10262507	446975	7108903	N	W
136.08779689	64.09437955	446975	7107984	N	W

Table 2: Dublin Gulch/VBW polygon coordinates using WGS 84 in zone 8N.

Longitude	Latitude	Easting	Northing	N/S	E/W
137.05232483	63.87127775	399168	7084292	N	W
137.05431226	63.87507405	399084	7084718	N	W
137.05438311	63.87520771	399081	7084733	N	W
137.04852078	63.87579359	399371	7084789	N	W
137.04558952	63.87608644	399516	7084817	N	W
137.04405872	63.87323521	399581	7084497	N	W
137.04347204	63.87216618	399606	7084377	N	W
137.03918715	63.86417368	399788	7083480	N	W
137.03801005	63.86197279	399838	7083233	N	W
137.03911316	63.86006295	399777	7083022	N	W
137.05533406	63.85840586	398974	7082863	N	W
137.04291951	63.83455744	399499	7080187	N	W
137.05281016	63.83356440	399009	7080092	N	W
137.05192836	63.83318190	399051	7080048	N	W
137.05853061	63.83032285	398716	7079740	N	W
137.05981205	63.83088815	398655	7079805	N	W
137.05884243	63.82902561	398696	7079596	N	W
137.05664163	63.82477455	398789	7079119	N	W
137.04915620	63.82553629	399160	7079192	N	W
137.04705723	63.82154402	399249	7078744	N	W
137.04495887	63.81755171	399338	7078296	N	W
137.14459081	63.80738909	394397	7077325	N	W
137.14885006	63.81556768	394218	7078243	N	W
137.16562521	63.81386267	393386	7078081	N	W
137.16967572	63.82161289	393216	7078951	N	W
137.18780417	63.81976828	392317	7078776	N	W
137.19198199	63.82775844	392142	7079673	N	W
137.18290515	63.82867697	392592	7079760	N	W
137.18918188	63.84064875	392329	7081104	N	W
137.19349979	63.84020620	392115	7081062	N	W
137.19860065	63.84041600	391865	7081094	N	W
137.20242519	63.84771097	391705	7081913	N	W
137.20422166	63.84753096	391616	7081896	N	W
137.20575049	63.86730472	391617	7084101	N	W
137.19660046	63.86744398	392067	7084101	N	W
137.19689456	63.87147073	392068	7084550	N	W
137.18774312	63.87160943	392518	7084550	N	W
137.18805635	63.87563590	392518	7084999	N	W
137.17888317	63.87577435	392969	7084999	N	W

137.17857055	63.87173889	392969	7084549	N	W
137.17827907	63.86771208	392968	7084100	N	W
137.16910840	63.86784990	393419	7084100	N	W
137.16849004	63.85956339	393418	7083176	N	W
137.11930819	63.86453012	395853	7083648	N	W
137.12140037	63.86852157	395765	7084096	N	W
137.11230802	63.86943571	396215	7084183	N	W
137.10881475	63.86981886	396388	7084220	N	W
137.11091459	63.87392705	396300	7084681	N	W
137.10151304	63.87481807	396765	7084765	N	W
137.09930745	63.87063947	396858	7084296	N	W
137.09842653	63.86892850	396895	7084104	N	W
137.09319021	63.86941735	397154	7084150	N	W
137.09207434	63.86727881	397201	7083910	N	W
137.08865972	63.86762443	397370	7083943	N	W
137.08659259	63.86363219	397457	7083495	N	W
137.07752032	63.86453489	397906	7083581	N	W
137.07958690	63.86853622	397819	7084030	N	W
137.07427228	63.86907040	398082	7084081	N	W
137.07053382	63.86944716	398267	7084117	N	W

Table 3: Clear Creek survey block polygon coordinates using WGS 84 in zone 8N.

2.0 Geophysical Data

Geophysical data are collected in a variety of ways and are used to aid in determination of geology, mineral deposits, oil and gas deposits, geotechnical investigations, contaminated land sites and UXO detection.

For the purposes of this survey, airborne magnetic and radiometric data were collected to serve in the exploration for gold deposits.

2.1 Magnetic Data

Magnetic surveying is the most common airborne survey type to be conducted for both mineral and hydrocarbon exploration. Aeromagnetic surveys measure and record the total intensity of the magnetic field at the magnetometer sensor, which is a combination of the desired magnetic field generated in the Earth as well as minute variations due to the temporal effects of the constantly varying solar wind and the magnetic field of the survey aircraft. By subtracting the solar, regional, and aircraft effects, the resulting aeromagnetic map shows the spatial distribution and relative abundance of magnetic minerals (most commonly the iron oxide mineral magnetite) in the upper levels of the Earth's crust, which in turn is related to lithology, structure, and alteration of bedrock. The type of survey specifications, instrumentation, and interpretation procedures depend on the objectives of the survey. Magnetic surveys are typically performed for:

1. Geological Mapping - to aid in mapping lithology, structure and alteration.
2. Depth to Basement Mapping - for exploration in sedimentary basins or mineralization associated with the basement surface.

2.2 Radiometric Data

Radiometric surveys detect and map natural radioactive emanations, called gamma rays, from rocks and soils. All detectable gamma radiation from Earth materials come from the natural decay products of three primary radioelements: uranium (U), thorium (Th), and potassium (K). The purpose of radiometric surveys is to determine either the absolute or relative amounts of U, Th, and K in surface rocks and soils which are then useful in mapping lithology, alteration, and structure.

Surficial debris, vegetation, standing water (lakes, marshes, swamps), and/or snow can effectively attenuate gamma rays originating from underlying rocks. Therefore, variations in isotope counts must be evaluated with respect to surficial conditions before they are attributed to changes in underlying geology. An increase in soil moisture can also significantly affect gamma radiation concentrations. For example, 10% increase in soil moisture can decrease the measured gamma radiation by about the same amount. Radon, formed naturally from the decay of radioactive elements such as uranium, attaches to dust particles in the atmosphere. The radioactive precipitation of these dust particles by rain can lead to apparent increases of more than 2000% in uranium ground concentration (IAEA, 2003). Therefore, gamma ray surveying should not be carried out during a rainfall, or shortly after a rainfall.

3.0 Survey Operations

The survey started on June 5, 2017, and was completed on June 8, 2017 in windy and dry conditions. The survey did not encounter any delays due to weather or technical problems. See Appendix C daily flight log report for details. The experience of the pilot helped to ensure that the data quality objectives were met and that the safety of the flight crew was never compromised given the potential risks involved in airborne geophysical surveying. Field processing and quality control checks were done daily.

3.1 Operations Base and Crew

The base of operations for the Dublin Gulch/VBW and Clear Creek surveys was at Victoria Gold's Eagle exploration camp, within the Dublin Gulch/VBW survey block (Figure 7) at Haggart Creek.

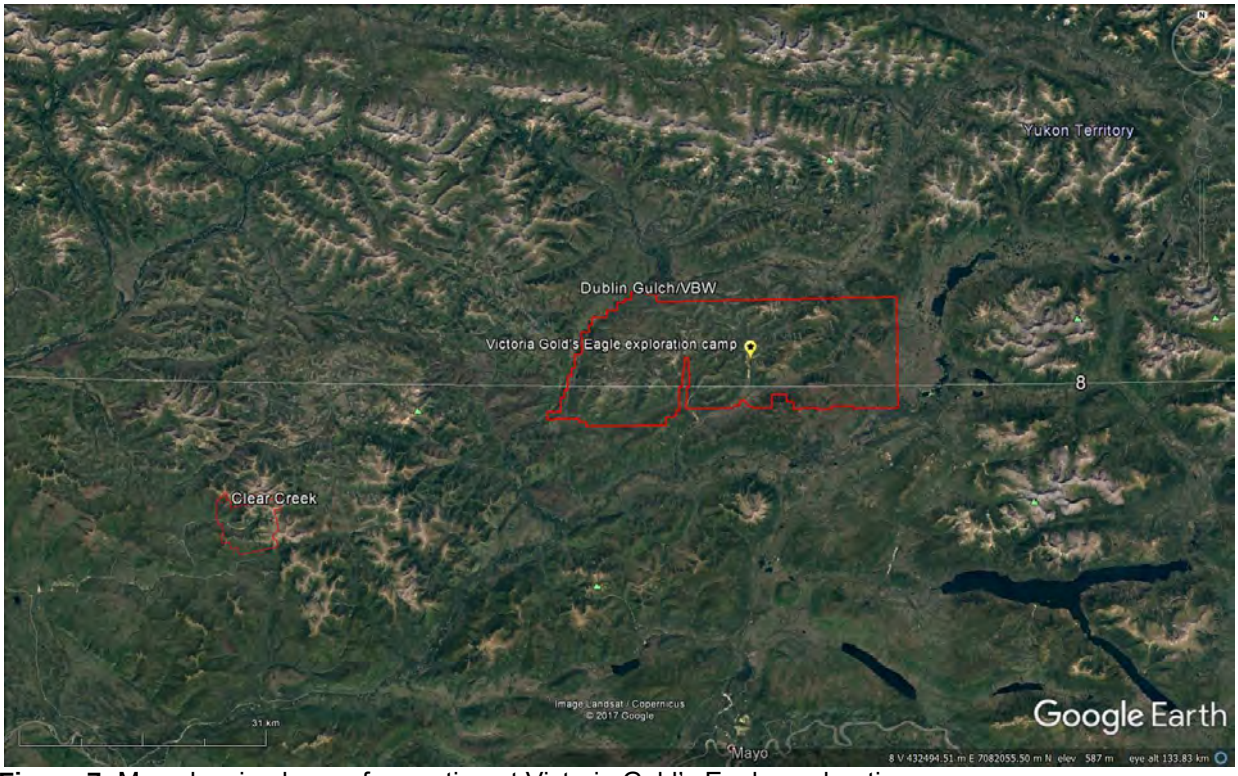

Figure 7: Map showing base of operation at Victoria Gold's Eagle exploration camp.

The Precision geophysical crew consisted of three members (Table 4):

Crew Member	Position
Lars Helgesen	Pilot
Shawn Walker, M.Sc., G.I.T.	Geophysicist and data processor (on-site)
Jenny Poon, P.Geo.	Geophysicist and data processor (off-site)

Table 4: List of survey crew members.

3.2 Base Station Specifications

Two GEM GSM-19T proton precession magnetometers were used to accurately record diurnal variations and geomagnetic storms in the survey area. Both base stations were set up north of the Eagle exploration camp, away from any sources of magnetic noise (Table 5; Figures 8 and 9).

Station name	Easting/Northing	Longitude/Latitude	Datum/ Projection
GEM 4 S/N 2105651	0458547E, 7100986N	135° 50' 54.67" W 64 ° 01' 59.41" N	WGS 84, Zone 8N
GEM 5 S/N 1094678	0458466E, 7101018N	135° 51' 0.68" W 64 ° 02' 0.38" N	WGS 84, Zone 8N

Table 5: Base station specifications.

Base station readings were reviewed at regular intervals to ensure that no airborne data were collected during periods of high diurnal magnetic activity (greater than 10 nT per minute). The magnetic base stations were installed in a magnetically noise-free area, away from metallic items such as ferromagnetic objects, vehicles, or power lines that could affect the base stations or survey data.

The diurnal magnetic variations recorded by the stationary base stations were removed from the magnetic data recorded in flight to ensure that the final magnetic data accurately represented the geomagnetic properties of the survey area and not contaminated by solar activity.

Figure 8: GEM 4 (left) and GEM 5 (right) magnetic base stations located in the field far away from metallic items/objects.

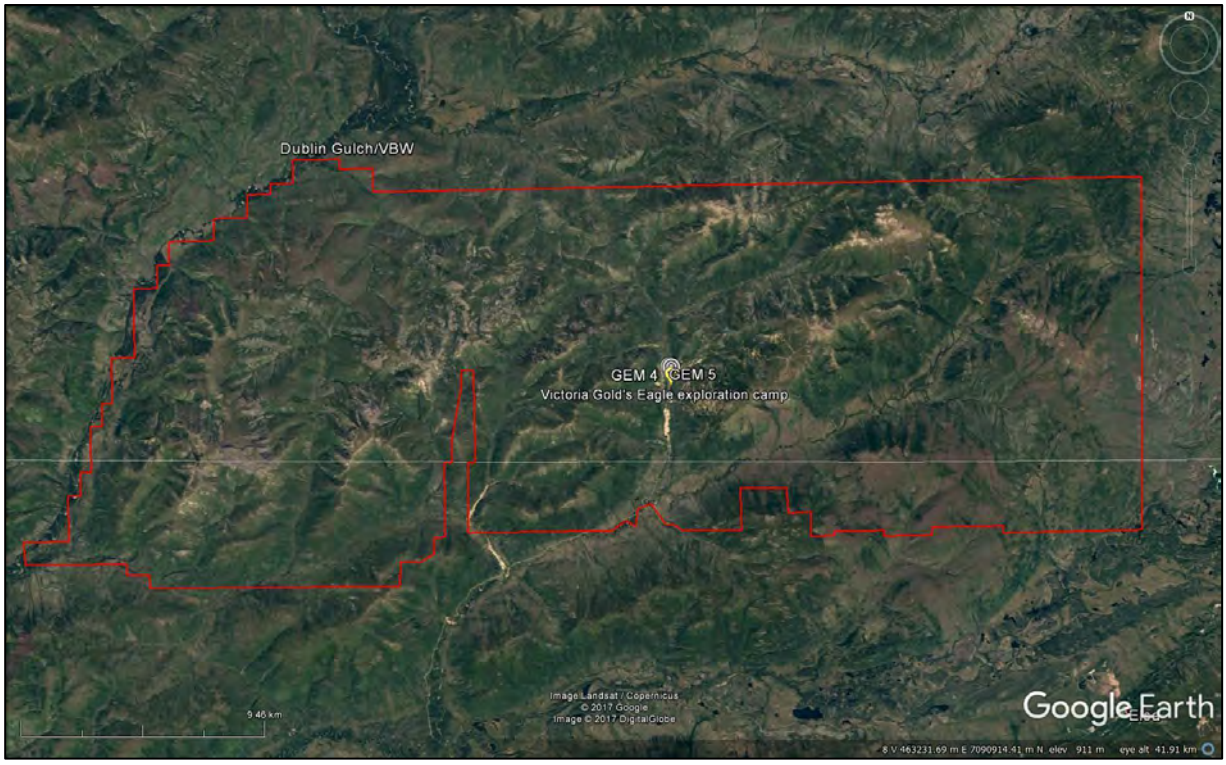

Figure 9: GEM 4 and GEM 5 magnetic base station locations within Dublin Gulch/VBW survey block.

3.3 Field Processing and Quality Control

On a flight-by-flight basis, the survey data were transferred from the helicopter's data acquisition system onto a USB flash drive and copied onto a field data processing laptop. The raw data files in PEI binary data format were converted into Geosoft GDB database format. Using Geosoft Oasis Montaj 9.1.3, the quality of the data was inspected to ensure that it met the contract specifications (Table 6, Figures 10 to 12).

Parameter	Specification	Details
Position	Line Spacing	Flight line deviation from flight path by more than 10 m left/right for 1 km or more.
	Height	Ground clearance by more than 10 m up/down for 1.0 km or more, provided line deviation from height is not due to tall trees, topography, cultural features, mitigation of wildlife harassment, or other obstacles beyond the pilot's control.

	GPS	Any flight lines where 3 or less GPS satellites received for distances of greater than 1 km, provided signal loss is not due to topography.
Magnetics	Diurnal Variations	Non-linear magnetic diurnal variations exceed 10 nT from a linear chord of length one (1) minute.
	Normalized 4th Difference	Magnetic data exceeding 0.10 nT peak to peak for distances greater than 1 km or more (provided noise is not due to geological or cultural features).
Radiometrics	Test Line Data	If signal from the four spectrometer windows (K, Th, U, TC) over the test line varies by more than 12%, the flights shall be re-flown or suspended.

Table 6: Contract re-flight specifications.

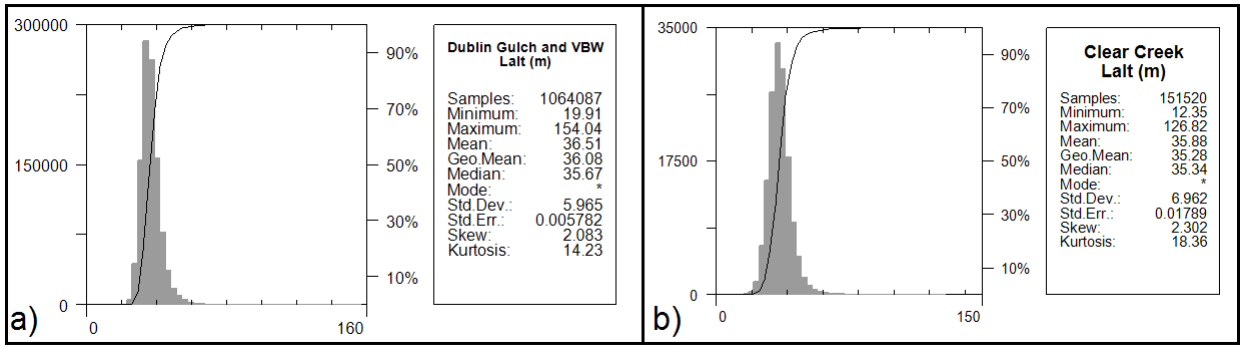

Figure 10: Histograms showing survey elevation vertically above ground. a) Dublin Gulch/VBW b) Clear Creek.

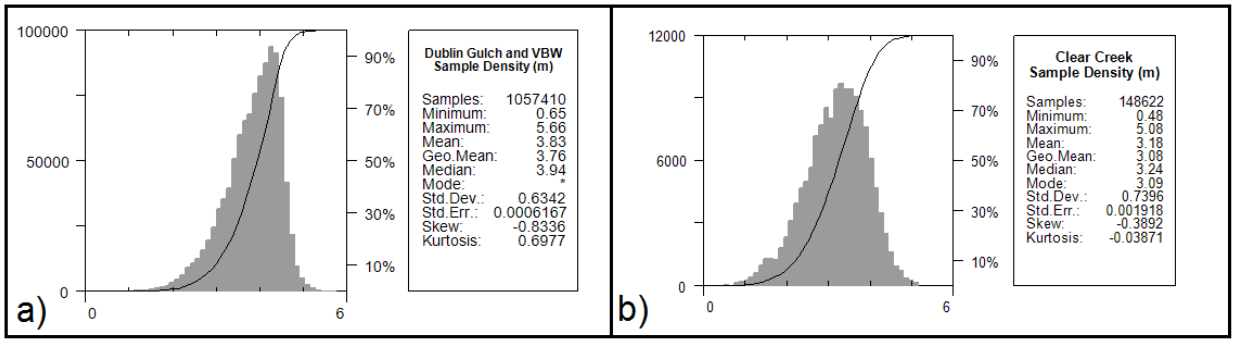

Figure 11: Histograms showing survey sample density. Linear distance in meters between adjacent measurement locations; sample frequency is 10 measurements per second. a) Dublin Gulch/VBW b) Clear Creek.

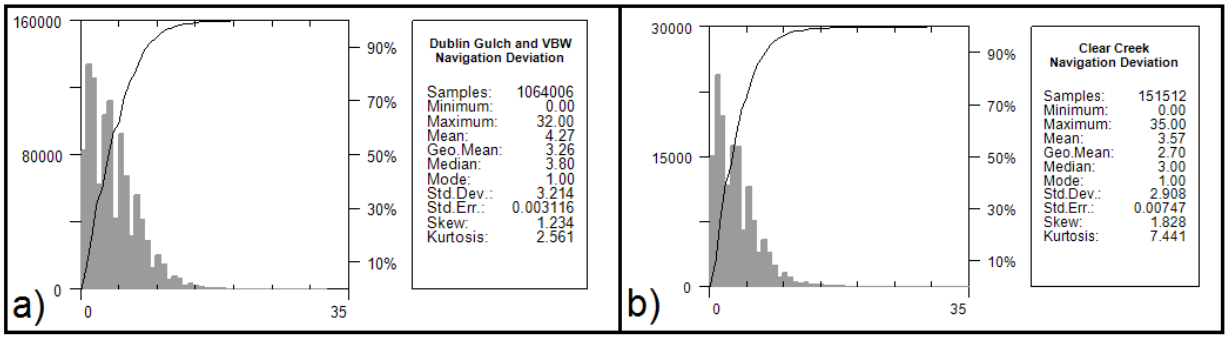

Figure 12: Histograms showing cross line navigation deviation. a) Dublin Gulch/VBW b) Clear Creek.

At Dublin Gulch/VBW survey block, several flight lines returned suspicious magnetic features that were investigated with re-flights. Part of L1870 was re-flown and the data consistently displayed the same magnetic linear high (Figure 13) parallel with the survey line. This confirmed the magnetic high feature to be real; therefore data from the first flight were used in the final database. Lines L440, L1520, and L1560 were also partially re-flown to confirm that suspicious magnetic features were real; data from the second flights were used in the final database.

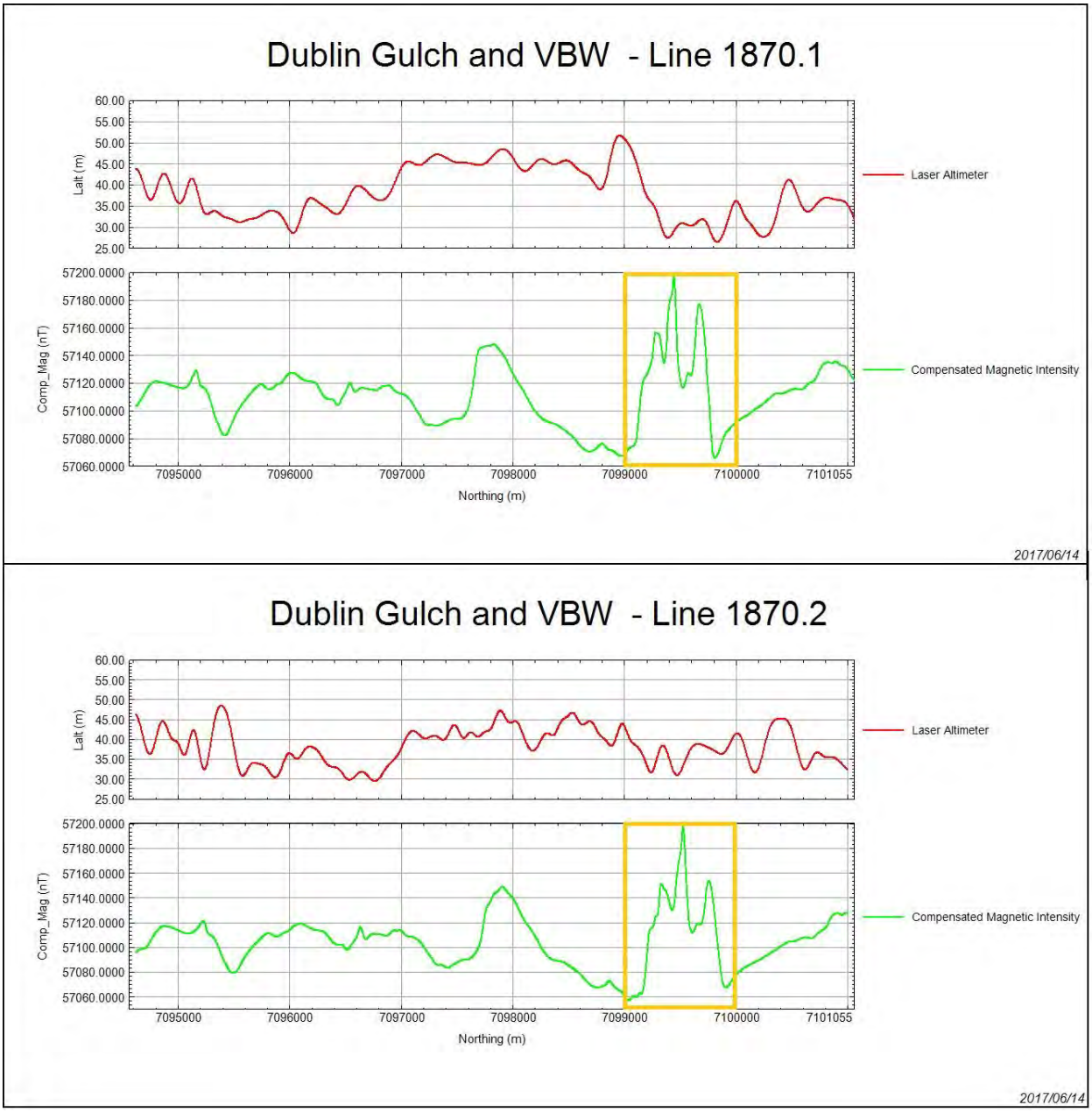

Figure 13: Profile plot of L1870 within Dublin Gulch/VBW survey block, looking west. Y-axis displaying laser altimeter readings in meters AGL (top, in red), compensated magnetic intensity (bottom, in green) and the x-axis displaying Y UTM coordinates. The high amplitude magnetic anomaly centered at UTM N 7099500 was reproduced on the re-flight.

At Dublin Gulch/VBW survey block, L1950 showed an isolated magnetic high-amplitude and short-wavelength anomaly which was not present on adjacent lines. The line was re-flown and the isolated magnetic high was not observed (Figure 14). Therefore the first flight returned an error in the data and data from the second flight were used in the final database.

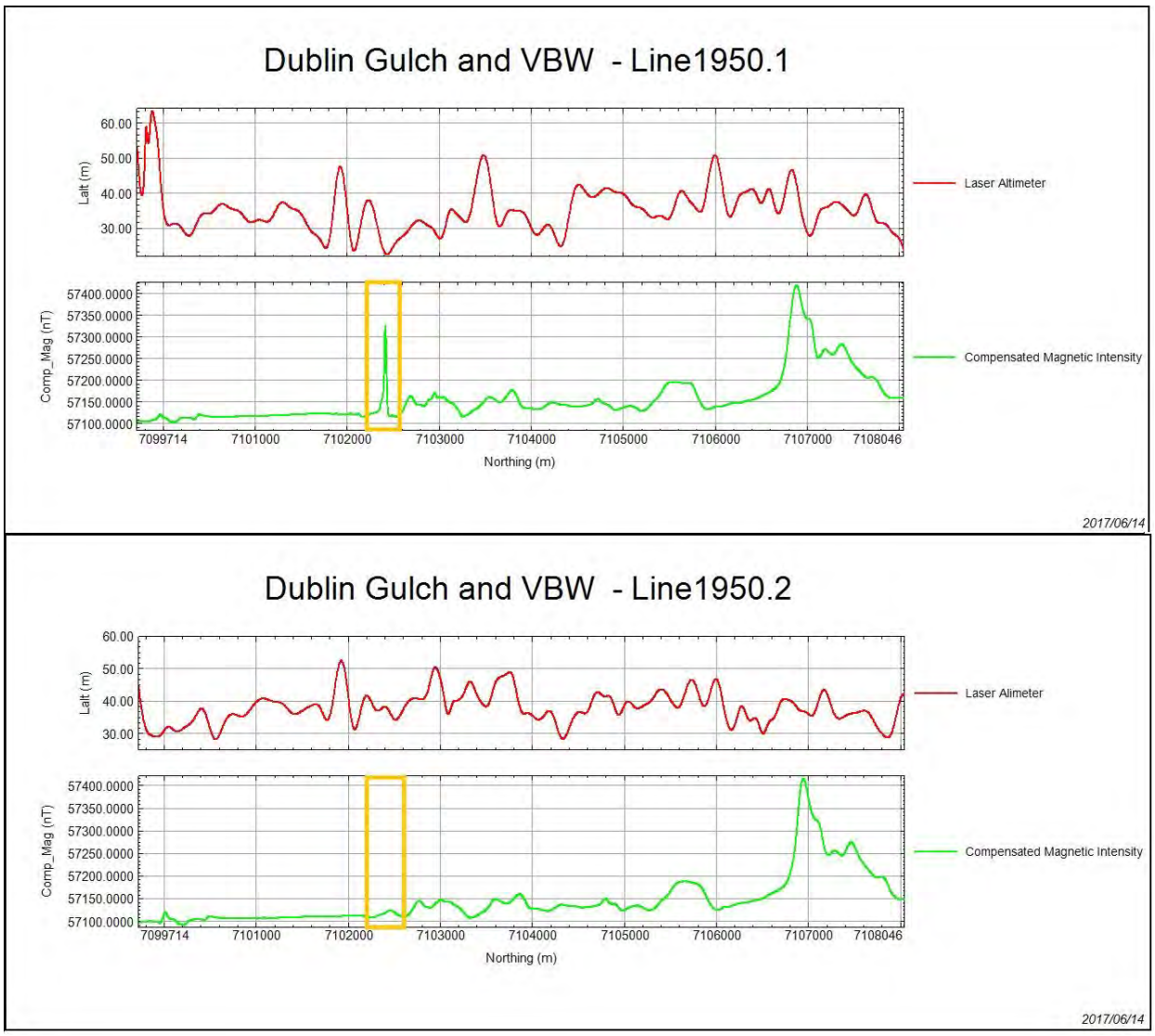

Figure 14: Profile plot of L1950 within the Dublin Gulch/VBW survey block, looking west. Y-axis displaying laser altimeter readings in meters AGL (top, in red), compensated magnetic intensity (bottom, in green) and the x-axis displaying Y UTM coordinates. The high amplitude narrow anomaly centered at UTM N 7102500 recorded on the first flight was not reproduced on the re-flight.

4.0 Aircraft and Equipment

All geophysical and subsidiary equipment were carefully installed on Precision GeoSurveys aircraft. For this survey, the survey magnetometer was carried in an approved "stinger" configuration to enhance flight safety and improve data quality.

4.1 Aircraft

Precision GeoSurveys flew the survey using an Airbus (formerly Eurocopter) AS350 helicopter, registration C-GSVY. The survey was flown at a constant height of 35 meters above ground for both the magnetometer and spectrometer.

4.2 Geophysical Equipment

The survey helicopter (Figure 15) was equipped with a magnetometer, spectrometer, data acquisition system, laser altimeter, magnetic compensation system, pilot guidance unit (PGU), and GPS navigation system. In addition, two magnetic base stations were used to record diurnal magnetic variations.

Figure 15: Geophysical survey helicopter equipped with geophysical equipment.

4.2.1 AGIS

The Airborne Geophysical Information System, AGIS (Figure 16), is the main computer used in data recording, data synchronizing, displaying real-time quality control data for the geophysical operator, and the generation of navigation information for the pilot and operator display systems. Information such as magnetic field components, total gamma count, counts of various

radioelements (K, U, Th, etc.), temperature, cosmic radiation, barometric pressure, atmospheric humidity, and survey altitude can all be monitored on the on-board AGIS display for immediate quality control.

The AGIS was manufactured by Pico Envirotec and uses standardized Pico software. External sensors are connected to the system via RS-232 serial communication cables. The AGIS data format is converted into Geosoft or ASCII file formats by a conversion program called PEIView. Additional Pico software allows for post or real time magnetic compensation and survey quality control procedures.

Figure 16: AGIS operator display installed in the Airbus AS350 survey helicopter, with screen displaying real time flight line recording and navigation parameters. Additional windows display real time geophysical data to operator.

4.2.2 Magnetometer

The airborne magnetic sensor was a Scintrex cesium vapor CS-3 magnetometer (S/N 1107379). The system was mounted on the front of the helicopter in an approved "stinger" configuration (Figure 17) to reduce influence from the aircraft's magnetic field. The CS-3 is a high sensitivity/low noise magnetometer with automatic hemisphere switching and a wide voltage range; the static noise rating for the unit is +/- 0.01 nT. Magnetic data were recorded at 10 Hz. A separate fluxgate magnetometer determined the helicopter's attitude (pitches, rolls, and yaws) relative to the inclination and declination of the Earth's magnetic field, which was necessary to remove magnetic noise created by the movement of the helicopter through a compensation process.

Figure 17: Scintrex cesium vapor CS-3 magnetometer mounted on the front of the helicopter in an approved "stinger" configuration. Sensor oriented 45° from vertical.

4.2.3 Spectrometer

The GRS-10 Radiometric Data Acquisition System, is a fully integrated gamma radiation detection system containing four NaI (T1) synthetic downward-looking crystals (Figure 18) and one NaI (T1) synthetic upward-looking crystal with 256 channel output at 1 Hz sampling rate. Each crystal has a volume of 4.2 liters, for a total of 21.0 liters. The downward-looking crystals are designed to measure gamma rays from below the aircraft and are equipped with upward-shielding high density RayShield® gamma-attenuating blankets to minimize cosmic and solar gamma noise. The upward-looking crystal measures solar gamma radiation from above the survey helicopter with a 6 mm thick lead plate used for downward-shielding. One of the downward-looking crystal packs was installed in the rear cabin of the aircraft, and the other downward-looking crystal pack was in the rear cargo box (total 16.8 liters downward-looking). The upward-looking crystal (total of 4.2 liters) was installed in the right cargo cheek.

Figure 18: GRS-10 Thallium-activated Sodium Iodide gamma spectrometer crystal pack. The open unit on the right shows two individual 4.2 liter detectors.

4.2.4 Base Station

To monitor and record the Earth's diurnal magnetic field variation, Precision GeoSurveys operates two GEM GSM-19T magnetometer base stations. The base stations were located in an area with low magnetic gradient, away from electric power transmission lines and moving ferrous objects, such as motor vehicles, that could affect the survey data integrity.

The GEM GSM-19T magnetometer (Figure 19) with integrated GPS time synchronization uses proton precession technology with a 0.5 Hz sampling rate. The GSM-19T has an absolute accuracy of +/- 0.2 nT and sensitivity of 0.15 nT at 1 Hz. Base station magnetic data were recorded on internal solid-state memory, and downloaded onto a field laptop computer using a serial cable and GEMLink 5.0 software. Profile plots of the base station readings were generated, updated, and reviewed at the end of each survey day.

Figure 19: GEM GSM-19T proton precession magnetometer.

4.2.5 Laser Altimeter

The pilot is provided with terrain guidance and clearance information from an Opti-Logic RS800 laser altimeter (Figure 20). This is attached to the aft end of the magnetometer boom. The RS800 laser is a time-of-flight sensor that measures distance by a rapidly-modulated and collimated laser beam that creates a dot on the target surface. The maximum range of the laser altimeter is 700 m off of natural surfaces with an accuracy of +/- 1 meter on 1 x 1 m^2 diffuse target with 50% (+/- 20%) reflectivity. Within the sensor unit, reflected signal light is collected by the lens and focused onto a photodiode. Through serial communications and digital outputs, the ground clearance data are transmitted to an RS-232 compatible port and recorded and displayed by the AGIS and PGU at 10 Hz in meters.

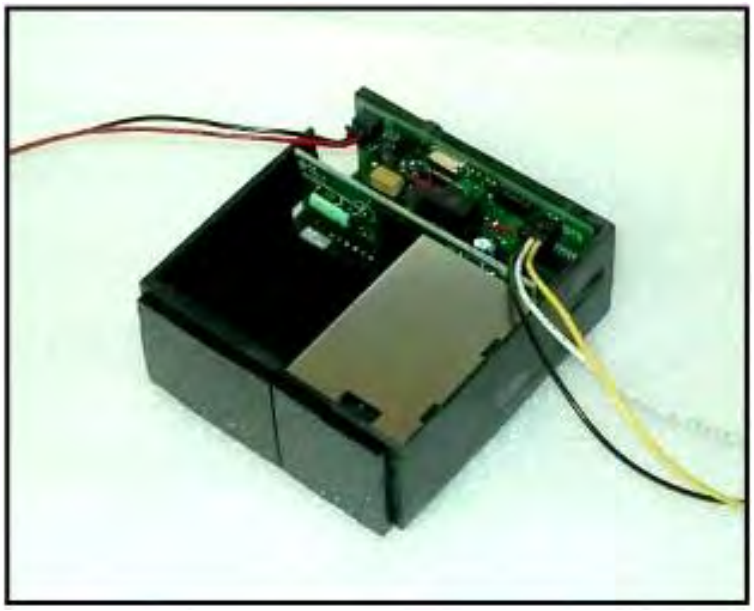

Figure 20: Opti-Logic RS800 laser altimeter.

4.2.6 Pilot Guidance Unit

The PGU (Pilot Guidance Unit) is a graphical display type unit that provides continuous steering and elevation information to the pilot (Figure 21). It is mounted remotely from the data system on top of the helicopter's instrument panel. The PGU assists the pilot in keeping the helicopter on the planned flight path, heading, and at the desired ground clearance.

Figure 21: PGU screen displaying navigation information.

The LCD monitor measures 7 inches, with a full VGA 800 x 600 pixel display. The CPU for the PGU is contained in a PC-104 console and uses Microsoft Windows operating system control, with input from the GPS antenna, embedded drape surface profile or laser altimeter, and AGIS.

4.2.7 GPS Navigation System

A Hemisphere R120 GPS receiver (Figure 22) navigation system integrated with the pilot display (PGU) and AGIS provided navigational information and control. The R120 GPS receiver supports fast updates and outputs messages at a rate of up to 20 Hz (20 times per second); delivering sub-meter positioning. It employs COAST technology that allows continuous operation for at least 40 minutes during temporary differential signal outages.

Figure 22: Hemisphere R120 GPS Receiver.

It can track GPS, SBAS (Satellite-Based Augmentation System), and L-Band (OmniSTAR HP and XP) differential corrections to provide accurate positioning.

5.0 Data Acquisition Equipment Checks and Calibration

Airborne equipment tests and calibrations were conducted at the start of the survey. There were three tests conducted for the airborne magnetometer: compensation flight, lag test, and heading error test. Three other tests were conducted for the airborne gamma ray spectrometer: calibration pad test, cosmic flight test, and the altitude correction and sensitivity test.

5.1 Magnetometer Tests

Before acquiring magnetic data the magnetometer was tested and calibrated. A series of dedicated flights were completed to collect data specifically for removing undesired side-effects of aircraft movement, speed, and heading direction.

5.1.1 Compensation Flight Test

During aeromagnetic surveying a small but significant amount of noise is introduced to the magnetic data by the aircraft itself, as the magnetometer is within the aircraft's magnetic field. Movement of the aircraft (roll, pitch and yaw) combined with the permanent magnetization of certain aircraft parts (in particular the engine and other ferrous magnetic objects) contribute to this noise. The aircraft was degaussed prior to starting the survey and the remaining magnetic

noise was removed by a process called magnetic compensation. Two magnetic compensation flights were completed prior to beginning the survey (Tables 7 and 8). The process consists of a series of prescribed maneuvers where the aircraft flies in the four orthogonal headings required for the survey (000°/090°/180°/270° and 045°/135°/225°/315° in the case of these surveys) at a sufficient altitude (typically > 2,500 m AGL) in an area of low magnetic gradient where the Earth's magnetic field becomes nearly uniform at the scale of the compensation flight. In each heading direction, three specified roll, pitch, and yaw maneuvers (total 36) are performed by the pilot at constant elevation so that any magnetic variation recorded by the airborne magnetometer can be attributed to aircraft movement. These maneuvers provide the data that are required to calculate the necessary parameters for compensating the magnetic data and removing aircraft noise from survey data.

Pre-Compensation					Post-Compensation				
Heading	**Roll**	**Pitch**	**Yaw**	**Total**	**Heading**	**Roll**	**Pitch**	**Yaw**	**Total**
091°	10.9596	6.8175	1.9134	19.6905	091°	0.1277	0.2231	0.2002	0.5510
180°	9.6973	8.0308	3.1968	20.9249	180°	0.1468	0.2364	0.2541	0.6373
271°	4.053	7.3072	2.1489	13.5091	271°	0.1452	0.2515	0.1301	0.5268
359°	8.5548	2.6197	1.7821	12.9566	359°	0.1468	0.1375	0.1934	0.4777
Total	33.2647	24.7752	9.0412		**Total**	0.5665	0.8485	0.7778	
FOM (nT) =67.0811					**FOM (nT) =2.1928**				

Table 7: Figure of Merit maneuver test results for 000°/090°/180°/270° compensation flight flown on June 5, 2017.

Pre-Compensation					Post-Compensation				
Heading	**Roll**	**Pitch**	**Yaw**	**Total**	**Heading**	**Roll**	**Pitch**	**Yaw**	**Total**
045°	9.4563	4.5829	2.9656	17.0048	045°	0.1153	0.0875	0.1726	0.3754
138°	10.8288	6.6106	3.6404	21.0798	138°	0.1757	0.1362	0.1962	0.5081
224°	6.0950	7.7755	3.8636	17.7341	224°	0.0997	0.1199	0.0746	0.2942
316°	5.4359	3.5705	1.7467	10.7531	316°	0.0882	0.1073	0.0837	0.2792
Total	31.8160	22.5395	12.2163		**Total**	0.4789	0.4509	0.5271	
FOM (nT) =66.5718					**FOM (nT) =1.4569**				

Table 8: Figure of Merit maneuver test results for 045°/135°/225°/315° compensation flight flown on June 8, 2017.

5.1.2 Lag Test

A lag test was performed to determine the relationship between the time the digital reading was recorded by the magnetic sensor instrument and the position fix time that the fiducial of the reading was obtained by the GPS system. The test was flown in the four orthogonal survey headings over an identifiable magnetic anomaly at survey speed and height. A lag of 16 fiducials (1.6 seconds) was determined from the lag test.

5.1.3 Heading Error Test

To determine the magnetic heading effect two cloverleaf pattern flight tests were conducted. The cloverleaf tests were flown in the same orthogonal headings as the survey and tie lines (000°/090°/180°/270° and 045°/135°/225°/315°) at >1000 m AGL in an area with low magnetic gradient. For each cloverleaf test, the survey aircraft must pass over the same mid-point all four times at the same elevation (Tables 9 and 10).

Heading	Fiducials	Mag (nT)	Correction (nT)
000°	882.7	57052.6635	4.8674
090°	1031.0	57062.2965	-4.7656
180°	735.6	57063.8482	-6.3173
270°	1149.7	57051.3154	6.2155
	Average	57057.5309	
	Total		**0.0000**

Table 9: Heading error test data format for Dublin Gulch/VBW flown on June 5, 2017.

Heading	Fiducials	Mag (nT)	Correction (nT)
045°	932.2	57074.5909	0.7471
135°	1147.3	57085.0857	-9.7477
225°	807.1	57075.6623	-0.3243
315°	1031.1	57066.0131	9.3249
	Average	57075.3380	
	Total		**0.0000**

Table 10: Heading error test data format for Clear Creek flown on June 8, 2017.

5.2 Gamma-ray Spectrometer Tests and Calibrations

Pre-survey calibrations and testing of the GRS-10 airborne gamma-ray spectrometry system were carried out prior to the start of the survey. The calibration of the spectrometer system involved three tests which enabled the conversion of airborne data to ground concentration of natural radioactive elements. These tests were the calibration pad test, cosmic flight test, and the altitude correction and sensitivity test. The measurements were made in accordance with IAEA technical report series No. 323, *Airborne Gamma Ray Spectrometer Surveying*, and AGSO Record 1995/60, *A Guide to the Technical Specification for Airborne Gamma-Ray Surveys*.

5.2.1 Calibration Pad Test

The calibration pad test was conducted by Pico Envirotec using GSC (Geological Survey of Canada) portable calibration pads. The pads are slabs of concrete containing known concentrations of the radioelements (K, Th, and U) and are used to simulate ideal geological sources of radiation. The measurements collected from the calibration pad test were used to determine the Compton scattering and Grasty backscatter (spectral overlap between element windows) coefficients.

5.2.2 Cosmic Flight Test

While the background source of gamma radiation from the aircraft itself is essentially constant, the amount of signal detected from ground sources varies with ground clearance. As the height of the aircraft increases, the distance between the ground and the spectrometer crystals increase, and the proportion of cosmic radiation in each spectral window increases exponentially due to radiation of cosmic origin. The cosmic flight test is conducted to determine the aircraft's background attenuation coefficients for the detector crystal packs and the cosmic coefficients. The pilot is required to fly over the same location repeatedly in opposite directions starting from 1,500 m to 3,000 m at 500 m intervals for approximately 2 minutes each to collect gamma data used to determine the amount of non-terrestrial gamma signal.

5.2.3 Altitude Correction and Sensitivity Test

The altitude and sensitivity test is similar to the cosmic flight test but is conducted at lower elevations (from ground level). The pilot is required to fly over the same location at the following elevations in meters above ground; 30, 50, 100, 150, 200, 250, and 300, for 2 minutes each. As the distance of the aircraft increases away from the radioactive ground source, the source signature exponentially degrades. As a result, this test is used to determine the altitude attenuation coefficients and the radio-element sensitivity of the airborne spectrometer system.

6.0 Data Processing

After all the data were collected from a survey flight, several procedures were undertaken to ensure that the data met a high standard of quality. All magnetic and radiometric data (Figure 23) were processed using Pico Envirotec software and Geosoft Oasis Montaj 9.1.3 geophysical processing software along with proprietary processing algorithms.

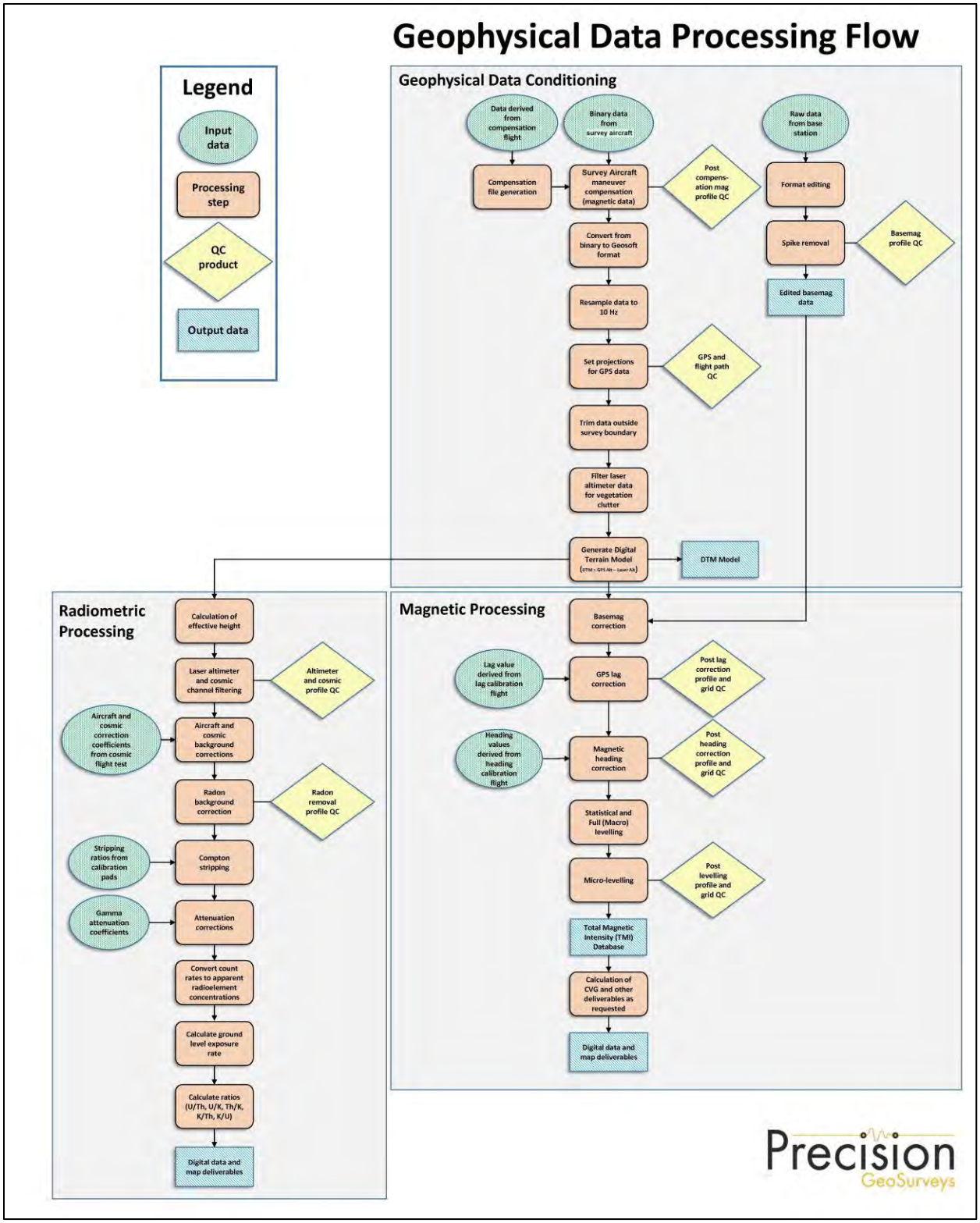

Figure 23: Magnetic and radiometric data processing flow.

6.1 Digital Terrain Model

Over glassy water or fog, the laser altimeter is unable to record a valid reading and causes the laser to drop out and record either an invalid reading or zeros. Areas with dense vegetation; thick tree covers, laser cannot penetrate through the trees to record actual ground clearance and high frequency variations are recorded. Corrections were applied to the laser altimeter data. To remove vegetation clutter, a Rolling Statistic filter was applied followed by a low pass filter which was used to smooth out the laser altimeter profile to eliminate isolated high frequency noise. Where the laser had dropped out, the invalid data or recorded zeros were replaced with ground clearance values computed from taking the difference between CDED (Canadian Digital Elevation Data) and GPS altitude of the aircraft.

A digital terrain model (DTM) channel was calculated by subtracting the processed laser altimeter data from the filtered GPS altimeter data defined by the WGS 84 ellipsoidal height.

6.2 Magnetic Processing

The data obtained from the compensation flight test were applied to the raw magnetic data before any further processing and editing. A computer program called PEIComp was used to create a model from the compensation flight test for each survey to remove the noise induced by aircraft movement; this model was applied to each survey flight so the data could be further processed.

The compensated raw magnetic data were then corrected for diurnal variations, lag, and heading. Any evidence of noise or spikes was removed. The initial corrected data from the survey and tie lines were then used to level the entire survey dataset. Lastly, the International Geomagnetic Reference Field (IGRF) was used to remove the background magnetic field of the Earth.

6.2.1 Diurnal Correction

The first step in processing the compensated magnetic data was to correct for diurnal variations. The base station data that were used for the correction came from GEM 5. The diurnal data were edited, plotted and merged into a Geosoft database (.GDB) on a daily bases. The airborne magnetic data were corrected for diurnal variations by subtracting the observed magnetic base station deviations from the data collected on the aircraft, which effectively removed the effects of diurnal variation, diurnal drift, and geomagnetic storms.

6.2.2 Lag Correction

Following the diurnal correction, a lag correction of 1.6 seconds was applied to the total magnetic field data to compensate for the combination of lag in the recording system and the magnetometer sensor flying 5.4 m ahead the GPS antenna.

6.2.3 Heading Correction

For each survey heading the magnetic instrument travels along a flight line, changes in instrument magnetic fields are detected and these systematic shifts are recorded. These values are used to construct a heading .TBL table file. An intersection table was created, containing all magnetic field values where tie lines intersected the survey lines and the overall average magnetic field value was calculated. For each of the four headings, the averages were calculated and then compared to the overall average to determine four values to be used for heading error correction.

6.2.4 Leveling and Micro-leveling

The initial Total Magnetic Intensity (TMI) data from survey and tie lines were used to level the entire survey dataset. Two forms of leveling were applied to the corrected data: conventional leveling and micro-leveling. There were two components to conventional leveling; Statistical Leveling to level tie lines and Full Leveling to level survey lines. The Statistical Leveling method corrected for miss-ties (SL/TL intersection errors) following a specific pattern or trend. Through the error channel, an algorithm calculated a least-squares trend line and derived a trend error curve, which was then added to the channel to be leveled. The second component was Full Leveling. This adjusted the magnetic value of the survey lines so that all lines matched the trended tie lines at each intersection point.

Lastly, micro-leveling was applied to the corrected conventional leveled data. This iterative grid-based process removed low amplitude components of flight line noise that still remained in the data after tie line and survey line leveling.

6.2.5 IGRF Removal

The International Geomagnetic Reference Field (IGRF) model is the empirical representation of the Earth's magnetic field (main core field without external sources) collected and disseminated from satellite data and from magnetic observatories around the world. The IGRF is generally revised and updated every five years by a group of modelers associated with the International Association of Geomagnetism and Aeronomy (IAGA). In this case, the IGRF values were calculated from the recently updated model (IGRF – 12) year 2015 and the actual survey dates were obtained from the "Date" channel.

By subtracting the calculated IGRF from TMI, Residual Magnetic Intensity (RMI) for each of the survey blocks were calculated. This created a more valid model of individual near-surface anomalies so that the data were not referenced to a specific time. This will allow for other magnetic data (historic or future) to be more easily incorporated into each survey database.

6.2.6 Reduced to Magnetic Pole

The Reduced to Magnetic Pole (RTP) was computed from the leveled Residual Magnetic Intensity (RMI) data. The RTP filter is applied in the Fourier domain and it migrates the observed magnetic inclination and declination field to what the field would look like at the magnetic pole.

6.2.7 Calculation of First Vertical Derivative

The first vertical derivative were computed from both the leveled Residual Magnetic Intensity (RMI) data and Reduced to Magnetic Pole (RTP). Long wavelengths and vertical rate of change were suppressed in the magnetic field. Therefore, the edges of magnetic anomalies were highlighted and spatial resolution was increased.

The first vertical derivative calculated from the RMI was designated as Calculated Vertical Derivative of RMI, or CVG. The first vertical derivative calculated from the RTP was designated as First Vertical Derivative of RTP, or 1VD.

6.3 Radiometric Processing

Radiometric surveys map the concentration of radioelements at or near the earth's surface; typically up to 1.5 meters below surface. Before any processing of the airborne radiometric data, the first step is to calibrate the spectrometer system. Once calibration of the system was complete, the radiometric data were processed by windowing the full spectrum to create channels for U, K, Th and total count.

Steps taken to process acquired radiometric data are summarized below:

- Calculation of effective height
- Aircraft and Cosmic background corrections
- Radon background correction
- Stripping ratios
- Attenuation corrections
- Conversion to apparent radioelement concentrations

6.3.1 Calculation of Effective Height

Laser/Radar altimeter data were converted to effective height (h_{ef}) in meters using the acquired laser/radar altimeter, temperature and pressure data, according to the formula below:

$$h_{ef} = h * \frac{273.15}{T + 273.15} * \frac{P}{1013.25}$$

where: h is the observed laser/radar altitude in meters
T is the measured air temperature in degrees Celsius
P is the barometric pressure in millibars

6.3.2 Intermediate Filtering

Some of the measured parameters are filtered as part of the pre-processing.

- Laser/radar altimeter is lightly filtered, a 5-point Hanning filter to smooth out rapid changes that may occur in rugged terrain.
- The Cosmic channel was smoothed with a 5-point Hanning filter to reduce statistical noise.

6.3.3 Aircraft and Cosmic Background Corrections

Aircraft background and cosmic stripping corrections are applied to all three elements, and total count, using the following formula:

$$C_{ac} = a_c + b_c * \mathrm{Cos}_f$$

where: C_{ac} is the background and cosmic corrected channel
a_c is the aircraft background for this channel
b_c is the cosmic stripping coefficient for this channel
Cos_f is the filtered cosmic channel

6.3.4 Radon Background Correction

To strip the effects of atmospheric radon from the downward-looking detectors, calibration constants are determined through the use of an upward-looking detector. The upward-looking detector uses crystal pack that is partially shielded from radiation from below to give the system a directional sensitivity and the ability to discriminate between radiation from the atmosphere and from the ground. Procedures to determine these calibration constants in detail are outlined in the IAEA 1363 report, *Guidelines for Radioelement Mapping using Gamma Ray Spectrometry Data*.

6.3.5 Compton Stripping

Spectral overlap corrections are applied to potassium, uranium, and thorium as part of the Compton stripping process. This is done by using the stripping ratios that have been calculated for the spectrometer by prior calibration; this breaks the corrected elemental values down into the apparent radioelement concentrations.

Stripping ratios α, β, and γ are first modified according to altitude. Then an adjustment factor (derived from the cosmic flight test), the reversed stripping ratio, uranium into thorium, is calculated.

$$\alpha_h = \alpha + h_{ef} * 0.00049$$

$$\beta_h = \beta + h_{ef} * 0.00065$$

$$\gamma_h = \gamma + h_{ef} * 0.00069$$

where: α, β, γ are the Compton stripping coefficients
α_h,β_h,γ_h are the height corrected Compton stripping coefficients
h_{ef} is the effective height above ground in metres at STP

The stripping corrections are then carried out using the following formulas:

$$Th_c = Th_{bc}(1 - g\beta_h) + U_{bc}(b\gamma_h - a) + K_{bc}(ag - b) / A$$

$$U_c = Th_{bc}(g\beta_h - \alpha_h) + U_{bc}(1 - b\beta_h) + K_{bc}(b\alpha_h - g) / A$$

$$K_c = [Th_{bc}(\alpha_h\gamma_h - \beta_h) + U_{bc}(a\beta_h - \gamma_h) + K_{bc}(1 - a\alpha_h)] / A$$

where: U_c, Th_c and K_c stripping corrected uranium, thorium and potassium
α_h,β_h,γ_h height corrected Compton stripping coefficients
U_{bc}, Th_{bc} and K_{bc} background corrected uranium, thorium and potassium
a is the spectral ratio Th/U
b is the spectral ratio Th/K
g is the spectral ratio U/K
$A = 1 - g\gamma_h - a(\alpha_h - g\beta_h) - b(\beta_h - \alpha_h\gamma_h)$ is the backscatter correction

6.3.6 Attenuation Corrections

The total count, potassium, uranium and thorium data are then corrected to a nominal survey altitude (corrected to remove vegetation clutter from radar/laser altimeter data), in this case the survey height was 35 meters. This is done according to the equation:

$$C_a = C * e^{\mu(h_{ef}-ho)}$$

where: C_a is the output altitude corrected channel
C is the input channel
μ is the attenuation correction for that channel
h_{ef} is the effective altitude, usually in m
h_0 is the nominal survey altitude used as datum

6.3.7 Conversion to Apparent Radioelement Concentrations

With all corrections applied to the radiometric data, the final step is to convert the corrected potassium, uranium, and thorium to apparent radioelement concentrations using the following formula:

$$eE = C_{cor} / s$$

where: *eE* is the element concentration K(%) and equivalent element concentration of U(ppm) & Th(ppm)
s is the experimentally determined sensitivity
C_{cor} is the fully corrected channel

Finally, the natural air exposure rate is determined by using the following formula:

$$E = [(13.08 * K + 5.43 * eU + 2.69 * eTh)/8.69]$$

where: *E* is the absorption dose rate in µR/h
K is the concentration of potassium (%)
eU is the equivalent concentration of uranium (ppm)
eTh is the equivalent concentration of thorium (ppm)

6.3.8 Radiometric Ratios

To calculate some of the common radiometric ratios (U/Th, Th/K, and U/K or their inverses) the guidelines of the IAEA are followed. Due to statistical uncertainties in the individual radioelement measurements, some care is taken in the calculation of the ratio in order to obtain statistically significant values. Following IAEA guidelines, the method of determining ratios of the eU/eTh, eU/K and eTh/K is as follows:

1. Any data points where the potassium concentration is less than 0.25% are neglected.
2. The element with the lowest corrected count rate is determined.
3. The element concentrations of adjacent points on either side of each data point are summed until they exceed a pre-determined threshold value. This threshold is set to be equivalent to 100 counts of the element with the lowest count rate. Additional minimum thresholds of 1.6% for potassium, 20 ppm for thorium, and 30 ppm for uranium are established to ensure meaningful ratios.
4. The ratios are calculated using the accumulated sums.

With this method, the errors associated with the calculated ratios are minimized and comparable for all data points.

6.4 Merging 2017 Geophysical Data with Historical Data

Parts of the 2017 Dublin Gulch/VBW and Clear Creek survey areas were previously flown with various geophysical technologies. The data from these surveys were provided to Precision with the intent of merging the data to improve coverage and resolution.

6.4.1 Dublin Gulch/VBW Survey area

Fugro flew a combined frequency domain electromagnetic and horizontal gradient[1] magnetic survey in 2004, over the eastern part of the 2017 survey area. The 2004 survey lines were spaced at 150 meters with lines oriented at 000/180°. The 2017 survey lines were planned as parallel and alternating with the 150 m Fugro lines, so that an effective line spacing of 75 m for the magnetic data was achieved where the previous survey coverage coincided with the 2017 survey.

The 2004 data were reported as being flown at an average height of 39.9 meters AGL with a standard deviation of 8.9 meters, and the 2017 data were flown at an average height of 36.5 meters AGL with a standard deviation of 6.0 meters, as shown in Table 11. The 2004 magnetic data were delivered by Fugro as total magnetic intensity. Therefore, the residual magnetic intensity was calculated so that it could readily be merged with 2017 data.

[1] Fugro's survey report is not clear if the magnetic gradient was measured in the lateral or longitudinal direction, or how Total Magnetic Intensity was derived from the multi-sensor horizontal gradiometer.

Parameter	2004 Fugro	2017 Precision
Survey Date(s)	Oct. 6 – Dec. 15, 2004	June 5-8, 2017
Sensors	Dighem EM and horizontal magnetic gradient	Total magnetic intensity by stinger and radiometrics
Survey area (km^2)	466.2	555.2
Total survey line km	3017.7	4068.4
Aircraft platform	helicopter	helicopter
Line orientation	000/180°	000/180°
Line spacing (m)	150	150
Survey ground clearance, Average (m)	39.9	36.5
Survey ground clearance, Std. Deviation (m)	8.9	6.0

Table 11: Comparison of 2004 and 2017 airborne survey specifications, Dublin Gulch area.

The residual magnetic field data from the 2004 and 2017 surveys were merged (Figure 24) so that the final product yielded 75 m line spacing and gridded at 18.75 meter cell size (25% of line spacing). The 2004 residual magnetic intensity data were leveled to 2017 RMI data by applying both conventional leveling and micro-leveling to the merged dataset. As the 2017 data had already been leveled as a standalone dataset, the statistical leveling was not performed a second time on the 2017 tie line data. Therefore, an intersection table was created for the merged dataset and a full level was performed on the 2004 survey line data in order to level it to the 2017 data. The 2017 survey line data had already been fully leveled to the 2017 tie lines. As a result, the data were unaffected by the full leveling component of the conventional leveling. Once the full leveling was complete, the dataset was reviewed to locate any problem areas that were not leveled properly. Such areas include, but are not limited to, intersection points between survey lines due to re-flights, portions of 2014 survey lines that were of specification, and areas with cultural features that may have changed with time.

Finally, micro-leveling was applied to the corrected conventional leveled and merged dataset (2004 and 2017). This iterative grid-based process removed low amplitude components of flight line noise that was introduced by the merging of the datasets and remained after the conventional leveling.

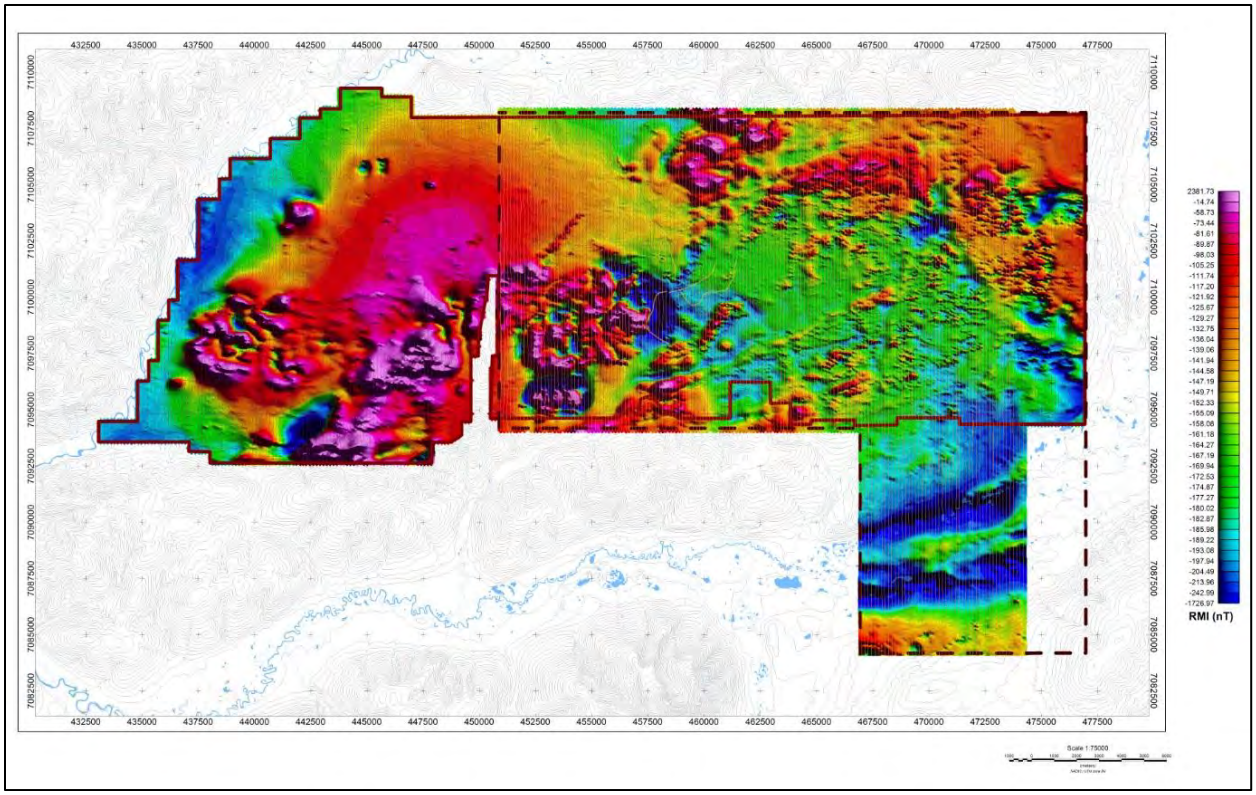

Figure 24: 2004 (Fugro) merged and leveled to 2017 (Precision) magnetic data with actual flight lines; residual magnetic intensity Dublin Gulch area.

6.4.2 Clear Creek Survey Area

In 1998, Newmont collected 1513.3 line km of total field magnetic and radiometric data in the Clear Creek area. The Newmont survey was flown in a 000-180° direction, without tie lines, at an average height of 74.1 meters AGL with a standard deviation of 22.2 meters, while the 2017 data were flown in a 045-225° direction at an average height of 35.9 meters AGL with a standard deviation of 7.0 meters, as shown in Table 12.

Parameter	1998 Newmont	2017 Precision
Survey Date(s)	August 11-14, 1998	June 7, 2017
Sensors	Total magnetic intensity by slung bird and radiometrics	Total magnetic intensity by stinger and radiometrics
Survey area (km2)	306.7	43.7
Total survey line km	1513.3	481.5
Aircraft platform	helicopter	helicopter
Line orientation	000/180°	045°/225°
Line spacing (m)	200	100
Survey ground clearance, Average (m) - magnetics	104.1	35.9
Survey ground clearance, Average (m) - radiometrics	134.1	35.9
Survey ground clearance, Std. Deviation (m) - magnetics	22.2	7.0
Survey ground clearance, Std. Deviation (m) - radiometrics	22.2	7.0

Table 12: Comparison of 1998 and 2017 airborne survey specifications, Clear Creek area. No tie lines were flown during the 1998 survey.

It was not possible to merge the 1998 data with the 2017 survey results due to the different line spacing, line direction, and flight height. However, the smaller 2017 magnetic and radiometric survey data were laid over the larger 1998 survey so that the more detailed 2017 results can be viewed in a more regional context (Figures 25 and 26).

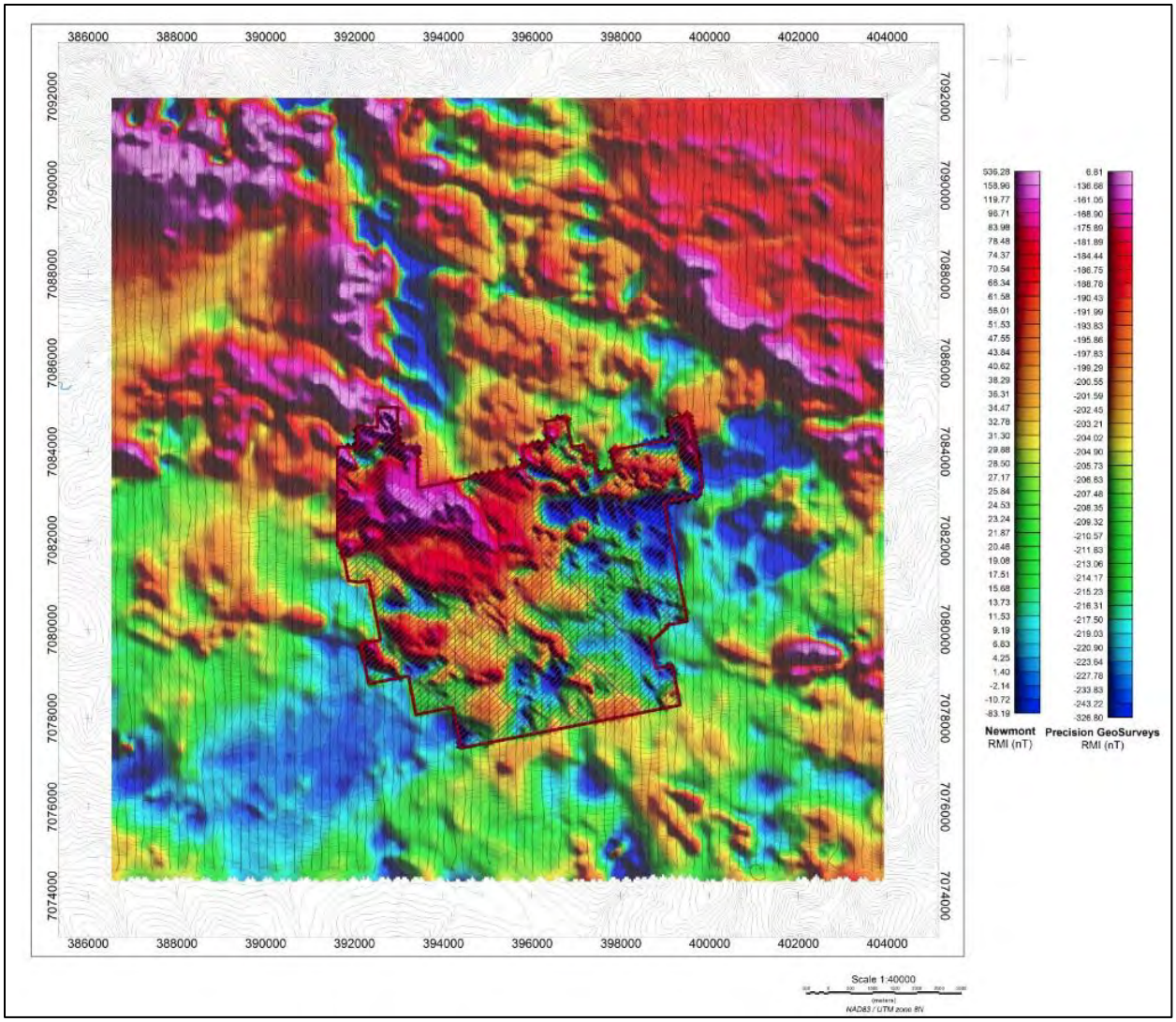

Figure 25: 2017 magnetic data laid over the larger 1998 magnetic data with actual flight lines; residual magnetic intensity Clear Creek area.

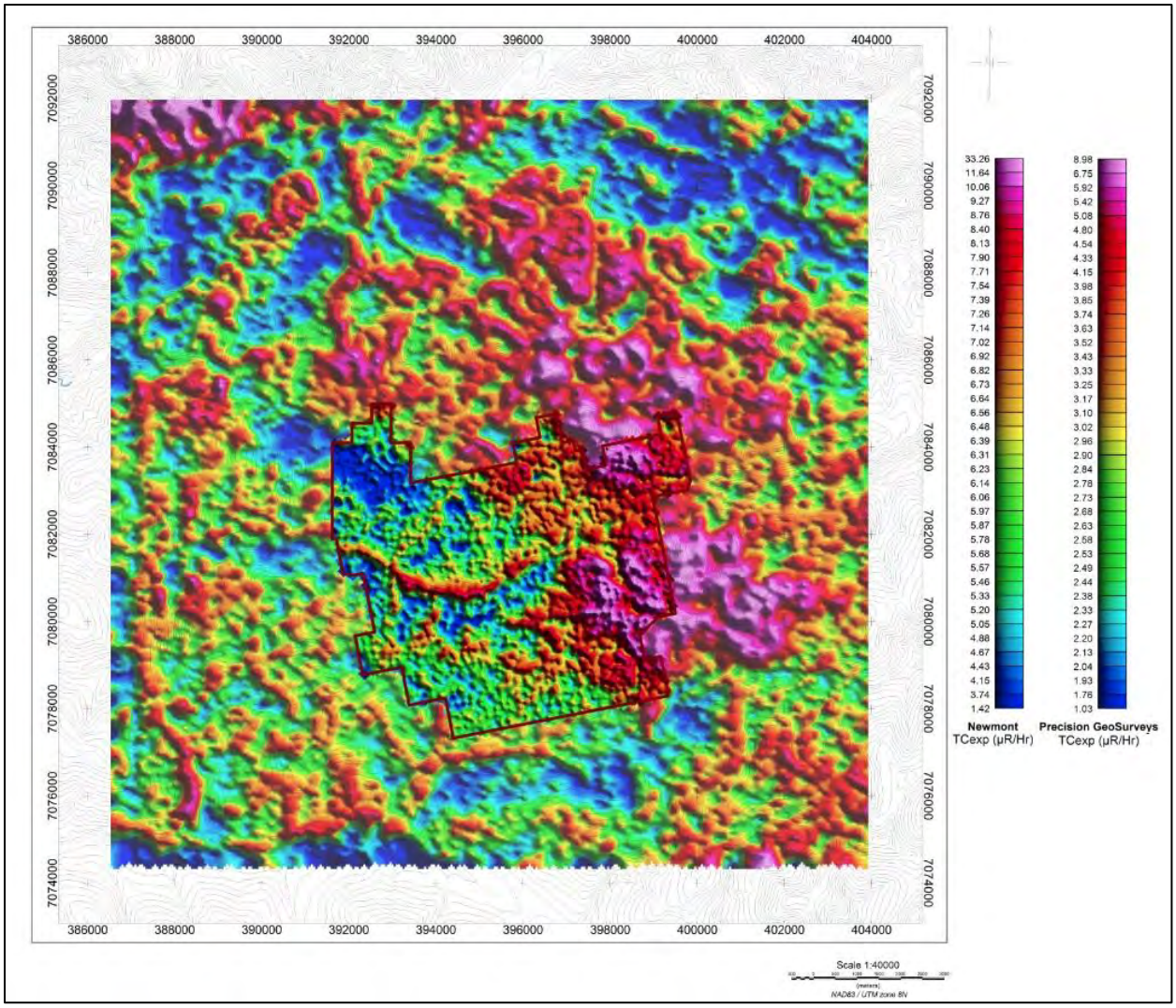

Figure 26: 2017 radiometric data laid over the larger 1998 radiometric data; total count exposure Clear Creek area.

7.0 Deliverables

All digital data are presented on a USB memory stick with the logistic report. The survey data are presented as digital databases, maps, and a report.

7.1 Digital Data

The digital files have been provided in two formats, the first is a .GDB file for use in Geosoft Oasis Montaj and the second format is a .XYZ (text) file. Full descriptions of the digital data and contents are included in the report (Appendix B).

The digital data were represented as grids, as listed below:

- Digital terrain model (DTM)
- Total magnetic intensity (TMI)
- Residual magnetic intensity (RMI) – removal of IGRF from TMI
- Calculated vertical gradient (CVG) - first vertical derivative of RMI
- Calculated horizontal gradient (CHG) – first horizontal derivative of RMI
- Reduced to Pole (RTP) – reduced to magnetic pole of RMI
- First Vertical Derivative of RTP (1VD) – first vertical derivative of RTP
- Potassium – Equivalent Concentration (%K)
- Thorium – Equivalent Concentration (eTh)
- Uranium – Equivalent Concentration (eU)
- Total Count – Equivalent Dose Rate (TCcor)
- Total Count – Exposure Rate (TCexp)
- Potassium over Thorium Ratio (%K/eTh)
- Potassium over Uranium Ratio (%K/eU)
- Uranium over Thorium Ratio (eU/eTh)
- Thorium over Potassium Ratio (eTh/%K)
- Uranium over Potassium Ratio (eU/%K)
- Ternary Map (TM)

7.1.1 Gridding

Digital data were gridded and displayed using the following Geosoft parameters for both Dublin Gulch/VBW and Clear Creek survey blocks:

- Grid cell size: 37.5 m (Dublin Gulch/VBW) and 25 m (Clear Creek)
- Low-pass desampling factor: 3
- Tolerance: 0.001
- % pass tolerance: 99.99
- Maximum iterations: 100

All grids were drawn with a histogram-equalized color shade; sun angle inclination at 45° and declination at 45°.

7.2 KMZ Grids

The digital data represented into grids were exported into kmz files which can be displayed using Google Earth. The grids can be draped onto topography and rendered to give a 3D view.

7.3 Maps

Digital maps were created for each of the survey blocks. The following map products were prepared:

Survey Overview Maps (colour images with elevation contour lines):

- Actual flight lines
- Digital elevation model

Magnetic Maps (colour images with elevation contour lines):

- Total magnetic intensity with actual plotted flight lines
- Total magnetic intensity
- Residual magnetic intensity
- Calculated vertical gradient of residual magnetic intensity
- Calculated horizontal gradient of residual magnetic intensity
- Reduced to magnetic pole of residual magnetic intensity
- First vertical derivative of reduced to magnetic pole

Radiometric Maps (colour images with elevation contour lines):

- Potassium – Equivalent Concentration in Percentage
- Thorium – Equivalent Concentration
- Uranium – Equivalent Concentration
- Total Count – Equivalent Dose Rate
- Total Count – Exposure Rate
- Potassium over Thorium Ratio
- Potassium over Uranium Ratio
- Uranium over Thorium Ratio
- Thorium over Potassium Ratio
- Uranium over Potassium Ratio
- Ternary Map

Data were collected in WGS 84 Zone 8N and all maps were prepared in NAD 83 and UTM zone 8N.

7.4 Report

The logistics report provides information on the acquisition procedures, magnetic and radiometric processing, and presentation of the Dublin Gulch/VBW and Clear Creek survey blocks data. A pdf copy of the report is included along with the digital data and maps that are provided on the USB stick.

8.0 Conclusions and Recommendations

The airborne magnetic and radiometric data were acquired to map the geophysical characteristics of the survey area, which are in turn related to the distribution and concentration of magnetic minerals and radioactive elements in the Earth. The geophysical data therefore will help explore and possibly discover new mineral deposits. As geophysical data are not a direct indication of mineral deposits, geophysical interpretation and careful integration with existing and new geological, geochemical, and other geophysical data are recommended to maximize value from the survey investment.

Appendix A

Equipment Specifications

- GEM GSM-19T Proton Precession Magnetometer (Base Station)
- Hemisphere R120 GPS Receiver
- Opti-Logic RS800 Laser Altimeter
- HC-S3 Temperature and Relative Humidity Probe
- Setra Model 276 Barometric Pressure
- Scintrex CS-3 Survey Magnetometer
- Bartington Mag-03 three-axis fluxgate magnetic field sensor
- Pico Envirotec GRS-10 Gamma Spectrometer
- Pico Envirotec AGIS data recorder system (for Navigation, Gamma Spectrometer, and Magnetometer Data Acquisition)

GEM GSM-19T Proton Precession Magnetometer (Base Station) Specifications

Configuration Options	15
Cycle Time	999 sec to 0.5 sec
Environmental	-40°C to +60°C
Gradient Tolerance	7,000 nT/m
Magnetic Readings	299,593
Operating Range	10, 000 to 120,000 nT
Power	12 V @ 0.62 A
Sensitivity	0.1 nT @ 1 sec
Weight (Console/ Sensor)	3.2 Kg
Integrated GPS	Yes

Hemisphere R120 GPS Receiver Specifications

GPS Sensor	Receiver Type	L1, C/A code, with carrier phase smoothing (Patented COAST technology during differential signal outage
	Channels	12-channel, parallel tracking (10-channel when tracking SBAS)
	Update Rate	Up to 20 Hz position
	Cold Start Time	<60 s
	SBAS Tracking	2-channel, parallel tracking
	Horizontal Accuracy	<0.02 m 95% confidence (RTK 1, 2) <0.28 m 95% confidence (L-Dif 1, 2) <0.6 m 95% confidence (DGPS 1,3) <2.5 m 95% confidence (autonomous, no SA1)
	Differential Options	SBAS, Autonomous, External RTCM, RTK, OmniSTAR (HP/XP)
Beacon Sensor Specifications	Channels	2-channel, parallel tracking
	Frequency Range	283.5 to 325 kHz
	MSK Bit Rates	50, 100, and 200 bps
L-Band Sensor	Channels	Single channel
	Frequency Range	1530 MHz to 1560 MHz
	Satellite Selection	Manual or Automatic (based on location)
	Startup and Satellite Reacquisition Time	15 seconds typical
Communications	Serial Ports	2 full duplex RS232C
	Baud Rates	4800 – 115200
	USB Ports	1 Communications
	Correction I/O Protocol	RTCM SC-104
	Data I/O Protocol	NMEA 0183
	Timing Output	1 PPS (HCMOS, active high, rising edge sync, 10 kΩ, 10 pF load)
	Raw Data	Proprietary binary (RINEX utility available)
Environmental	Operating Temperature	-30°C to +70°C
	Storage Temperature	-40°C to +85°C
	Humidity	95% non-condensing
Power GPS Sensor	Input Voltage Range	8 to 36 VDC
	Power Consumption	3 Watts
	Current Consumption	< 250 mA @ 12 VDC
	Antenna Voltage Output	5.0 VDC

[1]Depends on multipath environment, number of satellites in view, satellite geometry and ionospheric activity.
[2] Up to 5 km baseline length.
[3] Depends also on baseline length.

Opti-Logic RS800 Laser Altimeter Specifications

Accuracy	+/- 1 m on 1x1 m^2 diffuse target with 50% reflectivity
Resolution	0.2 m
Communication Protocol	RS232-8,N,1
Baud Rate	19200
Data Raw Counts	~200 Hz
Data Calibrated Range	~10 Hz
Calibrated Range Units	Feet, Meters, Yards
Laser	Class I (eye-safe) 905 nm +/- 10 nm
Power	7-9VDC conditioned required, current draw at full power (~ 1.8 W)
Laser Wavelength	RS100 905 nm +/- 10 nm
Laser Divergence	Vertical axis – 3.5 mrad half-angle divergence; Horizontal axis – 1 mrad half-angle divergence; (Approximate beam footprint at 100 m is 35 cm x 5 cm)
Data Rate	~200 Hz raw counts for un-calibrated operation; ~10 Hz for calibrated operation (averaging algorithm seeks 8 good readings)
Dimensions	32 x 78 x 84 mm (lens face cross section is 32 x 78 mm)
Weight	< 227 g (8 oz)
Casing	RS100/RS400/RS800 units are supplied as OEM modules consisting of an open chassis containing optics and circuit boards. Custom housings can be designed and built on request.

HC-S3 Temperature and Relative Humidity Probe Specifications

Operating Temperature	-40°C to +60°C
Temperature Output Signal Range	0 to 1.0 VDC
Temperature Resolution	0.1°C or better
Relative Humidity(RH) Measurement Range	0 to 100 % non-condensing
RH Output Signal Range	0 to 1.0 VDC
RH Accuracy At 23°C	± 1.5 % RH
RH Response Time	12 to 15 secs
RH Typical Long Term Stability	Better than 1% RH per year
Probe Length	168 mm (6.6 in.)
Probe Body Diameter	15.25 mm (0.6 in.)
Housing Material	Polycarbonate
Power Consumption	< 4 mA
Supply Voltage	3.5 to 50 VDC (typically 5 VDC)
Settling Time after power is switched on	3 secs

Setra Model 276 Barometric Pressure Specifications

Pressure Ranges	600 to 1100 hPa/mb 800 to 1100 hPa/mb 0 to 20 psia
Accuracy	±0.25% FS
Output	0.1 to 5.1 VDC 0.5 to 4.5 VDC
Excitation	12 VDC (9.0 to 14.5) 24 VDC (21.6 to 26.0) 5 VDC (4.9 to 7.1)
Size	2” dia. x 1” (5 cm x 2.5 cm)

Scintrex CS-3 Magnetometer Specifications

Operating Principal	Self-oscillation split-beam Cesium Vapor (non-radioactive Cs-133)
Operating Range	15,000 to 105,000 nT
Gradient Tolerance	40,000 nT/metre
Operating Zones	10° to 85° and 95° to 170°
Hemisphere Switching	a) Automatic b) Electronic control actuated by the control voltage levels (TTL/CMOS) c) Manual
Sensitivity	0.0006 nT √Hz rms
Noise Envelope	Typically 0.002 nT P-P, 0.1 to 1 Hz bandwidth
Heading Error	+/- 0.25 nT (inside the optical axis to the field direction angle range 15° to 75° and 105° to 165°)
Absolute Accuracy	<2.5 nT throughout range
Output	a) Continuous signal at the Larmor frequency which is proportional to the magnetic field (proportionality constant 3.49857 Hz/nT) sine wave signal amplitude modulated on the power supply voltage b) Square wave signal at the I/O connector, TTL/CMOS compatible
Information Bandwidth	Only limited by the magnetometer processor used
Sensor Head	Diameter: 63 mm (2.5”) Length: 160 mm (6.3”) Weight: 1.15 kg (2.6 lb)
Sensor Electronics	Diameter: 63 mm (2.5”) Length: 350 mm (13.8”) Weight: 1.5 kg (3.3 lb)
Cable, Sensor to Sensor Electronics	3 m (9’ 8”), lengths up to 5 m (16’ 4”) available
Operating Temperature	-40°C to +50°C
Humidity	Up to 100%, splash proof
Supply Power	24 to 35 Volts DC
Supply Current	Approx. 1.5 A at start up, decreasing to 0.5 A at 20°C
Power Up Time	Less than 15 minutes at -30°C

Bartington Mag-03 three-axis fluxgate magnetic field sensor Specifications

Number of Axes	3
Bandwidth	0 to 3 kHz at 50 µT peak
Internal Noise	Basic version: >10 to 20 pTrms/√Hz at 1 Hz Standard version: 6 to ≤10 pTrms/√Hz at 1 Hz Low Noise version: <6 pTrms/√Hz at 1 Hz
Scaling error (DC)	<±0.5%
Orthogonality error	<0.1°
Alignment error (Z axis to reference face)	<0.1°
Linearity error	<0.0015%
Frequency response	0 to 1 kHz maximally flat, ±5% maximum at 1 kHz
Input voltage	±12 V to ±17 V
Supply current	+30 mA, -10 mA (+1.4 mA per 100 µT for each axis)
Power supply rejection ratio	5 µV/V (-106 dB)
Analog output	±10 V (±12 V supply) swings to within 0.5 V of supply voltage
Output impedance	10 Ω
Operating temperature range	-40°C to +70°C
Environmental protection	IP51
Dimensions (W x H x L)	32 x 32 x 152mm
Weight	160 g
Enclosure material	Reinforced epoxy
Connector	ITT Cannon DEM-9P-NMB
Mating connector	ITT Cannon DEM-9S-NMB
Mounting	2 x M5 fixing holes

Pico Envirotec GRS-10 Gamma Spectrometer Specifications

Crystal volume	16.8 litres of NaI (Tl) synthetic downward looking crystals and 4.2 litres of NaI (Tl) synthetic upward looking crystals
Resolution	256/512 channels
Tuning	Automatic using peak determination algorithm
Detector	Digital Peak
Calibration	Fully automated detector
Real Time	Linearization and gain stabilization
Communication	RS232
Detectors	Expandable to 10 detectors and digital peak
Count Rate	Up to 60,000 cps per detector
Count Capacity per channel	65545
Energy detection range:	36 KeV to 3 MeV
Cosmic channel	Above 3 MeV
Upward Shielding	RayShield® non-radioactive shielding on downward looking crystals
Downward Shielding	6 mm thick lead plate is used for downward-shielding
Spectra	Collected spectra of 256/512 channels, internal spectrum resolution 1024
Software	Calibration: High voltage adjustment, linearity correction coefficients calculation, and communication test support Real Time Data Collection: Automatic Gain real time control on natural isotopes, and PC based test and calibration software suite
Sensor	Each box containing two (2) gamma detection NaI(Tl) crystals – each 4.2 liters. (256 cu in.) (approx. 100 x 100 x 650 mm) Total volume of approx 8.4 litres or 512 cu in with detector electronics
Spectra Stabilization	Real time automatic corrections on radio nuclei: Th, Ur, K. No implanted sources

Pico Envirotec AGIS data recorder system Specifications

(for Navigation, Gamma spectrometer, and Magnetometer Data Acquisition)

Functions	Airborne Geophysical Information System (AGIS) with integrated Global Positioning System Receiver (GPS) and all necessary navigation guidance software. Inputs for geophysical sensors - portable gamma ray spectrometer GRS-10, MMS4 Magnetometer, Totem 2A EM, A/D converter, temperature probe, humidity probe, barometric pressure probe, and laser altimeter. Output for the multi-parameter PGU (Pilot Guidance Unit)
Display	Touch screen with display of 800 x 600 pixels; customized keypad and operator keyboard. Multi-screen options for real-time viewing of all data inputs, fiducial points, flight line tracking, and GPS channels by operator.
GPS Navigation	Garmin 12-channel, WAAS-enabled
Data Sampling	Sensor dependent
Data Synchronization	Synchronized to GPS position
Data File	PEI Binary data format
Storage	80 GB
Supplied Software	PEIView: Allows fast data Quality Control (QC) Data Format: Geosoft GBN and ASCII output PEIConv: For survey preparation and survey plot after data acquisition
Software	Calibration: High voltage adjustment, linearity correction coefficients calculation, and communication test support Real Time Data Collection: Automatic Gain real time control on natural isotopes and PC based test and calibration software suite
Power Requirements	24 to 32 VDC
Temperature	Operating: -10°C to +55°C; storage: -20°C to +70°C

Appendix B

Digital File Descriptions

- Magnetic database description
- Radiometric database description
- Grids
- Maps

Magnetic Database:

Abbreviations used in the GDB files listed below:

CHANNEL	UNITS	DESCRIPTION
X_WGS84	m	UTM Easting – WGS 84 Zone 8 North
Y_WGS84	m	UTM Northing – WGS 84 Zone 8 North
X_NAD83	m	UTM Easting – NAD 83 Zone 8 North
Y_NAD83	m	UTM Northing – NAD 83 Zone 8 North
Lon_deg	degree	Longitude
Lat_deg	degree	Latitude
Date	yyyy/mm/dd	Dates of the survey flight(s)
FLT		Flight Line numbers
LineNo		Line numbers
STL		Number of satellite(s)
GPSfix		GPS fix
GPStime	Hours:min:secs	GPS time (UTC)
Geos_m	m	Geoidal separation
GHead_deg	degree	Heading of the aircraft
XTE_m	m	Flight line cross distance
Galt	m	GPS height – WGS 84 Zone 8 North (ASL)
Lalt	m	Laser Altimeter readings (AGL)
DTM	m	Digital Terrain Model
Sample_Density	m	Linear distance in metres between adjacent measurement locations; sample frequency is 10 measurements per second
basemag	nT	Base station diurnal data
IGRF		International Geomagnetic Reference Field 2015
Declin	Decimal degree	Calculated declination of magnetic field
Inclin	Decimal degree	Calculated inclination of magnetic field
TMI	nT	Total Magnetic Intensity
RMI	nT	Residual Magnetic Intensity

Radiometric Database:

Abbreviations used in the GDB files:

CHANNEL	UNITS	DESCRIPTION
X_WGS84	m	UTM Easting – WGS 84 Zone 8 North
Y_WGS84	m	UTM Northing – WGS 84 Zone 8 North
X_NAD83	m	UTM Easting – NAD 83 Zone 8 North
Y_NAD83	m	UTM Northing – NAD 83 Zone 8 North
Lon_deg	degree	Longitude
Lat_deg	degree	Latitude
Date	yyyy/mm/dd	Dates of the survey flight(s)
FLT		Flight numbers
LineNo		Line numbers
STL		Number of satellite(s)
GPStime	Hours:min:secs	GPS time (UTC)
Geos_m	m	Geoidal separation
GPSFix		GPS fix
GHead_deg	degree	Heading of the aircraft
XTE_m	m	Flight line cross distance
Galt	m	GPS height – WGS 84 Zone 8 North (ASL)
Lalt	m	Laser Altimeter readings (AGL)
DTM	m	Digital Terrain Model
Sample_Density	m	Linear distance in metres between adjacent measurement locations; sample frequency is 10 measurements per second
BaroSTP_kP	KiloPascal	Barometric Altitude (Press and Temp Corrected)
Temp_degC	Degrees C	Air Temperature
Press_kP	KiloPascal	Atmospheric Pressure
COSFILT	counts/sec	Spectrometer - Filtered Cosmic
UPUFILT	counts /sec	Spectrometer - Filtered Upward Uranium
Kcor	%	Equivalent Concentration - Potassium
Thcor	ppm	Equivalent Concentration - Thorium
Ucor	ppm	Equivalent Concentration - Uranium
TCcor	µR	Equivalent Dose Rate
TCexp	µR/hour	Exposure Rate - SUM(%k, eU, eTh) * determined factors
KThratio		Spectrometer –%K/eTh ratio
KUratio		Spectrometer –%K/eU ratio
ThKratio		Spectrometer – eTh/%K ratio
UKratio		Spectrometer – eU/%K ratio
UThratio		Spectrometer – eU/eTh ratio

Grids: Dublin Gulch/VBW, NAD 83 Datum, Zone 8N

FILE NAME	DESCRIPTION
DublinGulch_VBW_DTM_37.5m.grd	Digital terrain model gridded at 37.5 m cell size
DublinGulch_VBW_TMI_37.5m.grd	Total magnetic intensity gridded at 37.5 m cell size
DublinGulch_VBW_RMI_37.5m.grd	Residual magnetic intensity gridded at 37.5 m cell size
DublinGulch_VBW_RMI_wFL_04_17_18.8m.grd	2004 and 2017 integrated Residual magnetic intensity with flight lines gridded at 18.8 m cell size
DublinGulch_VBW_CVG_37.5m.grd	Calculated vertical gradient of RMI gridded at 37.5 m cell size
DublinGulch_VBW_CVG_04_17_18.8m.grd	2004 and 2017 integrated calculated vertical gradient of RMI gridded at 18.8 m cell size
DublinGulch_VBW_CHG_37.5m.grd	Calculated horizontal gradient of RMI gridded at 37.5 m cell size
DublinGulch_VBW_RTP_37.5m.grd	Reduced to magnetic pole of RMI gridded at 37.5 m cell size
DublinGulch_VBW_1VD_37.5m.grd	First vertical derivative of RTP gridded at 37.5 m cell size
DublinGulch_VBW_Kcor_37.5m.grd	Potassium (%K) - equivalent concentration in percentage gridded at 37.5 m cell size
DublinGulch_VBW_Thcor_37.5m.grd	Thorium (eTh) – equivalent concentration gridded at 37.5 m cell size
DublinGulch_VBW_Ucor_37.5m.grd	Uranium (eU) – equivalent concentration gridded at 37.5 m cell size
DublinGulch_VBW_TCcor_37.5m.grd	Total Count (TCcor) – equivalent dose rate gridded at 37.5 m cell size
DublinGulch_VBW_TCexp_37.5m.grd	Total Count (TCexp) – exposure rate gridded at 37.5 m cell size
DublinGulch_VBW_KThratio_37.5m.grd	Potassium over thorium ratio (%K/eTh) gridded at 37.5 m cell size
DublinGulch_VBW_KUratio_37.5m.grd	Potassium over uranium ratio (%K/eU) gridded at 37.5 m cell size
DublinGulch_VBW_UThratio_37.5m.grd	Uranium over thorium ratio (eU/eTh) gridded at 37.5 m cell size
DublinGulch_VBW_ThKratio_37.5m.grd	Thorium over potassium ratio (eTh/%K) gridded at 37.5 m cell size
DublinGulch_VBW_UKratio_37.5m.grd	Uranium over potassium ratio (eU/%K) gridded at 37.5 m cell size

Grids: Clear Creek, NAD 83 Datum, Zone 8N

FILE NAME	DESCRIPTION
ClearCreekBlock_DTM_25m.grd	Digital terrain model gridded at 25 m cell size
ClearCreekBlock_TMI_25m.grd	Total magnetic intensity gridded at 25 m cell size
ClearCreekBlock_RMI_25m.grd	Residual magnetic intensity gridded at 25 m cell size
ClearCreekBlock_CVG_25m.grd	Calculated vertical gradient of RMI gridded at 25 m cell size
ClearCreekBlock_CHG_25m.grd	Calculated horizontal gradient of RMI gridded at 25 m cell size
ClearCreekBlock_RTP_25m.grd	Reduced to magnetic pole of RMI gridded at 25 m cell size
ClearCreekBlock_1VD_25m.grd	First vertical derivative of RTP gridded at 25 m cell size
ClearCreekBlock_Kcor_25m.grd	Potassium (%K) - equivalent concentration in percentage gridded at 25 m cell size
ClearCreekBlock_Thcor_25m.grd	Thorium (eTh) – equivalent concentration gridded at 25 m cell size
ClearCreekBlock_Ucor_25m.grd	Uranium (eU) – equivalent concentration gridded at 25 m cell size
ClearCreekBlock_TCcor_25m.grd	Total Count (TCcor) – equivalent dose rate gridded at 25 m cell size
ClearCreekBlock_TCexp_25m.grd	Total Count (TCexp) – exposure rate gridded at 25 m cell size
ClearCreekBlock_KThratio_25m.grd	Potassium over thorium ratio (%K/eTh) gridded at 25 m cell size
ClearCreekBlock_KUratio_25m.grd	Potassium over uranium ratio (%K/eU) gridded at 25 m cell size
ClearCreekBlock_UThratio_25m.grd	Uranium over thorium ratio (eU/eTh) gridded at 25 m cell size
ClearCreekBlock_UKratio_25m.grd	Uranium over potassium ratio (eU/%K) gridded at 25 m cell size
ClearCreekBlock_ThKratio_25m.grd	Thorium over potassium ratio (eTh/%K) gridded at 25 m cell size

Maps: Dublin Gulch/VBW, NAD 83 Datum, Zone 8N (jpegs and pdfs)

FILE NAME	DESCRIPTION
DublinGulch_VBW_ActualFlightLines	Plotted actual flown flight lines
DublinGulch_VBW_DTM_37.5m	Digital terrain model gridded at 37.5 m cell size
DublinGulch_VBW_TMI_wFL_37.5m	Total magnetic intensity with plotted actual flight gridded at 37.5 m cell size
DublinGulch_VBW_TMI_37.5m	Total magnetic intensity gridded at 37.5 m cell size
DublinGulch_VBW_RMI_37.5m	Residual magnetic intensity gridded at 37.5 m cell size
DublinGulch_VBW_CVG_37.5m	Calculated vertical gradient of RMI gridded at 37.5 m cell size
DublinGulch_VBW_CHG_37.5m	Calculated horizontal gradient of RMI gridded at 37.5 m cell size
DublinGulch_VBW_RTP_37.5m	Reduced to magnetic pole of RMI gridded at 37.5 m cell size
DublinGulch_VBW_1VD_37.5m	First vertical derivative of RTP gridded at 37.5 m cell size
DublinGulch_VBW_Kcor_37.5m	Potassium (%K) - equivalent concentration in percentage gridded at 37.5 m cell size
DublinGulch_VBW_Thcor_37.5m	Thorium (eTh) – equivalent concentration gridded at 37.5 m cell size
DublinGulch_VBW_Ucor_37.5m	Uranium (eU) – equivalent concentration gridded at 37.5 m cell size
DublinGulch_VBW_TCcor_37.5m	Total Count (TCcor) – equivalent dose rate gridded at 37.5 m cell size
DublinGulch_VBW_TCexp_37.5m	Total Count (TCexp) – exposure rate gridded at 37.5 m cell size
DublinGulch_VBW_KThratio_37.5m	Potassium over thorium ratio (%K/eTh) gridded at 37.5 m cell size
DublinGulch_VBW_KUratio_37.5m	Potassium over uranium ratio (%K/eU) gridded at 37.5 m cell size
DublinGulch_VBW_UThratio_37.5m	Uranium over thorium ratio (eU/eTh) gridded at 37.5 m cell size
DublinGulch_VBW_UKratio_37.5m	Uranium over potassium ratio (eU/%K) gridded at 37.5 m cell size
DublinGulch_VBW_ThKratio_37.5m	Thorium over potassium ratio (eTh/%K) gridded at 37.5 m cell size
DublinGulch_VBW_TernaryMap	Displaying ratios of all three elements (%K, eTh, eU)
DublinGulch_VBW_RMI_wFL_04_17_18.8m	2004 and 2017 integrated residual magnetic intensity with flight lines gridded at 18.8 m cell size
DublinGulch_VBW_CVG_04_17_18.8m	2004 and 2017 integrated calculated vertical gradient of RMI gridded at 18.8 m cell size

Maps: Clear Creek, NAD 83 Datum, Zone 8N (jpegs and pdfs)

FILE NAME	DESCRIPTION
ClearCreek_ActualFlightLines	Plotted actual flown flight lines
ClearCreek_DTM_25m	Digital terrain model gridded at 25 m cell size
ClearCreek_TMI_wFL_25m	Total magnetic intensity with plotted actual flight gridded at 25 m cell size
ClearCreek_TMI_25m	Total magnetic intensity gridded at 25 m cell size
ClearCreek_RMI_25m	Residual magnetic intensity gridded at 25 m cell size
ClearCreek_CVG_25m	Calculated vertical gradient of RMI gridded at 25 m cell size
ClearCreek_CHG_25m	Calculated horizontal gradient of RMI gridded at 25 m cell size
ClearCreek_RTP_25m	Reduced to magnetic pole of RMI gridded at 25 m cell size
ClearCreek_1VD_25m	First vertical derivative of RTP gridded at 25 m cell size
ClearCreek_Kcor_25m	Potassium (%K) - equivalent concentration in percentage gridded at 25 m cell size
ClearCreek_Thcor_25m	Thorium (eTh) – equivalent concentration gridded at 25 m cell size
ClearCreek_Ucor_25m	Uranium (eU) – equivalent concentration gridded at 25 m cell size
ClearCreek_TCcor_25m	Total Count (TCcor) – equivalent dose rate gridded at 25 m cell size
ClearCreek_TCexp_25m	Total Count (TCexp) – exposure rate gridded at 25 m cell size
ClearCreek_KThratio_25m	Potassium over thorium ratio (%K/eTh) gridded at 25 m cell size
ClearCreek_KUratio_25m	Potassium over uranium ratio (%K/eU) gridded at 25 m cell size
ClearCreek_UThratio_25m	Uranium over thorium ratio (eU/eTh) gridded at 25 m cell size
ClearCreek_UKratio_25m	Uranium over potassium ratio (eU/%K) gridded at 25 m cell size
ClearCreek_ThKratio_25m	Thorium over potassium ratio (eTh/%K) gridded at 25 m cell size
ClearCreek_TernaryMap	Displaying ratios of all three elements (%K, eTh, eU)
ClearCreek_RMI_wFL_1998_2017	1998 RMI gridded at 50 m cell size and 2017RMI gridded at 25 m cell size with flight lines
ClearCreek_Kcor_1998_2017	1998 %K gridded at 50 m cell size and 2017 %K gridded at 25 m cell size
ClearCreek_Thcor_1998_2017	1998 eTh gridded at 50 m cell size and 2017 eTh gridded at 25 m cell size
ClearCreek_Ucor_1998_2017	1998 eU gridded at 50 m cell size and 2017 eU gridded at 25 m cell size
ClearCreek_TCexp_1998_2017	1998 TCexp gridded at 50 m cell size and 2017 TCexp gridded at 25 m cell size

Appendix C

Daily Flight Log Report

Date (yyyy/mm/dd)	Survey Block	Flight number	Distance flown km	Weather/Notes
2017/06/05	Dublin Gulch/VBW	1	686	Complete compensation and heading test flights (000°/090°/180°/270°). Started the Dublin Gulch and VBW survey block.
2017/06/06	Dublin Gulch/VBW	2	1387	Weather was good.
2017/06/07	Dublin Gulch/VBW	3	1708	Weather was good.
2017/06/08	Clear Creek	1	481	Complete compensation and heading test flights (045°/135°/225°/315°). Started and completed the Clear Creek survey block. Windy at peaks of the mountain.
	Dublin Gulch/VBW	4	290	Flew the remaining tie lines and re-flew a few partial lines. Survey completed.

Plates

Dublin Gulch/VBW Survey Block Maps

- Plate 1_DG_VBW: Dublin Gulch and VBW - Actual Flight Lines (FL)
- Plate 2_DG_VBW: Dublin Gulch and VBW - Digital Terrain Model (DTM)
- Plate 3_DG_VBW: Dublin Gulch and VBW - Total Magnetic Intensity with Plotted Flight Lines (TMI_wFL)
- Plate 4_DG_VBW: Dublin Gulch and VBW - Total Magnetic Intensity (TMI)
- Plate 5_DG_VBW: Dublin Gulch and VBW - Residual Magnetic Intensity (RMI)
- Plate 6_DG_VBW: Dublin Gulch and VBW - Calculated Vertical Gradient (CVG) of RMI
- Plate 7_DG_VBW: Dublin Gulch and VBW - Calculated Horizontal Gradient (CHG) of RMI
- Plate 8_DG_VBW: Dublin Gulch and VBW - Reduced to Pole (RTP) of RMI
- Plate 9_DG_VBW: Dublin Gulch and VBW - First Vertical Derivative (1VD) of RTP
- Plate 10_DG_VBW: Dublin Gulch and VBW - Potassium – Equivalent Concentration (%K)
- Plate 11_DG_VBW: Dublin Gulch and VBW - Thorium – Equivalent Concentration (eTh)
- Plate 12_DG_VBW: Dublin Gulch and VBW - Uranium – Equivalent Concentration (eU)
- Plate 13_DG_VBW: Dublin Gulch and VBW - Total Count – Equivalent Dose Rate (TCcor)
- Plate 14_DG_VBW: Dublin Gulch and VBW - Total Count – Exposure Rate (TCexp)
- Plate 15_DG_VBW: Dublin Gulch and VBW - Potassium over Thorium Ratio (%K/eTh)
- Plate 16_DG_VBW: Dublin Gulch and VBW - Potassium over Uranium Ratio (%K/eU)
- Plate 17_DG_VBW: Dublin Gulch and VBW - Uranium over Thorium Ratio (eU/eTh)
- Plate 18_DG_VBW: Dublin Gulch and VBW - Uranium over Potassium Ratio (eU/%K)
- Plate 19_DG_VBW: Dublin Gulch and VBW - Thorium over Potassium Ratio (eTh/%K)
- Plate 20_DG_VBW: Dublin Gulch and VBW - Ternary Map (TM)
- Plate 21_DG_VBW: Dublin Gulch and VBW – 2004 and 2017 Residual Magnetic Intensity with Flight Lines (RMI_wFL_04_17)
- Plate 22_DG_VBW: Dublin Gulch and VBW – 2004 and 2017 Calculated Vertical Gradient (CVG_04_17)

Plates

Clear Creek Survey Block Maps

- Plate 1_CC: Clear Creek - Actual Flight Lines (FL)
- Plate 2_CC: Clear Creek - Digital Terrain Model (DTM)
- Plate 3_CC: Clear Creek - Total Magnetic Intensity with Plotted Flight Lines (TMI_wFL)
- Plate 4_CC: Clear Creek - Total Magnetic Intensity (TMI)
- Plate 5_CC: Clear Creek - Residual Magnetic Intensity (RMI)
- Plate 6_CC: Clear Creek - Calculated Vertical Gradient (CVG) of RMI
- Plate 7_CC: Clear Creek - Calculated Horizontal Gradient (CHG) of RMI
- Plate 8_CC: Clear Creek - Reduced to Pole (RTP) of RMI
- Plate 9_CC: Clear Creek - First Vertical Derivative (1VD) of RTP
- Plate 10_CC: Clear Creek - Potassium – Equivalent Concentration (%K)
- Plate 11_CC: Clear Creek - Thorium – Equivalent Concentration (eTh)
- Plate 12_CC: Clear Creek - Uranium – Equivalent Concentration (eU)
- Plate 13_CC: Clear Creek - Total Count – Equivalent Dose Rate (TCcor)
- Plate 14_CC: Clear Creek - Total Count – Exposure Rate (TCexp)
- Plate 15_CC: Clear Creek - Potassium over Thorium Ratio (%K/eTh)
- Plate 16_CC: Clear Creek - Potassium over Uranium Ratio (%K/eU)
- Plate 17_CC: Clear Creek - Uranium over Thorium Ratio (eU/eTh)
- Plate 18_CC: Clear Creek - Uranium over Potassium Ratio (eU/%K)
- Plate 19_CC: Clear Creek - Thorium over Potassium Ratio (eTh/%K)
- Plate 20_CC: Clear Creek - Ternary Map (TM)
- Plate 21_CC: Clear Creek – 1998 and 2017 Residual Magnetic Intensity with Flight Lines (RMI_wFL_98_17)
- Plate 22_CC: Clear Creek – 1998 and 2017 Residual Magnetic Intensity (%K_98_17)
- Plate 23_CC: Clear Creek - 1998 and 2017 Residual Magnetic Intensity (eTh_98_17)
- Plate 24_CC: Clear Creek - 1998 and 2017 Residual Magnetic Intensity (eU_98_17)
- Plate 25_CC: Clear Creek - 1998 and 2017 Residual Magnetic Intensity (TCexp_98_17)

APPENDIX 3

RAVEN PETROGRAPHIC ANALYSIS - ULTRA PETROGRAPHY & GEOSCIENCE INC.

Ultra Petrography & Geoscience Inc.

Report for: Victoria Gold Corp.

Sent to: Mrs. Helena Kuikka

Petrographic Report on 9 polished thin sections from the exploration target "Raven" for Victoria Gold Corp.

DRAFT

Petrographic Report UPG210302

Effective Date: March 8, 2021

Prepared by: Fabrizio Colombo, Ph.D., P.Geo.

+1 778-855-3196 f.colombo@ultrapetrography.com www.ultrapetrography.com

Table of Contents

Conditions and Disclaimer

This report is issued subject to the following conditions:
This report has been prepared on the basis of information, as described in section 1 below. Other than as specifically noted in this report, Ultra Petrography and Geoscience Inc. has not conducted any work to verify the source, accuracy or completeness of the information provided, and is not responsible for any shortcomings in these regards.
Discussions, conclusions and/or summaries are presented to assist the reader in highlighting key points; however, they cannot be interpreted in isolation and must be considered with reference to and in the context of the body of the report.
Any reports, maps, graphs, logs or other information of a geological nature or otherwise, generated by Ultra Petrography and Geoscience Inc. and contained in this report or submitted separately, may be used for general information purposes, public disclosure, press releases, regulatory requirements, share exchange, financing and so forth by the Client to whom the information is addressed, provided any quotations, excerpts and references from the report are made in such a manner that their meaning and intent are not materially changed from the meaning and intent as contained in the report.
Ultra Petrography and Geoscience Inc. will not be held liable for loss or damages resulting from work undertaken or reported in terms of this assignment, or decisions taken based on such work and/or reporting.

1. Introduction

Mrs. Helena Kuikka of Victoria Gold Corp. submitted 9 polished thin sections to me for petrographic analysis. The client indicated that the samples were gathered from the exploration target "Raven", and provided ICP-MS analysis for some of the samples submitted for petrographic analysis.

The attached "Petrographic Descriptions" section provides the following for each sample:

1. The petrographic rock classification according to the British Geological Survey Classification Scheme (Gillespie and Styles, 1999; Gillespie et al., 2011; Hallsworth and Knox, 1999; Robertson, 1999). Upon request, I can follow the client's preferred classification scheme and database coding system.
2. A brief microstructural description linking the feature visible mesoscopically and on the stained offcut of the thin section (a 20x40 image of the offcut is included in the report) and the features detected under the microscope.
3. A table with the modal percentage and average grain size for each mineral;
4. A detailed description of the minerals in decreasing order of abundance.
5. Photomicrographs describing the most relevant microstructures and mineral intergrowths observed and described in points 1 and 4. The photomicrographs are in .tiff format, and the native copy of the high-resolution images included in the report are also provided separately.

The petrographic classification follows the recommendations of Gillespie et al. (2011), Gillespie and Styles (1999), and Robertson (1999).

The microstructural terminology used in this report follows the recommendations and definitions of Vernon (2004), Passchier and Trouw (2005), and Ramdohr (1980).

2. Summary of Results

Sample 1: 41676061—Galena-carbonate filling domain—This section is made up of abundant and massive galena, rare sphalerite, very rare pyrite, and an irregularly shaped domain of medium-grained carbonate.

Alteration: iron oxides/limonitic material: weak in the carbonate-rich domain

Sample 2: 2015738—Arsenopyrite-quartz-pyrite filling domain—Three domains can be distinguished in this sulphide-rich section. In the lower part, fractured arsenopyrite is associated with interstitial quartz. Quartz filled in an irregular and up to 5 mm thick monomineralic domain and in the upper part, fine-grained arsenopyrite, pyrite, and interstitial quartz and carbonate define a heterogeneous sub-domain.

Sample 3: 2015702—Arsenopyrite-pyrite-quartz-carbonate filling domain—Fractured domains of arsenopyrite and pyrite are filled in by inequigranular and xenomorphic crystals of quartz. Sphalerite is concentrated along the boundaries between the arsenopyrite-pyrite- and the quartz-rich domains.

Sample 4: 2057037—Quartz-arsenopyrite-pyrite-epidote filling domain—Inequigranular and xenomorphic crystals of quartz host heterogeneously dispersed and fractured crystals of arsenopyrite and pyrite. Interstitial aggregates of epidote occur in some of the interstitial positions between the quartz and the sulphides.

Sample 5: 2015702—Quartz-white mica-pyrite alteration zone & Carbonate veins—Xenomorphic crystals of quartz are associated with irregularly shaped replacement patches and pseudomorphic aggregates of white mica. The strongly altered rock is crosscut by irregular veins and veinlets of carbonate and hosts fine- to medium-grained pyrite and arsenopyrite crystals.

Alteration: quartz(?)-white mica: moderate to strong; pyrite: weak; carbonate-arsenopyrite-rutile: subtle

Sample 6: 2057035—Brecciated quartz-carbonate-arsenopyrite filling domain—This heterogeneous section is made up of inequigranular and xenomorphic crystals of quartz, filling domains of carbonate and irregularly shaped clusters of fine-grained idioblastic crystals of arsenopyrite and rare amoeboid crystals of galena.

Alteration: iron oxides/limonite: moderate; white mica: weak

Sample 7: 2015824—Arsenopyrite-quartz-carbonate filling domain—Abundant and fractured arsenopyrite is filled in by medium- to coarse-grained crystals of quartz and carbonate and subordinate chalcopyrite. Subhedral crystals of pyrite are dispersed within the arsenopyrite-rich filling domain.

Sample 8: 2015704—White mica-quartz alteration zone (altered granitoid?)—Irregularly shaped to subidiomorphic pseudomorphs of very fine- to fine-grained flakes of white mica are associated with monomineralic and polycrystalline domains of

quartz in the host rock, which is crosscut by a 15 mm thick arsenopyrite-carbonate vein.

Alteration: white mica: strong after feldspar; quartz(?): moderate to strong

Sample 9: 2015734—Deformed quartz-white mica-arsenopyrite filling domain—A strongly deformed domain of quartz hosts sparse alteromorphs of very fine-grained white mica and clusters of fractured crystals of arsenopyrite and subordinate pyrite.

Alteration: white mica: strong after feldspar

Based on the microscopic analysis, the petrogenetic sequence drafted in Figure 1 is interpreted.

Figure 1: The paragenetic sequence interpreted from the microstructures observed in the 9 samples described in this report.

	Magmatic	*Alteration*	*Infill Stage & Brittle Deformation*	*Oxidation*	*Comments*
quartz	———				
plagioclase	———				
[biotite?]	———				
arsenopyrite		———	———		
galena			—		
pyrite		——	——		
sphalerite			—		
chalcopyrite			—		
tetrahedrite/tennantite			—		Observed in one PTS (Sample 7) only
quartz		———	———		
carbonate			———		
white mica		———	———		
epidote			—		Observed in one PTS (Sample 4) only
rutile		——			Observed in one PTS (Sample 5) only
iron oxides/limonitic material				———	

Time →

Table 1: List of samples with their magnetic susceptibility and petrographic classification following the recommendations of Gillespie et al. (2011), Gillespie and Styles (1999), and Robertson (1999).

Sample No.	Sample ID	Rock Type	Alteration
1	41676061	Galena-carbonate filling domain	iron oxides/limonitic material: weak in the carbonate-rich domain
2	2015738	Arsenopyrite-quartz-pyrite filling domain	
3	2015702	Arsenopyrite-pyrite-quartz-carbonate filling domain	
4	2057037	Quartz-arsenopyrite-pyrite-epidote filling domain	
5	2015702	Quartz-white mica-pyrite alteration zone & Carbonate veins	quartz(?)-white mica: moderate to strong; pyrite: weak; carbonate-arsenopyrite-rutile: subtle
6	2057035	Brecciated quartz-carbonate-arsenopyrite filling domain	iron oxides/limonite: moderate; white mica: weak
7	2015824	Arsenopyrite-quartz-carbonate filling domain	
8	2015704	White mica-quartz alteration zone (altered granitoid?)	white mica: strong after feldspar; quartz(?): moderate to strong
9	2015734	Deformed quartz-white mica-arsenopyrite filling domain	white mica: strong after feldspar

3. Bibliography

Deer WA, Howie RA, Zussmann J (1992) An introduction to the rock-forming minerals. Longman, London

Gifkins C, Herrmann W, Large R (2005) Altered volcanic rocks, A guide to description and interpretation, Centre for Ore Deposits Research University of Tasmania, Australia

Gillespie MR, Barnes RP, Milodowski A (2011) British Geological Survey scheme for classifying discontinuities and fillings. In: British Geological Survey research report RR/10/05. http://www.bgs.ac.uk/downloads/start.cfm?id=1982. Accessed March 2021

Gillespie MR, Styles MT (1999) Classification of igneous rocks. British Geological Survey research report RR 99/06 (2nd edn), vol 1. http://www.bgs.ac.uk/downloads/start.cfm?id=7. Accessed March 2021

Passchier CW, Trouw RAJ (2005) Microtectonics (2nd edn). Springer, Heidelberg

Ramdohr P (1980) The ore minerals and their intergrowths (2nd edn), vol 1/2. Pergamon Press, Oxford

Tröger WE (1979) Optical determination of rock-forming minerals, part 1: determinative tables. Schweizerbart Science Publishers, Stuttgart

Vernon RH (2004) A practical guide to rock microstructure. Cambridge University Press, Cambridge

pyrite crystals are up to 0.2 mm across, are fractured, and are weakly altered by iron oxides' rims.

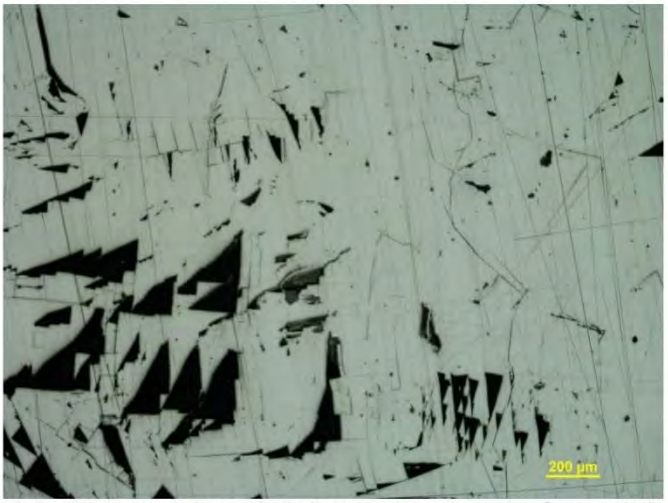

Photomicrograph 1a: Triangular poke marks in the massive aggregate of galena indicate the cubic symmetry of the mineral. Plane-polarized reflected light.

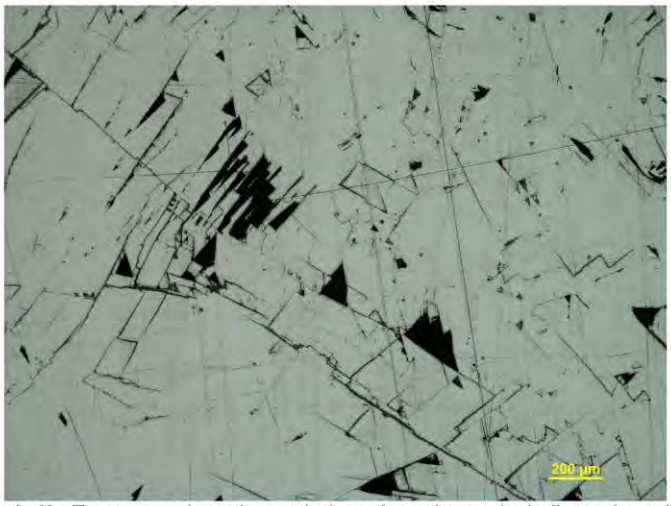

Photomicrograph 1b: Fractures orientation and triangular poke marks indicate the cubic symmetry of the massive galena. Plane-polarized reflected light.

Photomicrograph 1c: Medium-grained crystals of carbonate are intergrown with subordinate dispersions of partially oxidized pyrite and limonitic material. The carbonate domain shows an irregular boundary at the contact with the massive galena (in the lower part of this photomicrograph Plane-polarized transmitted light.

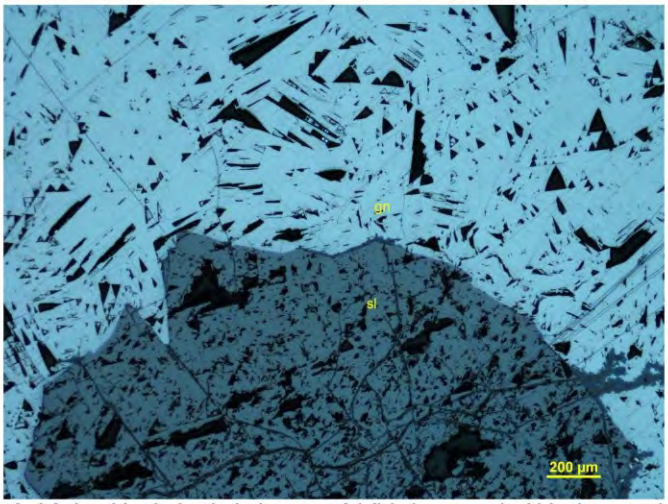

Photomicrograph 1d: A subhedral sphalerite crystal (sl) is immersed within the massive galena (gn). Plane-polarized reflected light.

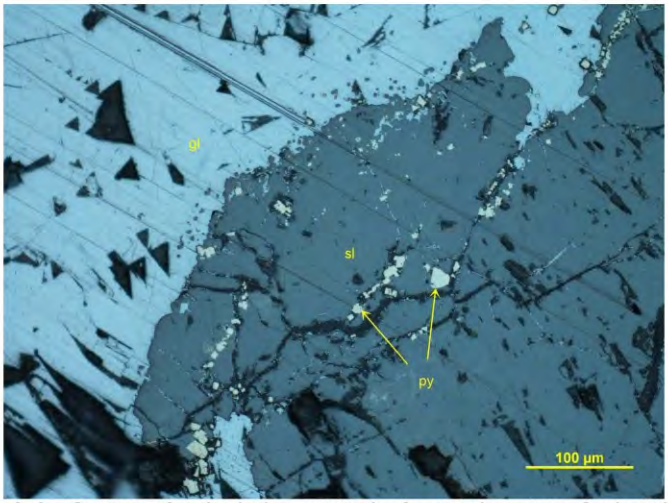

Photomicrograph 1e: Crystals of pyrite (py) populate the fractured crystals of sphalerite (sl) near the boundary with the hosting galena (gn). Plane-polarized reflected light.

Sample 2: 2015738

Arsenopyrite-quartz-pyrite filling domain

Three domains can be distinguished in this sulphide-rich section. In the lower part, fractured arsenopyrite is associated with interstitial quartz. Quartz filled in an irregular and up to 5 mm thick monomineralic domain and in the upper part, fine-grained arsenopyrite, pyrite, and interstitial quartz and carbonate define a heterogeneous sub-domain.

Mineral	*Alteration and Weathering Mineral*	*Modal %*	*Size Range (mm)*
arsenopyrite		60–62	0.1 to massive
quartz		22–24	up to 1.5 long
pyrite		15–17	up to 2.5
carbonate		1–2	up to 0.5

Arsenopyrite is concentrated in the lower part of the section as fine- to medium-grained crystals, which in some areas form massive and fractured aggregates. Subhedral to euhedral crystals of arsenopyrite are associated and intergrown with subordinate pyrite in the upper part of the section. In some cases, the arsenopyrite crystals are fractured, and the fractures are filled in by quartz and carbonate. The arsenopyrite is distinguished by its white colour and anisotropy from the creamy-white and isotropic pyrite (Photomicrograph 2a).

Quartz is concentrated within an irregular and up to 5 mm thick domain, which crosscut the sulphide-rich section (Photomicrograph 2c). In this domain, the quartz crystals are inequigranular (0.02–1.5 mm long) and xenomorphic. The quartz hosts abundant fluid inclusions, and in this domain, most of the crystals show a moderate to strong undulose extinction. Fine-grained interstitial crystals occupy the triangular microstructures and the interstices between the sulphide crystals in the arsenopyrite-rich and the arsenopyrite-pyrite-quartz-carbonate domain.

Pyrite forms inequigranular (up to 2.5 mm across) anhedral to subhedral crystals dispersed within the arsenopyrite-pyrite-quartz-carbonate domain. Medium-grained crystals of pyrite (Photomicrograph 2a) are concentrated along the boundary between the arsenopyrite-pyrite-quartz-carbonate domain and the quartz-rich filling domain. The pyrite crystals are fractured, and the fractures are filled in by arsenopyrite, quartz and subordinate carbonate (Photomicrograph 2b).

Carbonate is subordinate to the quartz in the arsenopyrite-pyrite-quartz-carbonate domain. The absence of a billet on which I can carry on the acid test does not allow me to distinguish

the carbonate.

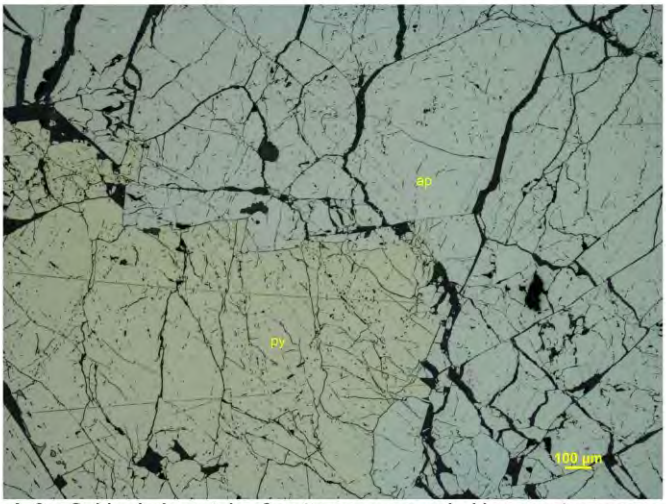

Photomicrograph 2a: Subhedral crystals of pyrite are surrounded by massive arsenopyrite, which in some cases filled in the pyrite's fractures. Plane-polarized reflected light.

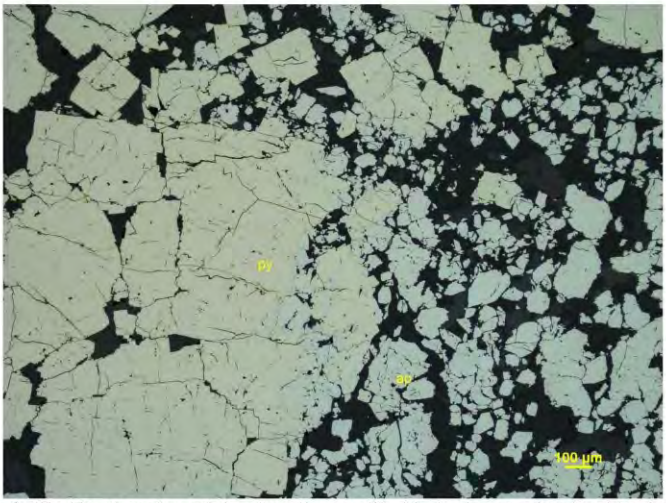

Photomicrograph 2b: Fractured crystals of pyrite are filled in by fine-grained subhedral crystals of arsenopyrite (ap), quartz and carbonate (both non-reflectant). Plane-polarized reflected light.

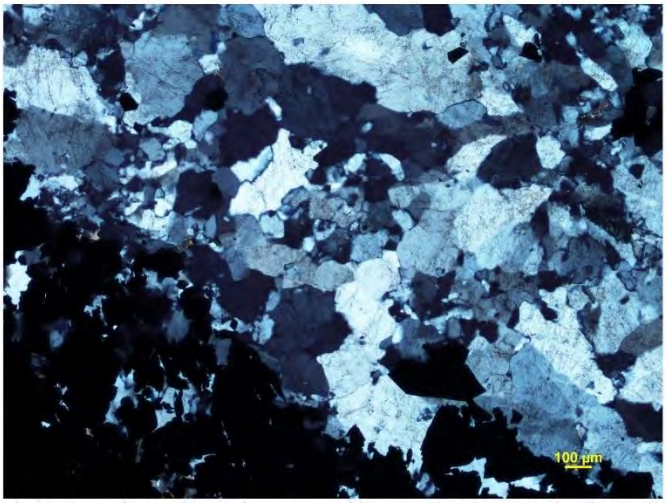

Photomicrograph 2c: Inequigranular and xenomorphic crystals of quartz dominate the composition of the quartz-rich filling domain. Crossed polarizers transmitted light.

Sample 3: 2015702

Arsenopyrite-pyrite-quartz-carbonate filling domain

Fractured domains of arsenopyrite and pyrite are filled in by inequigranular and xenomorphic crystals of quartz. Sphalerite is concentrated along the boundaries between the arsenopyrite-pyrite- and the quartz-rich domains.

Mineral	*Alteration and Weathering Mineral*	*Modal %*	*Size Range (mm)*
arsenopyrite		35–37	0.05 to massive
pyrite		25–27	up to 5
quartz		20–22	up to 2
carbonate		10–12	up to 5
sphalerite		8–10	up to 10 long
galena		tr	up to 0.1

Arsenopyrite occurs as fine- to medium-grained subhedral crystals, which in some cases coalesce to form a massive and fractured aggregate (Photomicrograph3a and 3c). Within the arsenopyrite, subidiomorphic to xenomorphic crystals of pyrite are heterogeneously dispersed.

Pyrite is heterogeneously dispersed within the arsenopyrite as fine- to medium-grained crystals up to 5 mm long. The pyrite is fractured and probably slightly pre-dated the crystallization of the arsenopyrite.

Quartz forms irregular domains of inequigranular (up to 7.5 mm long) and xenomorphic crystals, showing a moderate to strong undulose extinction. Similar to the quartz in Sample 2, the quartz crystals in this section host abundant and very fine-grained fluid inclusions and host sparse crystals (up to 7 mm across) of carbonate. Because of the tendency of the quartz to differentiate from the sulphide-rich domains, I interpret the quartz as having slightly post-dated the crystallization of most of the sulphides; however, fine-grained euhedral crystals of arsenopyrite are heterogeneously dispersed within the quartz.

Carbonate occurs as xenomorphic and inequigranular crystals (up to 5 mm across), which are spatially associated with the quartz, and like the quartz, show a strong undulose extinction.

Similar to the quartz, the **sphalerite**, which tends to form xenomorphic crystals (up to 10 mm long) between the sulphide-rich and the quartz-rich domains, can be considered as coeval

with the quartz and post-dating the arsenopyrite and pyrite. Most of the sphalerite crystals show subhedral growth zoning (Photomicrograph 3b).

Rare interstitial crystals of **galena**, filled in irregular fractures crosscutting the arsenopyrite and the pyrite, and forms clusters of fine-grained amoeboid crystals in the pyrite and arsenopyrite.

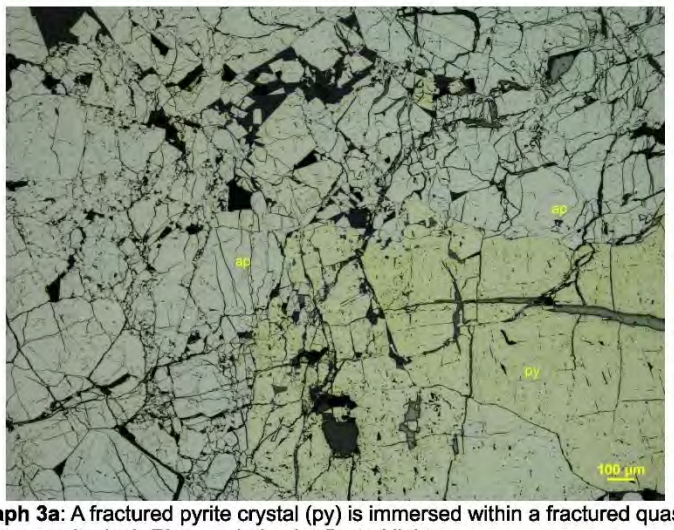

Photomicrograph 3a: A fractured pyrite crystal (py) is immersed within a fractured quasi-massive aggregate of arsenopyrite (ap). Plane-polarized reflected light.

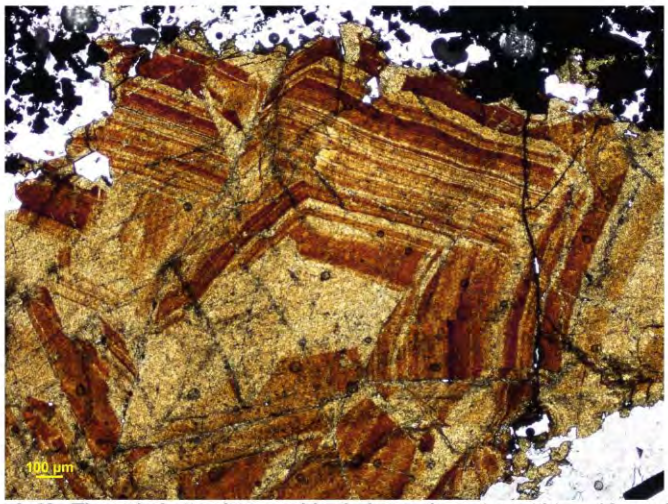

Photomicrograph 3b: The sphalerite shows subhedral growth zoning within a 10 mm long crystal. Plane-polarized transmitted light.

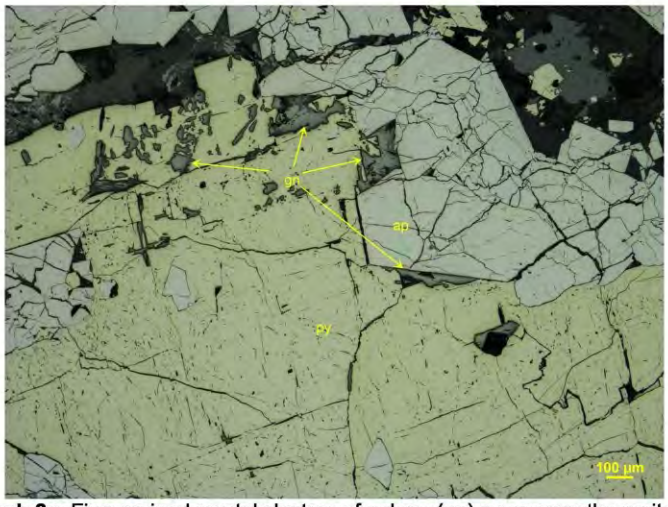

Photomicrograph 3c: Fine-grained crystal clusters of galena (gn) occur near the pyrite-arsenopyrite crystal boundary. Plane-polarized reflected light.

Sample 4: 2057037

Quartz-arsenopyrite-pyrite-epidote filling domain

Inequigranular and xenomorphic crystals of quartz host heterogeneously dispersed and fractured crystals of arsenopyrite and pyrite. Interstitial aggregates of epidote occur in some of the interstitial positions between the quartz and the sulphides.

Mineral	*Alteration and Weathering Mineral*	*Modal %*	*Size Range (mm)*
quartz		40–42	up to 3.5 long
arsenopyrite		35–37	0.02 to massive
pyrite		14–16	up to 5
epidote		8–9	up to 0.2
chalcopyrite		tr	up to 0.4 long

Quartz prevails over the sulphides as inequigranular (up to 3.5 mm long) xenomorphic crystals, which in most cases show moderate to strong undulose extinction, and in some cases, are fractured and developed sub-grain boundaries.

Arsenopyrite is the most abundant among the sulphides and occurs as subidiomorphic to massive and strongly fractured crystals (Photomicrograph 4a). The arsenopyrite is subtly oxidized along some of the fractures.

Pyrite is subordinate to the arsenopyrite and forms subidiomorphic to xenomorphic crystals intergrown with the arsenopyrite (photomicrograph 4a). Like the arsenopyrite, the pyrite is fractured, and some of the fractures are filled in by iron oxides and rare chalcopyrite.

Chalcopyrite is the least abundant among the sulphides and forms xenomorphic crystals dispersed within the quartz and arsenopyrite aggregates.

Epidote forms very fine-grained replacement patches and fine-grained radial aggregates occupying the interstices between the sulphides and the quartz (Photomicrograph 4c).

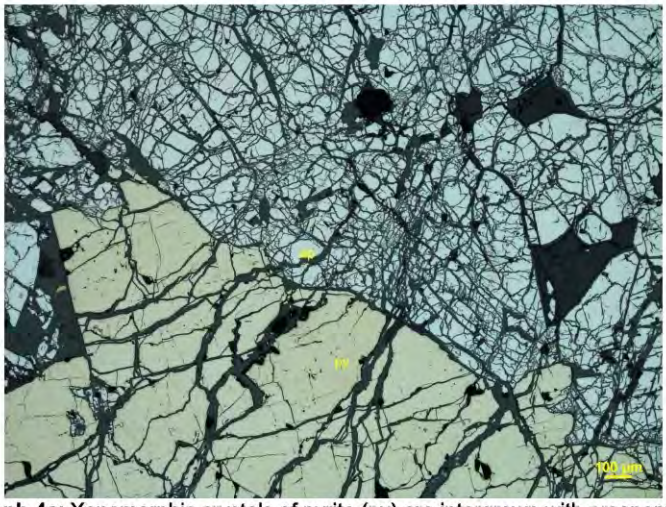

Photomicrograph 4a: Xenomorphic crystals of pyrite (py) are intergrown with arsenopyrite (ap). The arsenopyrite and the pyrite are strongly fractured. Plane-polarized reflected light.

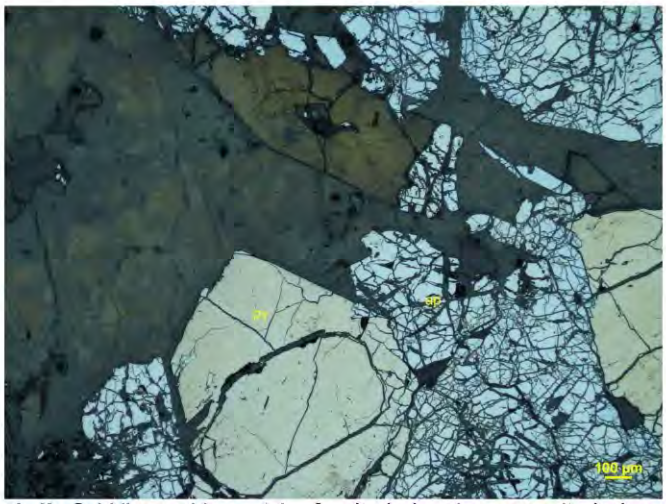

Photomicrograph 4b: Subidiomorphic crystals of pyrite (py) and arsenopyrite (ap) are intergrown with interstitial epidote and quartz (both non-reflectant, see Photomicrograph 4c for details). Plane-polarized reflected light.

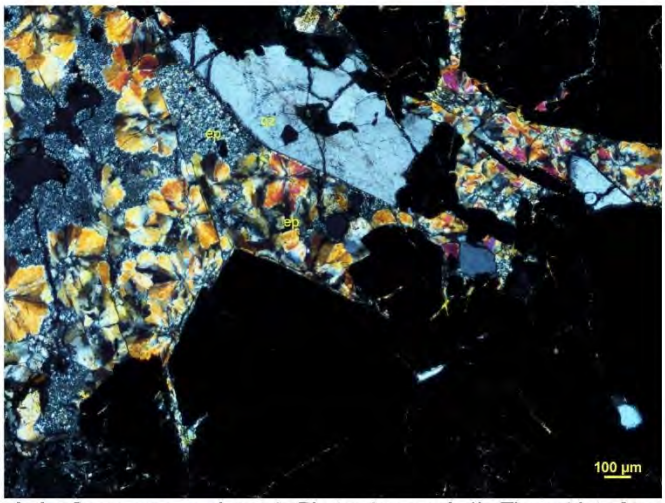

Photomicrograph 4c: Same area as shown in Photomicrograph 4b. The epidote forms very fine-grained crystals and fine-grained radial aggregates filling in the interstices between the quartz and the sulphides (opaque). Crossed polarizers transmitted light.

Sample 5: 2015702

Quartz-white mica-pyrite alteration zone

Carbonate veins

Xenomorphic crystals of quartz are associated with irregularly shaped replacement patches and pseudomorphic aggregates of white mica. The strongly altered rock is crosscut by irregular veins and veinlets of carbonate and hosts fine- to medium-grained pyrite and arsenopyrite crystals.

Alteration: quartz(?)-white mica: moderate to strong; **pyrite**: weak; **carbonate-arsenopyrite-rutile**: subtle

Mineral	*Alteration and Weathering Mineral*	*Modal %*	*Size Range (mm)*
alteration zone (~92% of PTS)			
quartz(?)	quartz	45–47	up to 3
[?]	white mica	38–40	up to 0.2
	pyrite	7–9	up to 1.2
	arsenopyrite	0.2–0.3	up to 0.4
	carbonate	tr	up to 0.1
	rutile	tr	up to 0.02
carbonate veins (~8% of PTS)			
carbonate		8	0.1 to massive
quartz		tr	up to 0.2

Quartz occurs as inequigranular xenomorphic to interlobate crystals, which tend to form monomineralic or quartz-rich domains. The interlobate crystals are strongly deformed and show a moderate to strong undulose extinction. It is hard to determine if the quartz recrystallized the quartz in a granular microstructure (i.e., a granitoid) or it is crystallized during a quartz-rich filling episode.

White mica is very fine- to fine-grained, and it forms irregularly shaped replacement patches intergrown with the quartz. In some cases, the white mica is concentrated within xenomorphic shapes, which I tentatively interpret as pseudomorphs after probable feldspar.

Carbonate crosscut the strongly altered section as irregular and up to 1.5 mm thick veins. The absence of the section offcut does not allow me to test with the HCl and determine if the carbonate is

calcite or dolomite/ankerite.

Pyrite is heterogeneously dispersed within the quartz-white mica, and it forms xenomorphic to idiomorphic crystals up to 1.2 mm across. Most of the pyrite crystals are fractured.

The **arsenopyrite** is subordinate to the pyrite, and it is dispersed as idiomorphic crystals up to 0.4 mm across (Photomicrograph 5b).

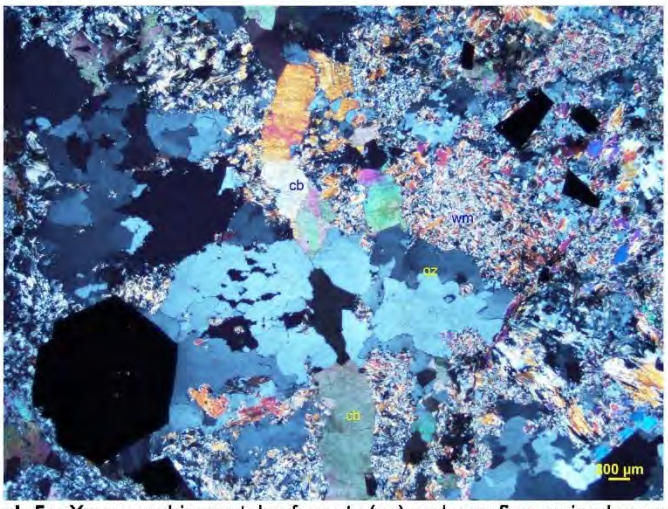

Photomicrograph 5a: Xenomorphic crystals of quartz (qz) and very fine-grained aggregates of white mica (wm) are crosscut by irregular carbonate veins (cb) and host sulphide minerals (opaque, see Photomicrograph 5b for details). Crossed polarizers transmitted light.

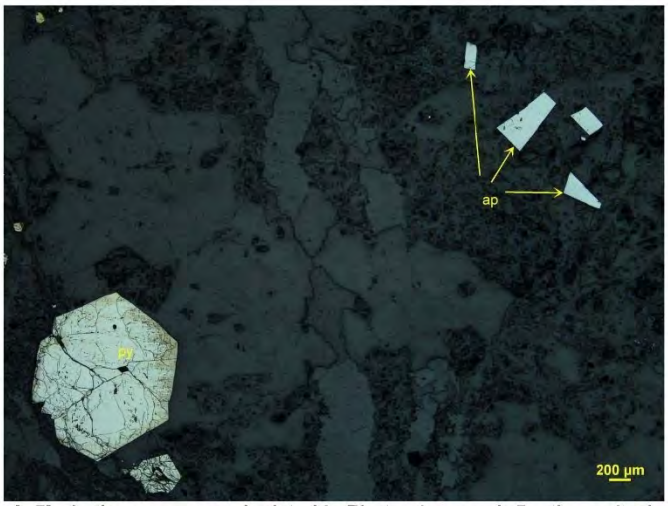

Photomicrograph 5b: In the same area depicted in Photomicrograph 5a, the pyrite (py) is idiomorphic, fractured, and shows a pale yellow colour. The arsenopyrite is idiomorphic, and it is white (ap). Plane-polarized reflected light.

Sample 6: 2057035

Brecciated quartz-carbonate-arsenopyrite filling domain

This heterogeneous section is made up of inequigranular and xenomorphic crystals of quartz, filling domains of carbonate and irregularly shaped clusters of fine-grained idioblastic crystals of arsenopyrite and rare amoeboid crystals of galena.

Alteration: iron oxides/limonite: moderate; **white mica**: weak

Mineral	*Alteration and Weathering Mineral*	*Modal %*	*Size Range (mm)*
quartz		50–52	up to 2.5 long
carbonate		30–27	up to 2.5
	iron oxide/limonite	10–12	<0.01
arsenopyrite		6–7	0.05–1.5 long
sphalerite		1.5–2.5	up to 1.8 long
	white mica	1–2	up to 0.05
galena		0.1–0.2	up to 2

Quartz tends to form fine- to medium-grained monomineralic aggregate, which I interpret as irregular filling domains, and very fine- to fine-grained domains, in which the fine-grained sub-prismatic crystals are randomly oriented within a very fine-grained and heterogeneous and unresolved aggregate of probable epidote, clay(?) and limonitic material.

Carbonate filled in the fractures of this section as fine- to medium-grained xenomorphic crystals showing a high relief and extreme birefringence. Most of the crystals of carbonate are fractured or show a strong undulose extinction. I tentatively interpret the fractured crystals of carbonate and the deformed medium-grained crystals of quartz as a deformed and brecciated filling domain.

Arsenopyrite occurs as fine-grained idiomorphic crystals concentrated within irregularly shaped clusters (Photomicrograph 6b) dispersed within the quartz-carbonate domains.

Sphalerite forms medium-grained xenomorphic crystals, which are spatially associated with the arsenopyrite clusters within the quartz-carbonate domains.

Very fine-grained flakes of **white mica** are heterogeneously dispersed within the quartz-rich domains.

Galena forms rare medium-grained (up to 2 mm across) amoeboid crystals dispersed within the quartz-carbonate domain.

Iron oxides and **limonitic material** are heterogeneously dispersed within this heterogeneous rock. Limonitic material filled in the carbonate's cleavage systems, and in some cases, define fine-grained boxwork microstructures.

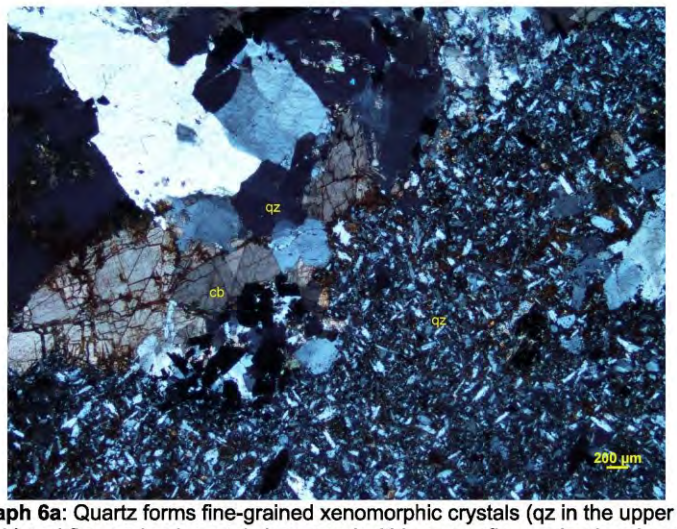

Photomicrograph 6a: Quartz forms fine-grained xenomorphic crystals (qz in the upper left of this photomicrograph) and fine-grained crystals immersed within a very fine-grained and unresolved matrix (qz in the right), and it is associated with medium-grained crystals of carbonate (cb) and dispersed sulphides (opaque). Crossed polarizers transmitted light.

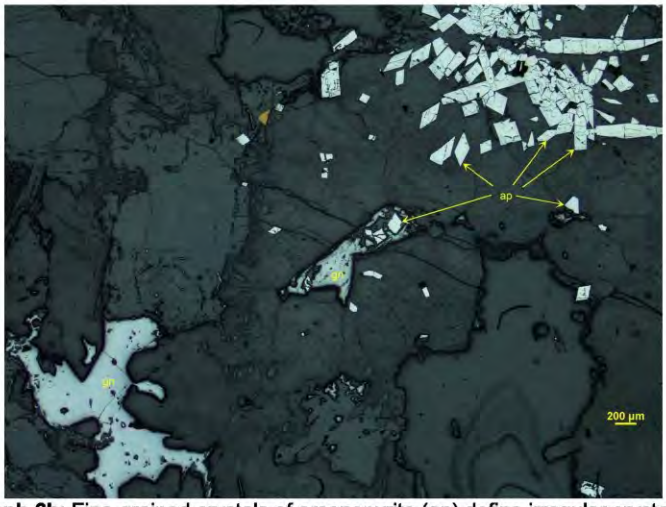

Photomicrograph 6b: Fine-grained crystals of arsenopyrite (ap) define irregular crystal clusters. The galena (gn) occurs as rare amoeboid crystals. Plane-polarized reflected light.

Sample 7: 2015824

Arsenopyrite-quartz-carbonate filling domain

Abundant and fractured arsenopyrite is filled in by medium- to coarse-grained crystals of quartz and carbonate and subordinate chalcopyrite. Subhedral crystals of pyrite are dispersed within the arsenopyrite-rich filling domain.

Mineral	*Alteration and Weathering Mineral*	*Modal %*	*Size Range (mm)*
arsenopyrite		80–82	0.05 to massive
quartz		10–12	up to 4.5 long
carbonate		5–7	up to 3
pyrite		3–4	up to 3
chalcopyrite		0.2–0.5	up to 0.5
galena		0.1–0.15	up to 1 long
tetrahedrite/tennantite		0.05–0.1	up to 0.5

Arsenopyrite forms fine-grained to massive aggregates, which are fractured and filled in by quartz, carbonate, chalcopyrite and pyrrhotite. The arsenopyrite is distinguished by its weak anisotropy and white colour under plane-polarized reflected light. I interpret the arsenopyrite as having post-dated the crystallization of the subidiomorphic crystals of pyrite (Photomicrograph 7a) and pre-dated the precipitation of the subordinate chalcopyrite and pyrrhotite.

Quartz forms medium- to coarse-grained interstitial crystals up to 4.5 mm long. The quartz crystals show moderate to strong undulose extinction within the interstitial positions defined by the arsenopyrite and the pyrite; therefore, I interpret the quartz and the carbonate as having crystallized during and immediately after the brittle deformation event that fractured the arsenopyrite, and to a lesser extent the pyrite.

Carbonate occupies the same microstructural position as the quartz, and the medium-to coarse-grained crystals are up to 3 mm long. Like the quartz, the carbonate was strained during the deformation and show moderate undulose extinction.

Pyrite is heterogeneously dispersed within the arsenopyrite-rich aggregate as medium- to coarse-grained (up to 3 mm across) subidiomorphic crystals. Some of the crystals are fractured and filled in by fine-grained crystals of arsenopyrite. This is the clue that the pyrite slightly pre-dated the crystallization of the arsenopyrite.

Chalcopyrite is subordinate to the arsenopyrite and the pyrite and mostly filled in the fractured crystals of arsenopyrite. The intergrowths with the less abundant tetrahedrite/tennantite (Photomicrograph 7b and 7c) suggest that the chalcopyrite and the tetrahedrite/tennantite precipitated together during the brittle deformation event.

Galena forms rare xenomorphic crystals, which preferentially precipitated along the boundary between the quartz and the fractured crystals of arsenopyrite, and within the fractures crosscutting the arsenopyrite (Photomicrograph 7d).

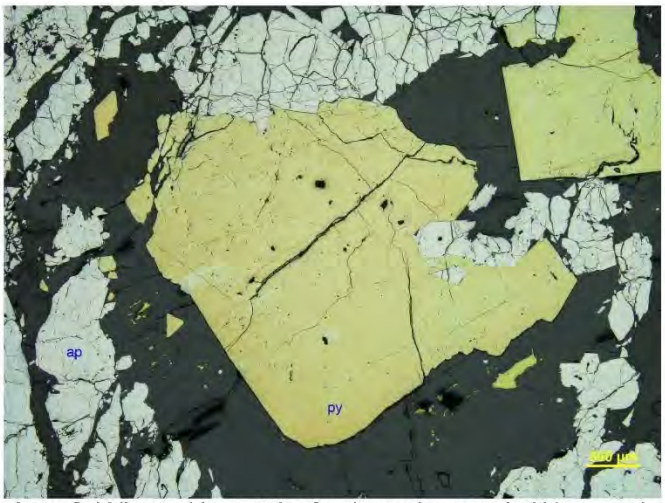

Photomicrograph 7a: Subidiomorphic crystals of pyrite are immersed within a quasi-massive aggregate of arsenopyrite (ap) and quartz (non-reflectant). Plane-polarized reflected light.

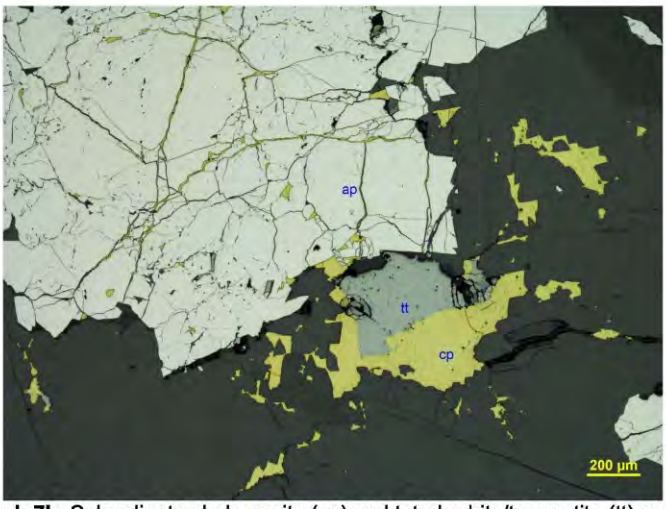

Photomicrograph 7b: Subordinate chalcopyrite (cp) and tetrahedrite/tennantite (tt) precipitated at the boundary between the arsenopyrite and the quartz. The chalcopyrite filled in the fractures within the arsenopyrite. Plane-polarized reflected light.

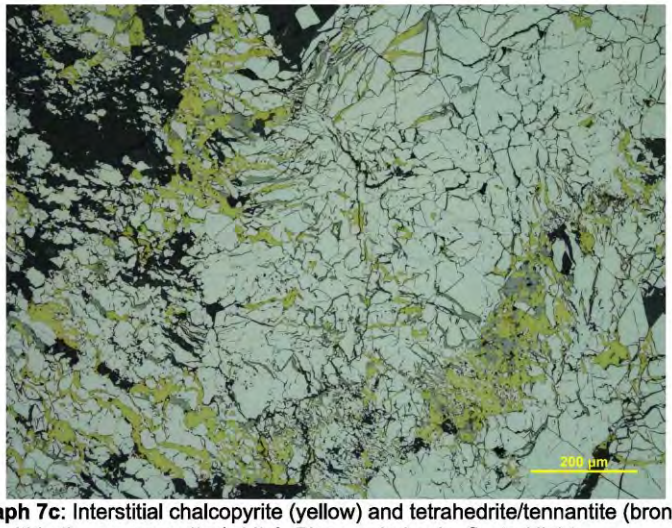

Photomicrograph 7c: Interstitial chalcopyrite (yellow) and tetrahedrite/tennantite (bronze-grey) filled in the fractures within the arsenopyrite (white). Plane-polarized reflected light.

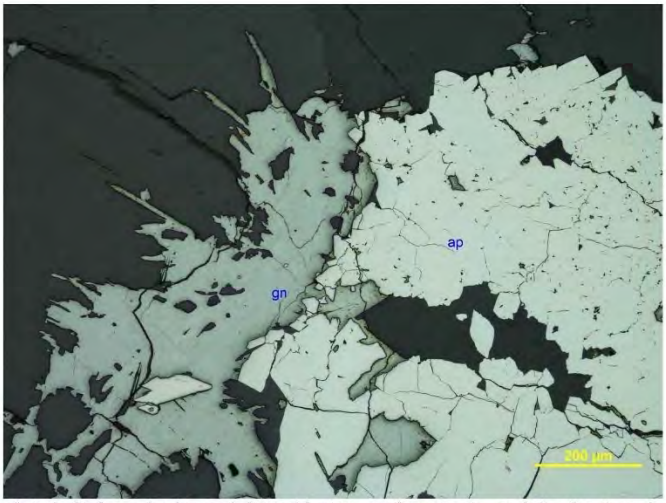

Photomicrograph 7d: Galena (gn) precipitated between the quartz and the fractured arsenopyrite (ap). Plane-polarized reflected light.

Sample 8: 2015704

White mica-quartz alteration zone (altered granitoid?)

Irregularly shaped to subidiomorphic pseudomorphs of very fine- to fine-grained flakes of white mica are associated with monomineralic and polycrystalline domains of quartz in the host rock, which is crosscut by a 15 mm thick arsenopyrite-carbonate vein.

Alteration: white mica: strong after feldspar; **quartz(?)**: moderate to strong

Mineral	*Alteration and Weathering Mineral*	*Modal %*	*Size Range (mm)*
alteration zone (~60% of PTS)			
[feldspar undiff.]	white mica	[2–3] 31–32	up to 0.1
quartz(?)	quartz	25–27	up to 1
arsenopyrite-carbonate vein (~40% of PTS)			
arsenopyrite		22–23	massive
carbonate		16–17	up to 5
quartz		0.2–0.3	up to 1
pyrite		0.1–0.2	up to 1.5 long

White mica is concentrated as very fine- to fine-grained flakes within pseudomorphic aggregates, which I tentatively interpret as having replaced feldspar minerals in the host rock. Relics of feldspar occur within some of the alteromorphs. The feldspar's refractive indexes are smaller than those of the quartz and suggest that the feldspar is either albite or alkali feldspar. The stained billet would indicate which feldspar occurs in this section.

Fine- to medium-grained crystals of **quartz** define monomineralic domains (Photomicrograph 8a) in the host rock. These domains probably are the result of the recrystallization of magmatic interstitial quartz in a granitoid rock. Fine-grained crystals of quartz are subordinate to the arsenopyrite and the carbonate in the vein.

Arsenopyrite forms massive and fractured aggregates in the 15 mm thick vein (Photomicrograph 8b). The arsenopyrite is relatively fresh, and its fractures are filled in by quartz, carbonate, and in rare cases, are subtly altered by iron oxides.

Carbonate forms inequigranular crystals intergrown with the arsenopyrite within the vein. Veinlets of carbonate branch off from the main vein and crosscut the host rock.

Pyrite is subordinate to the arsenopyrite and the carbonate, and forms fine-grained subidiomorphic crystals (up to 1.5 mm long) dispersed along the vein walls.

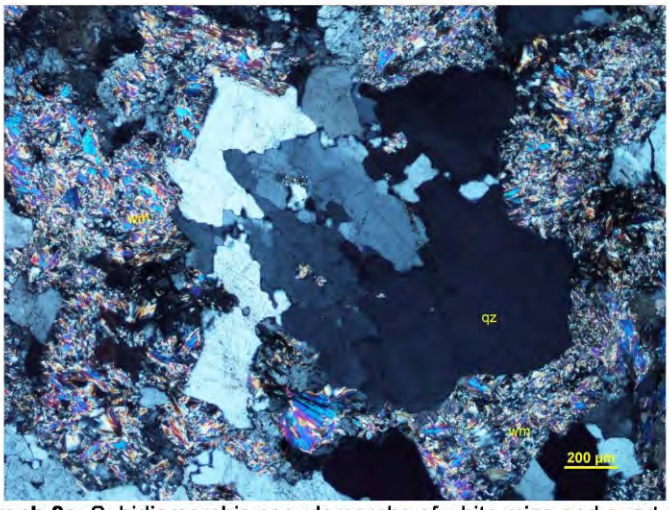

Photomicrograph 8a: Subidiomorphic pseudomorphs of white mica and quartz dominate the composition of the host rock. Crossed polarizers transmitted light.

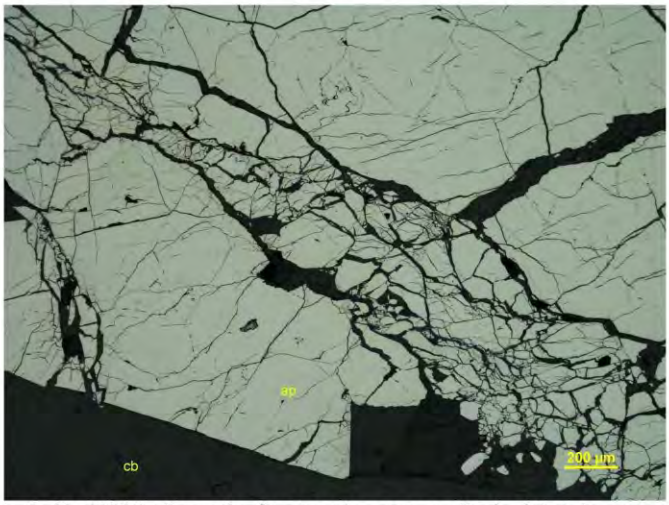

Photomicrograph 8b: Within the vein, fractured arsenopyrite (ap) is intergrown with carbonate (cb). Plane-polarized reflected light.

Sample 9: 2015734

Deformed quartz-white mica-arsenopyrite filling domain

A strongly deformed domain of quartz hosts sparse alteromorphs of very fine-grained white mica and clusters of fractured crystals of arsenopyrite and subordinate pyrite.

Alteration: white mica: strong after feldspar

Mineral	*Alteration and Weathering Mineral*	*Modal %*	*Size Range (mm)*
quartz		73–75	up to 10 long
white mica		15–17	up to 0.1
arsenopyrite		10–12	0.02 to massive
pyrite		0.2–0.3	up to 0.8

Quartz prevails in this section, which I interpret as a deformed quartz-rich filling domain flooding a white mica-quartz-altered rock similar to the host rock described as Sample 8. The quartz crystals are moderately to strongly deformed, and in some cases, are up to ~10 mm long (Photomicrograph 9a) and show a moderate to strong undulose extinction. Only in some domains, the quartz defines monomineralic domains intergrown with the white mica-rich alteromorphs. The elongate crystals of quartz are preferentially iso-oriented and define a weak foliation in this sample.

White mica is mostly fine-grained, and its flakes are concentrated within irregularly shaped alteromorphs (Photomicrograph 9c) and rare subhedral pseudomorphs, which I interpret as having replaced feldspar minerals.

Arsenopyrite is very fine- to medium-grained, and its crystals are concentrated within elongate to lenticular clusters oriented parallel to the weak foliation defined by the elongate crystals of quartz.

Rare subidiomorphic crystals of **pyrite** (up to 0.8 mm across) are spatially associated with the arsenopyrite clusters and are less fractured if compared to the arsenopyrite.

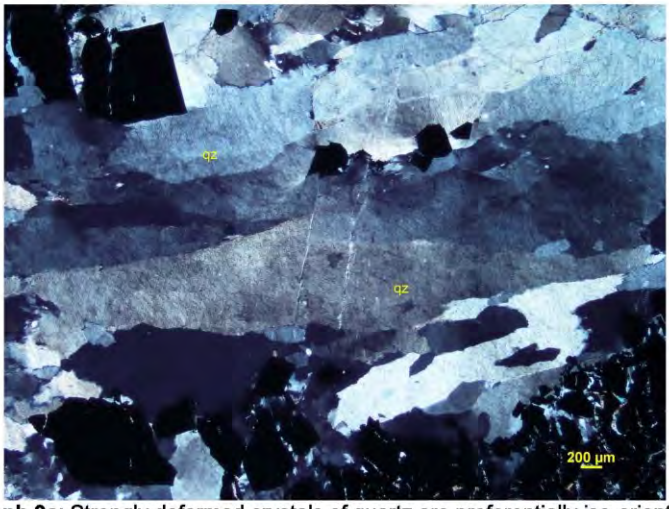

Photomicrograph 9a: Strongly deformed crystals of quartz are preferentially iso-oriented and define a weak foliation in this quartz-rich sample. Crossed polarizers transmitted light.

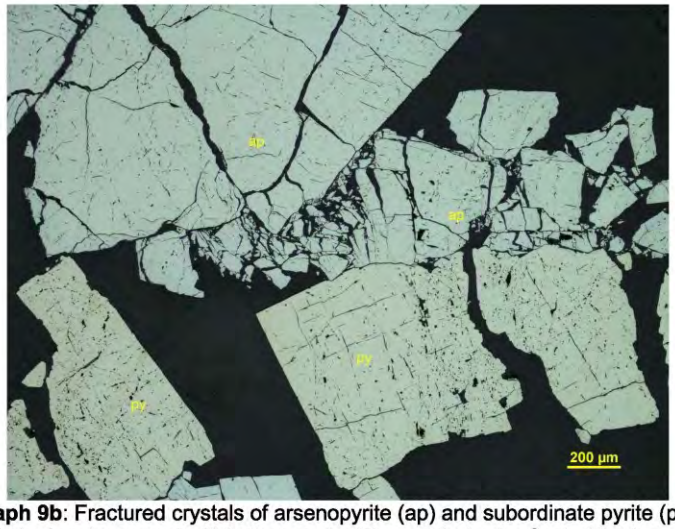

Photomicrograph 9b: Fractured crystals of arsenopyrite (ap) and subordinate pyrite (py) define elongate crystal clusters immersed within the quartz. Plane-polarized reflected light.

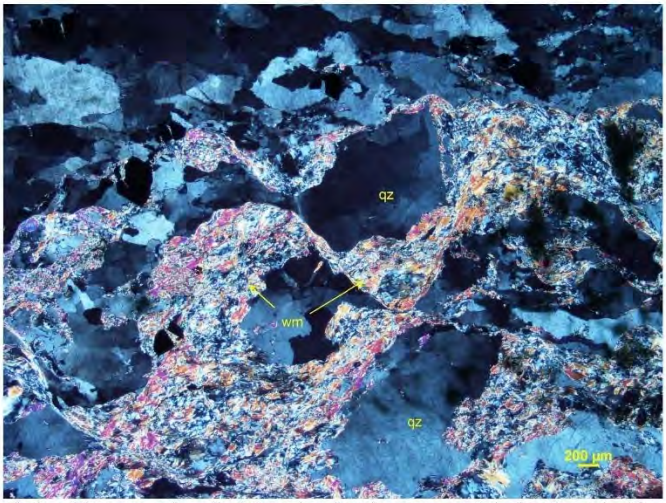

Photomicrograph 9c: Alteromorphs of white mica (wm) are associated with probable relic aggregates of quartz (qz). Crossed polarizers transmitted light.

APPENDIX 4

VARIOGRAM MODELS

Figure 1 Variogram Model – MSV Domain – Raven Gold Deposit

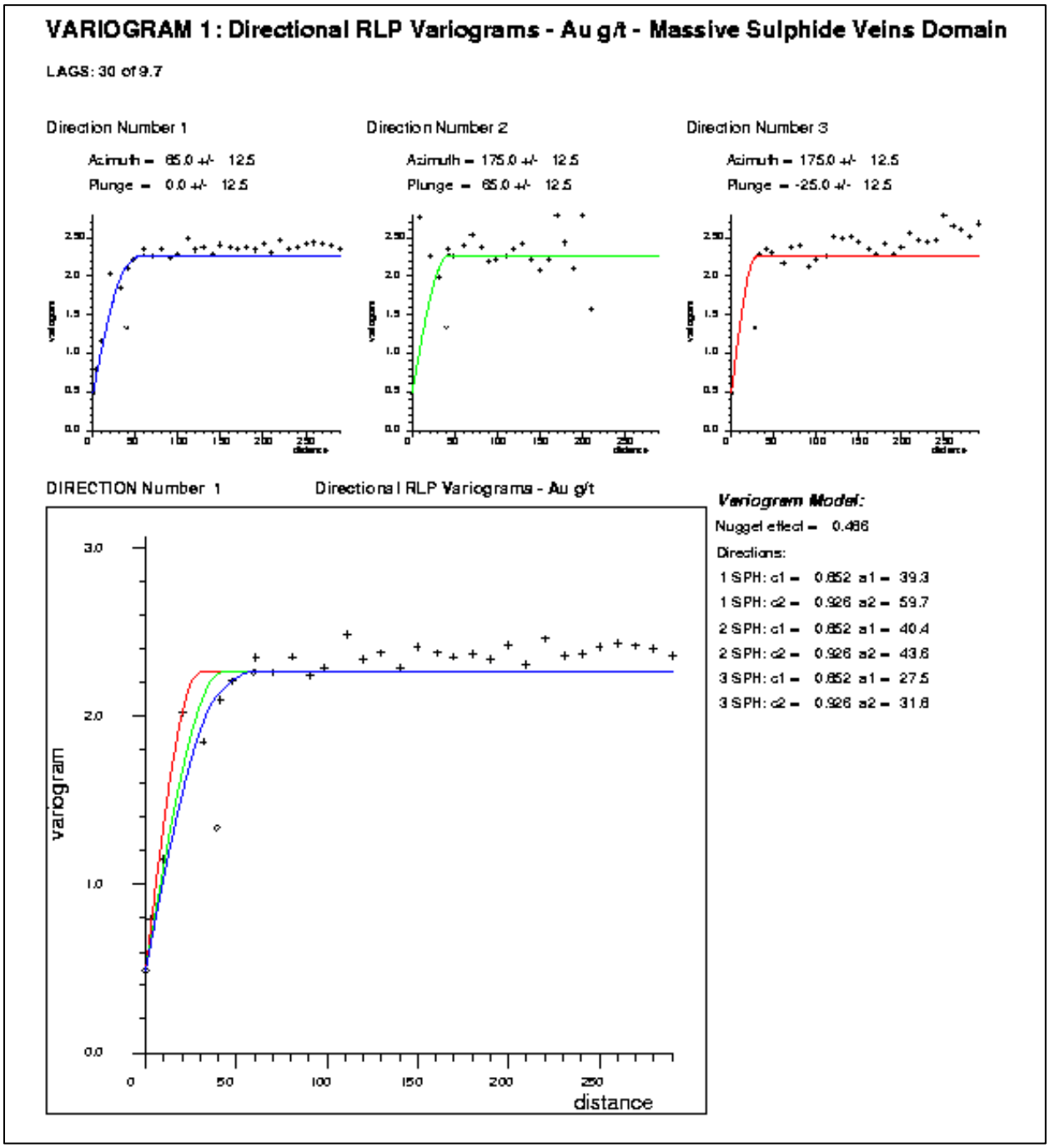

Source: Victoria Gold Corp. (2022)

Figure 2 Variogram Model – LG>0.2 Domain – Raven Gold Deposit

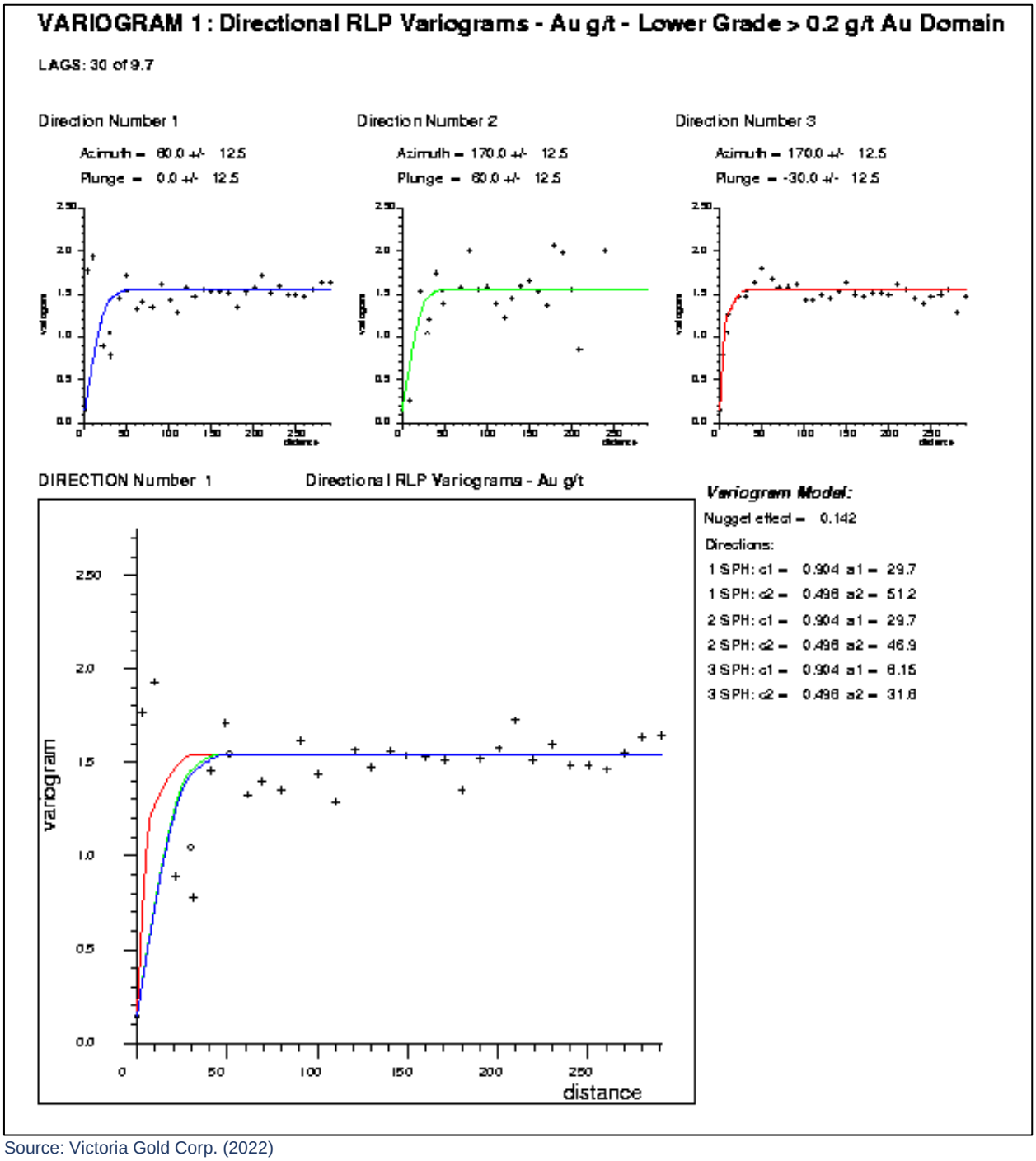

Source: Victoria Gold Corp. (2022)

Figure 3 Variogram Model – LG>0.6 Domain – Raven Gold Deposit

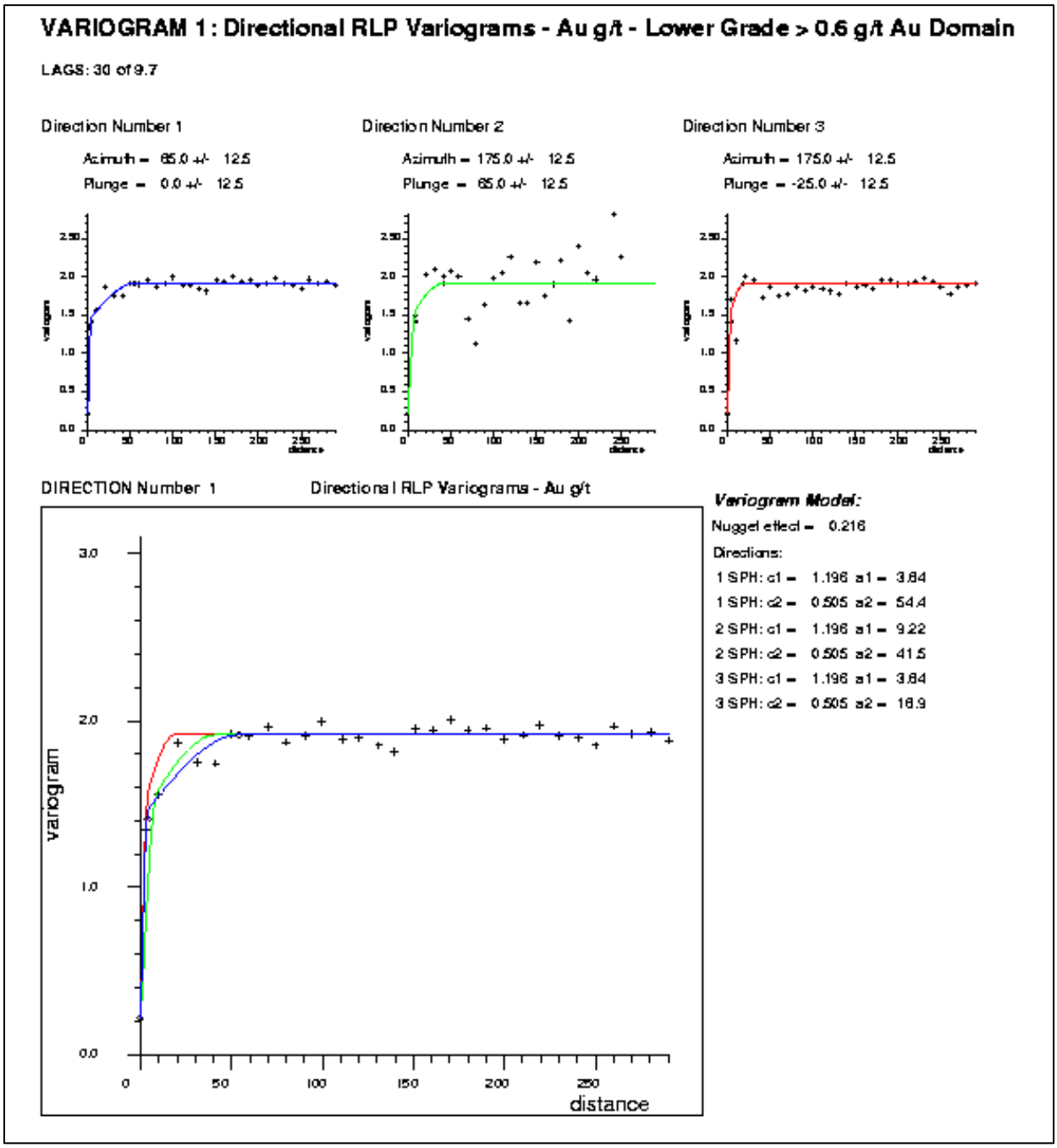

Source: Victoria Gold Corp. (2022)

Figure 4 Variogram Model – LG>4.0 Domain – Raven Gold Deposit

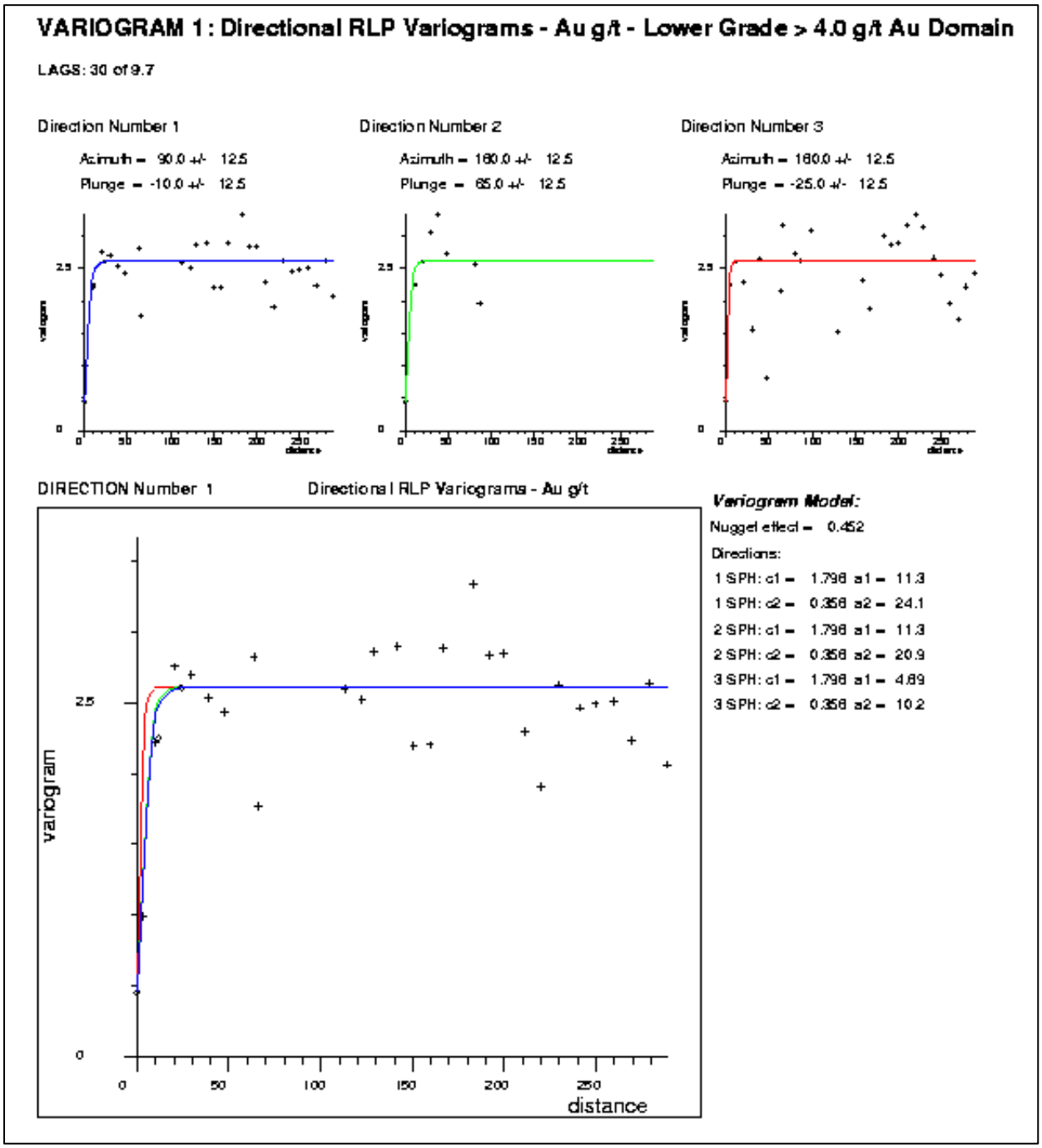

Source: Victoria Gold Corp. (2022)

APPENDIX 5

RAVEN DRILL HOLE LISTING – RESOURCE HOLES

Hole_ID	Location	UTM_E	UTM_N	Elevation	Azimuth	Dip	Depth (m)	Year
DG17-970C	Raven	472580	7104718	1027	165	-50	150	2017
NG18-001C	Raven	472028	7103049	1280	180	-45	204.22	2018
NG18-002C	Raven	472217	7102854	1301	0	-45	195.07	2018
NG18-003C	Raven	472558	7102684	1269	0	-45	213.36	2018
NG18-004C	Raven	472542	7102609	1267	0	-45	208.3	2018
NG18-005C	Raven	472667	7102516	1251	0	-45	205.74	2018
NG18-006C	Raven	473602	7101830	1248	175	-45	207.57	2018
NG18-007C	Raven	473606	7101838	1243	170	-65	213.36	2018
NG18-008C	Raven	473582	7101737	1252	172	-45	157.28	2018
NG19-009C	Raven	473585	7101722	1246	335	45	163.07	2019
NG19-010C	Raven	473524	7101832	1249	167	45	184.4	2019
NG19-011C	Raven	473671	7101758	1261	220	-45	165.2	2019
NG19-012C	Raven	473671	7101758	1261	160	-45	222.6	2019
NG19-013C	Raven	473679	7101840	1257	180	50	204.22	2019
NG19-014C	Raven	473706	7101670	1260	180	-45	179.83	2019
NG19-015C	Raven	473720	7101850	1259	180	-50	213.99	2019
NG19-016C	Raven	473676	7101877	1257	180	-45	185.93	2019
NG19-017C	Raven	473594	7101640	1257	160	-50	97.54	2019
NG20-018C	Raven	473835	7101857	1273	175	-45	201.17	2020
NG20-019C	Raven	473899	7101853	1268	170	-45	250.24	2020
NG20-020C	Raven	473964	7101860	1275	170	-45	291.39	2020
NG20-021C	Raven	473480	7101759	1242	174	-45	188.98	2020
NG20-022C	Raven	473951	7101789	1285	170	-45	255.66	2020
NG20-023C	Raven	473362	7101545	1217	170	-45	222.5	2020
NG20-024C	Raven	473928	7101741	1274	170	-45	230.73	2020
NG20-025C	Raven	473445	7101848	1237	170	-45	156.36	2020
NG20-026C	Raven	473491	7101850	1242	170	-45	262.13	2020
NG20-027C	Raven	473927	7101742	1274	218	-45	235.31	2020
NG20-028C	Raven	473466	7101933	1253	170	-45	251.16	2020
NG20-029C	Raven	473888	7101788	1267	170	-45	254.51	2020
NG20-030C	Raven	473563	7101927	1242	170	-45	217.93	2020
NG20-031C	Raven	473829	7101790	1266	170	-45	272.8	2020
NG20-032C	Raven	473638	7101931	1249	170	-45	275.84	2020
NG20-033C	Raven	474209	7101866	1270	170	-45	301.64	2020
NG20-034C	Raven	473743	7101930	1257	170	-45	256.64	2020
NG20-035C	Raven	473681	7101787	1265	170	-45	227.08	2020
NG20-036C	Raven	473970	7101916	1262	170	-45	281.94	2020
NG20-037C	Raven	473732	7101785	1268	170	-45	217.98	2020
NG20-038C	Raven	474020	7101861	1269	170	-45	291.08	2020
NG20-039C	Raven	473789	7101788	1266	170	-45	179.53	2020
NG20-040C	Raven	473765	7101680	1251	166	-45	216.41	2020
NG20-041C	Raven	473728	7101739	1268	170	-46	208.7	2020
NG20-042C	Raven	474013	7101815	1273	166	-46	335.28	2020
NG20-043C	Raven	473772	7101733	1267	170	-45	233.17	2020
NG20-044C	Raven	474015	7101767	1323	170	-45	322.04	2020
NG20-045C	Raven	473851	7101731	1325	170	-44	246.89	2020

NG20-046C	Raven	474024	7102023	1264	171	-43	242.32	2020
NG20-047C	Raven	473893	7101741	1321	170	-45	230.73	2020
NG20-048C	Raven	473785	7101850	1308	170	-45	94.49	2020
NG21-048C	Raven	473785	7101850	1300	170	-50	249.94	2021
NG21-049C	Raven	473815	7101670	1300	170	-50	256.03	2021
NG21-050C	Raven	473865	7101665	1300	170	-50	265.18	2021
NG21-051C	Raven	473865	7101665	1300	170	-70	298.7	2021
NG21-052C	Raven	473930	7101821	1300	170	-50	391.06	2021
NG21-053C	Raven	473903	7101701	1300	170	-50	259.38	2021
NG21-054C	Raven	474215	7101965	1500	170	-50	406.3	2021
NG21-055C	Raven	473909	7101642	1500	170	-55	207.26	2021
NG21-056C	Raven	474018	7101916	1500	170	-55	234.39	2021
NG21-057C	Raven	474174	7101909	1500	170	-50	362.71	2021
NG21-058C	Raven	473655	7101645	1500	170	-55	115.82	2021
NG21-059C	Raven	473655	7101645	1500	215	-55	153.9	2021
NG21-060C	Raven	473887	7101610	1500	170	-55	249.94	2021
NG21-061C	Raven	473656	7101698	1200	170	-55	188.98	2021
NG21-062C	Raven	474117	7101813	1500	170	-55	355.09	2021
NG21-063C	Raven	473654	7101644	1300	170	-55	155.45	2021
NG21-064C	Raven	473866	7101535	1300	170	-50	224.64	2021
NG21-065C	Raven	474066	7101812	1300	170	-50	352.04	2021
NG21-066C	Raven	473656	7101503	1200	170	-50	121.92	2021
NG21-067C	Raven	474120	7101859	1350	170	-45	349.9	2021
NG21-068C	Raven	473631	7101577	1210	170	-50	266.7	2021
NG21-069C	Raven	473714	7101595	1200	170	-50	155.45	2021
NG21-070C	Raven	473756	7101639	1200	170	-50	184	2021
NG21-072C	Raven	474069	7101859	1500	170	-50	429.77	2021
NG21-076C	Raven	473361	7101776	1288	170	-50	180.44	2021
NG21-077C	Raven	474117	7101813	1200	170	-50	324.61	2021
NG21-078C	Raven	473422	7101765	1200	165	-50	185.62	2021
NG21-079C	Raven	474065	7101765	1200	170	-55	289.56	2021
NG21-080C	Raven	473085	7101622	1200	189	-55	178.31	2021

APPENDIX 6

MINERAL TENURE INFORMATION

Regulation Type	Claim Name	Grant Number	Expiry Date	NTS Map Sheet
Claim	Bob 1 -7, 52, 86	YA17729 - YA17735, YA17780, YA43014	1-Mar-34	106D04
Claim	Dave 1 - 8, 17, 18	YA17802 - YA17809, YA17818, YA17819	1-Mar-34	106D04
Lease	Dave 13 - 16, 25, 27, 28	YA17814 - YA17817, YA42970, YA42972, YA42973	31-Jan-36	106D04
Claim	Dave 26	YA42971	1-Oct-24	106D04
Claim	Dave 29, 30, 31	YA42974, YA42975, YA43015	1-Mar-34	106D04
Claim	DG 43 - 55, 82, 83, 85, 100 - 103	YA14986 - YA14998, YA43044, YA43045, YA43046, YA43061 - YA43064	1-Mar-34	106D04
Claim	Dub 1 - 3	YC11075 - YC11077	1-Mar-34	106D04
Claim	Dub 4	YC11078	1-Mar-33	106D04
Claim	Dub 5 - 8	YC11079 - YC11082	1-Mar-32	106D04
Claim	Dub 9, 10	YC11083, YC11084	1-Mar-34	106D04
Claim	Dub 11 - 16	YC11085 - YC11090	1-Mar-33	106D04
Claim	Dub 17 - 20	YC11091 - YC11094	1-Mar-32	106D04
Claim	Dub 21	YC11095	1-Mar-37	106D04
Claim	Dub 22	YC11096	1-Mar-33	106D04
Claim	Dub 23	YC11097	1-Mar-37	106D04
Claim	Dub 24	YC11098	1-Mar-32	106D04
Claim	Dub 25	YC11099	1-Mar-37	106D04
Claim	Dub 26	YC11100	1-Mar-32	106D04
Claim	Dub 27	YC11101	1-Mar-34	106D04
Claim	Dub 28	YC11102	1-Mar-32	106D04
Claim	Dub 29	YC11103	1-Mar-37	106D04
Claim	Dub 30	YC11104	1-Mar-32	106D04

Regulation Type	Claim Name	Grant Number	Expiry Date	NTS Map Sheet
Claim	Dub 31	YC11105	1-Mar-36	106D04
Claim	Dub 32	YC11106	1-Mar-32	106D04
Claim	Dub 33	YC11107	1-Mar-37	106D04
Claim	Dub 34	YC11108	1-Mar-32	106D04
Claim	Dub 35	YC11109	1-Mar-36	106D04
Claim	Dub 36	YC11110	1-Mar-34	106D04
Claim	Dub 37	YC11111	1-Mar-32	106D04
Claim	Dub 38	YC11112	1-Mar-34	106D04
Claim	Dub 39	YC11113	1-Mar-32	106D04
Claim	Dub 40	YC11114	1-Mar-34	106D04
Claim	Dub 41	YC11115	1-Mar-32	106D04
Claim	Dub 42	YC11116	1-Mar-35	106D04
Claim	Dub 43, 44	YC11117, YC11118	1-Mar-32	106D04
Claim	Dub 45	YC11119	1-Mar-37	106D04
Claim	Dub 46	YC11120	1-Mar-32	106D04
Claim	Dub 47	YC11121	1-Mar-37	106D04
Claim	Dub 48	YC11122	1-Mar-32	106D04
Claim	Dub 49	YC11123	1-Mar-35	106D04
Claim	Dub 50	YC11124	1-Mar-32	106D04
Claim	Dub 51	YC11125	1-Mar-35	106D04
Claim	Dub 52	YC11126	1-Mar-32	106D04
Claim	Dub 53 - 56	YC11127 - YC11130	1-Mar-35	106D04
Claim	Dub 57 - 66	YC11131 - YC11140	1-Mar-37	106D04
Claim	Dub 67, 68	YC11141, YC11142	1-Mar-36	106D04
Claim	Dub 69	YC11143	1-Mar-37	106D04
Claim	Dub 70	YC11144	1-Mar-36	106D04

Regulation Type	Claim Name	Grant Number	Expiry Date	NTS Map Sheet
Claim	Dub 71	YC11145	1-Mar-37	106D04
Claim	Dub 72	YC11146	1-Mar-36	106D04
Claim	Dub 73 - 78	YC11147 - YC11152	1-Mar-32	106D04
Claim	Dub 79	YC11153	1-Mar-37	106D04
Claim	Dub 80	YC11154	1-Mar-32	106D04
Claim	Dub 81 - 85	YC11155 - YC11159	1-Mar-37	106D04
Claim	Dub 86	YC11160	1-Mar-35	106D04
Claim	Dub 87	YC11161	1-Mar-37	106D04
Claim	Dub 88	YC11162	1-Mar-35	106D04
Claim	Dub 89	YC11163	1-Mar-37	106D04
Claim	Dub 90	YC11164	1-Mar-35	106D04
Claim	Dub 91	YC11165	1-Mar-37	106D04
Claim	Dub 92	YC11166	1-Mar-35	106D04
Claim	Dub 93 - 102	YC11167 - YC11176	1-Mar-37	106D04
Claim	Dub 103, 104	YC11177, YC11178	1-Mar-36	106D04
Claim	Dub 105	YC11179	1-Mar-37	106D04
Claim	Dub 106	YC11180	1-Mar-32	106D04
Claim	Dub 107 - 111	YC11181 - YC11185	1-Mar-37	106D04
Claim	Dub 112	YC11186	1-Mar-33	106D04
Claim	Dub 113 - 129	YC11187 - YC11203	1-Mar-37	106D04
Claim	Dub 130 - 135	YC11204 - YC11209	1-Mar-35	106D04
Claim	Dub 136, 137	YC11210, YC11211	1-Mar-32	106D04
Claim	Dub 138 - 141	YC11212 - YC11215	1-Mar-34	106D04
Claim	Dub 142	YC11216	1-Mar-33	106D04
Claim	Dub 143 - 152	YC11217 - YC11226	1-Mar-37	106D04
Claim	Dub 153 - 159	YC11227 - YC11233	1-Mar-34	106D04

Regulation Type	Claim Name	Grant Number	Expiry Date	NTS Map Sheet
Claim	Dub 160	YC11234	1-Mar-36	106D04
Claim	Dub 161 - 165	YC11235 - YC11239	1-Mar-37	106D04, 105M13
Claim	Dub 166 - 170	YC11240 - YC11244	1-Mar-35	105M13
Claim	Dub 171 - 180	YC11245 - YC11254	1-Mar-34	105M13
Claim	Dub 181 - 189	YC11255 - YC11263	1-Mar-37	105M13
Claim	Dub 190	YC11264	1-Mar-34	105M13
Claim	Dub 191	YC11265	1-Mar-37	105M13
Claim	Dub 192	YC11266	1-Mar-32	105M13
Claim	Dub 193 - 197	YC11267 - YC11271	1-Mar-34	106D04, 105M13
Claim	Dub 198	YC11272	1-Mar-37	105M13
Claim	Dub 199 - 207	YC11273 - 11281	1-Mar-34	106D04, 105M13
Claim	Dub 208	YC11282	1-Mar-33	106D04
Claim	Dub 209 - 216	YC11283 - YC11290	1-Mar-37	106D04
Claim	Dub 217	YC11291	1-Mar-34	106D04
Claim	Dub 218	YC11292	1-Mar-35	106D04
Claim	Dub 219	YC11293	1-Mar-34	106D04
Claim	Dub 220 - 222	YC11297 - YC11296	1-Mar-35	106D04
Claim	Dub 223	YC11297	1-Mar-34	106D04
Claim	Dub 224	YC11298	1-Mar-35	106D04
Claim	Dub 225	YC11299	1-Mar-34	106D04
Claim	Dub 226	YC11300	1-Mar-35	106D04
Claim	Dub 227 - 229	YC11301 - YC11303	1-Mar-32	106D04
Claim	Dub 230 - 232	YC11304 - YC11306	1-Mar-34	106D04
Claim	Dub 233 - 240	YC11307 - YC11314	1-Mar-37	106D04

Regulation Type	Claim Name	Grant Number	Expiry Date	NTS Map Sheet
Claim	Dub 241 - 257	YC11315 - YC11331	1-Mar-35	106D04
Claim	Dub 258	YC11332	1-Mar-34	106D04
Claim	Dub 259, 260	YC11333, YC11334	1-Mar-35	106D04
Claim	Dub 261	YC11335	1-Mar-36	106D04
Claim	Dub 262 - 266	YC11336 - YC11340	1-Mar-33	106D04
Claim	Dub 267 - 272	YC11341 - YC11346	1-Mar-34	106D04
Claim	Dub 273 - 279	YC11347 - YC11353	1-Mar-35	106D04
Claim	Dub 280	YC11354	1-Mar-33	106D04
Claim	Dub 281 - 288	YC11355 - YC11362	1-Mar-34	106D04
Claim	Dub 289	YC11363	1-Mar-35	106D04
Claim	Dub 290	YC11364	1-Mar-34	106D04
Claim	Dub 291	YC11365	1-Mar-34	106D04
Claim	Dub 292, 293	YC11366, YC11367	1-Mar-34	106D04
Claim	Dub 294, 295	YC11368, YC11369	1-Mar-33	106D04
Claim	Dub 296	YC11370	1-Mar-34	106D04
Claim	Dub 297 - 299	YC11371 - YC11373	1-Mar-35	106D04
Claim	Dub 300 - 305	YC11374 - YC11379	1-Mar-34	106D04
Claim	Dub 306	YC11380	1-Mar-36	106D04
Claim	Dub 307 - 310	YC11381 - YC11384	1-Mar-34	106D04
Claim	Dub 311	YC11385	1-Mar-33	106D04
Claim	Dub 312	YC11386	1-Mar-34	106D04
Claim	Dub 313 - 324	YC11387 - YC11398	1-Mar-33	106D04
Claim	Dub 325 - 327	YC11399 - YC11401	1-Mar-34	106D04
Claim	Dub 328	YC11402	1-Mar-33	106D04
Claim	Dub 329	YC11403	1-Mar-34	106D04
Claim	Dub 330 - 338	YC11404 - YC11412	1-Mar-35	106D04

Regulation Type	Claim Name	Grant Number	Expiry Date	NTS Map Sheet
Claim	Dub 339	YC11413	1-Mar-36	106D04
Claim	Dub 340	YC11414	1-Mar-35	106D04
Claim	Dub 341	YC11415	1-Mar-37	106D04
Claim	Dub 342	YC11416	1-Mar-34	106D04
Claim	Dub 343	YC11417	1-Mar-36	106D04
Claim	Dub 344	YC11418	1-Mar-34	106D04
Claim	Dub 345	YC11419	1-Mar-36	106D04
Claim	Dub 346	YC11420	1-Mar-34	106D04
Claim	Dub 347	YC11421	1-Mar-36	106D04
Claim	Dub 348	YC11422	1-Mar-34	106D04
Claim	Dub 349	YC11423	1-Mar-36	106D04
Claim	Dub 350	YC11424	1-Mar-33	106D04
Claim	Dub 351	YC11425	1-Mar-36	106D04
Claim	Dub 352	YC11426	1-Mar-34	106D04
Claim	Dub 353	YC11427	1-Mar-37	106D04
Claim	Dub 354	YC11428	1-Mar-34	106D04
Claim	Dub 355	YC11429	1-Mar-37	106D04
Claim	Dub 356	YC11430	1-Mar-33	106D04
Claim	Dub 357 - 359	YC11431 - YC11433	1-Mar-34	106D04
Claim	Dub 360	YC11434	1-Mar-33	106D04
Claim	Dub 361 - 364	YC11435 - YC11438	1-Mar-34	106D04
Claim	Dub 365 - 368	YC11439 - YC11442	1-Mar-35	106D04
Claim	Dub 369 - 372	YC11443 - YC11446	1-Mar-33	106D04
Claim	Dub 373, 374	YC11447, YC11448	1-Mar-34	106D04
Claim	Dub 375, 376	YC11449, YC11450	1-Mar-37	106D04
Claim	Dub 377 - 384	YC11451 - YC11458	1-Mar-36	106D04

Regulation Type	Claim Name	Grant Number	Expiry Date	NTS Map Sheet
Claim	Dub 385 - 390	YC11459 - YC11464	1-Mar-37	106D04
Claim	Dub 391 - 396	YC11465 - YC11470	1-Mar-34	106D04
Claim	Dub 397	YC11471	1-Mar-35	106D04
Claim	Dub 398	YC11472	1-Mar-34	106D04
Claim	Dub 399, 400	YC11473, YC11474	1-Mar-35	106D04
Claim	Dub 401	YC11475	1-Mar-34	106D04
Claim	Dub 402	YC11476	1-Mar-33	106D04
Claim	Dub 403	YC11477	1-Mar-34	106D04
Claim	Dub 404	YC11478	1-Mar-33	106D04
Claim	Dub 405	YC11479	1-Mar-34	106D04
Claim	Dub 406	YC11480	1-Mar-33	106D04
Claim	Dub 407	YC11481	1-Mar-34	106D04
Claim	Dub 408	YC11482	1-Mar-33	106D04
Claim	Dub 409	YC11483	1-Mar-36	106D04
Claim	Dub 410	YC11484	1-Mar-37	106D04
Claim	Dub 411	YC11485	1-Mar-35	106D04
Claim	Dub 412	YC11486	1-Mar-37	106D04
Claim	Dub 413	YC11487	1-Mar-35	106D04
Claim	Dub 414	YC11488	1-Mar-36	106D04
Claim	Dub 415	YC11489	1-Mar-35	106D04
Claim	Dub 416	YC11490	1-Mar-36	106D04
Claim	Dub 417	YC11491	1-Mar-35	106D04
Claim	Dub 418	YC11492	1-Mar-36	106D04
Claim	Dub 419	YC11493	1-Mar-35	106D04
Claim	Dub 420	YC11494	1-Mar-37	106D04
Claim	Dub 421	YC11495	1-Mar-35	106D04

Regulation Type	Claim Name	Grant Number	Expiry Date	NTS Map Sheet
Claim	Dub 422	YC11496	1-Mar-33	106D04
Claim	Dub 423	YC11497	1-Mar-36	106D04
Claim	Dub 424	YC11498	1-Mar-37	106D04
Claim	Dub 425	YC11499	1-Mar-32	106D04
Claim	Dub 426	YC11500	1-Mar-36	106D04
Claim	Dub 427	YC11501	1-Mar-32	106D04
Claim	Dub 428	YC11502	1-Mar-35	106D04
Claim	Dub 429	YC11503	1-Mar-32	106D04
Claim	Dub 430	YC11504	1-Mar-35	106D04
Claim	Dub 431	YC11505	1-Mar-32	106D04
Claim	Dub 432 - 436	YC1150 - YC11510	1-Mar-35	106D04
Claim	Dub 437 - 440	YC11511 - YC11514	1-Mar-36	106D04
Claim	Dub 441 - 449	YC11515 - YC11523	1-Mar-32	106D04
Claim	Dub 450	YC11524	1-Mar-35	106D04
Claim	Dub 451	YC11525	1-Mar-34	106D04
Claim	Dub 452, 453	YC11526, YC11527	1-Mar-35	106D04
Claim	Dub 454	YC11528	1-Mar-36	106D04
Claim	Dub 455	YC11529	1-Mar-35	106D04
Claim	Dub 456	YC11530	1-Mar-36	106D04
Claim	Dub 457 - 479	YC11531 - YC11553	1-Mar-32	106D04
Claim	Dub 480 - 484	YC11554, YC32478 - YC32481	1-Mar-34	106D04
Claim	Dub 485 - 492	YC32482 - YC32489	1-Mar-32	105M13
Claim	Dub 493	YC32490	1-Mar-33	105M13
Claim	Dub 494 - 496	YC32491 -YC32493	1-Mar-32	105M13
Claim	Dub 497 - 516	YC32494 - YC32513	1-Mar-34	105M13
Claim	Dub 517	YC32514	1-Mar-33	105M13

Regulation Type	Claim Name	Grant Number	Expiry Date	NTS Map Sheet
Claim	Dub 518 - 544	YC32515 - YC32541	1-Mar-34	105M13
Claim	Dub 545 - 548	YC32542 - YC32545	1-Mar-32	105M13
Claim	Dub 567 - 581	YC32564 - YC32578	1-Mar-34	105M13
Claim	Dub 582 - 587	YC32579 - YC32584	1-Mar-32	105M13
Claim	Dub 588	YC32585	1-Mar-31	105M13
Claim	Dub 589	YC32586	1-Mar-32	105M13
Claim	Dub 590	YC32587	1-Mar-31	105M13
Claim	Dub 591	YC32588	1-Mar-32	105M13
Claim	Dub 592 - 603	YC32589 - YC32600	1-Mar-31	106D04, 105M13
Claim	Dub 604 - 662	YC32601 - YC32659	1-Mar-32	106D04, 105M13
Claim	Dub 663 - 678	YC32660 - YC32675	1-Mar-31	105M13, 105M14
Claim	Dub 679 - 682	YC32676 - YC32679	1-Mar-32	105M13
Claim	Dub 683 - 779	YC32680 - YC32700, YC38001 - YC38076	1-Mar-31	106D04, 105M13, 105M14
Claim	Dub 780	YC38077	1-Mar-32	106D04
Claim	Dub 781	YC38078	1-Mar-31	106D04
Claim	Dub 782	YC38079	1-Mar-32	106D04
Claim	Dub 783, 784	YC38080, YC38081	1-Mar-31	106D03
Claim	Dub 785 - 801	YC38082 - YC38098	1-Mar-32	106D03, 106D04
Claim	Dub 802 - 842	YC38099 - YC38139	1-Mar-31	106D03, 106D04
Claim	Dub 843 - 879	YC38140 - YC38176	1-Mar-32	106D04
Claim	Dub 880, 881	YC38177, YC38178	1-Mar-31	106D04
Claim	Dub 882	YC38179	1-Mar-32	106D04

Regulation Type	Claim Name	Grant Number	Expiry Date	NTS Map Sheet
Claim	Dub 883	YC38180	1-Mar-31	106D04
Claim	Dub 884, 885	YC38181, YC38182	1-Mar-32	106D04
Claim	Dub 886	YC38183	1-Mar-31	106D04
Claim	Dub 887 - 907	YC38184 - YC38204	1-Mar-32	106D04
Claim	Dub 908 - 927	YC38205 - YC38224	1-Mar-31	106D03, 106D04
Claim	Dub 928 - 953	YC38225 - YC38250	1-Mar-32	106D03, 106D04
Claim	Dub 954 - 969	YC38251 - YC38266	1-Mar-31	106D03, 106D04
Claim	Dub 970	YC38267	1-Mar-32	106D04
Claim	Dub 971	YC38268	1-Mar-31	106D04
Claim	Dub 972 - 975	YC38269 - YC38272	1-Mar-32	106D04
Claim	Dub 976 - 979	YC38273 - YC38276	1-Mar-31	106D04
Claim	Dub 980	YC38277	1-Mar-32	106D04
Claim	Dub 981	YC38278	1-Mar-31	106D04
Claim	Dub 982 - 999	YC38279 - YC38296	1-Mar-32	106D04
Claim	Dub 1000 - 1017	YC38297 - YC38314	1-Mar-31	106D03, 106D04
Claim	Dub 1018 - 1026	YC38315 - YC38323	1-Mar-32	1064D04
Claim	Dub 1027 - 1029	YC38324 - YC38326	1-Mar-31	106D04
Claim	Dub 1030	YC38327	1-Mar-32	106D04
Claim	Dub 1031 - 1033	YC38328 - YC38330	1-Mar-31	106D04
Claim	Dub 1034 - 1045	YC38331 - YC38342	1-Mar-32	106D04
Claim	Dub 1046 - 1063	YC38343 - YC38360	1-Mar-31	106D03, 106D04
Claim	Dub 1064 - 1103	YC38361 - YC38400	1-Mar-32	106D04
Claim	Dub 1104	YC38401	1-Mar-33	106D04

Regulation Type	Claim Name	Grant Number	Expiry Date	NTS Map Sheet
Claim	Dub 1105	YC38402	1-Mar-32	106D04
Claim	Dub 1106 - 1117	YC38403 - YC38414	1-Mar-33	106D04
Claim	Dub 1118 - 1127	YC38415 - YC38424	1-Mar-32	106D04
Claim	Dub 1128 - 1146	YC38425 - YC38443	1-Mar-31	106D03, 106D04
Claim	Dub 1147, 1148	YC38444, YC38445	1-Mar-32	106D04
Claim	Dub 1149, 1150	YC38446, YC38447	1-Mar-31	106D04
Claim	Dub 1151	YC38448	1-Mar-32	106D04
Claim	Dub 1152	YC38449	1-Mar-31	106D04
Claim	Dub 1153	YC38450	1-Mar-32	106D04
Claim	Dub 1154	YC38451	1-Mar-31	106D04
Claim	Dub 1155	YC38452	1-Mar-32	106D04
Claim	Dub 1156, 1157	YC38453, YC38454	1-Mar-31	106D04
Claim	Dub 1158	YC38455	1-Mar-32	106D04
Claim	Dub 1159	YC38456	1-Mar-31	106D04
Claim	Dub 1160	YC38457	1-Mar-32	106D04
Claim	Dub 1161	YC38458	1-Mar-31	106D04
Claim	Dub 1162 - 1190	YC38459 - YC38487	1-Mar-32	106D04
Claim	Dub 1191	YC38488	1-Mar-33	106D04
Claim	Dub 1192	YC38489	1-Mar-32	106D04
Claim	Dub 1193	YC38490	1-Mar-33	106D04
Claim	Dub 1194	YC38491	1-Mar-32	106D04
Claim	Dub 1195	YC38492	1-Mar-33	106D04
Claim	Dub 1196	YC38493	1-Mar-32	106D04
Claim	Dub 1197 - 1199	YC38494 - YC38496	1-Mar-33	106D04
Claim	Dub 1200 - 1209	YC38497 - YC38506	1-Mar-32	106D04

Regulation Type	Claim Name	Grant Number	Expiry Date	NTS Map Sheet
Claim	Dub 1210 - 1229	YC38507 - YC38526	1-Mar-31	106D03, 106D04
Claim	Dub 1230 - 1293	YC38527 - YC38590	1-Mar-32	106D04
Claim	Dub 1294	YC38591	1-Mar-31	106D04
Claim	Dub 1295	YC38592	1-Mar-32	106D04
Claim	Dub 1296	YC38593	1-Mar-31	106D04
Claim	Dub 1297	YC38594	1-Mar-32	106D04
Claim	Dub 1298	YC38595	1-Mar-31	106D04
Claim	Dub 1299	YC38596	1-Mar-32	106D04
Claim	Dub 1300	YC38597	1-Mar-31	106D04
Claim	Dub 1301	YC38598	1-Mar-32	106D04
Claim	Dub 1302	YC38599	1-Mar-31	106D04
Claim	Dub 1303	YC38600	1-Mar-32	106D04
Claim	Dub 1304	YC38601	1-Mar-31	106D04
Claim	Dub 1305	YC38602	1-Mar-33	106D04
Claim	Dub 1306 - 1310	YC38603 - YC38607	1-Mar-32	106D04
Claim	Dub 1311	YC38608	1-Mar-33	106D04
Claim	Dub 1312	YC38609	1-Mar-32	106D04
Claim	Dub 1313	YC38610	1-Mar-34	106D04
Claim	Dub 1314, 1315	YC38611, YC38612	1-Mar-32	106D04
Claim	Dub 1316	YC38613	1-Mar-31	106D04
Claim	Dub 1317	YC38614	1-Mar-32	106D04
Claim	Dub 1318	YC38615	1-Mar-31	106D04
Claim	Dub 1319 - 1321	YC38616 - YC38618	1-Mar-32	106D04
Claim	Dub 1322	YC38619	1-Mar-31	106D04

Regulation Type	Claim Name	Grant Number	Expiry Date	NTS Map Sheet
Claim	Dub 1323	YC38620	1-Mar-32	106D04
Claim	Dub 1324	YC38621	1-Mar-31	106D04
Claim	Dub 1325, 1326	YC38622, YC38623	1-Mar-32	106D04, 116A01
Claim	Dub 1327	YC38624	1-Mar-31	116A01
Claim	Dub 1328 - 1344, 1345, 1346, 1347	YC38625 - YC38641, YC39876, YC38642, YC38643	1-Mar-32	106D04
Claim	Dub 1348, 1349	YC38644, YC38645	1-Mar-33	106D04
Claim	Dub 1350 - 1359	YC38646 - YC38655	1-Mar-32	106D04
Claim	Dub 1360 - 1363	YC38656 - YC38659	1-Mar-31	106D04, 116A01
Claim	Dub 1364, 1365	YC38660, YC38661	1-Mar-32	106D04
Claim	Dub 1366, 1367	YC38662, YC38663	1-Mar-33	106D04
Claim	Dub 1368 - 1371	YC38664 - YC38667	1-Mar-34	106D04
Claim	Dub 1372 - 1395	YC38668 - YC38691	1-Mar-32	106D04
Claim	Dub 1396 - 1399	YC38692 - YC38695	1-Mar-31	106D04, 116A01
Claim	Dub 1400 - 1403	YC38969 - YC38699	1-Mar-32	106D04
Claim	Dub 1404 - 1419	YC38700 - YC38715	1-Mar-34	106D04
Claim	Dub 1420 - 1423	YC38716 - YC38719	1-Mar-32	106D04
Claim	Dub 1424 - 1437	YC38720 - YC38733	1-Mar-34	106D04
Claim	Dub 1438	YC38734	1-Mar-32	106D04
Claim	Dub 1439	YC38735	1-Mar-34	106D04
Claim	Dub 1440 - 1443	YC38736 - YC38739	1-Mar-32	106D04
Claim	Dub 1444 - 1457	YC38740 - YC38753	1-Mar-34	106D04
Claim	Dub 1458 - 1463	YC38754 - YC38759	1-Mar-32	106D04
Claim	Dub 1464	YC38760	1-Mar-34	106D04
Claim	Dub 1465	YC38761	1-Mar-32	106D04

Regulation Type	Claim Name	Grant Number	Expiry Date	NTS Map Sheet
Claim	Dub 1466	YC38762	1-Mar-34	106D04
Claim	Dub 1467	YC38763	1-Mar-32	106D04
Claim	Dub 1468	YC38764	1-Mar-34	106D04
Claim	Dub 1469	YC38765	1-Mar-32	106D04
Claim	Dub 1470	YC38766	1-Mar-34	106D04
Claim	Dub 1471	YC38767	1-Mar-32	106D04
Claim	Dub 1472	YC38768	1-Mar-34	106D04
Claim	Dub 1473	YC38769	1-Mar-32	106D04
Claim	Dub 1474	YC38770	1-Mar-34	106D04
Claim	Dub 1475 - 1499	YC38771 - YC38795	1-Mar-32	106D04, 116A01
Claim	Dub 1500	YC38795	1-Mar-31	116A01
Claim	Dub 1501	YC38796	1-Mar-32	116A01
Claim	Dub 1502	YC38797	1-Mar-31	116A01
Claim	Dub 1503	YC38798	1-Mar-32	116A01
Claim	Dub 1504 - 1512	YC38799 - YC38808	1-Mar-34	106D04
Claim	Dub 1513 - 1529	YC38809 - YC38825	1-Mar-32	106D04, 116A01
Claim	Dub 1530 - 1534	YC38826 - YC38830	1-Mar-34	106D04
Claim	Dub 1535	YC38831	1-Mar-32	106D04
Claim	Dub 1536 - 1538	YC38832 - YC38834	1-Mar-34	106D04
Claim	Dub 1539	YC38835	1-Mar-32	106D04
Claim	Dub 1540	YC38836	1-Mar-34	106D04
Claim	Dub 1541 - 1581	YC38837 - YC38877	1-Mar-32	106D04, 116A01
Claim	Dub 1582	YC38878	1-Mar-34	106D04
Claim	Dub 1583	YC38879	1-Mar-32	106D04

Regulation Type	Claim Name	Grant Number	Expiry Date	NTS Map Sheet
Claim	Dub 1584 - 1589	YC38880 - YC39856	1-Mar-31	106D04
Claim	Dub 1590 - 1619	YC39857 – YC39859, YC39866 – YC39875, YC39860 - YC39865, YC42226 - YC42236	1-Mar-32	106D04, 105M13
Claim	Dub Fr. 1620	YE55727	11-Feb-23	106D04
Claim	Fiji 1, 2, 3	YA63884, YB03409, YA63886	1-Mar-34	106D04
Claim	Fiji 5, 6	YA63888, YA63889	1-Mar-34	106D04
Claim	Hla 1 - 6, 7 - 14	YC10918 - YC10923, YC10828 - YC10835	1-Mar-29	106D04
Claim	Jan 1, 2	YB65585, YB65586	1-Mar-32	106D04
Claim	Jan 3	YB65587	16-Jan-24	106D04
Claim	Jan 4	YB65588	16-Jan-29	106D04
Claim	Jeff 17, 18, 33, 34, 113 - 115	YA17842, YA17843, YA17858, YA17859, YA42976 - YA142978	1-Mar-34	106D04
Claim	Jeff 116	YC39877	1-Mar-32	106D04
Claim	Jeff 117, 118, 120	YB03408, YA42981, YA42983	1-Mar-34	106D04
Claim	Len 1, 2	YC02730, YC02731	15-May-30	106D04
Claim	Len 3	YC02732	1-Mar-32	106D04
Claim	Len 4	YA30524	15-May-30	106D04
Claim	Len 5	YC02733	1-Mar-32	106D04
Claim	Len 6	YA30526	15-May-30	106D04
Claim	Len 7	YC02734	1-Mar-32	106D04
Claim	Len 8	YA30528	15-May-29	106D04
Claim	Len 9	YC02735	1-Mar-32	106D04
Claim	Len 10	YA30530	15-May-26	106D04
Claim	Len 11	YC02736	15-May-31	106D04
Claim	Len 12	YC02737	15-May-30	106D04
Claim	Len 13, 14	YC02738, YC02739	15-May-29	106D04

Regulation Type	Claim Name	Grant Number	Expiry Date	NTS Map Sheet
Claim	Len 15 - 18	YC02740 - YC02743	15-May-28	106D04
Claim	Len 19, 20	YC02744, YC02745	15-May-25	106D04
Claim	Len 21 - 23	YC02746 - YC02748	1-Mar-32	106D04
Claim	Len 24	YA30544	15-May-26	106D04
Claim	Len 25	YC02749	1-Mar-32	106D04
Claim	Len 26	YA30546	15-May-29	106D04
Claim	Len 27	YC02750	1-Mar-32	106D04
Claim	Len 28	YA30548	15-May-30	106D04
Claim	Len 29	YC02751	1-Mar-32	106D04
Claim	Len 30	YA30550	15-May-30	106D04
Claim	Len 31, 32	YC02752, YC02753	1-Mar-32	106D04
Claim	Lynx 1 - 18	YC10463 - YC10480	1-Mar-32	105M13
Claim	Lynx 19	YC10481	16-Jan-30	105M13
Claim	Lynx 20 - 23	YC10482 - YC10485	1-Mar-32	105M13
Claim	Lynx 24	YC10486	16-Jan-24	105M13
Claim	Lynx 25	YC10487	1-Mar-32	105M13
Claim	Lynx 26	YC10488	16-Jan-24	105M13
Claim	Lynx 27	YC10489	1-Mar-32	105M13
Claim	Lynx 28	YC10490	16-Jan-24	105M13
Claim	Lynx 29 - 32	YC10491 - YC10494	1-Mar-32	105M13
Claim	Lynx 33	YC10495	16-Jan-24	105M13
Claim	Lynx 34 - 40	YC10496 - YC10502	1-Mar-32	105M13
Claim	Lynx 41	YC10503	3-Mar-24	105M13
Claim	Lynx 42 - 57	YC10504 – YC10518, YC11555	1-Mar-32	105M13, 106D04

Regulation Type	Claim Name	Grant Number	Expiry Date	NTS Map Sheet
Claim	Mar 1 - 12, 14 - 22, 24, 31, 33 - 40	YA14896 - YA14907, YA14909 - YA14917, YA14919, YA42984, YA43101 - YA43108	1-Mar-34	106D04
Claim	Mary 1 - 8	YA63876 - YA63883	1-Mar-34	106D04
Claim	Neera 1, 2	YC10822, YC10823	1-Mar-29	106D04
Grant	Olive Crown Grant	GR1054	N/A	106D04
Claim	R & D 1 - 8, 10, 12, 14 - 16	YA01393 - YA01400, YA01402, YA01404, YA01406 - YA01408	1-Mar-34	106D04
Lease	R & D No. 9, 11, 13	YA01401, YA01403, YA01405	31-Jan-36	106D04
Claim	Roni 1 - 14	YB64630 - YB64643	1-Mar-34	106D04
Claim	Smoky 1 - 10, 23, 25 - 30, 37 - 41, 44 - 47, 48, 49, 51 - 54, 56, 58, 62 - 65, 66 - 71, 74 - 77, 78, 80, 83 - 85, 91 - 100, 107 - 109	YA17930 - YA17939, YA17952, YA17954 - YA17959, YA17966 - YA17970, YA30072 - YA30075, YA17973, YA17974, YA30076 - YA30079, YA17977, YA17979, YA30080 - YA30083, YA17983 - YA17988, YA30084 - YA30087, YA17991, YA17993, YA43120 - YA43122, YA43128 - YA43137, YA43144 - YA43146	1-Mar-34	106D04
Claim	Smoky Fr. 55	YE55726	6-Dec-2022	106D04
Claim	Tin Dome 1 - 4, 5 - 12	YC02842 - YC02845, YC02848 - YC02855	1-Mar-32	106D04
Claim	West 167 - 172, 174, 182, 184	YB18934 - YB18939, YB18941, YB18949, YB18951	1-Mar-34	106D04, 105M13

Source: Victoria Gold Corp. (2022)